WATER-USE EFFICIENCY: ADVANCES AND CHALLENGES IN A CHANGING CLIMATE

EDITED BY: Manoj Menon, Stuart Anthony Casson, Jeffrey M. Warren, Bhabani S. Das and Michael Vincent Mickelbart

PUBLISHED IN: Frontiers in Plant Science

frontiers Research Topics

frontiers

ISSN 1664-8714
ISBN 978-2-88963-098-1
DOI 10.3389/978-2-88963-098-1

About Frontiers

Frontiers is more than just an open-access publisher of scholarly articles: it is a pioneering approach to the world of academia, radically improving the way scholarly research is managed. The grand vision of Frontiers is a world where all people have an equal opportunity to seek, share and generate knowledge. Frontiers provides immediate and permanent online open access to all its publications, but this alone is not enough to realize our grand goals.

Frontiers Journal Series

The Frontiers Journal Series is a multi-tier and interdisciplinary set of open-access, online journals, promising a paradigm shift from the current review, selection and dissemination processes in academic publishing. All Frontiers journals are driven by researchers for researchers; therefore, they constitute a service to the scholarly community. At the same time, the Frontiers Journal Series operates on a revolutionary invention, the tiered publishing system, initially addressing specific communities of scholars, and gradually climbing up to broader public understanding, thus serving the interests of the lay society, too.

Dedication to Quality

Each Frontiers article is a landmark of the highest quality, thanks to genuinely collaborative interactions between authors and review editors, who include some of the world's best academicians. Research must be certified by peers before entering a stream of knowledge that may eventually reach the public - and shape society; therefore, Frontiers only applies the most rigorous and unbiased reviews.
Frontiers revolutionizes research publishing by freely delivering the most outstanding research, evaluated with no bias from both the academic and social point of view. By applying the most advanced information technologies, Frontiers is catapulting scholarly publishing into a new generation.

What are Frontiers Research Topics?

Frontiers Research Topics are very popular trademarks of the Frontiers Journals Series: they are collections of at least ten articles, all centered on a particular subject. With their unique mix of varied contributions from Original Research to Review Articles, Frontiers Research Topics unify the most influential researchers, the latest key findings and historical advances in a hot research area! Find out more on how to host your own Frontiers Research Topic or contribute to one as an author by contacting the Frontiers Editorial Office: researchtopics@frontiersin.org

WATER-USE EFFICIENCY: ADVANCES AND CHALLENGES IN A CHANGING CLIMATE

Topic Editors:
Manoj Menon, University of Sheffield, United Kingdom
Stuart Anthony Casson, University of Sheffield, United Kingdom
Jeffrey M. Warren, Oak Ridge National Laboratory (DOE), United States
Bhabani S. Das, Indian Institute of Technology Kharagpur, India
Michael Vincent Mickelbart, Purdue University, United States

Citation: Menon, M., Casson, S. A., Warren, J. M., Das, B. S., Mickelbart, M. V., eds. (2019). Water-Use Efficiency: Advances and Challenges in a Changing Climate. Lausanne: Frontiers Media. doi: 10.3389/978-2-88963-098-1

Table of Contents

frontiers in Plant Science

ORIGINAL RESEARCH
published: 28 June 2019
doi: 10.3389/fpls.2019.00830

Species-Specific Shifts in Diurnal Sap Velocity Dynamics and Hysteretic Behavior of Ecophysiological Variables During the 2015–2016 El Niño Event in the Amazon Forest

Bruno O. Gimenez[1†], Kolby J. Jardine[2†], Niro Higuchi[1], Robinson I. Negrón-Juárez[2], Israel de Jesus Sampaio-Filho[1], Leticia O. Cobello[1], Clarissa G. Fontes[3], Todd E. Dawson[3], Charuleka Varadharajan[2], Danielle S. Christianson[2], Gustavo C. Spanner[1], Alessandro C. Araújo[4], Jeffrey M. Warren[5], Brent D. Newman[6], Jennifer A. Holm[2], Charles D. Koven[2], Nate G. McDowell[7] and Jeffrey Q. Chambers[2,8]*

[1] National Institute of Amazonian Research (INPA), Manaus, Brazil, [2] Climate and Ecosystem Sciences Division, Lawrence Berkeley National Laboratory, Berkeley, CA, United States, [3] Department of Integrative Biology, University of California, Berkeley, Berkeley, CA, United States, [4] Embrapa Amazônia Oriental, Belém, Brazil, [5] Environmental Sciences Division and Climate Change Science Institute, Oak Ridge National Laboratory, Oak Ridge, TN, United States, [6] Earth and Environmental Sciences Division, Los Alamos National Laboratory, Los Alamos, NM, United States, [7] Pacific Northwest National Laboratory, Richland, WA, United States, [8] Department of Geography, University of California, Berkeley, Berkeley, CA, United States

OPEN ACCESS

Edited by:
Sebastian Leuzinger,
Auckland University of Technology,
New Zealand

Reviewed by:
Howard Scott Neufeld,
Appalachian State University,
United States
Mario Bretfeld,
University of Wyoming, United States

***Correspondence:**
Bruno O. Gimenez
bruno.oliva.gimenez@gmail.com

[†]These authors have contributed equally to this work

Specialty section:
This article was submitted to Plant Physiology, a section of the journal Frontiers in Plant Science

Received: 29 October 2018
Accepted: 07 June 2019
Published: 28 June 2019

Citation:
Gimenez BO, Jardine KJ, Higuchi N, Negrón-Juárez RI, Sampaio-Filho IdJ, Cobello LO, Fontes CG, Dawson TE, Varadharajan C, Christianson DS, Spanner GC, Araújo AC, Warren JM, Newman BD, Holm JA, Koven CD, McDowell NG and Chambers JQ (2019) Species-Specific Shifts in Diurnal Sap Velocity Dynamics and Hysteretic Behavior of Ecophysiological Variables During the 2015–2016 El Niño Event in the Amazon Forest. Front. Plant Sci. 10:830. doi: 10.3389/fpls.2019.00830

Current climate change scenarios indicate warmer temperatures and the potential for more extreme droughts in the tropics, such that a mechanistic understanding of the water cycle from individual trees to landscapes is needed to adequately predict future changes in forest structure and function. In this study, we contrasted physiological responses of tropical trees during a normal dry season with the extreme dry season due to the 2015–2016 El Niño-Southern Oscillation (ENSO) event. We quantified high resolution temporal dynamics of sap velocity (V_s), stomatal conductance (g_s) and leaf water potential (Ψ_L) of multiple canopy trees, and their correlations with leaf temperature (T_{leaf}) and environmental conditions [direct solar radiation, air temperature (T_{air}) and vapor pressure deficit (VPD)]. The experiment leveraged canopy access towers to measure adjacent trees at the ZF2 and Tapajós tropical forest research (near the cities of Manaus and Santarém). The temporal difference between the peak of g_s (late morning) and the peak of VPD (early afternoon) is one of the major regulators of sap velocity hysteresis patterns. Sap velocity displayed species-specific diurnal hysteresis patterns reflected by changes in T_{leaf}. In the morning, T_{leaf} and sap velocity displayed a sigmoidal relationship. In the afternoon, stomatal conductance declined as T_{leaf} approached a daily peak, allowing Ψ_L to begin recovery, while sap velocity declined with an exponential relationship with T_{leaf}. In Manaus, hysteresis indices of the variables $T_{leaf}-T_{air}$ and Ψ_L-T_{leaf} were calculated for different species and a significant difference ($p < 0.01$, $\alpha = 0.05$) was observed when the 2015 dry season (ENSO period) was compared with the 2017 dry season ("control scenario"). In some days during the 2015 ENSO event,

T_{leaf} approached 40°C for all studied species and the differences between T_{leaf} and T_{air} reached as high at 8°C (average difference: 1.65 ± 1.07°C). Generally, T_{leaf} was higher than T_{air} during the middle morning to early afternoon, and lower than T_{air} during the early morning, late afternoon and night. Our results support the hypothesis that partial stomatal closure allows for a recovery in Ψ_L during the afternoon period giving an observed counterclockwise hysteresis pattern between Ψ_L and T_{leaf}.

Keywords: tropical forests, sap velocity, stomatal conductance, direct solar radiation, vapor pressure deficit, leaf temperature, hysteresis

INTRODUCTION

Evapotranspiration by terrestrial ecosystems delivers an estimated 62,000 km^3 of water to the atmosphere every year, with the majority associated with plant transpiration (Jasechko et al., 2013). In the Amazon Basin, an estimated 25–50% of precipitation is recycled back to the atmosphere through forest transpiration (Eltahir and Bras, 1994; Chambers and Artaxo, 2017), with important implications for the interactions between the biosphere and atmosphere (Araújo et al., 2002; Negrón-Juárez et al., 2007). Under climate change scenarios, vegetation resilience will depend on the capacity to exploit water resources (Grossiord et al., 2017), and a mechanistic understanding of the water cycles from individual trees to landscape scales is necessary in order to predict changes in the forest structure (Chambers et al., 2014).

At the leaf level, transpiration flux is a function of vapor pressure deficit (VPD) between the leaf and the air and stomatal conductance (g_s), according to Fick's law of diffusion (Costa et al., 2010). Although numerous environmental factors influence g_s, net radiation, VPD and soil moisture are often considered the most important (Jarvis, 1976; Jones, 1998; Lloyd and Farquhar, 2008; Daloso et al., 2017). High leaf temperatures (T_{leaf}) and VPD are known to induce stomatal closure in order to minimize excessive water loss (Farquhar, 1978; Meinzer et al., 1993; Tinoco-Ojanguren and Pearcy, 1993; Oren et al., 1999b; McAdam et al., 2016; Brodribb et al., 2017). The degree of stomatal closure is a balancing act between preventing hydraulic damage while still allowing enough CO_2 influx for carbon fixation to avoid carbon-starvation (Adams et al., 2017). In addition, stomatal closure limits water lost through transpiration, and thereby indirectly regulates leaf temperatures. Given that the tropics have among the narrowest seasonal temperature range of any biome globally, they may be particularly sensitive to even small increases in temperature associated with climate change (Field et al., 2014). Indeed, rising temperature and VPD are environmental factors clearly associated with increased tree mortality in the tropics (McDowell et al., 2018), with more pronounced impacts during extreme drought events in the Amazon forest, such as the El Niño-Southern Oscillation (ENSO). This reinforces the importance of having more studies that investigate the effect of these variables (temperature and VPD) in the tropics, especially focusing on comparisons between two distinct periods, such as normal years (control scenario) and years with ENSO. This kind of approach can be considered as a "natural experiment" and allow to expand our understanding of the coupling of tree water use (and concurrent carbon uptake) and the environmental factors that affect stomatal conductance – solar radiation, CO_2, air temperature, leaf temperature and humidity.

The water potential gradient that regulates water movement through trees is anchored by soil moisture availability on one end, and atmospheric moisture availability VPD on the other. VPD is indirectly estimated from measurements of relative humidity (R_H) and air temperature (T_{air}) using micrometeorological sensors (Ewers and Oren, 2000). However, as T_{leaf} and T_{air} can differ by several degrees, the use of T_{leaf} instead of T_{air} to calculate VPD (ΔVPD) results in a more accurate representation of the true water vapor pressure gradient between the substomatal cavity and the boundary layer of the air near the leaf surface (Ewers and Oren, 2000). Therefore, T_{leaf} measurements are vital for better interpretation of plant hydraulic responses to environmental drivers in order to develop more accurate earth system models (ESMs) (Michaletz et al., 2016). However, sap velocity, T_{leaf} and environmental drivers are rarely measured together, especially in the tropics where the canopy layers are often hard to access (Chave et al., 2005; Segura and Kanninen, 2005). Thus, the response of a plant's transpiration to changes in environmental and physiological conditions remains highly uncertain in ESMs (Jasechko et al., 2013).

In relation to environmental drivers, clockwise hysteresis patterns between sap flow and VPD have been reported with higher sap flow rates during the morning period relative to the afternoon (O'Brien et al., 2004; Zeppel et al., 2004; Zhang et al., 2014). In addition, a counterclockwise hysteresis pattern has been observed in tropical and temperate forests when sap flow is plotted as function of irradiance (O'Brien et al., 2004; Zeppel et al., 2004; Bretfeld et al., 2018; Brum et al., 2018). In the case of transpiration, it has been established that the hysteresis phenomena are influenced by the temporal lag between solar radiation, which tends to peak in the late morning to mid-day, and VPD which tends to peak in the early afternoon (O'Brien et al., 2004; Zeppel et al., 2004; Zhang et al., 2014; Novick et al., 2016). Also, hysteresis between sap flux and environmental drivers are influenced by the stored stem water and the time lag between basal sap velocity and upper canopy transpiration, as an effect of hydraulic capacitance and resistance (Phillips et al., 1997; Ward et al., 2012). However, coupled field observations of physiological and environmental variables that include not only diurnal sap velocity and environmental driving data, but also concurrent leaf level data such as g_s, T_{leaf} and Ψ_L has been very limited in the tropics. Yet such data, are needed to verify

the relationships between V_s and environmental/physiological drivers in tropical forests.

In this study, we present *in situ* field observations of environmental (direct solar radiation, T_{air} and VPD) and physiological (V_s, g_s, and Ψ_L) variables and their correlations with T_{leaf} during the 2015–2016 ENSO. In order to observe the interactions between physiological variables and fast changing environmental conditions, we collected high temporal frequency data (15–60 min) in two primary rainforest sites located in the Eastern (Santarém) and in the Central (Manaus) Amazon. Since the 2015–2016 ENSO event was the warmest period in the Amazon forest over the past 13 years (Fontes et al., 2018), we expected peak T_{leaf} to increase and subsequently hysteretic behavior of water use vs. T_{leaf} to become more pronounced. In this study, we explored the mechanisms that regulate tree transpiration and the diurnal hysteresis patterns between physiological and environmental variables to contrast different tree species responses to the extreme 2015 dry season (ENSO) and a normal 2017 dry season ("control scenario").

MATERIALS AND METHODS

Study Area

The field activities occurred in two sites near the cities of Manaus and Santarém, Brazil (**Supplementary Figure S1**). Near the city of Manaus, trees with leaves accessible from the K-34 walkup tower were selected for study. The 50-meter tall K-34 tower is located at the Reserva Biológica do Cuieiras, also known as ZF-2, and contains roughly 22,000 ha adjacent to extensive areas of undisturbed tropical forest (Araújo et al., 2002). The mean value of rainfall is ∼2,500 mm year^{-1} with the driest months of the year concentrated from July to September (Araújo et al., 2002). Field data were collected at the K-34 tower site between July 01, 2015 and December 01, 2017.

Near the city of Santarém, four trees near the K-67 triangle tower were selected for study, located in the Tapajós National Forest with approximately 527,000 ha near the Santarém-Cuiabá highway (BR-163). The K-67 tower is located ∼6 km west of the BR-163 and ∼6 km east of Tapajós river, in an area of largely contiguous forest from north to south (Hutyra et al., 2007). The site receives ∼2,000 mm year^{-1} of rainfall and has a five-month dry season from mid-July to mid-December (Saleska et al., 2003; Wu et al., 2017). In Santarém, field data were collected during the period of April 01, 2016 to December 31, 2016.

Species Selection

Different species were selected in a plateau area of Tapajós National Forest (Santarém) and Reserva Biológica do Cueiras (ZF-2 – Manaus) (eight species in total; **Table 1**). Tree selection criteria were based on the proximity of the crowns to the two canopy access towers (K-34 and K-67). This approach enabled measurement of physiological variables including sap velocity at breast height, T_{leaf}, g_s, and Ψ_L from leaves at the top of the crowns, together with environmental variables including direct solar radiation, T_{air}, and R_H above the canopy (**Supplementary Figure S2**).

Sap Velocity (V_s) Measurements

One heat pulse sap velocity sensor (SFM1, ICT international®) was installed per tree near breast height (DBH) following the protocols previously described by Christianson et al. (2017). The SFM1 sensor consists of a heater and two temperature-sensing probes to determine sap velocity (cm h^{-1}) at 0.75 cm depth in the stem using the heat ratio method (Burgess et al., 2001; Green et al., 2003; Steppe et al., 2010). The heater needle was configured to emit a 20 Joule pulse of thermal energy every 15 min (sap heat ratio measurements for 5 min 32 s following the pulse). Biophysical characteristics (diameter and bark thickness) for each tree were used as input into the Sap Flow Tool version 1.4.1 (Phyto-IT®) to calculate sap velocity from raw data downloaded from the SFM1 sensors in the field.

The heat pulse method can be used for accurate measurements of sap flow (Lambers et al., 2008), but this method is unable to measure low rates due to its inability to distinguish heat-pulse velocities below a threshold velocity of 3–4 cm h^{-1} (Green et al., 2003). The probe spacing is also an important parameter and the sap velocity (V_s) is dependent upon the exact distance between needles as the following equation shows:

$$V_S = \frac{k}{x}\ln\left(\frac{v_1}{v_2}\right) * 3600 \text{ cm hr}^{-1} \quad (1)$$

where: k is the thermal diffusivity of wet wood; x is the distance between the heat source (heater) and temperature sensors; v_1 and v_2 are the increases in temperature (from ambient) at equidistant points downstream and upstream from the heater.

In this study, we used the factory default setting of 5 mm of needle spacings, as recommended by the manufacturer (Burgess and Downey, 2014), using a metal drill guide to ensure equidistant sensor placing. This 5 mm spacing is suitable to a theoretical maximum of 54 cm h^{-1} (Burgess and Downey, 2014).

It should be noted that following the protocols of 5 mm probe spacing of the SFM1 sensors, it is possible that the instrumental maximum was reached at relatively modest flows (16 cm h^{-1} for *Pouteria anomala* for example) on some days. Other available methods to estimate sap flow like the thermal dissipation method and the heat field deformation also underestimate V_s, where the error tends to increase with further increases in V_s (Steppe et al., 2010). However, evidence that the maximum observed V_s was not due to a sensor saturation includes: (1) different maximum values of V_s between species (plateau in the scatter plots); (2) the state theoretical maximum of 54 cm h^{-1} of the ICT user manual; and (3) on the same trees (Grossiord et al., under review) found no statistical difference between sap velocities determined by ICT and Granier sensors.

T_{leaf}, T_{air}, VPD and Direct Solar Radiation Measurements

To measure T_{leaf}, a single infrared radiometer sensor (IRR SI-111 analogic for the species *P. anomala*, *Pouteria erythrochrysa*, and *Couepia longipendula* or IRR SI-131 digital for the species *Eschweilera cyathiformis*, *Erisma uncinatum*, *Lecythis* sp. and *Chamaecrista xinguensis*, Apogee®) was positioned from the tower's structure with the field of view targeting the top of

TABLE 1 | List of tree species instrumented with sap velocity and T_{leaf} sensors in Manaus and Santarém.

Site	Tree species	Family	DBH (cm)	Height (m)	IRR viewing height (m)	IRR viewing angle	T_{leaf} target area (m^2)
Manaus K-34	**Eschweilera cyathiformis* S.A.Mori	Lecythidaceae	14.3	19.8	3.0	25°	2.41
Manaus K-34	***Pouteria anomala* (Pires) T.D.Penn.	Sapotaceae	35.3	31.0	0.2	10°	0.02
Manaus K-34	***Pouteria erythrochrysa* T.D.Penn.	Sapotaceae	36.5	29.3	0.2	10°	0.02
Manaus K-34	***Couepia longipendula* Pilg.	Chrysobalanaceae	28.1	23.9	0.6	10°	0.19
Santarém K-67	*Erisma uncinatum* Warm.	Vochysiaceae	94.8	39.2	6.5	54°	49.03
Santarém K-67	*Lecythis* sp. Loefl.	Lecythidaceae	81.1	36.4	6.7	63°	18.13
Santarém K-67	*Chamaecrista xinguensis* (Ducke) H.S.Irwin & Barneby	Fabaceae	75.3	29.5	6.2	58°	65.44
Santarém K-67	**Manilkara* sp. Adans.	Sapotaceae	40.0	30.0	–	–	–

*Also, are shown the tree family, DBH, tree height, IRR viewing height, IRR viewing angle, and T_{leaf} target area. *Species with diurnal measurements of g_s. **Species with diurnal measurements of Ψ_L.*

individual tree crowns (one IRR sensor per tree). Five-min averages of T_{leaf} were recorded using a CR-3000 (Campbell Scientific® for the SI-111 sensors) and EM-50 (Decagon® for the SI-131 sensors) dataloggers. The sensors were positioned with the viewing heights and viewing angles listed in **Table 1**. The field of view of each sensor (T_{leaf} target area) was calculated using the IRR calculator available in the website[1]. To validate the infrared radiometer sensors installed on the two sites, T_{leaf} measurements were made using Teflon insulated type T thermocouples (OM-CP-OCTTEMP-A Nomad®, Omega Engineering) directly attached to the abaxial side of the leaf using a breathable white tape and configured to register measurements every 15 s (**Supplementary Figure S3**). In addition, in Manaus direct solar radiation (W m^{-2}) with 5-min averages were collected at 35.0 m above the canopy using a SPN1-Sunshine Pyranometer (Delta-T Devices®). T_{air} and R_H data were obtained using a thermohygrometer (HC2S3, Campbell Scientific®) installed above the canopy at 51.1 m height on the K-34 tower structure.

In this study, a more accurate physiological approach to estimate VPD was applied. The Tetens equation was used to calculate the saturation vapor pressure of the air (e_o) using the variables air temperature (T_{air}) and relative humidity of the air (RH_o) (Eq. 2). To estimate the saturation vapor pressure inside the substomatal chamber (e_i) the Tetens equation was also used replacing T_{air} by T_{leaf} (Eq. 3). The relative humidity inside the substomatal cavity (RH_i) was assumed to be equal to 1 as demonstrated by many studies (Ward and Bunce, 1986; Buckley et al., 2017; Cernusak et al., 2018). With these variables it was possible to estimate the VPD difference between the substomatal chamber ($e_i \times RH_i$) and the atmosphere ($e_o \times RH_o$) (Eq. 4).

$$e_o = 0.611 \times 10^{\left(\frac{7.5\ x\ Tair}{Tair+237.3}\right)} \quad (2)$$

$$e_i = 0.611 \times 10^{\left(\frac{7.5\ x\ Tleaf}{Tleaf+237.3}\right)} \quad (3)$$

$$\Delta VPD = (e_i \times RH_i) - (e_o \times RH_o) \quad (4)$$

where: ΔVPD is the leaf-to-air water VPD (kPa); e_o is the air saturated water vapor pressure (kPa); e_i is the saturated water vapor pressure inside the substomatal chamber (kPa); RH_i is the relative humidity inside the substomatal cavity which is assumed to be equal to 1. RH_o is the relative humidity of the air near the leaf surface (expressed as a decimal); T_{leaf} is the leaf temperature in °C and T_{air} is the air temperature in °C.

Stomatal Conductance (g_s) Measurements

Diurnal observations of g_s were made on upper canopy leaves accessible from the walkup towers (K-34 in Manaus and a walkup tower 1 km from the K-67 triangle tower in Santarém). In Manaus, diurnal patterns of g_s were measured from individual leaves at the top the main crown near the towers from 6:00 to 18:00 using a Li-Cor 6400 XT portable photosynthesis system (Li-Cor, Lincoln®, NE, United States). g_s measurements on individual leaves were made for 10 min using Li-Cor 6400 XT. The CO_2 reference concentration was held constant at 400 μmol mol^{-1}. T_{block} and photosynthetically active radiation values were set every 15 min to match environmental conditions. Using the Li-Cor 6400 XT we set the T_{block} to achieve a target T_{leaf}, based on the infrared radiometers measurements recorded in the CR-3000 datalogger which have a screen that makes possible real time data reads without a computer. In Santarém, g_s measurements on individual leaves were made every 2 min using the SD-1 leaf porometer system (Decagon Devices®, WA, United States) throughout the day.

Leaf Water Potential (Ψ_L) Measurements

In Manaus Ψ_L data were collected from three trees together with T_{leaf} measurements (**Table 1**) to access potential diurnal hysteresis patterns similar to those observed with sap velocity, g_s, T_{air}, T_{leaf}, and ΔVPD. Hourly Ψ_L measurements (6:00 to 18:00 – 12 h) of healthy leaves without noticeable condensation on the surface of *P. anomala*, *P. erythrochysa*, and *C. longipendula* were performed in Manaus using a pressure chamber instrument (Model 1000, PMS Instrument Company®) connected to a high-pressure nitrogen cylinder. Small branches from the upper tree crowns were removed and a single leaf per tree was used to measure Ψ_L. The canopy position of each tree was also classified following the crown illumination index proposed by

[1]https://www.apogeeinstruments.com/irr-calculators/

Synnott (1979) (**Supplementary Table S1**). In this study, the leaf water potential measurements were performed in a single day of September during both 2015 and 2017 dry season.

Data Analysis

Data were analyzed using IGOR Pro® version 6.3 (WaveMetrics, Inc., United States) and R v. 3.0.2 (R Development Core Team, 2013) software packages. In Manaus, 4-month time series (August to November) were plotted to observe the correlations between T_{leaf} and T_{air} during the 2015 dry season (ENSO). Additionally, the two-dimensional kernel density function (*kde2d*) was used to observe potential offsets between T_{leaf} and T_{air} during the 2015 dry season. In Manaus, the 2015 dry season (ENSO period) was compared with the 2017 dry season ("control scenario") using hysteresis indexes (H_{index}) of the normalized values of T_{leaf}, T_{air}, and Ψ_L for the species *P. anomala*, *C. longipendula*, and *P. erythrochrysa*. For the normalization of each variable the min-max feature scaling method was used to standardize the range of the raw data. Hysteresis indices were calculated using the shoelace formula (Eq. 5; Braden, 1986), and a paired *t*-test was performed ($\alpha = 0.05$) to intercompare the H_{index} of the species between the 2015 and 2017 dry seasons. The H_{index} is a measure of the size of the hysteresis loop and enables quantitative comparisons of hysteresis behaviors during, for example, two contrasting periods like El Niño and regular season.

$$A = \frac{1}{2}\left|\sum_{i=1}^{n} x_i y_{i+1} + x_n y_1 - \sum_{i=1}^{n} x_i y_{i+1} - x_n y_1\right| \quad (5)$$

where: A is the area of the polygon, n is the number of sides of the polygon, and (x_i, y_i), $i = 1, 2, \ldots, n$ are the vertices (or "corners") of the polygon.

Additionally, normalized sap velocity and T_{leaf} hysteresis parameters of the species *E. cyathiformis*, *P. anomala*, and *P. erythrochysa* were compared separating the morning and afternoon/night periods during both 2015 and 2017 dry seasons (ENSO and regular season). In the morning period sigmoidal curves were fitted using 15 min interval data of the variables V_s and T_{leaf}. The statistical parameters of the sigmoidal curves were used to compare the ENSO and the regular season between species. The same approach was done to compare the afternoon/night period of the variables V_s and T_{leaf} but using power curves instead of sigmoidal functions.

RESULTS

V_s, T_{leaf}, and ΔVPD

Representative four-day time series of V_s as function of T_{leaf} and ΔVPD for *E. cyathiformis* in Manaus and V_s as function of T_{leaf} for *Lecythis* sp. in Santarém are presented in **Figure 1**. Despite expectations of a significant delay due to the large vertical distance between the observations of V_s and T_{leaf}, the two variables tightly track each other, during the day and night (**Figures 1A,E**). Additionally, normalized time series of V_s and T_{leaf} of six trees during a two-month period also show this tightly temporal track (**Supplementary Figure S4**). Moreover, temporal similarities were also graphically observed for the variables V_s and ΔVPD (**Figure 1B**).

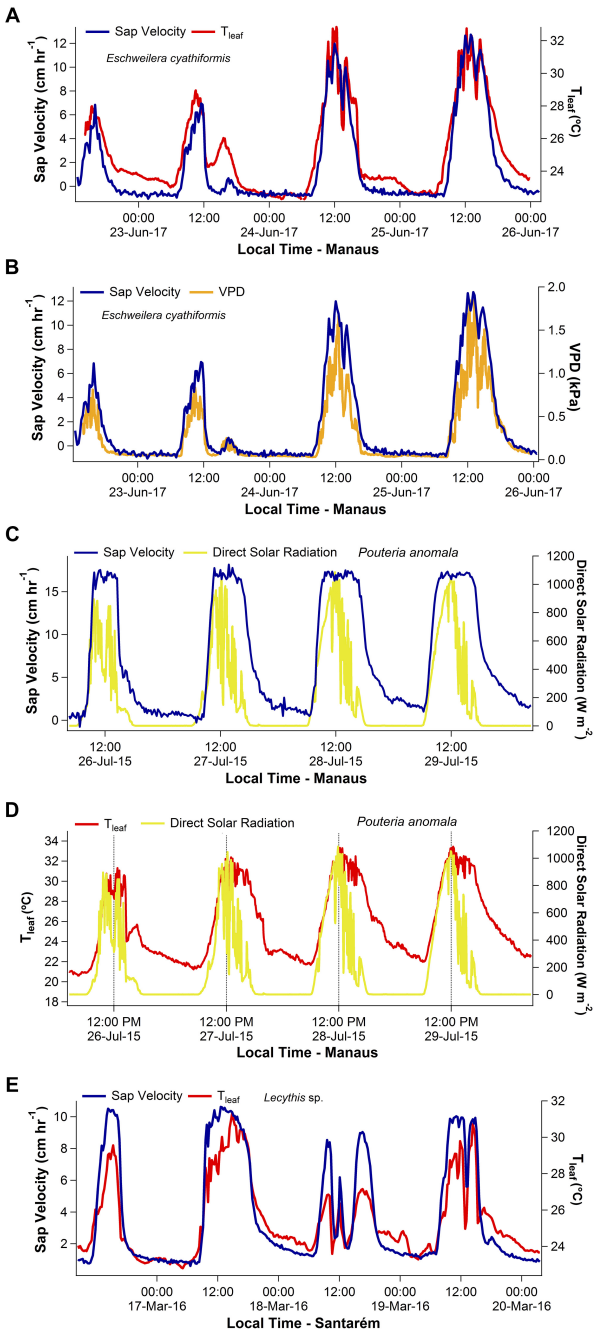

FIGURE 1 | Four-day time series showing the daily patterns of sap velocity (V_s), leaf temperature (T_{leaf}), and vapor pressure deficit (ΔVPD) for the species *Eschweilera cyathiformis*, *Pouteria anomala*, and *Lecythis* sp. Example of temporal similarities between V_s and T_{leaf} are shown in **(A,E)**. Temporal similarities were also observed for V_s and ΔVPD **(B)**. A temporal decoupling during the afternoon period was observed between V_s and direct solar radiation **(C)**. The contrasting patterns of direct solar radiation and T_{leaf} are also shown in **(D)**.

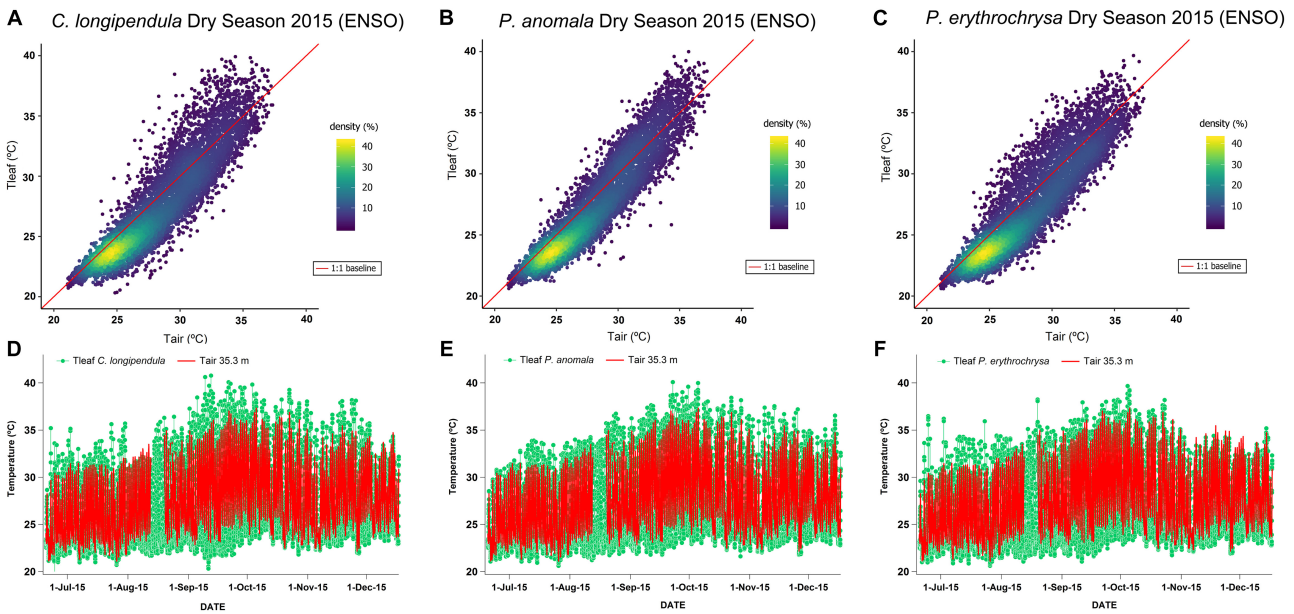

FIGURE 2 | Relationship between T_{leaf} and T_{air} for the species *C. longipendula*, *P. anomala*, and *P. erythrochrysa* during the 2015 ENSO dry season (August to November) near K-34 tower (Manaus). The scatter plot using the kernel density method allowed to visualize that the observations between T_{leaf} and T_{air} overlaps at maximum rates around 25°C of temperature (40% of density), with the majority of T_{leaf} values lower than T_{air} **(A–C)**. During the months of September and October of 2015, T_{leaf} reached, in some days, more than 40°C for all studied species **(D–F)**. In general, during the 2015 ENSO, maximum values of T_{leaf} for all species were higher than maximum values of T_{air}. However, during some days at the end of the 2015 dry season, T_{air} was higher than T_{leaf} for the species *C. longipendula* and *P. erythrochrysa* **(D,F)**.

Diurnal patterns of direct solar radiation differed from those of T_{leaf} in Manaus, especially during the afternoon period (**Figure 1D**). Direct solar radiation peaked about mid-day, then declined during the afternoon. In contrast, T_{leaf} and ΔVPD patterns peaked later, during the early afternoon and maintained high values until late afternoon even as solar radiation declined (**Figures 1A–E**). Thus, for Manaus, on average, a lag of 2 h and 22 min delay occurred between the peaks of direct solar radiation and T_{leaf}.

T_{leaf} and T_{air} Relations

The highest T_{leaf} values during the ENSO in the year of 2015 (2015 dry season – August to November) were observed during the months of September and October (**Figure 2**). On some days during the 2015 dry season, the differences between T_{leaf} and T_{air} were close to 8°C for some species (average difference between T_{leaf} and T_{air} for all species: 1.65 ± 1.07°C). For the species *C. longipendula* (**Figure 2A**) the maximum observed T_{leaf} value was 40.78°C (September 12, 2015 – 11:30 local time) and the difference between T_{leaf} and T_{air} was on average 1.70 ± 1.20°C (maximum observed difference 7.43°C); for the species *P. anomala* (**Figure 2B**) the maximum observed T_{leaf} value was 40.09°C (September 22, 2015 – 15:30 local time) and the difference between T_{leaf} and T_{air} was in average 1.49 ± 0.92°C (maximum observed difference 7.26°C); for the species *P. erythrochrysa* (**Figure 2C**) the maximum observed T_{leaf} value was 39.67°C (October 4, 2015 – 13:30 local time) and the difference between T_{leaf} and T_{air} was in average 1.75 ± 1.06°C (maximum observed difference 6.39°C). At the end of the 2015 dry season (November), there were some days when T_{air} reached higher values compared to T_{leaf} for the species *C. longipendula* and *P. erythrochrysa* (**Figures 2D,F**). The 1:1 baseline presented in **Figures 2A–C** provides a reference to examine deviations of T_{leaf} from T_{air}, where the densest observations are between 23 and 26°C with the majority of T_{leaf} values lower than T_{air}. This pattern is observed during the night period, when the lowest T_{air} and T_{leaf} values are recorded. In addition, hysteresis patterns between T_{leaf} and T_{air} were observed for the species *P. anomala*, *C. longipendula*, and *P. erythrochrysa* in Manaus during the 2015 and 2017 dry season (**Figure 3**). The area of the hysteresis loops (H_{index}) of *P. anomala*, *C. longipendula* and *P. erythrochrysa* during the 2015 dry season (ENSO) were statically larger ($p < 0.01$, $\alpha = 0.05$, *paired t*-test) than the 2017 dry season ("control scenario"; **Figure 3**). The H_{index} of the normalized variables T_{leaf} and T_{air} of the species *P. anomala*, *C. longipendula* and *P. erythrochrysa* during the 2015 dry season was, respectively: 0.0633; 0.0747; 0.0904. Moreover, the H_{index} calculated for *P. anomala*, *C. longipendula*, and *P. erythrochrysa* for the 2017 dry season was, respectively: 0.0355; 0.0406; 0.0523.

Using hourly averages for all the analyzed species it was possible to observe that generally T_{leaf} was higher than T_{air} from the middle of the morning period until the early afternoon in both the 2015 and 2017 dry seasons (**Figure 3**). In contrast, T_{air} was predominantly higher than T_{leaf} in the early morning, middle afternoon, and throughout the night in both the 2015 and 2017 dry seasons.

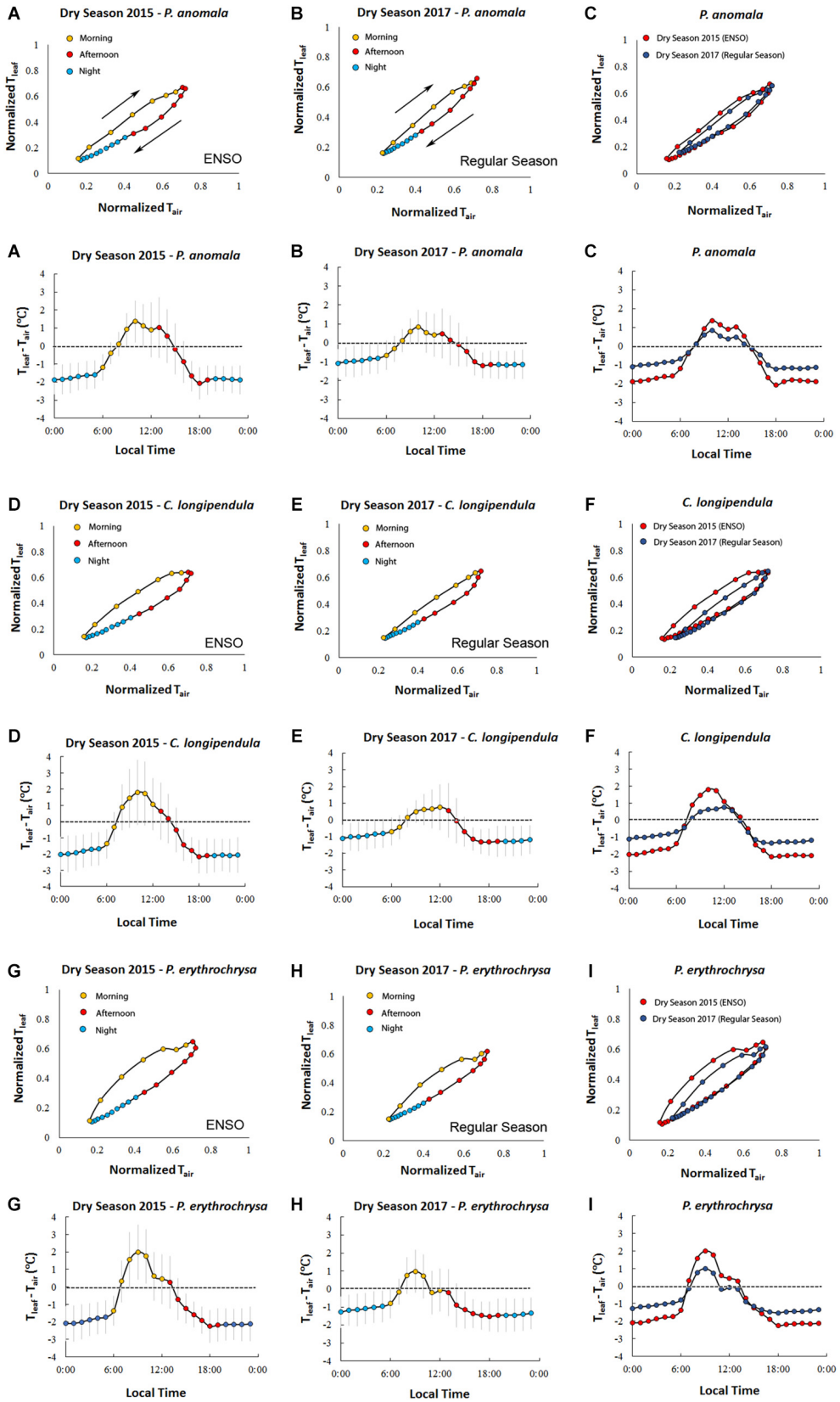

FIGURE 3 | Continued

FIGURE 3 | Hourly averages of T_{leaf} and T_{air} for the species *C. longipendula*, *P. anomala*, and *P. erythrochrysa* in Manaus site during the 2015 dry season (ENSO) and 2017 dry season ("control scenario"). The clockwise hysteresis pattern between T_{leaf} and T_{air} was observed for all the studied trees in Manaus. The orange dots represent the morning period (6:00–12:00), the red dots represent the afternoon period (13:00–19:00), and the blue dots represent the night period (20:00–5:00) **(A,B,D,E,G,H)**. A significant difference ($p < 0.01$) of T_{leaf} and T_{air} hysteresis loops (H_{index}) was observed when the 2015 dry season (ENSO period) was compared with the 2017 dry season ("control scenario") **(C,F,I)**. On average, in both 2015 and 2017 dry season, T_{leaf} was higher than T_{air} during the middle morning to early afternoon, and T_{air} was higher than T_{leaf} in the middle afternoon, night and early morning. The exception was for the species *P. erythrochrysa* where, on average, during the 2017 dry season T_{leaf} was higher than T_{air} only during the morning period (08:00–10:00) **(H)**.

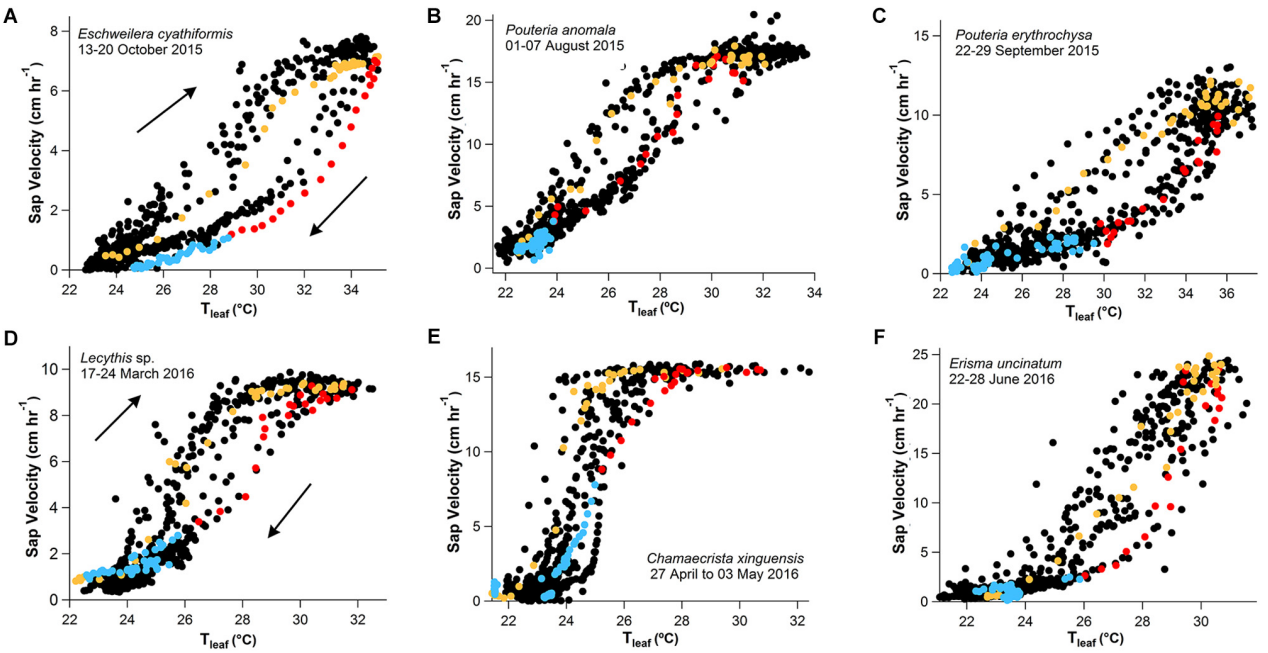

FIGURE 4 | One-week scatter plot data with 15-min observation intervals (black dots) showing the clockwise hysteresis of V_s and T_{leaf} for three trees of different species in Manaus **(A–C)**, and Santarém **(D–F)**. The hysteresis phenomenon is represented by a single day of data randomly selected, separated by morning (orange values, 6:00–14:00), afternoon (red values, 14:15–19:00), and nighttime (blue values, 19:15–5:45) periods.

V_s-T_{leaf}, $V_s-\Delta VPD$, and V_s-Direct Solar Radiation Diurnal Hysteresis

As an example, 1 week of V_s data were plotted as function of T_{leaf}, ΔVPD and direct solar radiation (**Figures 4**, **5**). The clockwise hysteresis in V_s-T_{leaf} and $V_s-\Delta VPD$ was evident with morning periods showing higher temperature sensitivities than afternoon and night periods and in this study is referred to as the "g_s effect" (**Figures 4**, **5**). In Manaus, the scatter plot of V_s-direct solar radiation revealed a counterclockwise hysteresis pattern, on the same day as the $V_s-\Delta VPD$ clockwise hysteresis (**Figure 5**). For the same direct solar radiation values, higher V_s values in the afternoon were observed relative to the morning period, and in this study this pattern is referred to as the "VPD effect."

V_s showed a sigmoid dependence on T_{leaf} and ΔVPD including a rapid increase, an inflection point, and a plateau. When V_s reached the maximum values for each species, it was insensitive to further increases in T_{leaf} and ΔVPD (**Figure 6** and **Supplementary Figure S5**). The sigmoid pattern was observed in all studied trees (**Supplementary Figure S5**), although the maximum V_s differed between species from 8 to 24 cm h^{-1}; detailed daily patterns of V_s-T_{leaf} revealed a sigmoid increase in V_s during the morning period followed by an exponential decrease in the afternoon and throughout the night (**Figure 6**). During the morning period the curve's maximum values (*max*) of the sigmoid function for the variables T_{leaf} and V_s were lower when the 2015 dry season (ENSO) was compared to the 2017 dry season (regular) for the species *E. cyathiformis* and *P. erythrochrysa* (**Figure 7**) (curve's maximum values (*max*): *E. cyathiformis* ENSO (2015): 0.6379 ± 0.017; *E. cyathiformis* regular dry season (2017): 0.9376 ± 0.028; *P. erythrochrysa* ENSO (2015): 0.6992 ± 0.029; *P. erythrochrysa* regular dry season (2017): 0.8837 ± 0.029). For the species *P. anomala* the *max* was statistically equal in both periods (curve's maximum values (*max*): *P. anomala* ENSO (2015): 0.7386 ± 0.082; *P. anomala* regular dry season (2017): 0.6960 ± 0.024). The inflection point (*xhalf*) of the sigmoidal curves also revealed different patterns between species. The *xhalf* values were lower for the species *E. cyathiformis* and *P. anomala* during the 2015 ENSO in comparison to the 2017 regular dry season (inflection point (*xhalf*): *E. cyathiformis* ENSO (2015): 0.3433 ± 0.006; *E. cyathiformis* regular dry season (2017): 0.5401 ± 0.006; *P. anomala* ENSO (2015): 0.2648 ± 0.024; *P. anomala* regular dry season (2017): 0.3423 ± 0.008. In

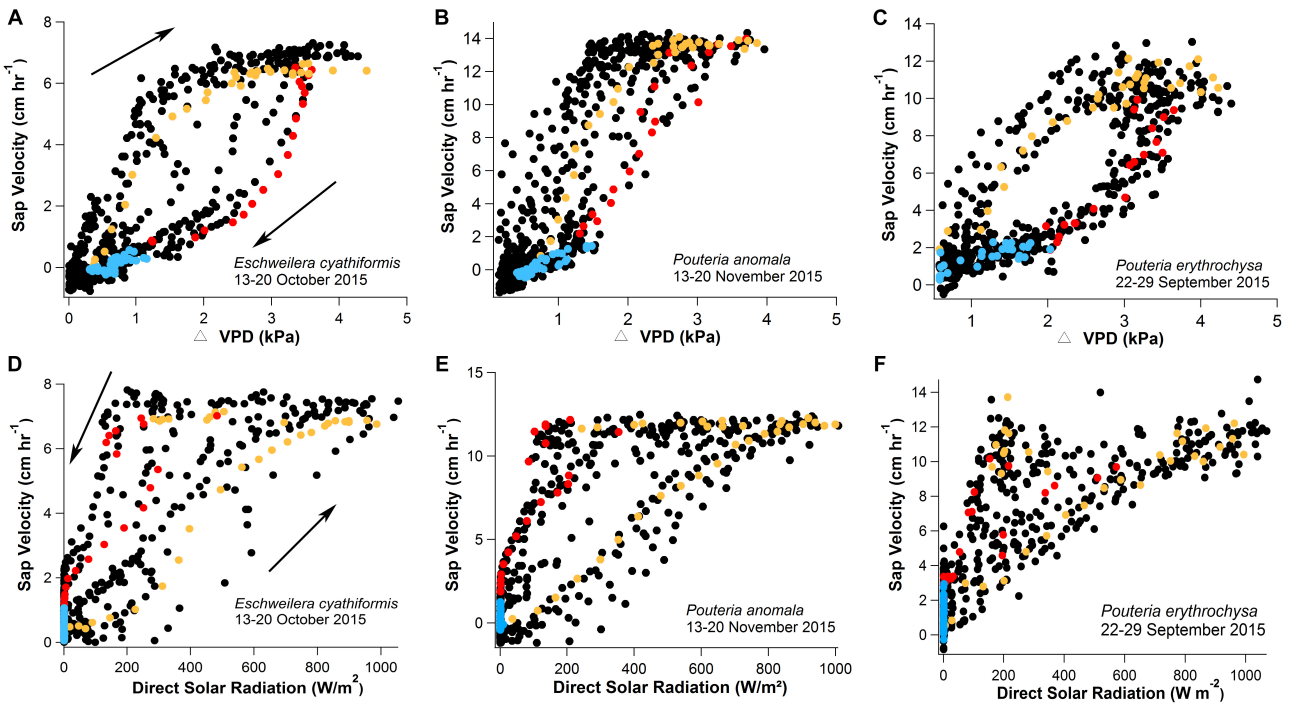

FIGURE 5 | One-week data with 15-min observation intervals showing clockwise hysteresis of V_s and ΔVPD **(A–C)** and counterclockwise hysteresis of V_s and direct solar radiation **(D–F)** for the species *E. cyathiformis*, *P. anomala*, and *P. erythrochrysa*. The clockwise and counterclockwise hysteresis phenomena were observed for each tree species using the data of the exact same week (black dots) and day (color dots) separated by morning (orange values, 6:00–14:00), afternoon (red values, 14:15–19:00), and nighttime periods (blue values, 19:15–5:45). During the morning period the V_s and ΔVPD clockwise hysteresis pattern showed higher temperature sensitivities compared to afternoon/night periods. In this study, this pattern was called the "g_s effect." During the afternoon period the counterclockwise hysteresis relationship between V_s and direct solar radiation showed higher temperature sensitivities compared to morning/night periods and it was called the "VPD effect." Both observed effects are a result of the Fick's law of diffusion (transpiration = g_s × VPD). For this interpretation, direct solar radiation was considered to have similar temporal patterns with g_s by circadian cycles.

contrast the *xhalf* value for the species *P. erythrochrysa* was higher during the ENSO in comparison to the 2017 regular dry season (inflection point (*xhalf*): *P. erythrochrysa* ENSO (2015): 0.4253 ± 0.012; *P. erythrochrysa* regular dry season (2017): 0.3064 ± 0.007). The statistical values of the power function during the afternoon/night period was relatively similar in both ENSO and regular dry season for the species *E. cyathiformis* and *P. anomala* (**Figure 7**). The exception was the species *P. erythrochrysa* which the exponent parameter (*pow*) were higher during ENSO compared to the 2017 regular dry season.

g_s-T_{leaf} and Ψ_L-T_{leaf} Diurnal Hysteresis

Clockwise hysteresis patterns were observed for g_s-T_{leaf} in Manaus and Santarém (**Supplementary Figure S6**). For the same T_{leaf}, the observed g_s values of *E. cyathiformis* and *Manilkara* sp. were greater during the morning period than the afternoon. The maximum observed g_s values occurred at a T_{leaf} of 33.3°C in Manaus and 32.6°C in Santarém (**Supplementary Figure S6**).

A counterclockwise hysteresis pattern was observed between Ψ_L and T_{leaf} (**Figure 8**). At the same T_{leaf} values, Ψ_L were more negative in the morning compared to the afternoon period. During September 2015 (peak of the El Niño) the H_{index} of the variables Ψ_L and T_{leaf} were significantly higher compared to September 2017 (regular dry season) ($p < 0.01$, $\alpha = 0.05$). The H_{index} calculated for the species *P. anomala*, *C. longipendula*, and *P. erythrochrysa* during the 2015 dry season was, respectively: 0.2379; 0.3116; 0.1605. Moreover, the H_{index} calculated for *P. anomala*, *C. longipendula*, and *P. erythrochrysa* for the 2017 dry season was, respectively: 0.0642; 0.1596; 0.0324.

DISCUSSION

Correlations Between Sap Velocity, T_{leaf}, T_{air} and ΔVPD

With a fine-scale measurement resolution of 15 min, temporal similarities between V_s and T_{leaf} were observed for all studied species. Delays between V_s-T_{leaf} and $V_s-\Delta VPD$, are expected due to the large differences in the heights of the measurements (basal sap velocity versus T_{leaf} in the upper canopy). This type of delays are related to the capacitance of the stems, where the evaporative demand in the branches near the crown are greater than the basal portions of the trunk, with an observed lag in the morning period between these two portions of the tree (Meinzer et al., 2003). Future research should aim to quantify these delays, using for example, simultaneous measurements of V_s at DBH height and V_s in the branches near the crown, as in Goldstein et al. (1998). At a small time resolution, similar results

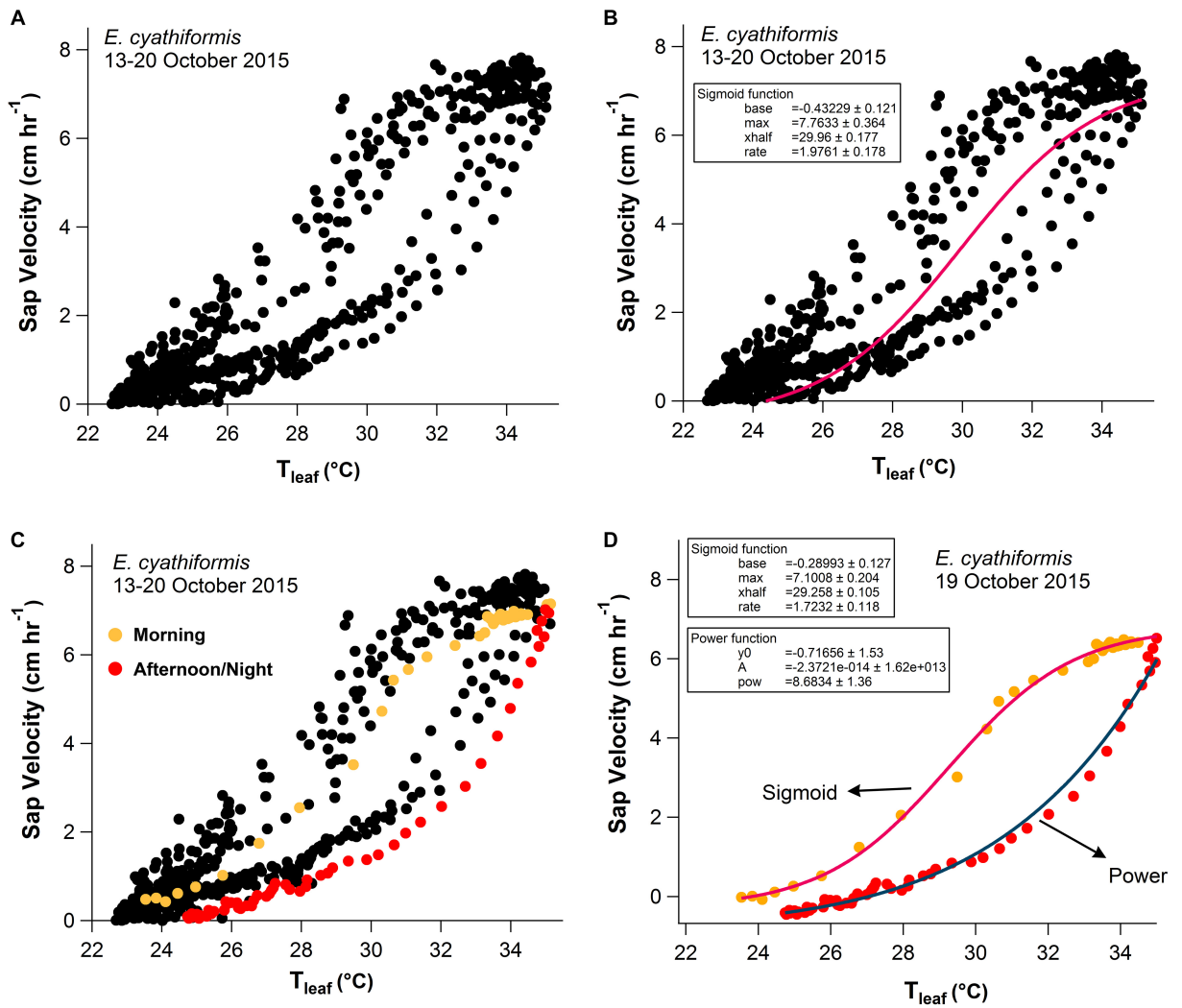

FIGURE 6 | One-week scatter plot data (13–20 October 2015) with 15-min observation intervals for *E. cyathiformis* **(A)**. The sigmoid function presented the best fit for one-week data of sap velocity (V_s) and T_{leaf} **(A,B)**. A single day data randomly selected, separated by two periods, presented different patterns **(C,D)**. During the morning period (orange dots 6:00–14:00) the sigmoid function presented the best fit $y = base + \left\{ \frac{max}{\left(1+exp\left(\frac{xhalf-x}{rate}\right)\right)} \right\}$ and during the afternoon/night period (red dots 14:15–5:45) the power function presented the best fit $y = y_0 + Ax^{pow}$ **(D)**.

were previously observed using Granier sap flow system and micrometeorological sensors in French Guiana (Granier et al., 1996), and North Carolina, United States (Oren et al., 1999a). At both sites (F. Guiana and N. Carolina), similar temporal correlations were observed between sap flow and VPD using a measurement resolution of 30 min. A recent study of Bretfeld et al. (2018) showed that V_s is largely in phase with VPD_{air} in an 80 year-old-forest which is similar to the observed results of this study. In addition, sigmoid patterns between V_s−VPD and V_s−T_{leaf} were also observed for all studied trees (**Supplementary Figure S5**), as also observed by O'Brien et al. (2004) in tropical species of Costa Rica, and da Costa et al. (2018) in the eastern Amazon. In this study, sap velocity displayed species-specific diurnal hysteresis patterns with a sigmoidal increase during the morning period and an exponential decrease during the afternoon/night period, with statistical differences between the extreme 2015 dry season (ENSO) and a normal 2017 dry season ("control scenario") (**Figures 6**, **7**).

Given the large diurnal T_{leaf} variation and the exponential dependence of VPD on T_{leaf} (Eqs 2, 3), changes in VPD during the daytime are largely driven by changes in T_{leaf} (Jackson et al., 1981; Ewers and Oren, 2000). The relationship between T_{leaf} and T_{air} represented by T_{leaf}−T_{air} offset is a good indicator of water stress in plants (Jackson et al., 1981). Over short time scales (e.g., 10 s) T_{leaf} is also partially related to the leaf mass per area (Michaletz et al., 2016), which can provide new insights about the water dynamics like capacitance. Low temperature values during rainstorms are associated with low VPD and high R_H in the Amazon forest (Moradi et al., 2016). Periods of days with the lowest observed V_s are related to the lowest observed values

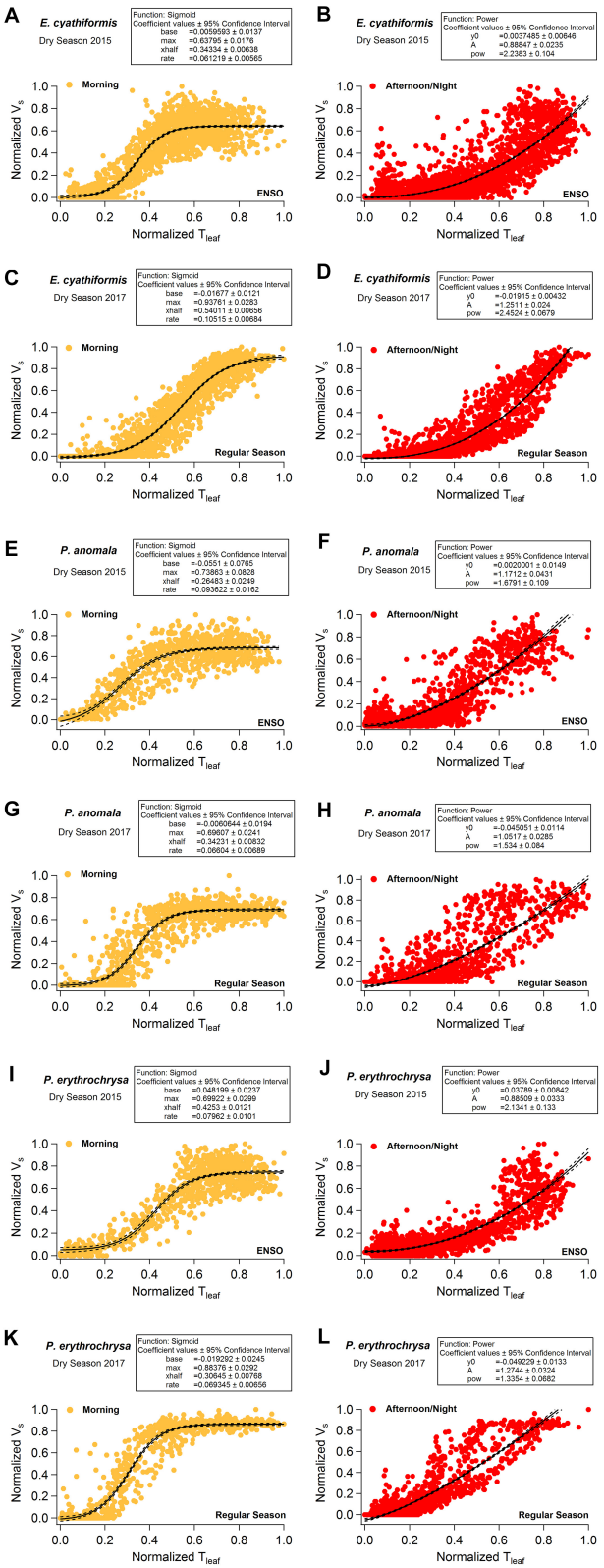

FIGURE 7 | Intercomparison of the hysteretic behavior of the normalized variables V_s and T_{leaf} for the species *E. cyathiformis*, *P. anomala*, and *P. erythrochrysa* during 2015 (ENSO) and 2017 (regular) dry seasons. During the morning period the curve's maximum values (*max*) of the sigmoid function for variables V_s and T_{leaf} were lower during the 2015 dry season (ENSO) in comparison to the 2017 dry season (Regular) for the species *E. cyathiformis* and *P. erythrochrysa* and statically equal for the species *P. anomala* **(A,C,E,G,I,K)**. The inflection point (*xhalf*) of the sigmoidal curves also revealed different patterns for the species when the 2015 dry season was compared to the 2017 dry season. The *xhalf* values were lower for the species *E. cyathiformis* and *P. anomala* during the 2015 ENSO in comparison to the 2017 regular dry season **(A,C,E,G)**. In contrast the *xhalf* value for the species *P. erythrochrysa* was higher during the ENSO in comparison to the 2017 regular dry season **(I,K)**. The statistical values of the power function during the afternoon/night period were relative similar in both ENSO and regular dry season for the species *E. cyathiformis* and *P. anomala* **(B,D,F,H)**. The exception was the species *P. erythrochrysa* which the exponent parameter (*pow*) where higher during ENSO compared to the 2017 regular dry season **(J,L)**.

of T_{leaf} and ΔVPD. This observation is consistent with previous studies in the Amazon where rain, cloud coverage, and reduced direct solar radiation were found to be the major factors that reduced xylem sap flow rates (Kunert et al., 2017). In addition, other researchers in tropical sites like Costa Rica found that significant leaf wetness also reduces sap flow by up to 28% by impacting VPD (Aparecido et al., 2016).

The positive nighttime V_s observed in Manaus and Santarém also apparently followed T_{leaf}, similar to that observed by Burgess and Dawson (2004) which found strong positive similarities between nighttime sap flow and VPD in *Sequoia sempervirens*. These observations of positive nighttime V_s in the first hours of the night are probably related to the capacitance of stem tissues and radial water transport (Steppe et al., 2012), as well as incomplete stomatal closure (Snyder et al., 2003; Barbour and Buckley, 2007; Dawson et al., 2007) which also allows trees to increase their water content through foliar water uptake (Eller et al., 2013). Another explanation for nighttime transpiration is the water outlet through lenticels, small pores on stem surfaces of many tropical tree species (Roth, 1981). However, it should be noted that no treatment was done to correct V_s for small potential offsets (less than 1 cm h^{-1} – lower scales) to estimate the standard deviation of V_s, and the possibility of positive nighttime water flow where, in this study, the V_s values are generally close to zero.

Hysteresis Patterns

In the current study, clockwise hysteresis patterns were observed for V_s−T_{leaf} and V_s−ΔVPD (**Figures 4**, **5**). Similar results were previously described for sap flow and VPD in tropical forests of Costa Rica (O'Brien et al., 2004) and in tropical secondary forests in Panama (Bretfeld et al., 2018), in temperate forests of Australia (Zeppel et al., 2004), in eastern Amazon trees (Brum et al., 2018) and in a grass-land ecosystem (Zhang et al., 2014). The observed hysteresis phenomenon for sap velocity has been described as a result of the temporal offset of g_s that tends to peak, in the tropics, during late morning to mid-day (10:30–12:00) (Slot and Winter, 2017a) (**Supplementary Figure S6**) and VPD that tends to peak in the early afternoon (13:00–14:30). The hysteresis phenomenon can also be visualized with variables T_{leaf} and direct solar radiation (irradiance). In normal conditions g_s

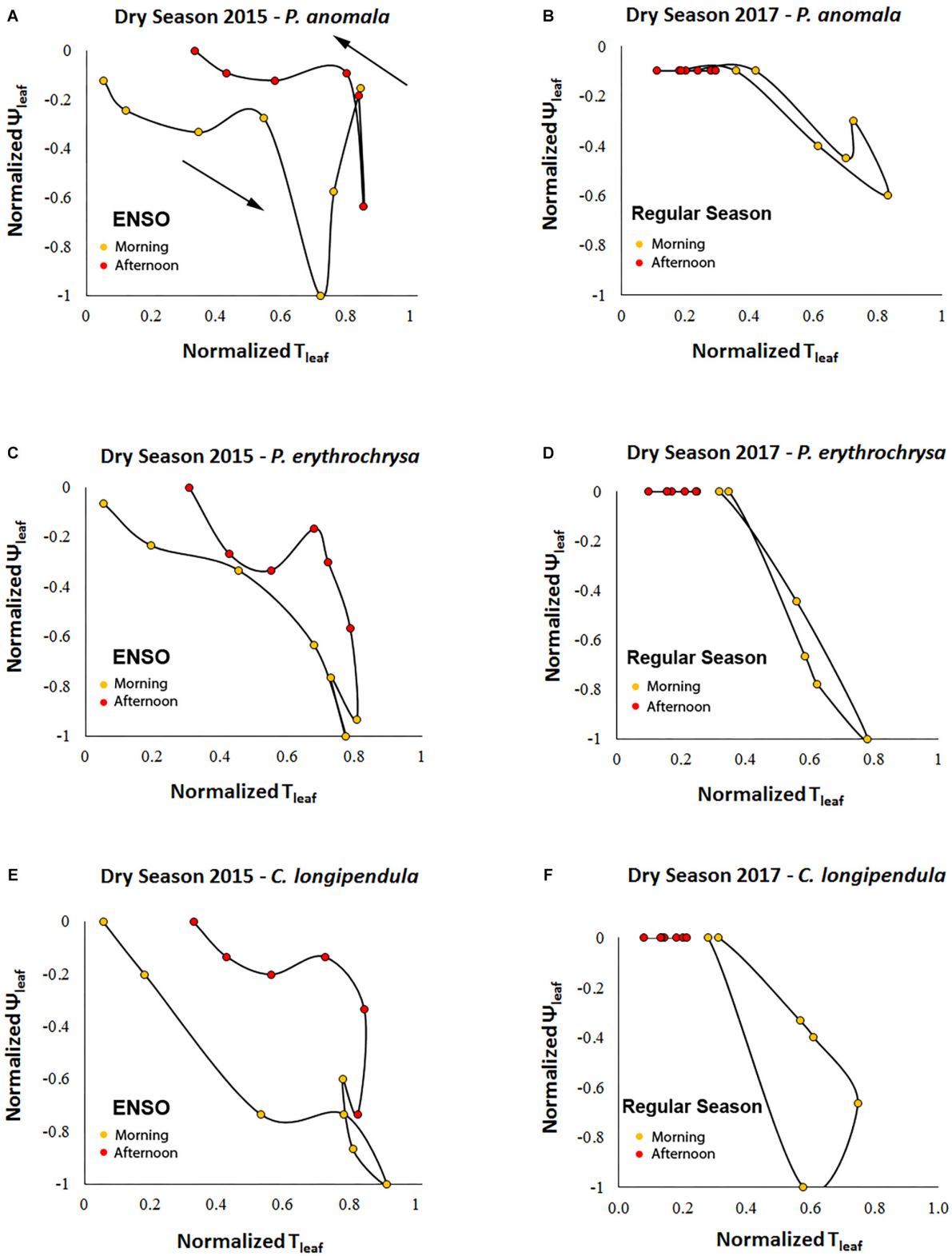

FIGURE 8 | Counterclockwise hysteresis of Ψ_L and T_{leaf} for the species *C. longipendula*, *P. anomala*, and *P. erythrochrysa* in Manaus during the 2015 and 2017 dry seasons. The stomata resistance acts to minimize the water loss during the afternoon periods given the observed counterclockwise pattern for Ψ_L–T_{leaf}. During September 2015 (peak of the El Niño) the H_{index} of the variables Ψ_L and T_{leaf} was significant higher **(A,C,E)** compared to September 2017 (regular dry season) ($p < 0.01$, $\alpha = 0.05$) **(B,D,F)**.

respond positively to irradiance (Hennessey and Field, 1991; Gorton et al., 1993; Motzer et al., 2005) and the temporal similarities between these two variables are supposed to be associated with circadian cycles (daily patterns), as demonstrated in some hysteretic behaviors of this study separating the morning, afternoon, and night periods.

In terms of temperature, g_s was found to reach a maximum at a T_{leaf} of 31–33°C, which relates with the optimum temperature for photosynthesis (T_{opt}) previously determined for many tropical species (Slot and Winter, 2017b). Interestingly, this T_{opt} range seems to match with the inflection point (*xhalf*) in the V_s-T_{leaf} hysteresis plots in Manaus (**Figures 4–7**). Thus, we speculate that it may be possible to determine T_{opt} using V_s-T_{leaf} diurnal hysteresis plots for individual trees. The observed inflection points patterns of V_s-T_{leaf} during the morning period for the species *E. cyathiformis*, *P. anomala,* and *P. erythrochrysa* (**Figure 7**) seems to be influenced by the canopy position and the resistance to drought once, in this study, species-specific shifts emerged when the 2015 ENSO was compared to the 2017 dry season. Additionally, the calculation of an index to quantify the hysteresis loops (H_{index}) was performed by this study, similar to a previous approach of Zuecco et al. (2016) which described hysteresis patterns of hydrological variables and runoff events. A quantitative comparison of hysteresis loops from a large number of species using an index approach would be a way of constraining ranges of hysteresis effects in models. Satellite observations revealed that September 2015 exhibited the warmest monthly averaged surface air temperature of any other month over the past 13 years in the Central Amazon (Fontes et al., 2018). These extreme temperatures also modified T_{leaf} patterns, as observed by this study (**Figure 3**). Higher T_{leaf} values were reflected in a significantly higher H_{index} for the variables $T_{leaf}-T_{air}$ and Ψ_L-T_{leaf} when the 2015 dry season (ENSO period) was compared to the 2017 dry season ("control scenario"). Even though H_{index} for V_s was not calculated in this study, we found species-specific shifts in diurnal sap velocity dynamics in both 2015 and 2017 dry seasons contradicting the expected higher values of transpiration during 2015 ENSO compared to other periods due to the high evaporative demand. Brum et al. (2018), for example, found significant differences in the H_{index} for transpiration between dry and wet seasons during the 2015–2016 ENSO in the Eastern Amazon. Nevertheless, the effect of g_s during drought events needs to be clarified because trees are expected to show a strong stomatal control under drought conditions, which would offset the expected increase in transpiration H_{index}. The higher T_{leaf} values compared to T_{air} during the middle morning to early afternoon observed by this study for the species *P. anomala*, *C. longipendula*, and *P. erythrochrysa* also contradicts with the expected decrease in T_{leaf} due the transpiration effect. One possible explanation for this pattern is the leaf flushing which is, in the Central Amazon, concentrated in the five driest months (Lopes et al., 2016). On this period, it is possible that the leaf photosynthesis apparatus and tissues aren't fully developed, reflecting directly in the g_s and transpiration patterns. Also, the increasing of light availability in the Amazon forest during the dry season can, maybe, exert an overriding effect in T_{leaf} patterns relative to the cooling effect of transpiration.

Changes in g_s are associated with changes in Ψ_L via their mutual effects on the balance between V_s and transpiration rates. Consistent with the clockwise hysteresis between V_s-T_{leaf} and $V_s-\Delta VPD$, a counterclockwise hysteresis pattern was observed between Ψ_L-T_{leaf}. At the same T_{leaf}, Ψ_L were more negative during morning than afternoon suggesting that partial stomatal closure in the afternoon allows the leaf to recover to less negative Ψ_L (**Figure 8**; Jarvis, 1976). The results suggest that during 2015–2016 ENSO the trees of this study located in a plateau area have a strong isohydric behavior, by reducing stomatal conductance in the warm afternoon periods in order to reduce transpiration rates, thereby minimizing the chances for embolism (Sade et al., 2012; Roman et al., 2015). The same process can be observed in the clockwise hysteresis between V_s-T_{leaf}, and $V_s-\Delta VPD$ where the partial stomatal closure in the afternoon period reduce the V_s rates compared to the morning (**Figures 4**, **5**). In this study this pattern was called the "g_s effect." It should be emphasized that the daily hysteresis patterns with the morning, afternoon and night periods separated by colors make it possible to observe both the "g_s effect" and "VPD effect" (**Figure 5**).

Interestingly, the counterclockwise hysteresis pattern of V_s-direct solar radiation is not driven by the partial stomatal closure in the late morning until the afternoon period, but by the high ΔVPD. At the same solar radiation intensity, higher V_s occurs during the afternoon relative to the morning and in this study was called the "VPD effect" (**Figure 5**). This observations suggests that partial stomatal closure in the afternoon can be offset by the effect of high ΔVPD in maintaining elevated transpiration rates under high afternoon temperatures, as previously shown in other ecosystems (O'Brien et al., 2004; Zeppel et al., 2004; Zhang et al., 2014; Novick et al., 2016; Bretfeld et al., 2018; Brum et al., 2018). Also, these results support recent findings that heat waves can be associated with sustained transpirational cooling as a key mechanism of thermotolerance (Drake et al., 2018). However, the mechanisms of transpiration cooling can be exceeded by the heat intensity during El Niño events, which increase tree mortality in the Amazon forest (Aleixo et al., 2019). Finally, the range of H_{index} for the variables T_{leaf} and T_{air} presented for the first time in this study, can be a useful tool to predict future impacts on tree mortality during extreme drought events in comparison to other periods.

The observed differences of the maximum V_s rates (curve's maximum values (*max*) of sigmoidal functions during the morning period – **Figure 7**)) between species can be related to the diameter of the vessels (Dünisch and Morais, 2002), wood density (Eller et al., 2018) and with the susceptibility to embolism (Lovisolo and Schubert, 1998). Tree height is also an important factor which influences sun exposure and therefore the temperature of the leaves and transpiration rates (Goldstein et al., 1998). In Manaus, *E. cyathiformis* was the thinnest and shortest studied tree with 14.3 cm of DBH and 19.8 m of height and was the tree with the lowest observed V_s rates

(~8 cm h^{-1}) during ENSO (**Figure 4**). In contrast, the *Pouteria* genus (*P. anomala* and *P. erythrochysa*) have large DBHs (35.3 cm and 36.5 cm) and high rates of V_s during ENSO (18 and 12 cm h^{-1}, respectively) (**Figure 4**). This is consistent with other studies where DBH, height and sap flow showed a positive correlation (Motzer et al., 2005). Likewise, the same correlations were observed in Santarém, where the larger DBHs showed the higher sap velocity. Also, the observed differences in curve's maximum values (*max*) of sigmoidal curves observed for V_s and T_{leaf} during ENSO period and the regular dry season (**Figure 7**), may be associated with the high range of functional traits and susceptibility to embolism of some trees in the Amazon forest along hydro-topographic gradients (Cosme et al., 2017; Oliveira et al., 2019). Other important issue is that mortality rates during droughts are substantially higher for large DBH's (Meakem et al., 2017), and maybe this is potentially aggravated by high transpiration rates and the crown exposure to the direct light. Another study of rain exclusion in the eastern Amazon by Rowland et al. (2015) support this observation. However, other factors are also involved since it has been shown that early-successional forests experienced more drought stress than trees in late-successional forests (Bretfeld et al., 2018). In fact, more studies are needed in the tropics, especially in the Amazon, due to the large diversity of terrestrial plants (Ter Steege et al., 2013), the wide range of functional traits and evolutionary strategies to avoid cavitation, carbon starvation, and other aspects related to drought which can modify T_{leaf} and V_s patterns.

CONCLUSION

For the first time in the Amazon forest, the quantitative differences and the hysteresis pattern between T_{leaf} and T_{air} were demonstrated and compared during the 2015 (ENSO) and 2017 ("control scenario") dry seasons. The relationship between T_{leaf} and T_{air} was significantly different between these two periods and, in general, T_{leaf} was higher than T_{air} during the middle morning to early afternoon. The use of the variable T_{leaf} together with T_{air} are extremely important to ecophysiological observations due to the differences in terms of magnitude and temporal patterns. Also, T_{leaf} is an important variable to estimate the true water vapor pressure gradient between the substomatal cavity and the boundary layer of the air near the leaf surface (ΔVPD). Moreover, sap velocity displayed species-specific diurnal hysteresis patterns that were strongly linked to g_s and VPD and reflected by changes in T_{leaf}. In the morning, g_s was linearly related to T_{leaf} and sap velocity displayed a sigmoidal relationship with T_{leaf}. In the afternoon, stomatal conductance declined as T_{leaf} approached a daily peak, allowing Ψ_L to begin recovery, while sap velocity declined with an exponential relationship with T_{leaf}. Hysteresis indices (T_{leaf} : T_{air} and T_{leaf} : Ψ_L) were much more pronounced during the ENSO event than during a typical dry season and varied between species, which reflects species-specific capacitance and tree hydraulic traits. Future research may address a new modeling approach using the magnitude of the hysteresis loops (H_{index}) to measure, for example, the intensity of the droughts and how it impacts plant communities. Finally, the hysteretic behavior of the transpiration separated by morning, afternoon and night periods is the key to understand the complexity of this process in a changing climate and improve the current models.

AUTHOR CONTRIBUTIONS

BG, KJ, RN-J, IS-F, CF, LC, JH, JC, NH, TD, and NM performed the experiments and analyzed the data. JC, NH, TD, and NM planned and designed the experiments. BG and KJ wrote the manuscript. CF, AA, JW, BN, CV, DC, GS, CK, and NM improved the manuscript.

FUNDING

This material is based upon work supported as part of the Next Generation Ecosystem Experiments-Tropics (NGEE-Tropics), as part of DOE's Terrestrial Ecosystem Science Program – Contract No. DE-AC02-05CH11231. Additional funding for this research was provided by the Coordenação de Aperfeiçoamento de Pessoal de Nível Superior (CAPES).

ACKNOWLEDGMENTS

The authors are thankful to the logistical and scientific support provided by the Laboratório de Manejo Florestal (LMF) and the Large-Scale Biosphere-Atmosphere Program (LBA) at the National Institute of Amazonian Research (INPA).

SUPPLEMENTARY MATERIAL

The Supplementary Material for this article can be found online at: https://www.frontiersin.org/articles/10.3389/fpls.2019.00830/full#supplementary-material

REFERENCES

Adams, H. D., Zeppel, M. J., Anderegg, W. R., Hartmann, H., Landhäusser, S. M., Tissue, D. T., et al. (2017). A multi-species synthesis of physiological mechanisms in drought-induced tree mortality. *Nat. Ecol. Evol.* 1, 1285–1291. doi: 10.1038/s41559-017-0248-x

Aleixo, I., Norris, D., Hemerik, L., Barbosa, A., Prata, E., Costa, F., et al. (2019). Amazonian rainforest tree mortality driven by climate and functional traits. *Nat. Clim. Change* 9, 384–388. doi: 10.1038/s41558-019-0458-0

Aparecido, L. M. T., Miller, G. R., Cahill, A. T., and Moore, G. W. (2016). Comparison of tree transpiration under wet and dry canopy conditions in a costa rican premontane tropical forest. *Hydrol. Process.* 30, 5000–5011. doi: 10.1002/hyp.10960

Araújo, A., Nobre, A., Kruijt, B., Elbers, J., Dallarosa, R., Stefani, P., et al. (2002). Comparative measurements of carbon dioxide fluxes from two nearby towers in a central amazonian rainforest: the manaus LBA site. *J. Geophys. Res. Atmos.* 107:8090. doi: 10.1029/2001JD000676

Barbour, M. M., and Buckley, T. N. (2007). The stomatal response to evaporative demand persists at night in *Ricinus communis* plants with high nocturnal

conductance. *Plant Cell Environ.* 30, 711–721. doi: 10.1111/j.1365-3040.2007.01658.x

Braden, B. (1986). The surveyor's area formula. *College Math. J.* 17, 326–337. doi: 10.2307/2686282

Bretfeld, M., Ewers, B. E., and Hall, J. S. (2018). Plant water use responses along secondary forest succession during the 2015–2016 El Niño drought in panama. *New Phytol.* 219, 885–899. doi: 10.1111/nph.15071

Brodribb, T. J., McAdam, S. A., and Carins Murphy, M. R. (2017). Xylem and stomata, coordinated through time and space. *Plant Cell Environ.* 40, 872–880. doi: 10.1111/pce.12817

Brum, M., Gutiérrez López, J., Asbjornsen, H., Licata, J., Pypker, T., Sanchez, G., et al. (2018). ENSO effects on the transpiration of eastern amazon trees. *Philos. Trans. R. Soc. B Biol. Sci.* 373:20180085. doi: 10.1098/rstb.2018.0085

Buckley, T. N., John, G. P., Scoffoni, C., and Sack, L. (2017). The sites of evaporation within leaves. *Plant Physiol.* 173, 1763–1782. doi: 10.1104/pp.16.01605

Burgess, S., and Downey, A. (2014). *SFM1 Sap Flow Meter Manual*. Armidale, NSW: ICT international Pty Ltd.

Burgess, S. S., Adams, M. A., Turner, N. C., Beverly, C. R., Ong, C. K., Khan, A. A., et al. (2001). An improved heat pulse method to measure low and reverse rates of sap flow in woody plants. *Tree Physiol.* 21, 589–598. doi: 10.1093/treephys/21.9.589

Burgess, S. S. O., and Dawson, T. E. (2004). The contribution of fog to the water relations of *Sequoia sempervirens* (D. Don): foliar uptake and prevention of dehydration. *Plant Cell Environ.* 27, 1023–1034. doi: 10.1111/j.1365-3040.2004.01207.x

Cernusak, L. A., Ubierna, N., Jenkins, M. W., Garrity, S. R., Rahn, T., Powers, H. H., et al. (2018). Unsaturation of vapour pressure inside leaves of two conifer species. *Sci. Rep.* 8:7667. doi: 10.1038/s41598-018-25838-2

Chambers, J., Davies, S., Koven, C., Kueppers, L., Leung, R., McDowell, N., et al. (2014). *Next Generation Ecosystem Experiment (NGEE) Tropics*. Berkeley, CA: Lawrence Berkeley National Laboratory.

Chambers, J. Q., and Artaxo, P. (2017). Biosphere-atmosphere interactions: deforestation size influences rainfall. *Nat. Clim. Change* 7, 175–176. doi: 10.1038/nclimate3238

Chave, J., Andalo, C., Brown, S., Cairns, M., Chambers, J., Eamus, D., et al. (2005). Tree allometry and improved estimation of carbon stocks and balance in tropical forests. *Oecologia* 145, 87–99. doi: 10.1007/s00442-005-0100-x

Christianson, D. S., Varadharajan, C., Christoffersen, B., Detto, M., Faybishenko, B., Gimenez, B. O., et al. (2017). A metadata reporting framework (FRAMES) for synthesis of ecohydrological observations. *Ecol. Inform.* 42, 148–158. doi: 10.1016/j.ecoinf.2017.06.002

Cosme, L. H., Schietti, J., Costa, F. R., and Oliveira, R. S. (2017). The importance of hydraulic architecture to the distribution patterns of trees in a central Amazonian forest. *New Phytol.* 215, 113–125. doi: 10.1111/nph.14508

Costa, M. H., Biajoli, M. C., Sanches, L., Malhado, A. C. M., Hutyra, L. R., da Rocha, H. R., et al. (2010). Atmospheric versus vegetation controls of amazonian tropical rain forest evapotranspiration: are the wet and seasonally dry rain forests any different? *J. Geophys. Res. Biogeosci.* 115:G04021. doi: 10.1029/2009JG001179

da Costa, A. C., Rowland, L., Oliveira, R. S., Oliveira, A. A., Binks, O. J., Salmon, Y., et al. (2018). Stand dynamics modulate water cycling and mortality risk in droughted tropical forest. *Glob. Chang. Biol.* 24, 249–258. doi: 10.1111/gcb.13851

Daloso, D. M., Medeiros, D. B., Anjos, L., Yoshida, T., Araújo, W. L., and Fernie, A. R. (2017). Metabolism within the specialized guard cells of plants. *New Phytol.* 216, 1018–1033. doi: 10.1111/nph.14823

Dawson, T. E., Burgess, S. S., Tu, K. P., Oliveira, R. S., Santiago, L. S., Fisher, J. B., et al. (2007). Nighttime transpiration in woody plants from contrasting ecosystems. *Tree Physiol.* 27, 561–575. doi: 10.1093/treephys/27.4.561

Drake, J. E., Tjoelker, M. G., Vårhammar, A., Medlyn, B. E., Reich, P. B., Leigh, A., et al. (2018). Trees tolerate an extreme heatwave via sustained transpirational cooling and increased leaf thermal tolerance. *Glob. Chang. Biol.* 24, 2390–2402. doi: 10.1111/gcb.14037

Dünisch, O., and Morais, R. R. (2002). Regulation of xylem sap flow in an evergreen, a semi-deciduous, and a deciduous meliaceae species from the amazon. *Trees* 16, 404–416. doi: 10.1007/s00468-002-0182-6

Eller, C. B., Barros, F. V., Bittencourt, P. R. L., Rowland, L., Mencuccini, M., and Oliveira, R. S. (2018). Xylem hydraulic safety and construction costs determine tropical tree growth. *Plant Cell Environ.* 41, 548–562. doi: 10.1111/pce.13106

Eller, C. B., Lima, A. L., and Oliveira, R. S. (2013). Foliar uptake of fog water and transport belowground alleviates drought effects in the cloud forest tree species, *Drimys brasiliensis* (winteraceae). *New Phytol.* 199, 151–162. doi: 10.1111/nph.12248

Eltahir, E. A., and Bras, R. L. (1994). Precipitation recycling in the Amazon basin. *Q. J. R. Meteorol. Soc.* 120, 861–880. doi: 10.1002/qj.49712051806

Ewers, B. E., and Oren, R. (2000). Analyses of assumptions and erros in the calculation of stomatal conductance from sap flux measurements. *Tree Physiol.* 20, 579–589. doi: 10.1093/treephys/20.9.579

Farquhar, G. (1978). Feedforward responses of stomata to humidity. *Funct. Plant Biol.* 5, 787–800. doi: 10.1071/PP9780787

Field, C. B., Barros, V. R., Mach, K., and Mastrandrea, M. (2014). *Climate Change 2014: Impacts, Adaptation, and Vulnerability*. Cambridge: Cambridge University Press.

Fontes, C. G., Dawson, T. E., Jardine, K., McDowell, N., Gimenez, B. O., Anderegg, L., et al. (2018). Dry and hot: the hydraulic consequences of a climate change–type drought for amazonian trees. *Philos. Trans. R. Soc. B Biol. Sci.* 373:20180209. doi: 10.1098/rstb.2018.0209

Goldstein, G., Andrade, J., Meinzer, F., Holbrook, N., Cavelier, J., Jackson, P., et al. (1998). Stem water storage and diurnal patterns of water use in tropical forest canopy trees. *Plant Cell Environ.* 21, 397–406. doi: 10.1046/j.1365-3040.1998.00273.x

Gorton, H. L., Williams, W. E., and Assmann, S. M. (1993). Circadian rhythms in stomatal responsiveness to red and blue light. *Plant Physiol.* 103, 399–406. doi: 10.1104/pp.103.2.399

Granier, A., Huc, R., and Barigah, S. (1996). Transpiration of natural rain forest and its dependence on climatic factors. *Agric. For. Meteorol.* 78, 19–29. doi: 10.1016/0168-1923(95)02252-X

Green, S., Clothier, B., and Jardine, B. (2003). Theory and practical application of heat pulse to measure sap flow. *Agron. J.* 95, 1371–1379. doi: 10.2134/agronj2003.1371

Grossiord, C., Sevanto, S., Borrego, I., Chan, A. M., Collins, A. D., Dickman, L. T., et al. (2017). Tree water dynamics in a drying and warming world. *Plant Cell Environ.* 40, 1861–1873. doi: 10.1111/pce.12991

Hennessey, T. L., and Field, C. B. (1991). Circadian rhythms in photosynthesis: oscillations in carbon assimilation and stomatal conductance under constant conditions. *Plant Physiol.* 96, 831–836. doi: 10.1104/pp.96.3.831

Hutyra, L. R., Munger, J. W., Saleska, S. R., Gottlieb, E., Daube, B. C., Dunn, A. L., et al. (2007). Seasonal controls on the exchange of carbon and water in an Amazonian rain forest. *J. Geophys. Res. Biogeosci.* 112:G03008. doi: 10.1029/2006JG000365

Jackson, R. D., Idso, S., Reginato, R., and Pinter, P. (1981). Canopy temperature as a crop water stress indicator. *Water Resour. Res.* 17, 1133–1138. doi: 10.1029/WR017i004p01133

Jarvis, P. (1976). The interpretation of the variations in leaf water potential and stomatal conductance found in canopies in the field. *Philos. Trans. R. Soc. Lond. B Biol. Sci.* 273, 593–610. doi: 10.1098/rstb.1976.0035

Jasechko, S., Sharp, Z. D., Gibson, J. J., Birks, S. J., Yi, Y., and Fawcett, P. J. (2013). Terrestrial water fluxes dominated by transpiration. *Nature* 496, 347–350. doi: 10.1038/nature11983

Jones, H. G. (1998). Stomatal control of photosynthesis and transpiration. *J. Exp. Bot.* 49, 387–398.

Kunert, N., Aparecido, L. M. T., Wolff, S., Higuchi, N., dos Santos, J., de Araujo, A. C., et al. (2017). A revised hydrological model for the central amazon: the importance of emergent canopy trees in the forest water budget. *Agric. For. Meteorol.* 239, 47–57. doi: 10.1016/j.agrformet.2017.03.002

Lambers, H., Chapin, F. S., and Pons, T. L. (2008). "Plant water relations," in *Plant Physiological Ecology*, eds L. P. Thijs, H. Lambers, and F. S. Chapin (New York, NY: Springer), 163–223.

Lloyd, J., and Farquhar, G. D. (2008). Effects of rising temperatures and [CO2] on the physiology of tropical forest trees. *Philos. Trans. R. Soc. B Biol. Sci.* 363, 1811–1817. doi: 10.1098/rstb.2007.0032

Lopes, A. P., Nelson, B. W., Wu, J., de Alencastro Graça, P. M. L., Tavares, J. V., Prohaska, N., et al. (2016). Leaf flush drives dry season green-up of the central amazon. *Remote Sens. Environ.* 182, 90–98. doi: 10.1016/j.rse.2016.05.009

Lovisolo, C., and Schubert, A. (1998). Effects of water stress on vessel size and xylem hydraulic conductivity in *Vitis vinifera* L. *J. Exp. Bot.* 49, 693–700. doi: 10.1093/jxb/49.321.693

McAdam, S. A., Sussmilch, F. C., and Brodribb, T. J. (2016). Stomatal responses to vapour pressure deficit are regulated by high speed gene expression in angiosperms. *Plant Cell Environ.* 39, 485–491. doi: 10.1111/pce.12633

McDowell, N., Allen, C. D., Anderson-Teixeira, K., Brando, P., Brienen, R., Chambers, J., et al. (2018). Drivers and mechanisms of tree mortality in moist tropical forests. *New Phytol.* 219, 851–869. doi: 10.1111/nph.15027

Meakem, V., Tepley, A. J., Gonzalez-Akre, E. B., Herrmann, V., Muller-Landau, H. C., Wright, S. J., et al. (2017). Role of tree size in moist tropical forest carbon cycling and water deficit responses. *New Phytol.* 219, 947–958. doi: 10.1111/nph.14633

Meinzer, F., Goldstein, G., Holbrook, N., Jackson, P., and Cavelier, J. (1993). Stomatal and environmental control of transpiration in a lowland tropical forest tree. *Plant Cell Environ.* 16, 429–436. doi: 10.1111/j.1365-3040.1993.tb00889.x

Meinzer, F. C., James, S. A., Goldstein, G., and Woodruff, D. (2003). Whole-tree water transport scales with sapwood capacitance in tropical forest canopy trees. *Plant Cell Environ.* 26, 1147–1155. doi: 10.1046/j.1365-3040.2003.01039.x

Michaletz, S. T., Weiser, M. D., McDowell, N. G., Zhou, J., Kaspari, M., Helliker, B. R., et al. (2016). The energetic and carbon economic origins of leaf thermoregulation. *Nat. Plants* 2:16129. doi: 10.1038/nplants.2016.129

Moradi, I., Arkin, P., Ferraro, R., Eriksson, P., and Fetzer, E. (2016). Diurnal variation of tropospheric relative humidity in tropical regions. *Atmos. Chem. Phys.* 16, 6913–6929. doi: 10.5194/acp-16-6913-2016

Motzer, T., Munz, N., Küppers, M., Schmitt, D., and Anhuf, D. (2005). Stomatal conductance, transpiration and sap flow of tropical montane rain forest trees in the southern ecuadorian andes. *Tree Physiol.* 25, 1283–1293. doi: 10.1093/treephys/25.10.1283

Negrón-Juárez, R. I., Hodnett, M. G., Fu, R., Goulden, M. L., and von Randow, C. (2007). Control of dry season evapotranspiration over the amazonian forest as inferred from observations at a southern Amazon forest site. *J. Clim.* 20, 2827–2839. doi: 10.1175/JCLI4184.1

Novick, K. A., Miniat, C. F., and Vose, J. M. (2016). Drought limitations to leaf-level gas exchange: results from a model linking stomatal optimization and cohesion–tension theory. *Plant Cell Environ.* 39, 583–596. doi: 10.1111/pce.12657

O'Brien, J., Oberbauer, S., and Clark, D. (2004). Whole tree xylem sap flow responses to multiple environmental variables in a wet tropical forest. *Plant Cell Environ.* 27, 551–567. doi: 10.1111/j.1365-3040.2003.01160.x

Oliveira, R. S., Costa, F. R., van Baalen, E., de Jonge, A., Bittencourt, P. R., Almanza, Y., et al. (2019). Embolism resistance drives the distribution of amazonian rainforest tree species along hydro-topographic gradients. *New Phytol.* 221, 1457–1465. doi: 10.1111/nph.15463

Oren, R., Phillips, N., Ewers, B., Pataki, D., and Megonigal, J. (1999a). Sap-flux-scaled transpiration responses to light, vapor pressure deficit, and leaf area reduction in a flooded *Taxodium distichum* forest. *Tree Physiol.* 19, 337–347. doi: 10.1093/treephys/19.6.337

Oren, R., Sperry, J., Katul, G., Pataki, D., Ewers, B., Phillips, N., et al. (1999b). Survey and synthesis of intra-and interspecific variation in stomatal sensitivity to vapour pressure deficit. *Plant Cell Environ.* 22, 1515–1526. doi: 10.1046/j.1365-3040.1999.00513.x

Phillips, N., Nagchaudhuri, A., Oren, R., and Katul, G. (1997). Time constant for water transport in loblolly pine trees estimated from time series of evaporative demand and stem sapflow. *Trees* 11, 412–419. doi: 10.1007/s004680050102

R Development Core Team (2013). *RA Lang. Environ. Stat. Comput.* 55, 275–286.

Roman, D., Novick, K., Brzostek, E., Dragoni, D., Rahman, F., and Phillips, R. (2015). The role of isohydric and anisohydric species in determining ecosystem-scale response to severe drought. *Oecologia* 179, 641–654. doi: 10.1007/s00442-015-3380-9

Roth, I. (1981). *Structural Patterns of Tropical Barks*. Berlin: Gebruder Borntraeger.

Rowland, L., da Costa, A. C. L., Galbraith, D. R., Oliveira, R., Binks, O. J., Oliveira, A., et al. (2015). Death from drought in tropical forests is triggered by hydraulics not carbon starvation. *Nature* 528, 119–122. doi: 10.1038/nature15539

Sade, N., Gebremedhin, A., and Moshelion, M. (2012). Risk-taking plants: anisohydric behavior as a stress-resistance trait. *Plant Signal. Behav.* 7, 767–770. doi: 10.4161/psb.20505

Saleska, S. R., Miller, S. D., Matross, D. M., Goulden, M. L., Wofsy, S. C., Da Rocha, H. R., et al. (2003). Carbon in amazon forests: unexpected seasonal fluxes and disturbance-induced losses. *Science* 302, 1554–1557. doi: 10.1126/science.1091165

Segura, M., and Kanninen, M. (2005). Allometric models for tree volume and total aboveground biomass in a tropical humid forest in costa rica. *Biotropica* 37, 2–8. doi: 10.1111/j.1744-7429.2005.02027.x

Slot, M., and Winter, K. (2017a). In situ temperature relationships of biochemical and stomatal controls of photosynthesis in four lowland tropical tree species. *Plant Cell Environ.* 40, 3055–3068. doi: 10.1111/pce.13071

Slot, M., and Winter, K. (2017b). In situ temperature response of photosynthesis of 42 tree and liana species in the canopy of two panamanian lowland tropical forests with contrasting rainfall regimes. *New Phytol.* 214, 1103–1117. doi: 10.1111/nph.14469

Snyder, K., Richards, J., and Donovan, L. (2003). Night-time conductance in C3 and C4 species: do plants lose water at night? *J. Exp. Bot.* 54, 861–865. doi: 10.1093/jxb/erg082

Steppe, K., Cochard, H., Lacointe, A., and Ameglio, T. (2012). Could rapid diameter changes be facilitated by a variable hydraulic conductance? *Plant Cell Environ.* 35, 150–157. doi: 10.1111/j.1365-3040.2011.02424.x

Steppe, K., De Pauw, D. J. W., Doody, T. M., and Teskey, R. O. (2010). A comparison of sap flux density using thermal dissipation, heat pulse velocity and heat field deformation methods. *Agric. For. Meteorol.* 150, 1046–1056. doi: 10.1016/j.agrformet.2010.04.004

Synnott, T. J. (1979). *A Manual of Permanent Plot Procedures for Tropical Rainforests*. Oxford: University of Oxford.

Ter Steege, H., Pitman, N. C., Sabatier, D., Baraloto, C., Salomão, R. P., Guevara, J. E., et al. (2013). Hyperdominance in the amazonian tree flora. *Science* 342:1243092. doi: 10.1126/science.1243092

Tinoco-Ojanguren, C., and Pearcy, R. W. (1993). Stomatal dynamics and its importance to carbon gain in two rainforest piper species. I. VPD effects on the transient stomatal response to lightflecks. *Oecologia* 94, 388–394. doi: 10.1007/BF00317115

Ward, D. A., and Bunce, J. A. (1986). Novel evidence for a lack of water vapour saturation within the intercellular airspace of turgid leaves of mesophytic species. *J. Exp. Bot.* 37, 504–516. doi: 10.1093/jxb/37.4.504

Ward, E. J., Bell, D. M., Clark, J. S., and Oren, R. (2012). Hydraulic time constants for transpiration of loblolly pine at a free-air carbon dioxide enrichment site. *Tree Physiol.* 33, 123–134. doi: 10.1093/treephys/tps114

Wu, J., Guan, K., Hayek, M., Restrepo-Coupe, N., Wiedemann, K. T., Xu, X., et al. (2017). Partitioning controls on Amazon forest photosynthesis between environmental and biotic factors at hourly to interannual timescales. *Glob. Chang. Biol.* 23, 1240–1257. doi: 10.1111/gcb.13509

Zeppel, M. J., Murray, B. R., Barton, C., and Eamus, D. (2004). Seasonal responses of xylem sap velocity to VPD and solar radiation during drought in a stand of native trees in temperate Australia. *Funct. Plant Biol.* 31, 461–470. doi: 10.1071/FP03220

Zhang, Q., Manzoni, S., Katul, G., Porporato, A., and Yang, D. (2014). The hysteretic evapotranspiration—vapor pressure deficit relation. *J. Geophys. Res. Biogeosci.* 119, 125–140. doi: 10.1002/2013JG002484

Zuecco, G., Penna, D., Borga, M., and Meerveld, H. (2016). A versatile index to characterize hysteresis between hydrological variables at the runoff event timescale. *Hydrol. Process.* 30, 1449–1466. doi: 10.1002/hyp.10681

Conflict of Interest Statement: The authors declare that the research was conducted in the absence of any commercial or financial relationships that could be construed as a potential conflict of interest.

frontiers in Plant Science

ORIGINAL RESEARCH
published: 17 April 2019
doi: 10.3389/fpls.2019.00492

Genotypic, Developmental and Environmental Effects on the Rapidity of g_s in Wheat: Impacts on Carbon Gain and Water-Use Efficiency

*Michele Faralli[1], James Cockram[2], Eric Ober[2], Shellie Wall[1], Alexander Galle[3], Jeroen Van Rie[3], Christine Raines[1] and Tracy Lawson[1]**

[1] School of Biological Sciences, University of Essex, Colchester, United Kingdom, [2] The John Bingham Laboratory, NIAB, Cambridge, United Kingdom, [3] BASF Agricultural Solutions Belgium NV, Ghent, Belgium

Stomata are the primary gatekeepers for CO_2 uptake for photosynthesis and water loss via transpiration and therefore play a central role in crop performance. Although stomatal conductance (g_s) and assimilation rate (A) are often highly correlated, studies have demonstrated an uncoupling between A and g_s that can result in sub-optimal physiological processes in dynamic light environments. Wheat (*Triticum aestivum* L.) is exposed to changes in irradiance due to leaf self-shading, moving clouds and shifting sun angle to which both A and g_s respond. However, stomatal responses are generally an order of magnitude slower than photosynthetic responses, leading to non-synchronized A and g_s responses that impact CO_2 uptake and water use efficiency ($_iWUE$). Here we phenotyped a panel of eight wheat cultivars (estimated to capture 80% of the single nucleotide polymorphism variation in North–West European bread wheat) for differences in the speed of stomatal responses (to changes in light intensity) and photosynthetic performance at different stages of development. The impact of water stress and elevated [CO_2] on stomatal kinetics was also examined in a selected cultivar. Significant genotypic variation was reported for the time constant for stomatal opening (K_i, $P = 0.038$) and the time to reach 95% steady state A ($P = 0.045$). Slow g_s opening responses limited A by ∼10% and slow closure reduced $_iWUE$, with these impacts found to be greatest in cultivars Soissons, Alchemy and Xi19. A decrease in stomatal rapidity (and thus an increase in the limitation of photosynthesis) ($P < 0.001$) was found during the post-anthesis stage compared to the early booting stage. Reduced water availability triggered stomatal closure and asymmetric stomatal opening and closing responses, while elevated atmospheric [CO_2] conditions reduced the time for stomatal opening during a low to high light transition, thus suggesting a major environmental effect on dynamic stomatal kinetics. We discuss these findings in terms of exploiting various traits to develop ideotypes for specific environments, and suggest that intraspecific variation in the rapidity of stomatal responses could provide a potential unexploited breeding target to optimize the physiological responses of wheat to dynamic field conditions.

Keywords: stomatal rapidity, *Triticum aestivum* L., photosynthesis, stomatal conductance, water-use efficiency, water stress, elevated [CO_2]

OPEN ACCESS

Edited by:
Stuart Anthony Casson, The University of Sheffield, United Kingdom

Reviewed by:
Shardendu Kumar Singh, United States Department of Agriculture, United States
Caspar Christian Cedric Chater, The University of Sheffield, United Kingdom

***Correspondence:**
Tracy Lawson
tlawson@essex.ac.uk

Specialty section:
This article was submitted to Plant Physiology, a section of the journal Frontiers in Plant Science

Received: *07 September 2018*
Accepted: *01 April 2019*
Published: *17 April 2019*

Citation:
Faralli M, Cockram J, Ober E, Wall S, Galle A, Van Rie J, Raines C and Lawson T (2019) Genotypic, Developmental and Environmental Effects on the Rapidity of g_s in Wheat: Impacts on Carbon Gain and Water-Use Efficiency. Front. Plant Sci. 10:492. doi: 10.3389/fpls.2019.00492

INTRODUCTION

Wheat (*Triticum aestivum* L.) is one of the most important food crops globally, accounting for 20% of human calorie consumption (Ray et al., 2013). Significant yield gains have been achieved in the last century following both genetic improvements and advances in crop management (Slafer et al., 2015). However, more recently, evidence of stagnation in yield improvement, combined with the predicted environmental changes associated with global warming (Ray et al., 2012), highlight the need to identify optimized crop ideotypes and new genetic targets for incorporation into current wheat breeding programs to maintain and/or improve future productivity.

Crop yield is the product of the cumulative rates of photosynthesis over the growing season and the subsequent capacity of sinks to accept and store these products (Zelitch, 1982). Although previous work suggested that selecting for elevated photosynthetic rate on a leaf area basis does not always produce significant results in terms of yield (Evans, 1996), free-air concentration enrichment experiments (Long et al., 2006) and bioengineering approaches (Driever et al., 2017) have provided promising results, and highlight the possibility of yield gains via elevated rates of photosynthesis. In many crops, while harvest index and light interception capacity are approaching theoretical maximum (∼0.64 and 0.8–0.9 respectively, Long et al., 2006), the efficiency of energy conversion into biomass (i.e., radiation-use efficiency and thus photosynthesis) still has substantial room for improvement (Long et al., 2006). Most of the intraspecific natural variation in photosynthesis for C_3 plants is mainly due to differences in biochemical capacity including electron transport rates and carboxylation efficiency (Driever et al., 2014; Carmo-Silva et al., 2017). In addition, under natural dynamic conditions photosynthetic process can also be limited by factors such as activation of Calvin cycle enzymes and/or stomatal dynamics (Lawson and Blatt, 2014; Taylor and Long, 2017; Salter et al., 2019).

Stomata control CO_2 and water vapor exchange between the leaf and the atmosphere, and thus play a unique role in crop productivity and yield (Lawson et al., 2010, 2012). Stomata respond to environmental changes by modifying pore aperture, and both internal and external signals are involved (Lawson and Blatt, 2014). Although external environmental stimuli (e.g., VPD, light, water availability, heat) often occur in combination, stomata generally open in response to high or increasing light intensity, low CO_2 concentration [CO_2] and low vapor pressure deficit (VPD), while stomata close in the opposite conditions (Outlaw, 2003; Lawson et al., 2014). In the field, leaf self-shading, cloud cover and sun angle often lead to rapid changes in photosynthetic photon flux density (PPFD), to which photosynthesis rapidly responds while stomatal responses are an order of magnitude slower (Lawson et al., 2010, 2012; Lawson and Blatt, 2014; Slattery et al., 2018). Slow stomatal responses can lead to (i) reduced A due to restricted CO_2 diffusion during a low to high light transition, or (ii) unnecessary water loss during a high to low light transition when stomata lag behind decreases in A. Indeed, recent reports suggested that in wheat stomatal limitation of photosynthesis can be up to 10% (McAusland et al., 2016) leading to potential impacts on crop productivity (Lawson and Blatt, 2014; Taylor and Long, 2017; Vialet-Chabrand et al., 2017; Faralli et al., 2019; Vialet-Chabrand and Lawson, 2019). These findings highlight the advantage of selecting genotypes with fast stomatal responses to changes in irradiance, as rapid stomatal opening can increase photosynthetic rate whilst rapid stomatal closure can enhance water use efficiency at the crop level, leading to increased soil moisture conservation and therefore delay the onset of stress during periods of low rainfall (McAusland et al., 2016; Qu et al., 2016).

Although interspecific variation in stomatal responses to changes in light intensity have been previously reported (Vico et al., 2011; McAusland et al., 2016), to our knowledge there are no reports demonstrating intraspecific variation in the rapidity of stomatal responses in wheat. In addition, there are limited reports on the effects of developmental and environmental factors on stomatal rapidity (e.g., Leakey et al., 2002; Gerardin et al., 2018; Haworth et al., 2018). In particular, climate change has been associated with more frequent periods of water stress (Ray et al., 2012) and a significant increase in atmospheric [CO_2] (Ainsworth and Rogers, 2007), two environmental conditions that strongly affect both A, and g_s and therefore crop productivity. Therefore, the main aims of this work were, (i) to assess the extent of natural variation in the speed of stomatal responses in selected wheat cultivars; (ii) to determine the influence of developmental stage (late vegetative, booting, and post-anthesis stages) on such variation; and (iii) to evaluate the impact of reduced water availability and elevated atmospheric [CO_2] on the rapidity of stomatal responses. A panel of eight winter wheat genotypes, capturing ∼80% of the United Kingdom single nucleotide polymorphism variability (Gardner et al., 2016), was phenotyped at different developmental stages for stomatal rapidity and photosynthetic capacity. In addition, a selected genotype was used to assess the impact reduced water availability and elevated [CO_2] on stomatal kinetics.

MATERIALS AND METHODS

Plant Material

Eight elite wheat varieties adapted to the United Kingdom were selected: Alchemy, Brompton, Claire, Hereward, Rialto, Robigus, Soissons, and Xi19. These are the founder lines of the 'NIAB Elite MAGIC' multi-parent advanced generation inter-cross (MAGIC) population (Mackay et al., 2014). Seeds were sown in plastic trays containing compost and germinated in a growth cabinet (Reftech BV, Sassenheim, Netherlands) at ∼200 μmol m^{-2} s^{-1} PPFD, 14 h/10 h photoperiod (light/dark), ∼15°C on average and ∼60% relative humidity (RH). The compost material (Levington F2S) contained fertilizer (144 mg L^{-1} N, 73 mg L^{-1} P, 239 mg L^{-1} K, adjusted to pH 5.3–6.0 with dolomitic lime) and incorporated coir and sand. Plants were watered every 2 days. At BBCH (Biologische Bundesanstalt, Bundessortenamt und Chemische Industrie) growth stage (GS) 12 (GS12, two seedling leaves unfolded; Lancashire et al., 1991) seedlings were moved into a cold room for vernalization: 4°C, ∼50 μmol m^{-2} s^{-1} PPFD

at 10 h/14 h photoperiod (light/dark) for 8 weeks. After vernalization, seedlings (one per pot) were transplanted into 1.5 L (15 cm diameter; 12 cm deep) or 4 L (16.5 cm diameter; 21 cm deep) pots (depending on the experiment) containing Levington F2S compost (Everris, Ipswich, United Kingdom). After which plants where transferred to either the glasshouse or controlled growth environment depending on experimental design (see below).

Growth Conditions and Experimental Design

Experiment 1: Phenotyping Stomatal Rapidity at Different Developmental Stages

To assess the presence of natural variation for stomatal rapidity and to determine the influence of developmental stage on this trait, plants were grown in a greenhouse in a fully randomized block design, in six blocks (n = 6). Solar radiation was supplemented with sodium vapor lamps (∼200 to 400 μmol m^{-2} s^{-1}. Hortilux Schreder 600W, Monster, Netherlands) and maintaining a 12 h photoperiod. Air temperature was on average ∼20°C during the day and ∼15°C at night. Water was applied daily to avoid soil moisture deficit, while full strength Hoagland's nutrients solution (∼100 mL per pot) was applied weekly. Owing to the different developmental pattern of the lines studied in this work, plants were visually scored for growth stage every 2 days. All phenotypic measurements were collected at BBCH GS25-31 (vegetative growth, tillering to start of stem extension), GS41-45 (early reproductive growth, booting stage) and GS71-75 (post-anthesis; 'watery ripe' to 'medium milk' stages of grain).

Experiment 2: Stomatal Rapidity Under Reduced Water Availability

To evaluate the impact of reduced water availability on stomatal dynamics, plants (cv. Soissons) were transplanted into 4 L pots and watered daily to avoid soil moisture deficit until the start of the treatment, and nutrients were supplied with Hoagland's solution (∼100 mL per pot, until the start of water availability manipulation). Between GS45 and GS51, pots were watered daily to ensure full soil water capacity by weighing the pots (∼3000 g of pot target weight). The non-stressed plants (well-watered, WW, n = 6) were watered daily throughout the experiment, whereas the progressive soil drying treatment was applied by removing watering to the water stressed plants (WS, n = 6). Water content in the pot was expressed as the fraction of transpirable soil water (FTSW). The FTSW method was recently summarized by King and Purcell (2017), and briefly described as follows: FTSW = (Pg – Pd)/TTSW, where (i) total transpirable soil water (TTSW) was the difference between the pot weights at 100% water holding capacity (WHC) (pot weight ∼3000 g including plant and plastic pot) and when transpiration rate of the stressed plants decreased to 10% of the control plants, (ii) Pg was the actual pot weight on a given date, and (iii) Pd was the pot weight at the time when transpiration rate of stressed plants was 10% of the control plants (∼1300 g of pot weight). Gas exchange analyses were carried out when FTSW was ∼0.2–0.3 for WS plants, and ∼0.8–0.9 for the WW treatment. The value at which WS plants were analyzed was chosen to represent a soil water stress condition at which wheat has previously been found to show typical stress symptoms (e.g., significant reduction of g_s, leaf water potential and leaf relative water content) (Weldearegay et al., 2016). Two sets of soil drying treatments where carried out separately (n = 3 for WS for each cycle) to avoid overlaps between replicates during the phenotypic analysis (**Supplementary Figure 1**).

Experiment 3: Stomatal Rapidity Under Elevated Atmospheric [CO_2]

To evaluate the impact of elevated atmospheric [CO_2] on the rapidity of stomatal responses a third experiment was carried out in growth chambers in which atmospheric [CO_2] was manipulated (Conviron Adaptis A1000, Conviron, Canada). Plants (cv. Soissons) were transplanted into in 1.5 L pots (one per pot) and placed into two growth chambers, one set of pots (n = 6) at ambient [CO_2] ([CO_2] 446 ± 31 μmol mol^{-1} on average) and the other (n = 6) at elevated [CO_2] (706 ± 6 μmol mol^{-1} on average) (**Supplementary Figure 2**). The light level inside both chambers at leaf height was ∼400–800 μmol m^{-2} s^{-1} with a 12 h photoperiod. Air temperature was maintained at ∼20°C through the day and ∼15°C at night, and RH maintained at ∼60%. Plants were watered every 2 days with Hoagland's solution (∼100 mL per pot). Phenotypic analyses were carried out at GS25-31 (33–42 days after sowing) as described below (**Supplementary Figure 2**).

Phenotypic Analysis

Analyses of the Rapidity of g_s to Changes in Light Intensity

In each experiment, the third fully expanded leaf at GS31, and the flag leaf at GS41 and GS71 were tagged on each plant at the onset of each selected growth stage. Prior to gas exchange analysis, plants were transferred from the greenhouse to a temperature and humidity-controlled room (∼20°C temperature and ∼60% RH) and gas exchange measurements performed on the middle of the leaf lamina using an open infrared gas exchange system fitted with a 2 cm^2 leaf cuvette and integral blue–red LED light source (LI-6400–40; LI-COR, Lincoln, NE, United States). All measurements were collected between 8:30 and 15:00 and randomized to avoid any potential diurnal influence over a 8 week measurement period. Prior to measurement, leaves were first equilibrated at a PPFD of 100 μmol m^{-2} s^{-1} until both A and g_s reached 'steady state,' defined as a ∼2% maximum change in rate during a 10 min period (generally 60 min). After equilibration, PPFD was increased to 1500 μmol m^{-2} s^{-1} for 1 h, and subsequently returned to 100 μmol m^{-2} s^{-1} for 1 h. The conditions inside the leaf cuvette were kept constant at 20 ± 0.1°C leaf temperature, at VPD of 1 kPa with a dew point generator (LI-610; LI-COR, Lincoln, NE, United States) and at 400 μmol CO_2 mol^{-1} air (ambient CO_2 concentration, C_a). In Experiment 3 the plants grown at ∼700 μmol mol^{-1} [CO_2] were analyzed at 700 μmol mol^{-1} C_a. Values were logged every minute throughout the three h measurement cycle. Intrinsic water use efficiency ($_iWUE$) was

calculated as ${}_iWUE = A/g_s$. All data were analyzed according to the exponential model of Vialet-Chabrand et al. (2013) as described in McAusland et al. (2016). Variables estimated with the exponential model were steady-state photosynthesis at saturating light (A), steady state stomatal conductance at saturating light (g_s), K_i (time constant for rapidity of stomatal opening), K_d (time constant for rapidity of stomatal closing) and 'time to reach 95% A' ($T_{95\%A}$) (**Figures 1A,B**). The limitation of A by g_s ($g_s\text{limit}A$) was calculated by estimating a hypothetical A if no stomatal limitation was present (McAusland et al., 2016) and determining the differences with the measured kinetic values. The 'time to restore ${}_iWUE$' (T_{iWUE}) was defined as the time necessary to recover the maximum ${}_iWUE$ value during the high to low light transition. T_{iWUE} was calculated using segmented regression and estimated as the intersection between the two linear segments (**Figure 1B**). The g_s at the point of intercept was used to determine the 'limitation of ${}_iWUE$ by g_s' ($g_s\text{limit}_iWUE$) by calculating the integrated difference with measured values following the high to low light transition (**Figure 1B**).

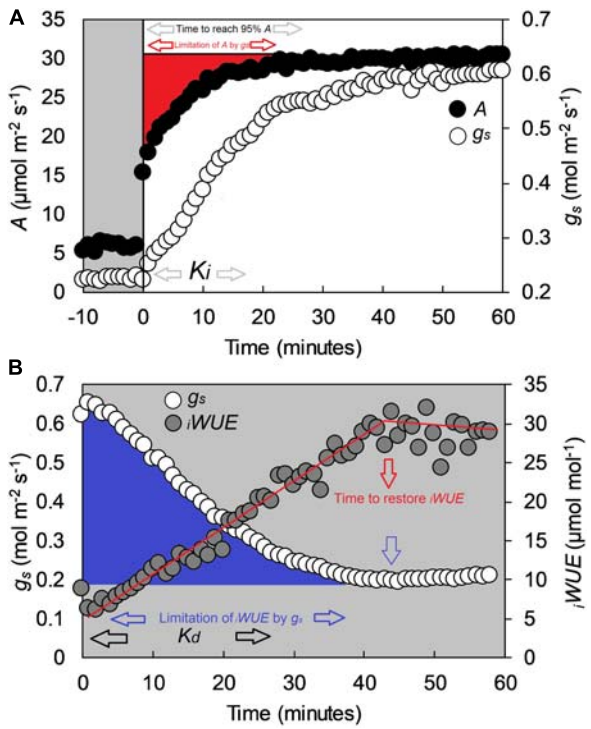

FIGURE 1 | Example of a step-change in light for the flag leaf of a wheat plant (cv. Soissons), collected with a Li-Cor 6400 at GS41. **(A)** Step-change from low to high light (100 to 1500 μmol m^{-2} s^{-1} PPFD), and **(B)** step-change from high to low light (1500 to 100 μmol m^{-2} s^{-1} PPFD). In **(A)**, black dots represent CO_2 assimilation rate (A), whereas white dots represent stomatal conductance (g_s). In **(B)**, white dots represent stomatal conductance (g_s) while gray dots represent intrinsic water-use efficiency (${}_iWUE$) calculated as ${}_iWUE = A/g_s$. White areas represent 1500 μmol m^{-2} s^{-1} PPFD, gray areas 100 μmol m^{-2} s^{-1} PPFD. Estimated variables with the exponential model described by Vialet-Chabrand et al. (2013) are K_i (time constant for rapidity of stomatal opening), K_d (time constant for rapidity of stomatal closing) and time to reach 95% A ($T_{95\%A}$.) The limitation of A by g_s ($g_s\text{limit}A$) was estimated by assuming a hypothetical A if no stomatal limitation was present immediately after a low to high light transition (McAusland et al., 2016). Time to restore ${}_iWUE$ (T_{iWUE}) was calculated with segmented regression, and estimated as the intercept between the two linear segments. The g_s at the two ${}_iWUE$ intercepts were used to calculate the limitation of ${}_iWUE$ by g_s ($g_s\text{limit}_iWUE$) by assuming an instantaneous stomatal closure after a high to low light transition.

A/Ci Curves

Photosynthesis measurements (A/C_i curves) were performed between 9:00 and 12:00 on the fully emerged flag leaf at GS41-45 in Experiment 1. Measurements of the response of A to sub-stomatal CO_2 concentrations (C_i) were performed in the middle of the tagged leaf using an open infrared gas exchange system and a 2 cm^2 leaf cuvette with an integral blue–red LED light source (LI-6400–40; LI-COR, Lincoln, NE, United States). In the cuvette, PPFD was maintained at a saturating level of 1500 μmol m^{-2} s^{-1}, a leaf temperature of 20 ± 0.1°C, a VPD between 0.9 and 1.3 kPa and a C_a of 400 μmol mol^{-1}. When steady-state conditions were achieved, C_a was sequentially decreased to 300, 200, 100, and 75 μmol mol^{-1} before returning to the initial concentration of 400 μmol mol^{-1}. This was followed by a sequential increase to 550, 700, 1000, and 1200 μmol mol^{-1}. Readings were recorded when A had stabilized to the new conditions. The maximum velocity of Rubisco for carboxylation (V_{cmax}) and the maximum rate of electron transport demand for Ribulose 1,5-bisphosphate (RuBP) regeneration (J_{max}) were derived by curve fitting, as described by Sharkey et al. (2007).

Stomatal Density Analysis

At GS41-45 in Experiment 1, stomatal impressions were collected at the same point of the leaf lamina used for gas exchange analyses, on both the adaxial (n = 6) and abaxial (n = 6) side of the leaf. A negative impression was made using a dental polymer (Xantoprene, Heraesus Kulzer, Ltd., Hanau, Germany) (Weyers and Johansen, 1985). After the material had dried, a positive impression was produced using nail polish on a microscope slide. Stomatal density and pore length were determined using a light microscope by averaging the value of six fields of view for each leaf with a size of ∼1250 μm^2 captured from each impression and using a 5 MP eye-piece camera (MicroCAM 5 MP, Bresser Optics, Rhede, Germany).

Statistical Analysis

Statistical analyses were conducted using SPSS (v.16; SPSS, Inc., Chicago, IL, United States) and R[1]. A two-way analysis of variance (ANOVA) was used for gas exchange data when two factors (genotype × growth stage) were present (i.e., for the variables A, g_s, K_i, K_d, $T_{95\%A}$, $g_s\text{limit}A$, T_{iWUE} for Experiment 1). Single factor analyses were carried out using one-way ANOVA (i.e., for A, g_s, K_i, K_d in Experiments 2 and 3). Shapiro–Wilk and Levene's tests were used to test data for normality and homogeneity of variance, respectively. Duncan's test was used for multiple comparisons. When present, linear curves were fitted with

[1]http://www.r-project.org/

major axis regression thus minimizing the variability for the traits of interest in both the axes. The strength of trait associations at GS41-45 (between steady-state and dynamic gas exchange, anatomical and photosynthetic capacity traits) and for all developmental stages (between steady-state and dynamic gas exchange traits) were measured using Pearson's correlation coefficient.

RESULTS

Speed of Stomatal Responses at Different Developmental Stages

Significant genotypic variation ($P < 0.001$) in steady-state A and g_s at 1500 μmol m^{-2} s^{-1} was recorded for the eight wheat cultivars investigated (**Figures 2A–F**). Soissons and Xi19 showed the highest A and g_s values, whereas Hereward showed consistently lower values. There was a significant effect of growth stage on A and g_s ($P < 0.001$ for both), with most of the cultivars showing higher values at GS41. Significant variation in the time constants for stomatal opening (K_i) was recorded between cultivars ($P = 0.038$) (**Figures 2G–I**) and developmental stage significant impact K_i ($P < 0.001$) in the majority of cultivars, with a lower time constant (thus faster g_s responses) at GS31 and GS41 compared with GS71. However, in cultivars Claire, Rialto and Robigus, there was no significant effect of growth stage on K_i. Similarly, K_d varied significantly between the different growth stages ($P < 0.001$), although no significant genotypic differences were found ($P = 0.343$) (**Figures 2J–L**). Most of the cultivars achieved 95% A between 7 and 15 min following a step increase in light intensity when analyzed at GS31 and GS41 and significant variation ($P = 0.045$) existed between cultivars (**Figures 2M–O**). At GS71, $T_{95\%A}$ was significantly longer than GS31 and GS41 ($P < 0.001$), between 14 and 25 min.

When plants were subjected to a step increase in light intensity, photosynthesis was limited by the slow increase in g_s, with an average limitation ($g_{s\text{limit}}A$) between 7 and 15% across genotypes ($P = 0.019$) and growth stages (**Figures 3A–C**). Soissons and Alchemy showed the greatest limitation of A by g_s (∼12% on average) while, Rialto, Hereward and Claire were less limited at ∼8% on average. Generally, $g_{s\text{limit}}A$ was exacerbated at GS71 ($P < 0.001$), although some genotypes (Claire, Rialto) did not show any significant increases in $g_{s\text{limit}}A$ at GS71 compared to GS41.

The time to restore ${}_iWUE$ (T_{iWUE}) was generally faster at GS31 compared to GS41 and GS71 ($P < 0.001$) (**Figures 4A–C**). Hereward was the quickest to restore ${}_iWUE$ due to fast stomatal closure (low K_d) at GS31 and GS41, whilst the slowest responses were observed in Alchemy at GS31 and Soissons at both GS41 and GS71 ($P = 0.014$). $g_{s\text{limit}i}WUE$ was significantly different between cultivars ($P = 0.030$) and growth stages ($P < 0.001$) (**Figures 4D–F**). Across all of the growth stages measured, the temporal response of g_s for opening and closing were significantly correlated with $T_{95\%A}$ and $g_{s\text{limit}}A$ (**Figure 5**). At the same time, significant correlations were found between T_{iWUE} and the time constant for stomatal closing.

Photosynthetic Capacity at Flag Leaf Stage

Significant genotypic variation in V_{cmax} ($P < 0.024$) was observed within the eight cultivars analyzed (**Figures 6A,B**). Rialto, Soissons, and Xi19 showed the highest values for both V_{cmax} and J_{max} (∼160 and 260 μmol m^{-2} s^{-1} on average, respectively) whereas Robigus and Hereward displayed the lowest values. Significant positive correlations were observed between photosynthetic capacity traits (A, V_{cmax}, J_{max}), g_s, speed of stomatal responses and stomatal density (**Figure 7**). A significant positive relationships was observed between g_s and A whilst a negative relationship between g_s and ${}_iWUE$ was recorded. In addition, A was significantly and positively correlated with most of the stomatal kinetics related traits (K_i, K_d, $T_{95\%A}$, $g_{s\text{limit}}A$). Interestingly, ${}_iWUE$ positively correlated with the $g_{s\text{limit}}A$. Significant and positive correlations were found between the $g_{s\text{limit}}A$, $T_{95\%A}$, and K_i.

Stomatal Anatomical Features at Flag Leaf Stage

Stomatal density and pore length were significantly different between the cultivars ($P = 0.002$ for abaxial and $P < 0.001$ for adaxial stomatal density while $P = 0.013$ for abaxial and $P = 0.001$ for adaxial pore length) (**Table 1**). The abaxial density ranged from 63.7 to 81.6 stomata mm^{-2} while the adaxial density was between 61.0 and 90.4 mm^{-2}. Stomatal density was correlated with K_i (adaxial, positive) and $T_{95\%A}$ (abaxial, negative) (**Figure 7**) while abaxial pore length was negatively correlated with abaxial stomatal density (**Figure 7**).

Speed of Stomatal Responses Under Reduced Water Availability

Using the variety Soissons, reduced water availability significantly reduced A and g_s at 1500 μmol m^{-2} s^{-1} PPFD by 45 and 63% respectively ($P < 0.001$) (**Figures 8A,B**). The time constant K_i was increased ($P = 0.036$) in plants grown under water stress (WS) conditions compared to the well-watered controls (WW) (**Figure 8C**). In contrast, a significantly lower K_d ($P = 0.022$) was recorded under WS compared with WW (**Figure 8D**).

Speed of Stomatal Responses Under Elevated [CO_2]

The cv. Soissons grown under 700 μmol mol^{-1} [CO_2] showed a 25% increase in A compared to the rate in control plants grown at 400 μmol mol^{-1} [CO_2] (**Figure 8E**). In contrast, a small reduction in g_s (6%) was recorded under elevated [CO_2], although this was not significantly different from g_s at 400 μmol mol^{-1} [CO_2] (**Figure 8F**). Elevated [CO_2] significantly reduced K_i ($P = 0.047$), while no differences were found for K_d (**Figures 8G,H**).

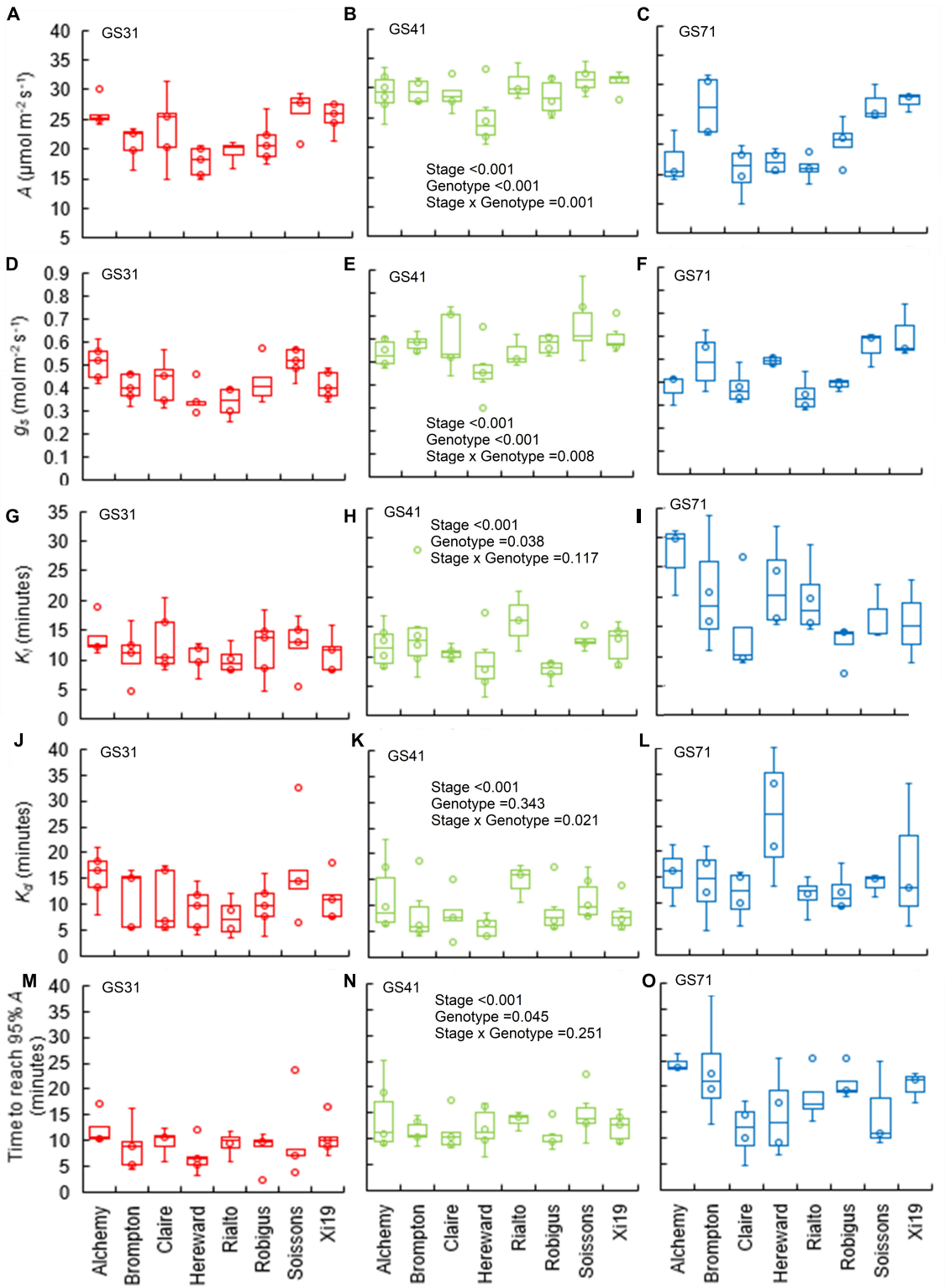

FIGURE 2 | Box plots for steady-state and estimated parameters from step-changes in light at three growth stages on a panel of eight wheat genotypes. Data were collected at collected at GS31, GS41, and GS71 respectively (see graph); **(A–C)** *A*, CO_2 assimilation rate at saturating light after 60 min of induction at 1500 µmol m^{-2} s^{-1} PPFD. **(D–F)** g_s, stomatal conductance at saturating light after 60 min of induction at 1500 µmol m^{-2} s^{-1} PPFD. **(G–I)** K_i, time constant for stomatal opening. **(J–L)** K_d, time constant for stomatal closure. **(M–O)** 'Time to reach 95% *A*' ($T_{95\%A}$). Data were analyzed using two-way ANOVA and means separation was carried out with Duncan's test (**Supplementary Table S1**). All data are means of n = 4–7.

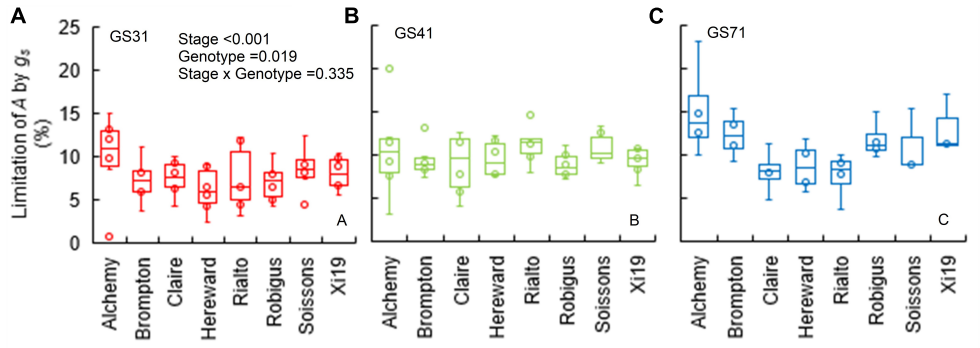

FIGURE 3 | Limitation of *A* by g_s ($g_{slimit}A$) after 30 min of the step change from low to high light (100 to 1500 μmol m^{-2} s^{-1} PPFD) assessed for eight wheat genotypes over three key stages of development (GS31, GS41, and GS71 as **A–C** respectively). Data were estimated by assuming a hypothetical *A* if no stomatal limitation was present immediately after a low to high light transition. Data were analyzed using two-way ANOVA [means separation was carried out with Duncan's test (**Supplementary Table S1**)]. Data are means (n = 4–7).

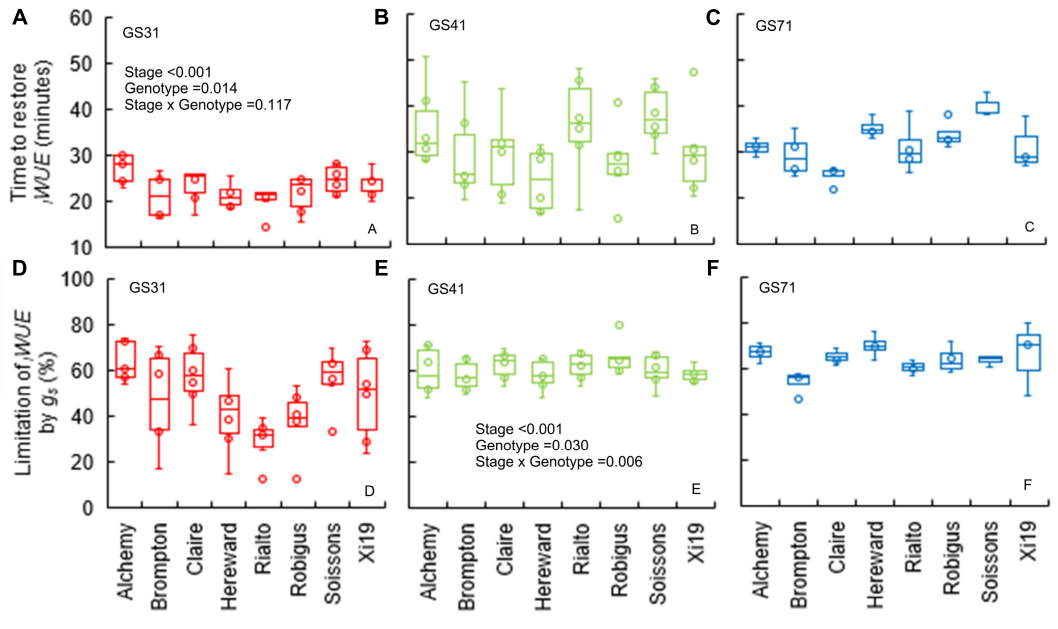

FIGURE 4 | Time to restore $_iWUE$ (T_{iWUE}) **(A–C)** and limitation of $_iWUE$ by g_s ($g_{slimit}{}_iWUE$) **(D–F)** of the step change from high to low light (1500 to 100 μmol m^{-2} s^{-1} PPFD) assessed for eight wheat genotypes over three key stage of development (GS31, GS41, and GS71). Time to restore $_iWUE$ was calculated with segmented regression, and estimated as the intercept between the two linear segments. The g_s at the two $_iWUE$ intercepts was used to calculate the limitation of $_iWUE$ by g_s by assuming an instantaneous stomatal closure after a high to low light transition. Data were analyzed by using two-way ANOVA [means separation was carried out with Duncan's test (**Supplementary Table 1**)] and shown as means (n = 4–7).

DISCUSSION

Genotypic Variation for Stomatal Rapidity in Wheat

Previous work has demonstrated the presence of significant interspecific (Vico et al., 2011; McAusland et al., 2016) and intraspecific (e.g., rice, Qu et al., 2016) variation in the rapidity of stomatal responses or photosynthetic induction (Salter et al., 2019) in crops. Here, we show that significant genotypic variation in the rapidity of g_s is present in wheat in response to step changes in irradiance. Consistent with the conclusions of previous work (e.g., Vico et al., 2011; Lawson et al., 2012; McAusland et al., 2016), the time to reach maximum steady state g_s ranged from 7 to 27 min between cultivars. Cultivars with faster g_s opening responses (lower K_i) (e.g., Hereward, Claire) achieved 95% *A* more rapidly than those cultivars with slower g_s kinetics (e.g., Xi19, Soissons) supported by the positive correlation between K_i and $T_{95\%A}$. At the same time, cultivars with faster stomatal closing (lower K_d, e.g., Hereward and Claire at GS41) following a high to low light transition achieve a

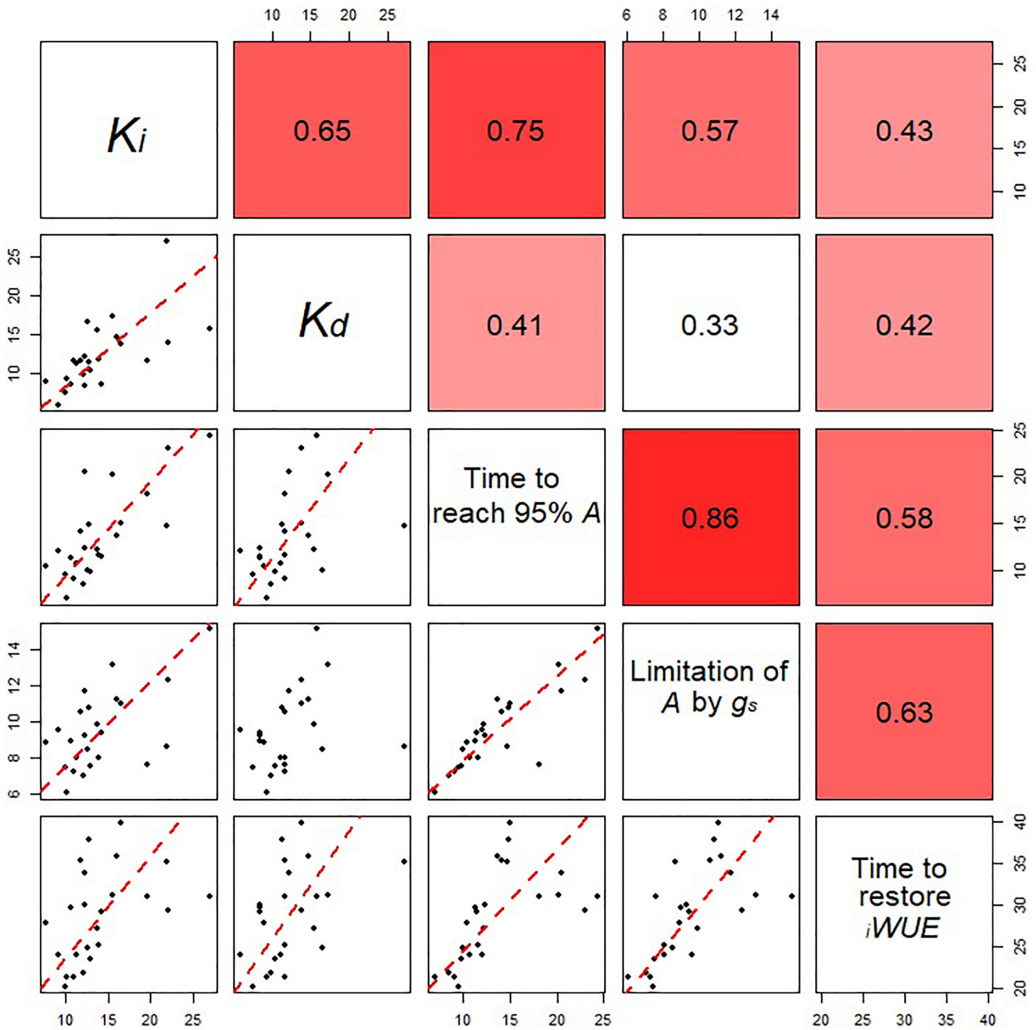

FIGURE 5 | Relationships between the estimated parameters for stomatal opening and closing for all eight wheat varieties at all the growth stages analyzed. Data points are means (n = 4–7) for the eight cultivars at three different growth stages. Correlation coefficients between parameters are shown in the top right panels. In the bottom panels, regression was fitted using major axis regression. Fitting lines are shown only when the correlation is significant ($P < 0.05$).

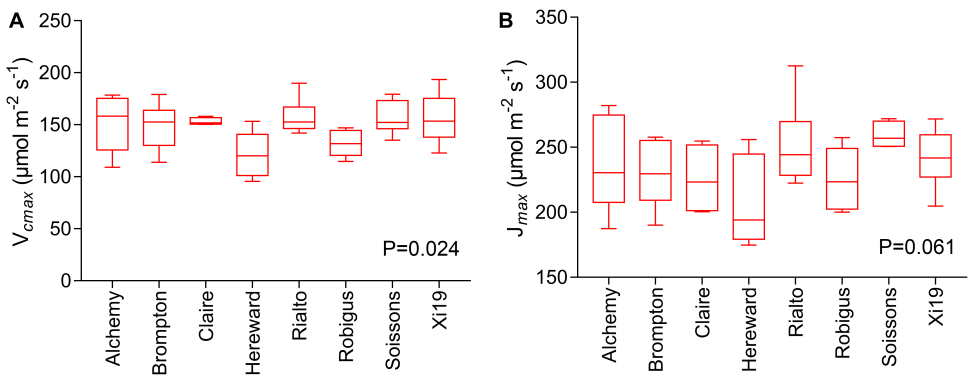

FIGURE 6 | Measures of photosynthetic capacity for the flag leaf of the wheat panel at GS41-45, estimated through A/C_i curves for eight wheat varieties. Data are means (n = 5–6 ± standard error of the means). **(A)** The maximum velocity of Rubisco for carboxylation (V_{cmax}). **(B)** The maximum rate of electron transport demand for RuBP regeneration (J_{max}).

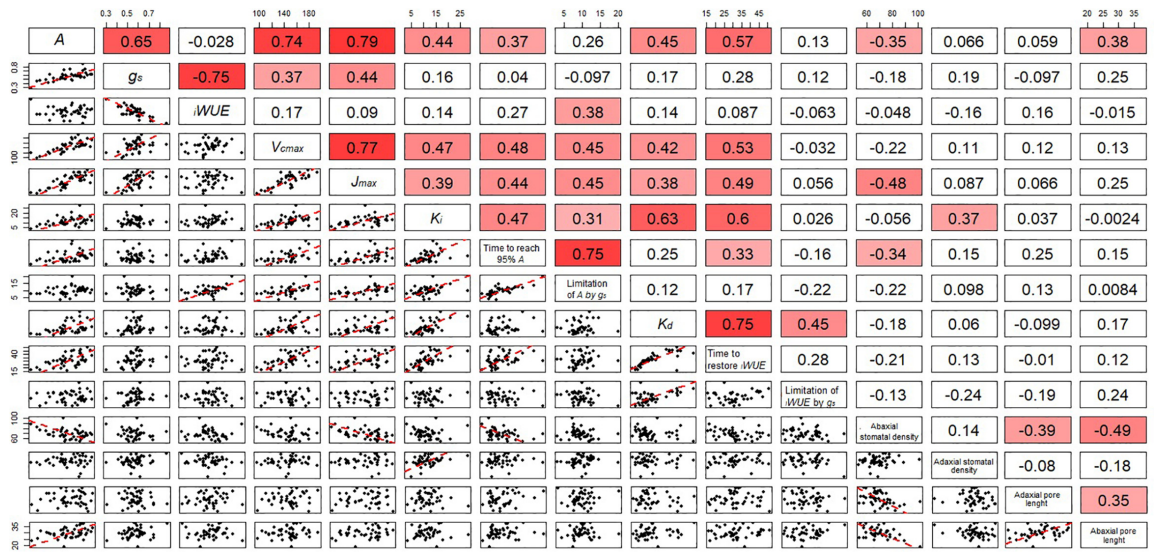

FIGURE 7 | Correlation matrix including the correlation coefficient between parameters describing the temporal response of g_s during opening and closing, photosynthetic capacity and anatomical features for stomata of the flag leaf of wheat plants at GS41. In the bottom panels, regression was fitted by using major axis regression. Fitting line is shown only when the correlation was significant ($P < 0.05$).

higher $_iWUE$, more rapidly. These findings support previous reports in which the 'speedy stomata' trait has been considered a potential target for maximizing CO_2 diffusion and A, as well as $_iWUE$, particularly under dynamic light regimes (Lawson and Vialet-Chabrand, 2018). Significant differences in stomatal density and pore length were also observed between cultivars; interestingly, the variation in stomatal density was greater on the adaxial than the abaxial surface. However, only a weak correlation between stomatal density (adaxial) and K_i was apparent, indicating minimal anatomical influence on the speeds of g_s response in the panel of wheat cultivars analyzed. Additionally, our findings are contrary to previous research on the relationship between stomatal speed and density in the non-domesticated species of the dicot genus *Banksia* that have reported higher stomatal density results in faster responses (Drake et al., 2013).

In rice (Qu et al., 2016) and other species (McAusland et al., 2016), asymmetric stomatal responses (e.g., faster stomatal closure that opening) have been suggested as a strategy of prioritizing water conservation over CO_2 uptake. In our work, the relatively conserved ratio of K_i:K_d (at all growth stages) in all the cultivars studied indicates a balance between carbon gain and water conservation. However, although the time constant for opening and closure were comparable, the fact that T_{iWUE} was significantly higher than $T_{95\%A}$ indicates that slow g_s responses had a greater impact on $_iWUE$ than A. While the varieties studied in this work are adapted to a north–west European environment (Mackay et al., 2014), and therefore likely optimized for carbon gain rather than $_iWUE$, wheat cultivars adapted to lower rainfall regimes may provide a more extensive natural diversity for water conservation (i.e., faster stomatal closure rather than opening). To our knowledge, this is the first report demonstrating natural variation in the speed of stomatal responses in wheat at the leaf level. However, new cutting-edge technologies, for example whole plant gas-exchange (Jauregui et al., 2018), would enable the impact of the speed of stomatal responses on whole plant net carbon assimilation and water use to be evaluated. Cultivars with fast g_s responses (e.g., Claire, Robigus, and Hereward) were followed by lower A and g_s values thus showing potential elevated adaptation to dynamic light environment and potentially water deficit conditions. In contrast, Soissons and Xi19 demonstrated high overall g_s values, but slow g_s responses, traits that may be useful for environments in which light is high and constant with higher temperatures but with sufficient water to support high g_s and evaporative cooling. These data suggest that phenotyping wheat lines for stomatal rapidity has the potential to identify novel targets for improving wheat productivity for exploitation in breeding programs.

Photosynthetic Capacity and Speed of Stomatal Responses

In our study, a significant variation for V_{cmax} and steady-state A and g_s was found between cultivars, consistent with previous studies in wheat (e.g., Driever et al., 2014; Gaju et al., 2016). However, cultivars with greater g_s rapidity displayed lower photosynthetic capacity demonstrated by the positive relationship between A and g_s with $T_{95\%A}$, and the time constants for stomatal opening and closing (K_i and K_d), respectively. This suggests a compromise between the rapidity of stomatal behavior and the values of steady state A and g_s achieved. Stomatal movement involves a series of hierarchical processes based on the transport, accumulation, and release of osmotically active solutes (Lawson and Blatt, 2014) as well as subsidiary cell physiology (Raissig et al., 2017), and any variation in these processes could result in differences in stomatal behavior. For

example, variation in vascular connectivity (e.g., vein density) could explain the positive relationship between steady state A and g_s and the speed of g_s. Feldman et al. (2017) recently showed stronger photosynthetic performance in rice with increased leaf vein densities via mutagenesis. It is therefore conceivable that concurrent improvements for stomatal rapidity, photosynthetic capacity and for maximum A and g_s could be attained if vein density and hydraulic efficiency were improved.

Leaf Age Affects the Rapidity of g_s in Wheat

A novel finding of this work is the significant effect of growth stage on stomatal responses. The rapidity of g_s was reduced at post-anthesis stage (GS71) compared to the earlier developmental stages (GS31 and GS41) and this corresponded with a significant decrease in both steady-state A and g_s. The decrease in post-anthesis photosynthetic capacity, and therefore reduction in radiation use-efficiency in cereals, has been reported previously (Bingham et al., 2007; Carmo-Silva et al., 2017), and mainly attributed to the onset of leaf senescence (Gaju et al., 2016). The activation of the senescence signaling pathway, thought to be triggered by sink feedback (e.g., Bingham et al., 2007), leads to degradation of chlorophyll and Rubisco and subsequent re-allocation of nutrients from the senescing parts (i.e., leaves) to the growing sink (i.e., grain), thus leading to reduction in the efficiency of the source (Camargo et al., 2016).

TABLE 1 | Stomatal density and pore length for wheat flag leaf analyzed on both the abaxial and the adaxial surface (n = 6) and in the eight wheat cultivars.

	Abaxial stomatal density (mm^{-2})	Adaxial stomatal density (mm^{-2})	Abaxial pore length (μm)	Adaxial pore length (μm)
Alchemy	65.6 a	77.9 bc	29.9 bc	31.3 cd
Brompton	81.6 c	90.4 d	25.4 a	26.2 a
Claire	64.2 a	78.1 bc	27.0 ab	28.5 abc
Hereward	76.6 bc	80.3 bcd	24.3 a	27.2 ab
Rialto	65.6 a	73.4 b	26.5 ab	28.5 abc
Robigus	68.7 ab	61.0 a	27.4 abc	30.7 bcd
Soissons	63.7 a	88.3 cd	28.6 abc	32.7 d
Xi19	63.7 a	72.4 b	31.5 c	33.7 d
d.f.	40	40	40	40
P-value	0.002	<0.001	=0.013	=0.001

Data were analyzed by using one-way ANOVA and different letters represent significant differences according to Duncan's test.

However, to our knowledge, this is the first report showing developmental effects on stomatal responses to changes in light intensity. In particular, the data highlight growth stage- and genotype-dependent variation in stomatal rapidity, and the importance of taking into account these variables when quantifying dynamic stomatal traits. Additionally, periods of low precipitation and/or high temperature are more common during the post-anthesis stage, often leading to significant

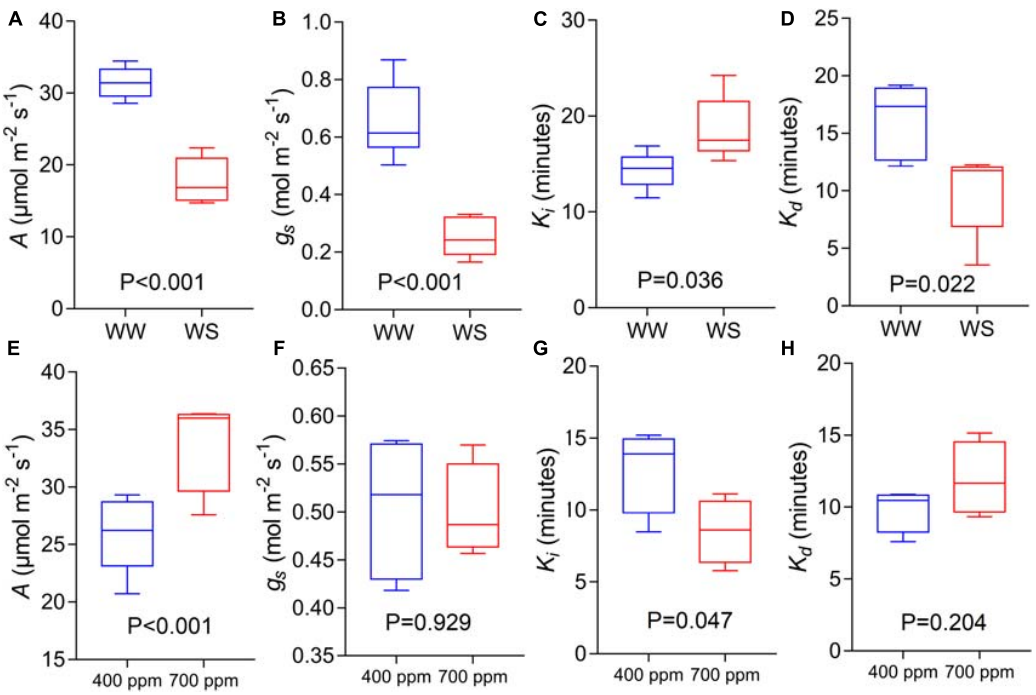

FIGURE 8 | CO_2 assimilation rate at saturating light after 60 min of induction at 1500 μmol m^{-2} s^{-1} PPFD **(A,E**, A), stomatal conductance at saturating light after 60 min of induction at 1500 μmol m^{-2} s^{1} PPFD **(B,F**, g_s), time constant for stomatal opening **(C,G**, K_i), and time constant for stomatal closing **(D,H**, K_d) estimated from step-changes in light collected in Experiments 2 and 3 (well-watered conditions and reduced water availability, WW and WS respectively, **A–D**; ambient and elevated atmospheric [CO_2] conditions, 400 and 700 μmol mol^{-1} respectively, **E–H**) collected at GS45-51 and GS31 respectively on cv. Soissons. Data were analyzed with one-way ANOVA and shown as means (n = 4–6 ± standard error of the means).

yield reductions. Faster stomatal opening could facilitate greater utilization of sudden increases in irradiance, and thus not only provide more assimilates for grain filling, but avoid any potential damage from excess excitation pressure (Yamasaki et al., 2002). Increased A is particularly important in view of the potential source-limitation (or at least source-sink co-limitation), which has been reported during grain filling in several wheat cultivars (Álvaro et al., 2008; Acreche and Slafer, 2009). Additionally, as wheat is extremely sensitive to temperature (Yamasaki et al., 2002) rapid g_s responses to increasing irradiance will facilitate maintenance of nearer optimal leaf temperatures to support maximum photosynthetic performance (Lawson and Vialet-Chabrand, 2018).

On the other hand, water conservation strategies would be enhanced by faster stomatal closure when carbon gain is reduced (e.g., during high to low light transition), thus improving the water-use budget and helping to reduce early soil water exhaustion (Bodner et al., 2015). For example, Hereward, Claire, and Robigus showed very quick g_s responses overall with minimal developmental effects (apart from Hereward at GS71), thus being good candidates for breeding exploitation for stomatal rapidity. The fact that a significant variation was observed for K_i, as well as a stage × genotype interaction for K_d and T_{iWUE}, suggests that the targeted exploitation of existing natural variation could be used to facilitate carbon gain for photosynthesis and optimize water-use under dynamic field environments and at different stages of wheat development.

Water Stress and Elevated CO_2 Concentration Affects Stomatal Rapidity

The effect of elevated [CO_2] and water stress on stomatal rapidity has received little attention to date. A recent report on *Arundo donax* (Haworth et al., 2018), showed that water stress increases the rapidity of stomatal closure and reduced the speed of opening, consistent with our data in wheat. Similarly, in Lawson and Blatt (2014), *Vicia faba* plants subjected to water stress showed a faster g_s reduction during a shade fleck whilst a slower g_s increase was recorded for a sun fleck. However, recent work by Gerardin et al. (2018) reported an increase in rapidity for both the opening and the closing phase in *Nicotiana tabacum* under reduced water availability. It should be noted that in *N. tabacum* a strong asymmetry between the opening and closing phase (due to a faster closing phase) under control conditions was also reported. Under optimal soil water availability, asymmetric stomatal responses have not been previously described in wheat (e.g., McAusland et al., 2016), thus suggesting that the opening/closing ratio under optimal growth conditions might be species-specific and strongly influenced by water status. Thus, the presence of asymmetric stomatal responses under stress conditions could be considered as: (1) an adaptation to reduce water loss (stronger coordination between A and g_s) and (2) a mechanism to limit increasing g_s after steady state A has been achieved (McAusland et al., 2016). Our data suggests that both possibilities are conceivable under reduced water availability, with both high K_i and low K_d values observed in wheat. Water stress therefore exacerbates conservative responses under dynamic light in wheat allowing further opportunities for adaptation to reduced water availability conditions.

Only a handful of studies have examined the effect of atmospheric [CO_2] on stomatal kinetics, with most research focusing on the effects for steady stage g_s or changes in stomatal anatomy (Ainsworth and Rogers, 2007). Leakey et al. (2002) reported that in *Shorea leprosula*, the relative enhancement of biomass driven by elevated [CO_2] was greater under dynamic irradiance compared to uniform irradiance. Consistent with our findings in wheat, Leakey et al. (2002) suggested that faster stomatal opening under dynamic conditions reduced the time to reach maximum g_s and reduced CO_2 limitation of A. Therefore, a faster stomatal opening phase (in response to an increase in irradiance) might be a leaf trait that has an additional positive effect under elevated [CO_2] that deserves further investigation at the field level. Further efforts should focus on understanding and quantifying the effects of these major environmental factors on stomatal dynamics under fluctuating light environments.

CONCLUSION

To our knowledge, this is the first report showing significant genotypic variation in wheat for the rapidity of stomatal responses. Our work illustrates that slow g_s responses can limit A during a low to high light transition by 7–15%, while slow reduction of g_s during a high to low light transition strongly limits water conservation. Measurements obtained post-anthesis suggest that leaf age might exacerbate stomatal limitations by reducing the rapidity of stomatal responses, whilst environmental cues (i.e., water stress and [CO_2]) also affected this. Evidence of significant genotypic variation for these traits highlights them as novel and as yet unexploited targets for crop improvement programs, which aim to develop cultivars that maximize photosynthesis and minimize the waste of water in the dynamic light environments encountered in the field. This work lends to a greater understanding of the interactions between stomatal behavior, environmental cues and leaf performance, which guides the establishment of ideotypes for specific growth environments. For example, the cultivar Hereward demonstrated fast g_s responses at GS 31 and 41 and minimal limitation of A, with potential for exploitation to provide ideotypes for environments in which conservation of water use is a priority. On the other hand, cultivars such as Soissons and Xi19 demonstrated high photosynthetic capacity, high overall g_s values, but slow g_s responses, traits that may be useful for high-light and high-temperature environments. Improvement of stomatal responses under a dynamic light environment might support the optimization of resource use and yield in major crops, and therefore inform the development of new crop ideotypes with higher yield potential and resilience to future environmental changes.

AUTHOR CONTRIBUTIONS

MF and TL design the experiments, analyzed the data, and wrote the manuscript. MF executed all the experiments and acquired

all the data. SW analyzed stomatal density and pore length. JC, EO, AG, CR, and JVR helped with interpretation of data and edit the manuscript. TL, JC, EO, and CR acquired project funding and resources.

FUNDING

MF was supported by Biotechnology and Biological Sciences Research Council (BBSRC) grants to TL (BB/NO16831/1) and JC (BB/N01698X/1), with IPA co-funding from BASF. SW was supported through a BBSRC Industrial Studentship (1775930) award to BASF (JVR), Essex (TL), and NAIB (JC). Dr. Silvère Vialet-Chabrand was acknowledged for the development of the R scripts.

SUPPLEMENTARY MATERIAL

The Supplementary Material for this article can be found online at: https://www.frontiersin.org/articles/10.3389/fpls.2019.00492/full#supplementary-material

TABLE S1 | Duncan's multiple comparisons test output carried out for the gas-exchange data in Experiment 1. The test was performed on both "cultivar" and "stage" factors. In the analysis of the factor "stage", vegetative, flag, and heading represents GS31, 41, and 71 respectively.

REFERENCES

Acreche, M. M., and Slafer, G. A. (2009). Grain weight, radiation interception and use efficiency as affected by sink-strength in Mediterranean wheats released from 1940 to 2005. *Field Crop. Res.* 110, 98–105. doi: 10.1016/j.fcr.2008.07.006

Ainsworth, E. A., and Rogers, A. (2007). The response of photosynthesis and stomatal conductance to rising [CO2]: mechanisms and environmental interactions. *Plant Cell Environ.* 30, 258–270. doi: 10.1111/j.1365-3040.2007.01641.x

Álvaro, F., Royo, C., García del Moral, L. F., and Villegas, D. (2008). Grain filling and dry matter translocation responses to source–sink modifications in a historical series of durum wheat. *Crop Sci.* 48, 1523–1531. doi: 10.2135/cropsci2007.10.0545

Bingham, I. J., Blake, J., Foulkes, M. J., and Spink, J. (2007). Is barley yield in the UK sink limited?: I. Post-anthesis radiation interception, radiation-use efficiency and source–sink balance. *Field Crop. Res.* 101, 198–211. doi: 10.1111/pce.12801

Bodner, G., Nakhforoosh, A., and Kaul, H. P. (2015). Management of crop water under drought: a review. *Agron. Sustain. Dev.* 35, 401–442. doi: 10.1007/s13593-015-0283-4

Camargo, A. V., Mott, R., Gardner, K. A., Mackay, I. J., Corke, F., Doonan, J. H., et al. (2016). Determining phenological patterns associated with the onset of senescence in a wheat MAGIC mapping population. *Front. Plant Sci.* 7:1540. doi: 10.3389/fpls.2016.01540

Carmo-Silva, E., Andralojc, P. J., Scales, J. C., Driever, S. M., Mead, A., Lawson, T., et al. (2017). Phenotyping of field-grown wheat in the UK highlights contribution of light response of photosynthesis and flag leaf longevity to grain yield. *J. Exp. Bot.* 68, 3473–3486. doi: 10.1093/jxb/erx169

Drake, P. L., Froend, R. H., and Franks, P. J. (2013). Smaller, faster stomata: scaling of stomatal size, rate of response, and stomatal conductance. *J. Exp. Bot.* 64, 495–505. doi: 10.1093/jxb/ers347

Driever, S. M., Lawson, T., Andralojc, P. J., Raines, C. A., and Parry, M. A. (2014). Natural variation in photosynthetic capacity, growth, and yield in 64 field-grown wheat genotypes. *J. Exp. Bot.* 65, 4959–4973. doi: 10.1093/jxb/eru253

Driever, S. M., Simkin, A. J., Alotaibi, S., Fisk, S. J., Madgwick, P. J., Sparks, C. A., et al. (2017). Increased SBPase activity improves photosynthesis and grain yield in wheat grown in greenhouse conditions. *Phil. Trans. R. Soc. B.* 372:20160384. doi: 10.1098/rstb.2016.0384

Evans, L. T. (1996). *Crop Evolution, Adaptation and Yield*. Cambridge: Cambridge Univ. Press.

Faralli, M., Matthews, J., and Lawson, T. (2019). Exploiting natural variation and genetic manipulation of stomatal conductance for crop improvement. *Curr. Opin. Plant Biol.* 49, 1–7. doi: 10.1016/j.pbi.2019.01.003

Feldman, A. B., Leung, H., Baraoidan, M., Elmido-Mabilangan, A., Canicosa, I., Quick, W. P., et al. (2017). Increasing leaf vein density via mutagenesis in rice results in an enhanced rate of photosynthesis, smaller cell sizes and can reduce interveinal mesophyll cell number. *Front. Plant Sci.* 8:1883. doi: 10.3389/fpls.2017.01883

Gaju, O., DeSilva, J., Carvalho, P., Hawkesford, M. J., Griffiths, S., Greenland, A., et al. (2016). Leaf photosynthesis and associations with grain yield, biomass and nitrogen-use efficiency in landraces, synthetic-derived lines and cultivars in wheat. *Field Crop. Res.* 193, 1–15. doi: 10.1016/j.fcr.2016.04.018

Gardner, K. A., Wittern, L. M., and Mackay, I. J. (2016). A highly recombined, high-density, eight-founder wheat MAGIC map reveals extensive segregation distortion and genomic locations of introgression segments. *Plant Biotechnol. J.* 14, 1406–1417. doi: 10.1111/pbi.12504

Gerardin, T., Douthe, C., Flexas, J., and Brendel, O. (2018). Shade and drought growth conditions strongly impact dynamic responses of stomata to variations in irradiance in *Nicotiana tabacum*. *Environ. Exp. Bot.* 153, 188–197. doi: 10.1016/j.envexpbot.2018.05.019

Haworth, M., Marino, G., Cosentino, S. L., Brunetti, C., De Carlo, A., Avola, G., et al. (2018). Increased free abscisic acid during drought enhances stomatal sensitivity and modifies stomatal behaviour in fast growing giant reed (*Arundo donax* L.). *Environ. Exp. Bot.* 147, 116–124. doi: 10.1016/j.envexpbot.2017.11.002

Jauregui, I., Rothwell, S. A., Taylor, S. H., Parry, M. A., Carmo-Silva, E., and Dodd, I. C. (2018). Whole plant chamber to examine sensitivity of cereal gas exchange to changes in evaporative demand. *Plant Methods* 14:97. doi: 10.1186/s13007-018-0357-9

King, C. A., and Purcell, L. C. (2017). Evaluation of methods for estimating transpiration response to soil drying for container-grown plants. *Crop Sci.* 57, 2143–2148. doi: 10.2135/cropsci2016.12.1000

Lancashire, P. D., Bleiholder, H., Boom, T. V. D., Langelüddeke, P., Stauss, R., Weber, E., et al. (1991). A uniform decimal code for growth stages of crops and weeds. *Ann. Appl. Biol.* 119, 561–601. doi: 10.1111/j.1744-7348.1991.tb04895.x

Lawson, T., and Blatt, M. R. (2014). Stomatal size, speed, and responsiveness impact on photosynthesis and water use efficiency. *Plant Phys.* 164, 1556–1570. doi: 10.1104/pp.114.237107

Lawson, T., Kramer, D. M., and Raines, C. A. (2012). Improving yield by exploiting mechanisms underlying natural variation of photosynthesis. *Current Opin. Biotechnol.* 23, 215–220. doi: 10.1016/j.copbio.2011.12.012

Lawson, T., Simkin, A. J., Kelly, G., and Granot, D. (2014). Mesophyll photosynthesis and guard cell metabolism impacts on stomatal behaviour. *New Phytol.* 203, 1064–1081. doi: 10.1111/nph.12945

Lawson, T., and Vialet-Chabrand, S. (2018). Speedy stomata, photosynthesis and plant water use efficiency. *New Phytol.* 221, 93–98. doi: 10.1111/nph.15330

Lawson, T., von Caemmerer, S., and Baroli, I. (2010). "Photosynthesis and stomatal behaviour," in *Progress in Botany*, eds U. E. Luttge, W. Beyschlag, B. Budel, and D. Francis (Berlin: Springer), 265–304.

Leakey, A. D. B., Press, M. C., Scholes, J. D., and Watling, J. R. (2002). Relative enhancement of photosynthesis and growth at elevated CO2 is greater under sunflecks than uniform irradiance in a tropical rain forest tree seedling. *Plant Cell Environ.* 25, 1701–1714. doi: 10.1046/j.1365-3040.2002.00944.x

Long, S. P., Zhu, X. G., Naidu, S. L., and Ort, D. R. (2006). Can improvement in photosynthesis increase crop yields? *Plant Cell Environ.* 29, 315–330.

Mackay, I. J., Bansept-Basler, P., Barber, T., Bentley, A. R., Cockram, J., Gosman, N., et al. (2014). An eight-parent multiparent advanced generation inter-cross population for winter-sown wheat: creation, properties, and validation. *Genes Genom. Genet.* 4, 1603–1610. doi: 10.1534/g3.114.012963

McAusland, L., Vialet-Chabrand, S., Davey, P., Baker, N. R., Brendel, O., and Lawson, T. (2016). Effects of kinetics of light-induced stomatal responses on

photosynthesis and water-use efficiency. *New Phytol.* 211, 1209–1220. doi: 10.1111/nph.14000

Outlaw, W. H. Jr. (2003). Integration of cellular and physiological functions of guard cells. *Crit. Rev. Plant Sci.* 22, 503–529. doi: 10.1080/713608316

Qu, M., Hamdani, S., Li, W., Wang, S., Tang, J., Chen, Z., et al. (2016). Rapid stomatal response to fluctuating light: an under-explored mechanism to improve drought tolerance in rice. *Funct. Plant Biol.* 43, 727–738. doi: 10.1071/FP15348

Raissig, M. T., Matos, J. L., Gil, M. X. A., Kornfeld, A., Bettadapur, A., Abrash, E., et al. (2017). Mobile MUTE specifies subsidiary cells to build physiologically improved grass stomata. *Science* 355, 1215–1218. doi: 10.1126/science.aal3254

Ray, D. K., Mueller, N. D., West, P. C., and Foley, J. A. (2013). Yield trends are insufficient to double global crop production by 2050. *PLoS One* 8:e66428. doi: 10.1371/journal.pone.0066428

Ray, D. K., Ramankutty, N., Mueller, N. D., West, P. C., and Foley, J. A. (2012). Recent patterns of crop yield growth and stagnation. *Nat. Commun.* 3:1293. doi: 10.1038/ncomms2296

Salter, W. T., Merchant, A. M., Richards, R. A., Trethowan, R., and Buckley, T. N. (2019). Rate of photosynthetic induction in fluctuating light varies widely among genotypes of wheat. *J. Exp. Bot.* doi: 10.1093/jxb/erz100 [Epub ahead of print].

Sharkey, T. D., Bernacchi, C. J., Farquhar, G. D., and Singsaas, E. L. (2007). Fitting photosynthetic carbon dioxide response curves for C3 leaves. *Plant Cell Environ.* 30, 1035–1040. doi: 10.1111/j.1365-3040.2007.01710.x

Slafer, G. A., Elia, M., Savin, R., García, G. A., Terrile, I. I., Ferrante, A., et al. (2015). Fruiting efficiency: an alternative trait to further rise wheat yield. *Food Energy Secur.* 4, 92–109. doi: 10.1002/fes3.59

Slattery, R. A., Walker, B. J., Weber, A. P., and Ort, D. R. (2018). The impacts of fluctuating light on crop performance. *Plant Phys.* 176, 990–1003. doi: 10.1104/pp.17.01234

Taylor, S. H., and Long, S. P. (2017). Slow induction of photosynthesis on shade to sun transitions in wheat may cost at least 21% of productivity. *Phil. Trans. R. Soc. B.* 372:20160543. doi: 10.1098/rstb.2016.0543

Vialet-Chabrand, S., Dreyer, E., and Brendel, O. (2013). Performance of a new dynamic model for predicting diurnal time courses of stomatal conductance at the leaf level. *Plant Cell Environ.* 3, 1529–1546. doi: 10.1111/pce.12086

Vialet-Chabrand, S., and Lawson, T. (2019). Dynamic leaf energy balance: deriving stomatal conductance from thermal imaging in a dynamic environment. *J. Exp. Bot.* doi: 10.1093/jxb/erz068 [Epub ahead of print].

Vialet-Chabrand, S. R., Matthews, J. S., McAusland, L., Blatt, M. R., Griffiths, H., and Lawson, T. (2017). Temporal dynamics of stomatal behaviour: modelling and implications for photosynthesis and water use. *Plant Phys.* 174, 603–613. doi: 10.1104/pp.17.00125

Vico, G., Manzoni, S., Palmroth, S., and Katul, G. (2011). Effects of stomatal delays on the economics of leaf gas exchange under intermittent light regimes. *New Phytol.* 192, 640–652. doi: 10.1111/j.1469-8137.2011.03847.x

Weldearegay, D. F., Yan, F., Rasmussen, S. K., Jacobsen, S. E., and Liu, F. (2016). Physiological response cascade of spring wheat to soil warming and drought. *Crop Pasture Sci.* 67, 480–488. doi: 10.1071/CP15211

Weyers, J. D., and Johansen, L. G. (1985). Accurate estimation of stomatal aperture from silicone rubber impressions. *New Phytol.* 101, 109–115. doi: 10.1111/j.1469-8137.1985.tb02820.x

Yamasaki, T., Yamakawa, T., Yamane, Y., Koike, H., Satoh, K., and Katoh, S. (2002). Temperature acclimation of photosynthesis and related changes in photosystem II electron transport in winter wheat. *Plant Phys.* 128, 1087–1097. doi: 10.1104/pp.010919

Zelitch, I. (1982). The close relationship between net photosynthesis and crop yield. *Bioscience* 32, 796–802. doi: 10.2307/1308973

Conflict of Interest Statement: The authors declare that the research was conducted in the absence of any commercial or financial relationships that could be construed as a potential conflict of interest.

frontiers in Plant Science

REVIEW
published: 06 March 2019
doi: 10.3389/fpls.2019.00225

Impact of Stomatal Density and Morphology on Water-Use Efficiency in a Changing World

*Lígia T. Bertolino[1,2], Robert S. Caine[2] and Julie E. Gray[2]**

[1]Grantham Centre for Sustainable Futures, University of Sheffield, Sheffield, United Kingdom, [2]Department of Molecular Biology and Biotechnology, University of Sheffield, Sheffield, United Kingdom

Global warming and associated precipitation changes will negatively impact on many agricultural ecosystems. Major food production areas are expected to experience reduced water availability and increased frequency of drought over the coming decades. In affected areas, this is expected to reduce the production of important food crops including wheat, rice, and maize. The development of crop varieties able to sustain or improve yields with less water input is, therefore, a priority for crop research. Almost all water used for plant growth is lost to the atmosphere by transpiration through stomatal pores on the leaf epidermis. By altering stomatal pore apertures, plants are able to optimize their CO_2 uptake for photosynthesis while minimizing water loss. Over longer periods, stomatal development may also be adjusted, with stomatal size and density being adapted to suit the prevailing conditions. Several approaches to improve drought tolerance and water-use efficiency through the modification of stomatal traits have been tested in the model plant *Arabidopsis thaliana*. However, there is surprisingly little known about the stomata of crop species. Here, we review the current understanding of how stomatal number and morphology are involved in regulating water-use efficiency. Moreover, we discuss the potential and limitations of manipulating stomatal development to increase drought tolerance and to reduce water loss in crops as the climate changes.

Keywords: water-use efficiency, stomatal conductance, stomatal density and size, drought response, crops

OPEN ACCESS

Edited by:
Michael Vincent Mickelbart, Purdue University, United States

Reviewed by:
Fulai Liu, University of Copenhagen, Denmark
Jeroni Galmes, Universitat de les Illes Balears, Spain

****Correspondence:***
Julie E. Gray
j.e.gray@sheffield.ac.uk

Specialty section:
This article was submitted to Plant Physiology, a section of the journal Frontiers in Plant Science

Received: *28 September 2018*
Accepted: *11 February 2019*
Published: *06 March 2019*

Citation:
Bertolino LT, Caine RS and Gray JE (2019) Impact of Stomatal Density and Morphology on Water-Use Efficiency in a Changing World. Front. Plant Sci. 10:225. doi: 10.3389/fpls.2019.00225

INTRODUCTION

Changes in climate are already negatively affecting the yields of staple crops in agricultural areas around the world (Lobell et al., 2011; IPCC, 2014). As the globe continues to warm, changes in the hydrological cycles are, in general, increasing aridity and the incidence of droughts (Dai, 2013; Sherwood and Fu, 2014). Agriculture will need to adapt quickly to ensure that water is used more efficiently, while maintaining food security in a world where human population is rapidly growing. Sustainable and climate-smart management of water, land, and biodiversity will be important for achieving these objectives (discussed in Howden et al., 2007; Campbell et al., 2014; Lipper et al., 2014; Iglesias and Garrote, 2015). Moreover, the development of crop varieties that have improved water-use efficiency (WUE) under predicted future climates will also be critical (Flexas, 2016; Varshney et al., 2018). WUE can be estimated at different scales; at an agronomic level, it is described as the ratio of water used in crop production versus

biomass or yield (Condon et al., 2004; Medrano et al., 2015). From a plant physiology point of view, and as it will be primarily addressed here, WUE is the amount of CO_2 fixed in photosynthesis (A) relative to the amount of water vapor lost to the atmosphere (Willmer and Fricker, 1996; Condon et al., 2004; Bacon, 2004). As stomata play a fundamental role in regulating plant water use and carbon gain, they present a key target for improving WUE. Here, we review how changes in stomatal developmental traits can affect plant WUE and also drought tolerance.

Stomata are microscopic structures consisting of a pair of specialized guard cells that surround a central pore. They are found on aerial surfaces of most plants, providing access to mesophyll cells (Zeiger et al., 1987; Hetherington and Woodward, 2003). By actively adjusting guard cell turgor pressure, plants can alter stomatal pore aperture, thereby moderating gas exchange rates between the leaf interior and the atmosphere (Zeiger et al., 1987; Kollist et al., 2014). Increases in guard cell turgor pressure lead to a greater stomatal pore aperture, which enhances the rates of CO_2 uptake for A and of water loss, *via* a process termed stomatal conductance (g_s) (Condon et al., 2002; Hetherington and Woodward, 2003). On the other hand, reductions in guard cell turgor pressure lead to decreases in stomatal aperture and in g_s. The signals governing the fluxes of CO_2 and water to and from the plant mesophyll are highly coordinated, allowing plants to finely balance the need for carbon with the need to moderate water loss (Wong et al., 1979; Haworth et al., 2016; Sorrentino et al., 2016). This internal crosstalk is influenced by many environmental factors, including changes in temperature, light intensity, atmospheric CO_2 concentration, air humidity, and soil moisture content (Farquhar and Sharkey, 1982; Schroeder et al., 2001; Mott, 2009; Assmann and Jegla, 2016; Chaves et al., 2016). For example, when water becomes limited, signals such as reduced hydraulic conductivity and increased abscisic acid (ABA) arise, causing guard cell turgor pressure decreases, which result in reduced stomatal aperture and g_s (Schroeder et al., 2001; Mustilli, 2002; Tombesi et al., 2015; Bartlett et al., 2016; McAdam et al., 2016). These changes lead to an improved water conservation, but often at the expense of A (Flexas and Medrano, 2002). Conversely, when water is plentiful in the soil or air, guard cell turgor increases, leading to increases in stomatal pore aperture and in g_s, with A also often increasing.

Over longer periods, external signals perceived by mature leaves can also lead to systemic responses that moderate stomatal development on the new leaf epidermis, resulting in changes in stomatal patterning (Casson and Gray, 2008; Casson et al., 2010; Pillitteri and Torii, 2012; Chater et al., 2014; Qi and Torii, 2018).

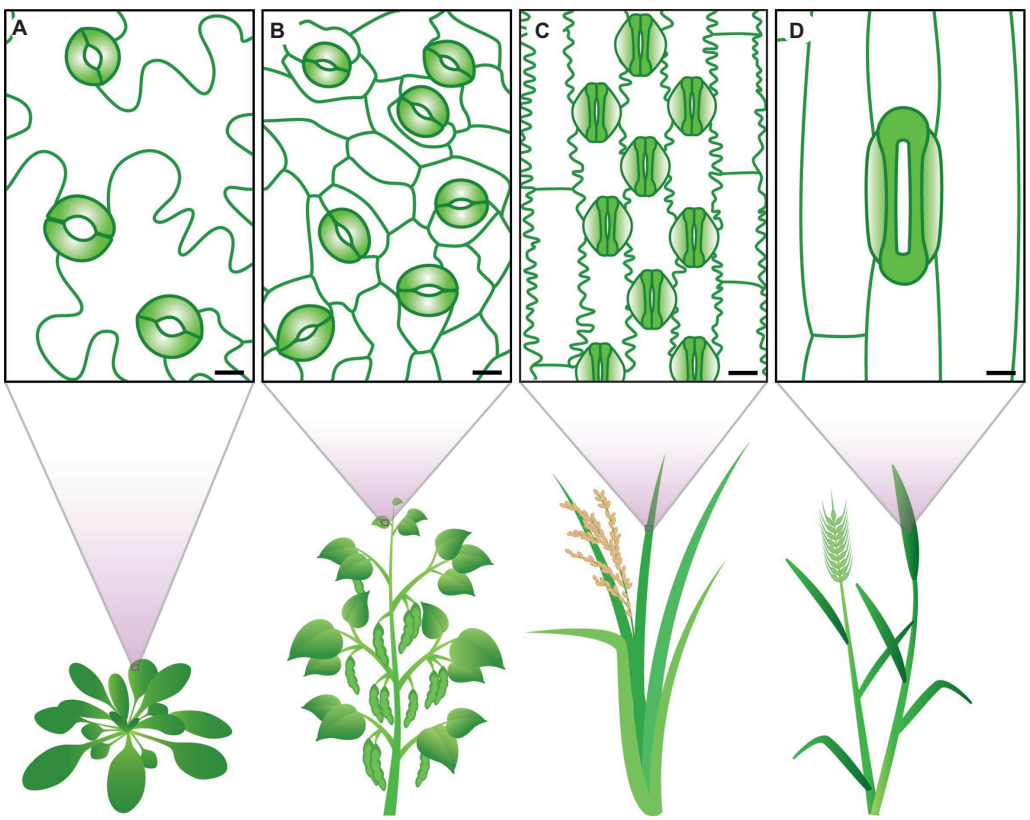

FIGURE 1 | Stomatal traits vary between species. The eudicots **(A)** *Arabidopsis thaliana* and **(B)** *Phaseolus vulgaris* display kidney-shaped guard cells (colored in green). The grasses **(C)** *Oryza sativa* and **(D)** *Triticum aestivum* show dumbbell-shaped guard cells (solid green) and specialized subsidiary cells (light green gradient). Clear differences in stomatal size and stomatal density can be observed. Scale bars 10 μM.

Exposure of mature leaves to high CO_2 or low light levels, for example, is known to cause reductions in stomatal density (*SD,* number of stomata per unit of area) and in stomatal index (*SI*, ratio of stomata to epidermal cells plus stomata, multiplied by 100) of new developing leaves (Lake et al., 2001; Miyazawa et al., 2006). Conversely, low CO_2 and high light generally have the opposite effect. The impact of water availability on stomatal development is less understood, with mixed responses and differences among species being reported (Clifford et al., 1995; Xu and Zhou, 2008; Doheny-Adams et al., 2012; Sun et al., 2014; Zhao et al., 2015). In Arabidopsis, plants grown under water restriction do not show altered *SD*; however, reductions in stomatal size (*SS*, guard cell area, based on guard cell pair length and width) were observed (Doheny-Adams et al., 2012). These plastic modulations of number and size of stomata allow plants to adjust their stomatal pore area in response to the surrounding environment, ultimately affecting their maximum and minimum gas exchange.

Stomata exhibit a diverse range of shapes, sizes, and numbers across different plant species (**Figure 1**). There are profound differences in how the stomata of different groups develop and are patterned on the epidermis (Sack, 1994; Caine et al., 2016; Raissig et al., 2016; Rudall et al., 2017). Morphological differences include *SD*, *SS*, guard cell shape, and presence or absence of subsidiary cells. All of these parameters have the potential to influence stomatal movement and, consequently, plant *A*, g_s, and WUE. Over evolutionary time, various stomatal traits have altered, potentially aiding in adapting plant species to new environments (Taylor et al., 2012; Drake et al., 2013; Haworth et al., 2018). Eudicots, for example, typically have kidney-shaped stomata that are formed on the leaf epidermis without a pre-determined location (MacAlister et al., 2007; Pillitteri and Dong, 2013). While in monocots, stomata can either be kidney-shaped or, as with the grasses, be composed of dumbbell-shaped stomata with neighboring subsidiary cells, collectively termed a stomatal complex (Rudall et al., 2017). In grasses, stomatal development is constrained to the leaf base, with stomatal pores being formed in specified cell files adjacent to veins (Stebbins and Shah, 1960; Rudall et al., 2013; Hepworth et al., 2018).

Although stomatal behavior, patterning and morphology are important factors that contribute to WUE (Lawson and Blatt, 2014; Lawson and Vialet-Chabrand, 2019), relatively little is known about how targeted modifications of stomatal traits affect physiological responses in crop plants, especially in field experiments. Efforts to improve WUE have often led to decreases in yield (Flexas, 2016). By attempting to alter stomatal features to improve water conservation, reductions in g_s may arise, potentially leading to detrimental effects on *A*, evaporative cooling, and plant fertility. However, recent findings suggest that under at least some greenhouse and controlled environment growth conditions, changing stomatal traits may improve WUE without such undesirable yield penalties (Yu et al., 2013; Hughes et al., 2017; Caine et al., 2019). While these studies are encouraging, they offer only a snapshot of how plants with modifications in stomatal features might perform. Here, we discuss our current understanding of how alterations in *SS*, *SD,* and stomatal morphology contribute to altered WUE and drought tolerance with particular emphasis on the latest advances in crop species.

VARIATION IN *SS* AND *SD* INFLUENCES GASEOUS EXCHANGE AND WUE

Dynamic adjustments to the opening degree of stomatal pores are responsible for regulating g_s in the short term, allowing plants to quickly reduce water loss according to external cues (Farquhar and Sharkey, 1982). Over a longer term, anatomical adjustments, such as changes to *SS* and *SD*, can modify the range of g_s by altering the maximum stomatal conductance (g_{smax}) (Franks et al., 2009; Dow et al., 2014a). G_{smax} refers to the maximal potential gas exchange in a state where all stomata are fully open. It is a theoretical estimate that is calculated using empirical stomatal anatomical measurements, including *SD*, stomatal pore depth (estimated as guard cell width), and maximum stomatal pore area (calculated based on pore length) (Franks and Beerling, 2009; Dow and Bergmann, 2014; Sack and Buckley, 2016). Despite operating g_s normally being significantly lower than its maximum capacity (Fanourakis et al., 2015; McElwain et al., 2016), measured g_s positively correlates with calculated g_{smax} (Franks et al., 2009). Furthermore, it is suggested that adaptations in g_{smax} allow plants to adjust their operating gas exchange rates while maintaining guard cells turgor pressure in an optimum state. This is believed to provide better stomatal sensitivity and rapid adjustment of aperture response (Franks et al., 2012; Dow and Bergmann, 2014). Therefore, although *SS* and *SD* are not the only variables determining leaf gas exchange, changes to these stomatal traits do permit plants to adjust both *A* and water use (Franks et al., 2009; Franks and Beerling, 2009; de Boer et al., 2011; Dow et al., 2014a).

Variation in size and density of stomata may arise due to genetic factors and/or growth under different environmental conditions. A negative correlation has frequently been suggested between these two stomatal traits. This inverse relationship has been observed in plastic developmental responses to changes in environment and also during long-term evolutionary adaptation (Dilcher et al., 2000; Ohsumi et al., 2007; Franks et al., 2009, 2012; Franks and Beerling, 2009; Doheny-Adams et al., 2012; Taylor et al., 2012; Sun et al., 2014; Fanourakis et al., 2015; de Boer et al., 2016; Dittberner et al., 2018). Analysis of herbarium and fossilized plant remains suggest that *SS* and *SD* have changed in response to atmospheric CO_2 concentration over evolutionary time, probably to enable adjustments to g_{smax} and CO_2 diffusion into the leaf (Woodward, 1987; Dilcher et al., 2000; Franks and Beerling, 2009). In samples from periods when CO_2 concentrations were low, a reduction in *SS* and an increase in *SD* have been observed. On the other hand, when atmospheric CO_2 levels have been high, *SS* has increased and *SD* decreased. Such adaptive responses to CO_2 are also found in many extant lineages; however, this is not always the case in all species surveyed (Casson and Gray, 2008; Haworth et al., 2013; Field et al., 2015).

Although various combinations of *SS* and *SD* can result in similar alteration to g_{smax}, there are limitations as to how much

of the epidermis can be patterned by stomata. First, other functionally important leaf structures such as veins and trichomes are also absolutely required. Second, stomata need to be spaced by at least one epidermal cell to function efficiently (Franks and Farquhar, 2007; Dow et al., 2014b). Therefore, changes to *SS* and *SD* are limited to a finite portion of the epidermis (Franks et al., 2009; Franks and Beerling, 2009; de Boer et al., 2016). In general, plants optimize g_{smax} through investing in increases in *SD* coupled with reductions in *SS* (Franks and Beerling, 2009; de Boer et al., 2012). According to Franks and Beerling (2009) and Franks and Farquhar (2007), changes toward increased *SD* in combination with reduced *SS* could maintain or improve total pore area (due to increased *SD*) but can also provide a shorter diffusion path (due to the smaller pore depth), potentially resulting in improved gas exchange.

While small *SS* coupled with high *SD* often leads to a higher g_{smax}, it is also possible for g_{smax} to be reduced by a smaller *SS* alone. Decreases in g_{smax} due to a smaller *SS* have been associated with higher water conservation, as reported for plants exposed to drought (Doheny-Adams et al., 2012) and ABA treatment (Franks and Farquhar, 2001). Smaller stomata are also associated with improved WUE in *Arabidopsis thaliana* (Dittberner et al., 2018); and rice varieties with smaller *SS* have the ability to strongly decrease g_s under drought (Ouyang et al., 2017). Growth under low soil moisture conditions has been shown to cause a decrease in *SS* in several species (Xu and Zhou, 2008; Doheny-Adams et al., 2012; Sun et al., 2014; Zhao et al., 2015), but the effect on *SD* is less consistent (Clifford et al., 1995; Xu and Zhou, 2008; Doheny-Adams et al., 2012; Sun et al., 2014; Zhao et al., 2015). Stomatal size and density responses to vapor pressure deficit (VPD) are also variable. Under high VPD conditions, the woody angiosperm, *Toona ciliata*, displays smaller *SS* and higher *SD* (Carins Murphy et al., 2014), while tomato and sweet pepper show decreases in both stomatal traits (Bakker, 1991), and in poplar, changes in *SD* are dependent on CO_2 concentration. (Miyazawa et al., 2006). Thus, changes in *SS* and *SD* in response to soil moisture or VPD appear to be specific to species and environmental variables (Bakker, 1991; Miyazawa et al., 2006; Xu and Zhou, 2008; Sun et al., 2014). Nutrient availability can also affect plant development. However, as described for soil moisture and VPD responses, adjustments in stomatal development in response to nutrient availability appear to be variable with no consistent response emerging (Gao et al., 2006; Sekiya and Yano, 2008; Yan et al., 2012; Sun et al., 2014; Hepworth et al., 2016).

ARE SMALL STOMATA FASTER?

Small stomatal size can provide a reduction in total leaf pore area and might also facilitate faster aperture response (Franks and Beerling, 2009; Drake et al., 2013; Lawson and Blatt, 2014). The higher cell surface area to volume ratio of smaller cells is believed to permit faster ion fluxes, leading to faster guard cell turgor changes and a more rapid g_s response (Lawson and Vialet-Chabrand, 2019). This faster stomatal behavior in plants with smaller *SS* has been observed in response to changes in light intensity across species of *Banksia*, rainforest trees, and in cereal species with dumbbell-shaped guard cells (Drake et al., 2013; McAusland et al., 2016; Kardiman and Raebild, 2017). However, although rapid stomatal movements might help to maximize WUE under fluctuating light environments, this is unlikely to have much impact on water loss over long periods of water stress under field conditions.

SS is clearly not the only anatomical trait influencing stomatal behavior. The shape of guard cells and the presence of subsidiary cells are also suggested to impact on stomatal responses (as discussed in "Stomatal morphology and improved WUE" below). In addition, the distribution of stomata between leaf abaxial and adaxial surfaces may also affect plant responses to environmental stresses. For example, stomata on the abaxial surfaces of wheat leaves show a stronger decrease in g_s than adaxial stomata when they are exposed to water stress (Lu, 1989), and abaxial and adaxial stomata of cotton show differing responses to light quality (Lu et al., 1993). Moreover, as shown by Elliott-Kingston et al. (2016), Haworth et al. (2018), and McAusland et al. (2016), simple differences in *SS* do not always correlate with stomatal speed, especially when comparing distant taxa. Comparisons of cultivars or mutants of the same species with altered *SS*, but similar *SD*, would improve our understanding of the effect of guard cell size on speed of stomatal movement and explore if there is potential for *SS* as trait for improving WUE. Although a correlation between *SS* and genome size has been documented (Beaulieu et al., 2008; Jordan et al., 2015; Monda et al., 2016), the genetic and molecular mechanisms regulating *SS* remain unstudied, which currently limits our understanding of this trait.

TARGETED CHANGES IN *SD* LEADING TO ALTERATIONS IN WUE

Reductions in *SD* also have the potential to constrain g_s and transpiration (E), representing a shift towards a more conservative use of water. If not limiting A or evaporative cooling, this reduction in water loss should represent an advantage under low water availability scenarios. In comparison to *SS*, significant advances have been made in understanding the molecular signals regulating stomatal density and patterning, which allow the study of the physiological effects of altering *SD*. Stomatal development in *Arabidopsis thaliana* is controlled by a complex genetic network, of which the basic helix-loop-helix (bHLH) transcription factors SPCH, MUTE, and FAMA together with either ICE1/SCREAM (SCRM) or SCRM2 control the sequential cell fate transitions. Additionally, an intercellular signaling pathway that includes peptide ligands, leucine-rich repeat receptor kinases (LRR-RKs) and a MAPK cascade, regulates the activity of the bHLHs (reviewed in Bergmann and Sack, 2007; Vatén and Bergmann, 2012; Zoulias et al., 2018). This signaling network includes the secretory peptides EPIDERMAL PATTERNING FACTOR1 (EPF1), EPF2, and EPF-like 9. EPF1 and EPF2 both negatively regulate stomatal density, with EPF1 also preventing stomatal clustering (Hara et al., 2007; Hunt and Gray, 2009), while EPFL9

functions antagonistically to promote stomatal development (Hunt et al., 2010; Sugano et al., 2010; Lee et al., 2015).

In Arabidopsis, the overexpression of *AtEPF2* results in plants with particularly low *SD*. Despite a coupled increase in *SS*, these plants have significantly lower g_s and g_{smax}, with minor reductions in carbon assimilation, leading to an increase in intrinsic WUE (iWUE, estimated by A/g_s to water vapor) (Doheny-Adams et al., 2012; Franks et al., 2015). The large reduction in *SD* resulted in plants with improved tolerance to drought, without detrimental effects to uptake of nitrogen or phosphate (Hepworth et al., 2015, 2016). Improved plant drought responses were also achieved by Wang et al. (2016) in poplar plants overexpressing *PdEPF1*. Transgenic poplar lines showed a 28% reduction in *SD*, which led to a 30% decrease in *E*, despite an increase in *SS*. WUE and drought tolerance were improved in poplar plants with lower *SD*, which also showed relatively lower decreases in levels of *A* and biomass under water restricted conditions (Wang et al., 2016). The manipulation of another regulator of stomatal development, the subtilisin-like protease STOMATAL DENSITY AND DISTRIBUTION1 (SDD1), also leads to a significant alteration to *SD* in Arabidopsis, with overexpression of this gene reducing *SD* by 40% (Von Groll et al., 2002). This reduction was translated into a lower g_s under high light intensities; however, *A* was compromised under some light conditions (Büssis et al., 2006). A more encouraging result was achieved by Yoo et al. (2010) by manipulating a transcriptional repressor of SDD1, GT-2 LIKE 1 (GTL1). GTL1 loss-of-function Arabidopsis mutants had higher *SDD1* expression resulting in lower *SD* and g_s, without detrimental effects to the photosynthetic rates over a range of light levels. The lower water loss observed in the *gtl1* mutants significantly improved WUE, when water loss versus shoot dry weight was assessed. Taken together, these data indicate that it is possible to improve WUE by altering g_{smax} and g_s using genetic engineering tools. It is not fully understood, however, how severe reductions in g_{smax} may limit short-term stomatal responses or whether adjustments to stomatal development in response to changes in environmental conditions would be affected in these genetically modified plants.

Although stomatal development in grasses differs from that of eudicots in various aspects, recent findings demonstrate that several components of the stomatal signaling pathway, including bHLH transcription factors (Liu et al., 2009; Raissig et al., 2016, 2017) and peptide signals controlling stomatal density, mediate similar events (Hughes et al., 2017; Yin et al., 2017; Caine et al., 2019). This has allowed researchers to begin to test the implications of targeted manipulations in stomatal density in grasses, a family of plants that comprises many important food crops. Research on barley and rice (further discussed below) shows that the overexpression of *EPF1* can result in improved WUE without yield penalty, despite in some cases small reductions in photosynthetic rate under well-watered conditions (Hughes et al., 2017; Caine et al., 2019). Interestingly, in both crops, an increase in guard cell size was not observed in plants with reduced *SD*, contrasting with that described for poplar and Arabidopsis above. These observations suggest that the response of *SS* to altered *SD* may be differentially regulated between monocots and eudicots.

STOMATAL MORPHOLOGY AND IMPROVED WUE

The shape of guard cells and the presence or absence of subsidiary cells have implications for the mechanics and responsiveness of stomatal movement (Franks and Farquhar, 2007). Diversity in stomatal morphology is commonly observed across species and can be linked to adaptability to certain environments (Chen et al., 2017; Müller et al., 2017). In the grass family, for example, stomatal morphology has often been hypothesized to have contributed to successful diversification, particularly in habitats with fluctuating water availability (Hetherington and Woodward, 2003; Cai et al., 2017; Chen et al., 2017). In contrast to the two kidney-shaped guard cells observed in many species, grass species develop stomatal complexes formed by a pair of dumbbell-shaped guard cells, which are flanked by two paracytic subsidiary cells (Stebbins and Shah, 1960; Sack, 1994; Rudall et al., 2017; Hepworth et al., 2018; McKown and Bergmann, 2018). Several studies comparing stomatal opening and closing responses, between grasses and species with kidney-shaped stomata, suggest that grasses exhibit faster and more efficient stomatal regulation (Grantz and Zeiger, 1986; Vico et al., 2011; Merilo et al., 2014; McAusland et al., 2016; Haworth et al., 2018). The linear dumbbell-shaped guard cells require only small changes in volume to bring about stomatal opening and, consequently, to achieve a higher diffusible pore area (Hetherington and Woodward, 2003). The large and rapid responses of grass stomata are also related to the physical interaction between dumbbell-shaped guard cells and flanking subsidiary cells. Subsidiary cells are not only able to limit but also to accommodate guard cell movement, providing a mechanical advantage (Franks and Farquhar, 2007). They function by promptly supplying ions to guard cells, facilitating a reciprocal change in turgor pressure (Raschke and Fellows, 1971; Franks and Farquhar, 2007; Schäfer et al., 2018). This efficient osmotic flux aids rapid stomatal movement and therefore is believed to confer adaptive advantages to grasses.

Slow stomatal responses are proposed to lead to less efficient uptake of CO_2 during stomatal opening and unnecessary water loss during stomatal closure (McAusland et al., 2016; Lawson and Vialet-Chabrand, 2019). Under particular environmental conditions (e.g., fluctuations in irradiance), plants with stomata which are highly responsive might achieve higher WUE. Recently, the absence of subsidiary cells was investigated in *Brachypodium distachyon* plants with a mutation in *BdMUTE*, an ortholog of an Arabidopsis bHLH gene. Mutant plants lacking subsidiary cells failed to open guard cells as widely as control plants and also showed slower stomatal responses to changes in light intensity, further suggesting that subsidiary cells are integral for efficient stomatal functioning in grasses (Raissig et al., 2017). The receptor-like proteins PANGLOSS (PAN) 1 and PAN2 are also integral for the formation of subsidiary cells, primarily by enabling subsidiary mother cells to polarize in the correct orientation to guard mother cells during stomatal

development (Cartwright et al., 2009; Zhang et al., 2012; Sutimantanapi et al., 2014). Defective *pan1* and *pan2* mutants and *pan1/pan2* double mutants have misshapen subsidiary cells, which could impact on stomatal responsiveness; however, it is not known whether gas exchange is affected in these mutant plants. Despite the relatively recent discoveries of MUTE and PAN proteins in grasses, there are still many unanswered questions in relation to subsidiary and guard cell interactions, especially in non-grass species, which show a diversity of stomatal complex morphologies, with different numbers and positions of subsidiary cells (Rudall et al., 2017). Further study of how the diversity of stomatal complex morphologies affects plant physiology could improve our understanding of how these features might contribute to improved WUE.

GENETIC MANIPULATION OF STOMATAL DEVELOPMENT IN CROPS, THE IMPLICATIONS FOR WUE, AND DROUGHT RESPONSES

An increasing number of genetic resources are enabling researchers to test whether targeted alterations in stomatal development can improve WUE and drought tolerance in crop species (Winter et al., 2007; Goodstein et al., 2012; Yin et al., 2017). Although results are yet to be demonstrated in the field, in overexpressing orthologs of Arabidopsis *SDD1* in maize and tomato, respectively, Liu et al. (2015) and Morales-Navarro et al. (2018) have been able to reduce leaf *SD*, leading to reduced water consumption and improved drought tolerance in both crops, as well as improved WUE in maize. Similar results were achieved in barley by overexpressing *HvEPF1* (Hughes et al., 2017). With approximately 50% reduction in *SD* and shorter guard cells, under drought conditions, transgenic barley lines were able to retain higher levels of soil water content. These plants were able to avoid water stress for longer periods, showing drops in photosystem II activity 4–5 days later than the control plants. Carbon isotope analysis suggested that plants with reduced *SD* had improved WUE under the water stress treatment, and despite small reductions in *A*, no detrimental effects on plant growth or yield were observed (Hughes et al., 2017). Similarly, overexpression of rice *OsEPF1* resulted in rice plants with improved WUE (Caine et al., 2019). Two genetically modified lines, one with moderate (~58%) and the other with severe (~88%) reductions in *SD*, had improved water conservation during the vegetative stage, using 42% and 38% less water, respectively, than the control.

An opposite effect on stomatal development was created by overexpressing the maize gene *SHORTROOT 1* (*ZmSHR1*) in rice, leading to higher *SD* and in some cases reduced *SS* (Schuler et al., 2018). Despite the changes in stomatal properties, neither *A* nor g_s was significantly different from controls suggesting that increased *SD* neither positively or negatively impacted on gaseous exchange. In this particular study, WUE was not reported, but based on *A* and g_s values, alterations seem unlikely. Given the predicted temperature increases for the coming century, however, crop plants with more stomata and potentially increased gas exchange capacity may be important in mitigating the effects of heat stress through increased transpiration-mediated cooling.

While most of the crop studies discussed above have characterized drought and photosynthetic performance, to better understand how crops with altered *SD*, *SS*, or function might perform under future climate scenarios, it is important to consider the combinatory effects of multiple abiotic factors. Of particular importance are the predicted reductions in water availability, increasing atmospheric CO_2, concentration, and increasing temperature. While reduced water availability and elevated CO_2 often result in stomatal closure leading to reduced g_s, increased temperature might have the opposite effect, forcing stomata to open to mitigate the effects of overheating (Zhou et al., 2007; Chaves et al., 2016; Caine et al., 2019). This essentially means that in future climates, if plants are going to conserve water, they may be less able to prevent overheating, possibly leading to photoinhibition, leaf damage, and reduction in yields.

This trade-off between WUE and evaporative cooling was recently investigated in the *OsEPF1* overexpressing (*OsEPF1oe*) rice. Under well-watered conditions at high temperature (40°C), plants with substantially reduced *SD* (and *SS*) exhibited increased g_s, reaching similar rates as control plants. The increase in gas exchange rates were seemingly achieved through regulation of

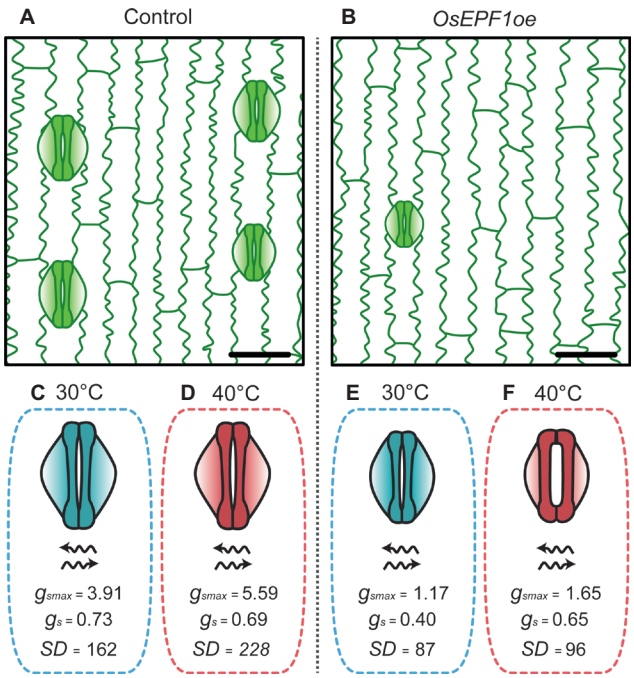

FIGURE 2 | *OsEPF1oe* rice plants with reduced stomatal density and size are able to maintain high rates of gas exchange under heat stress conditions by opening their stomatal pores (adapted from Caine et al., 2019). Epidermis of **(A)** non-transgenic control and **(B)** *OsEPF1oe* plants grown at 30°C, bars = 25 μM. Stomata of control plants grown at **(C)** 30°C and **(D)** 40°C. Control plants show increases in stomatal density and in maximum leaf stomatal conductance average values under high temperature conditions. *OsEPF1oe* plants grown at **(E)** 30°C and **(F)** 40°C. Transgenic line shows an increase in stomatal aperture at 40°C, reaching similar g_s levels as control plants, despite lower maximum stomatal conductance. Units: g_{smax} and g_s = mol m^{-2} s^{-1}, *SD* = mm^{-2}.

stomatal apertures (**Figure 2**), with the trade-off being a loss of superior WUE relative to control plants (Caine et al., 2019). However, at 40°C, *OsEPF1oe* plants with severe *SD* reductions showed enhanced survival rates under drought stress, perhaps because of their improved soil water conservation under these conditions. Although these responses suggest that having low *SD* with reduced *SS* could be beneficial at very high temperature, at present the operational dynamics of stomata when temperature exceeds 40°C are not well understood. Modeling of g_{smax} suggested that despite the much reduced *SD*, *OsEPF1oe* plants still use only up to 40% of their theoretical maximum gas exchange capacity at 40°C, but the actual level of g_s (and *A* and WUE) at more extreme temperatures remains untested (Caine et al., 2019). These results raise a number of questions regarding the physiological behavior of these reduced *SD* plants. Firstly, will plants with fewer, smaller stomata be capable of continuing to increase g_s to maintain water flow and *A* at extreme temperatures, and will this be at the expense of WUE? If so, will plants with the lowest *SD* be less water-use efficient than plants with higher *SD* at very high temperatures in order to maintain cooling? The answers to such questions are critical to understand if targeted *SD* reductions are to be an effective tool to improve rice production in areas where drought and high temperatures are predicted to become more prevalent.

OTHER POTENTIAL STOMATAL-RELATED TARGETS TO IMPROVE WUE

The central position of stomata in the gas exchange process makes them an obvious target for improving WUE; nonetheless, the manipulation of other processes with potential for improving plant carbon and water relations has also been investigated (Lefebvre et al., 2005; Taylor et al., 2011; Ort et al., 2015; Kromdijk et al., 2016; Głowacka et al., 2018). Alterations in mesophyll conductance (g_m), for example, can have a great impact in *A*, and its coregulation with g_s is essential for plant WUE. Indeed, it has been suggested that increases in g_m coupled with decreases in g_s could improve WUE, without the potential detrimental impacts in *A* and yield (Flexas et al., 2013).

Moreover, stomata are not the only structures on the epidermis to prevent water loss – trichomes, the cuticle, and cuticular waxes are also important (Guo et al., 2016; Ichie et al., 2016; Bi et al., 2017; Zeisler-Diehl et al., 2018). While research into crop plant stomata is of long-standing (Teare et al., 1971; Gay and Hurd, 1975; Liao et al., 2005; Ohsumi et al., 2007), new approaches are looking at drought-tolerant relatives of crops or desert-growing species for novel ways to increase WUE. For example, by crossing the wild drought tolerant tomato relative, *Solanum pennellii* (which has abundant trichomes), with the cultivated species *Solanum lycopersicum*, Galdon-Armero et al. (2018) showed that the coordinated development of trichomes and stomata may be a key tool for enhancing WUE in crops. It was found that the plants with the best WUE were those with the highest ratio of trichomes to stomata. One possible explanation for this is that plants with fewer stomata and abundant trichomes have a more significant boundary layer, thus creating a greater resistance to diffusion of water from the leaf (Galdon-Armero et al., 2018). Another example of increased resistance to diffusion of water due to adaptations to the epidermis has also recently been reported in the desert crop, date palm (*Phoenix dactylifera*) (Müller et al., 2017). In this study, wax chimneys were detected on the cuticle that encircled stomata, which like trichomes, prevented excessive water loss, thereby potentially improving WUE. Further investigations exploring how stomata and other epidermal structures jointly contribute to regulate WUE may be a critical piece in the jigsaw of preserving water and negating drought. Indeed, the recent discovery of the *Fused Outer Cuticular Ledge1* stomata gene in Arabidopsis may help facilitate such studies (Hunt et al., 2017).

CONCLUSION

The knowledge relating to the genetics underpinning stomatal development and physiology in both Arabidopsis and crop species has advanced substantially, with noticeable advancements made in improving WUE. However, there are still many questions to answer, of particular importance is how *SS* is regulated at the genetic level and why do *SS*-*SD* responses vary so much between species. In addition to this, understanding how stomatal complex architecture is modified and how ion fluxes are directed between guard and subsidiary cells at the genetic level is the key area where further advances in knowledge are required. In crops, recent studies are showing that engineering plants to reduce stomatal number may be an effective tool to improve plant WUE and drought tolerance without yield reductions. Of course, as modified plants have typically been evaluated in laboratory conditions, it is still necessary to answer how such plants might perform in the real world. In a field context, many other environmental variables and stressors will impact on performance. Additional studies are necessary to understand how plants with altered stomatal development will respond to multiple stresses in different developmental phases. Moreover, combining changes in stomatal traits with other alterations associated with improved water relations, such as modifications to the leaf epidermis, photosynthesis, g_m, and root growth, among others, could further benefit plant WUE and drought tolerance under future predicted climate scenarios.

AUTHOR CONTRIBUTIONS

LB and RC wrote the paper. LB designed the figures. JG provided advice and comments. All authors read, commented on, and approved this version of the manuscript.

FUNDING

The authors are supported by the Grantham Centre for Sustainable Futures—Funded a PhD scholarship (LB) and the BBSRC Newton Fund—grant BB/N013646/1—Funded group's research (RC and JG). University of Sheffield library—to fund journal fees.

REFERENCES

Assmann, S. M., and Jegla, T. (2016). Guard cell sensory systems: recent insights on stomatal responses to light, abscisic acid, and CO_2. *Curr. Opin. Plant Biol.* 33, 157–167. doi: 10.1016/J.PBI.2016.07.003

Bacon, M. (2004). *Water use efficiency in plant biology*. Oxford, UK: Blackwell.

Bakker, J. C. (1991). Effects of humidity on stomatal density and its relation to leaf conductance. *Sci. Hortic.* 48, 205–212. doi: 10.1016/0304-4238(91)90128-L

Bartlett, M. K., Klein, T., Jansen, S., Choat, B., and Sack, L. (2016). The correlations and sequence of plant stomatal, hydraulic, and wilting responses to drought. *Proc. Natl. Acad. Sci. U. S. A.* 113, 13098–13103. doi: 10.1073/pnas.1604088113

Beaulieu, J. M., Leitch, I. J., Patel, S., Pendharkar, A., and Knight, C. A. (2008). Genome size is a strong predictor of cell size and stomatal density in angiosperms. *New Phytol.* 179, 975–986. doi: 10.1111/j.1469-8137.2008.02528.x

Bergmann, D. C., and Sack, F. D. (2007). Stomatal development. *Annu. Rev. Plant Biol.* 58, 163–181. doi: 10.1146/annurev.arplant.58.032806.104023

Bi, H., Kovalchuk, N., Langridge, P., Tricker, P. J., Lopato, S., and Borisjuk, N. (2017). The impact of drought on wheat leaf cuticle properties. *BMC Plant Biol.* 17:85. doi: 10.1186/s12870-017-1033-3

Büssis, D., Von Groll, B. U., Fisahn, J., and Altmann, T. (2006). Stomatal aperture can compensate altered stomatal density in *Arabidopsis thaliana* at growth light conditions. *Funct. Plant Biol.* 33, 1037–1043. doi: 10.1071/FP06078

Cai, S., Papanatsiou, M., Blatt, M. R., and Chen, Z. -H. (2017). Speedy grass stomata: emerging molecular and evolutionary features. *Mol. Plant* 10, 912–914. doi: 10.1016/j.molp.2017.06.002

Caine, R., Chater, C. C., Kamisugi, Y., Cuming, A. C., Beerling, D. J., Gray, J. E., et al. (2016). An ancestral stomatal patterning module revealed in the non-vascular land plant *Physcomitrella patens*. *Development* 143, 3306–3314. doi: 10.1242/dev.135038

Caine, R. S., Yin, X., Sloan, J., Harrison, E. L., Mohammed, U., Fulton, T., et al. (2019). Rice with reduced stomatal density conserves water and has improved drought tolerance under future climate conditions. *New Phytol.* 221, 371–384. doi: 10.1111/nph.15344

Campbell, B. M., Thornton, P., Zougmoré, R., van Asten, P., and Lipper, L. (2014). Sustainable intensification: what is its role in climate smart agriculture? *Curr. Opin. Environ. Sustain.* 8, 39–43. doi: 10.1016/J.COSUST.2014.07.002

Carins Murphy, M. R., Jordan, G. J., and Brodribb, T. J. (2014). Acclimation to humidity modifies the link between leaf size and the density of veins and stomata. *Plant Cell Environ.* 37, 124–131. doi: 10.1111/pce.12136

Cartwright, H. N., Humphries, J. A., and Smith, L. G. (2009). PAN1: a receptor-like protein that promotes polarization of an asymmetric cell division in maize. *Science* 323, 649–651. doi: 10.1126/science.1161686

Casson, S. A., Hetherington, A. M., Bergmann, D. C., and Fleming, A. J. (2010). Environmental regulation of stomatal development This review comes from a themed issue on Growth and Development Edited. *Curr. Opin. Plant Biol.* 13, 90–95. doi: 10.1016/j.pbi.2009.08.005

Casson, S., and Gray, J. E. (2008). Influence of environmental factors on stomatal development. *New Phytol.* 178, 9–23. doi: 10.1111/j.1469-8137.2007.02351.x

Chater, C. C. C., Oliver, J., Casson, S., and Gray, J. E. (2014). Putting the brakes on: abscisic acid as a central environmental regulator of stomatal development. *New Phytol.* 202, 376–391. doi: 10.1111/nph.12713

Chaves, M. M., Costa, J. M., Zarrouk, O., Pinheiro, C., Lopes, C. M., and Pereira, J. S. (2016). Controlling stomatal aperture in semi-arid regions—The dilemma of saving water or being cool? *Plant Sci.* 251, 54–64. doi: 10.1016/J.PLANTSCI.2016.06.015

Chen, Z. -H., Chen, G., Dai, F., Wang, Y., Hills, A., Ruan, Y. -L., et al. (2017). Molecular evolution of grass stomata. *Trends Plant Sci.* 22, 124–139. doi: 10.1016/j.tplants.2016.09.005

Clifford, S. C., Black, C. R., Roberts, J. A., Stronach, I. M., Singleton-Jones, P. R., Mohamed, A. D., et al. (1995). The effect of elevated atmospheric CO_2 and drought onstomatal frequency in groundnut (*Arachis hypogaea* (L.)). *J. Exp. Bot.* 46, 847–852. doi: 10.1017/CBO9781107415324.004

Condon, A. G., Richards, R. A., Rebetzke, G. J., and Farquhar, G. D. (2002). Improving intrinsic water-use efficiency and crop yield. *Crop Sci.* 42, 122–131. doi: 10.2135/cropsci2002.1220

Condon, A. G., Richards, R. A., Rebetzke, G. J., and Farquhar, G. D. (2004). Breeding for high water-use efficiency. *J. Exp. Bot.* 2447–2460. doi: 10.1093/jxb/erh277

Dai, A. (2013). Increasing drought under global warming in observations and models. *Nat. Clim. Chang.* 3, 52–58. doi: 10.1038/nclimate1633

de Boer, H. J., Eppinga, M. B., Wassen, M. J., and Dekker, S. C. (2012). A critical transition in leaf evolution facilitated the Cretaceous angiosperm revolution. *Nat. Commun.* 3, 1221. doi: 10.1038/ncomms2217

de Boer, H. J., Lammertsma, E. I., Wagner-Cremer, F., Dilcher, D. L., Wassen, M. J., and Dekker, S. C. (2011). Climate forcing due to optimization of maximal leaf conductance in subtropical vegetation under rising CO_2. *Proc. Natl. Acad. Sci. U. S. A.* 108, 4041–4046. doi: 10.1073/pnas.1100555108

de Boer, H. J., Price, C. A., Wagner-Cremer, F., Dekker, S. C., Franks, P. J., and Veneklaas, E. J. (2016). Optimal allocation of leaf epidermal area for gas exchange. *New Phytol.* 210, 1219–1228. doi: 10.1111/nph.13929

Dilcher, D., de Boer, H. J., Dekker, S. C., Dilcher, D. L., Lotter, A. F., and Wagner-Cremer, F. (2000). Toward a new synthesis: major evolutionary trends in the angiosperm fossil record. *Proc. Natl. Acad. Sci.* 97, 7030–7036. doi: 10.1073/pnas.97.13.7030

Dittberner, H., Korte, A., Mettler-Altmann, T., Weber, A. P. M., Monroe, G., and de Meaux, J. (2018). Natural variation in stomata size contributes to the local adaptation of water-use efficiency in *Arabidopsis thaliana*. *Mol. Ecol.* doi: 10.1111/mec.14838

Doheny-Adams, T., Hunt, L., Franks, P. J., Beerling, D. J., and Gray, J. E. (2012). Genetic manipulation of stomatal density influences stomatal size, plant growth and tolerance to restricted water supply across a growth carbon dioxide gradient. *Philos. Trans. R. Soc. Lond. Ser. B Biol. Sci.* 367, 547–555. doi: 10.1098/rstb.2011.0272

Dow, G. J., and Bergmann, D. C. (2014). Patterning and processes: how stomatal development defines physiological potential. *Curr. Opin. Plant Biol.* 21, 67–74. doi: 10.1016/j.pbi.2014.06.007

Dow, G. J., Bergmann, D. C., and Berry, J. A. (2014a). An integrated model of stomatal development and leaf physiology. *New Phytol.* 201, 1218–1226. doi: 10.1111/nph.12608

Dow, G. J., Berry, J. A., and Bergmann, D. C. (2014b). The physiological importance of developmental mechanisms that enforce proper stomatal spacing in *Arabidopsis thaliana*. *New Phytol.* 201, 1205–1217. doi: 10.1111/nph.12586

Drake, P. L., Froend, R. H., and Franks, P. J. (2013). Smaller, faster stomata: scaling of stomatal size, rate of response, and stomatal conductance. *J. Exp. Bot.* 64, 495–505. doi: 10.1093/jxb/ers347

Elliott-Kingston, C., Haworth, M., Yearsley, J. M., Batke, S. P., Lawson, T., and McElwain, J. C. (2016). Does size matter? Atmospheric CO_2 may be a stronger driver of stomatal closing rate than stomatal size in taxa that diversified under low CO_2. *Front. Plant Sci.* 7:1253. doi: 10.3389/fpls.2016.01253

Fanourakis, D., Giday, H., Milla, R., Pieruschka, R., Kjaer, K. H., Bolger, M., et al. (2015). Pore size regulates operating stomatal conductance, while stomatal densities drive the partitioning of conductance between leaf sides. *Ann. Bot.* 115, 555–565. doi: 10.1093/aob/mcu247

Farquhar, G. D., and Sharkey, T. D. (1982). Stomatal conductance and photosynthesis. *Annu. Rev. Plant Physiol.* 33, 317–345. doi: 10.1146/annurev.pp.33.060182.001533

Field, K. J., Duckett, J. G., Cameron, D. D., and Pressel, S. (2015). Stomatal density and aperture in non-vascular land plants are non-responsive to above-ambient atmospheric CO_2 concentrations. *Ann. Bot.* 115, 915–922. doi: 10.1093/aob/mcv021

Flexas, J. (2016). Genetic improvement of leaf photosynthesis and intrinsic water use efficiency in C3 plants: why so much little success? *Plant Sci.* 251, 155–161. doi: 10.1016/J.PLANTSCI.2016.05.002

Flexas, J., and Medrano, H. (2002). Drought-inhibition of photosynthesis in C3 plants: stomatal and non-stomatal limitations revisited. *Ann. Bot.* 89, 183–189. doi: 10.1093/aob/mcf027

Flexas, J., Niinemets, Ü., Gallé, A., Barbour, M. M., Centritto, M., Diaz-Espejo, A., et al. (2013). Diffusional conductances to CO_2 as a target for increasing photosynthesis and photosynthetic water-use efficiency. *Photosynth. Res.* 117, 45–59. doi: 10.1007/s11120-013-9844-z

Franks, P. J., and Beerling, D. J. (2009). Maximum leaf conductance driven by CO_2 effects on stomatal size and density over geologic time. *Proc. Natl. Acad. Sci. U. S. A.* 106, 10343–10347. doi: 10.1073/pnas.0904209106

Franks, P. J., Drake, P. L., and Beerling, D. J. (2009). Plasticity in maximum stomatal conductance constrained by negative correlation between stomatal

size and density: an analysis using *Eucalyptus globulus*. *Plant Cell Environ.* 32, 1737–1748. doi: 10.1111/j.1365-3040.2009.002031.x

Franks, P. J., and Farquhar, G. D. (2001). The effect of exogenous abscisic acid on stomatal development, stomatal mechanics, and leaf gas exchange in *Tradescantia virginiana*. Available at: www.plantphysiol.org (Accessed July 31, 2018).

Franks, P. J., and Farquhar, G. D. (2007). The mechanical diversity of stomata and its significance in gas exchange control. *Plant Physiol.* 143, 78–97. doi: 10.1104/pp.106.089367

Franks, P. J., Leitch, I. J., Ruszala, E. M., Hetherington, A. M., and Beerling, D. J. (2012). Physiological framework for adaptation of stomata to CO_2 from glacial to future concentrations. *Philos. Trans. R. Soc. Lond. Ser. B Biol. Sci.* 367, 537–546. doi: 10.1098/rstb.2011.0270

Franks, P. J., Doheny-Adams, W. T., Britton-Harper, Z. J., and Gray, J. E. (2015). Increasing water-use efficiency directly through genetic manipulation of stomatal density. *New Phytol.* 207, 188–195. doi: 10.1111/nph.13347

Galdon-Armero, J., Fullana-Pericas, M., Mulet, P. A., Conesa, M. A., Martin, C., and Galmes, J. (2018). The ratio of trichomes to stomata is associated with water use efficiency in tomato. *Plant J.* doi: 10.1111/tpj.14055

Gao, X., Zou, C., Wang, L., and Zhang, F. (2006). Silicon decreases transpiration rate and conductance from stomata of maize plants. *J. Plant Nutr.* 29, 1637–1647. doi: 10.1080/01904160600851494

Gay, A. P., and Hurd, R. G. (1975). The influence of light on stomatal density in the tomato. *New Phytol.* 75, 37–46. doi: 10.1111/j.1469-8137.1975.tb01368.x

Głowacka, K., Kromdijk, J., Kucera, K., Xie, J., Cavanagh, A. P., Leonelli, L., et al. (2018). Photosystem II subunit S overexpression increases the efficiency of water use in a field-grown crop. *Nat. Commun.* 9:868. doi: 10.1038/s41467-018-03231-x

Goodstein, D. M., Shu, S., Howson, R., Neupane, R., Hayes, R. D., Fazo, J., et al. (2012). Phytozome: a comparative platform for green plant genomics. *Nucleic Acids Res.* 40, D1178–D1186. doi: 10.1093/nar/gkr944

Grantz, D. A., and Zeiger, E. (1986). Stomatal responses to light and leaf-air water vapor pressure difference show similar kinetics in sugarcane and soybean. *Plant Physiol.* 81, 865–868. doi: 10.1104/pp.81.3.865

Guo, J., Xu, W., Yu, X., Shen, H., Li, H., Cheng, D., et al. (2016). Cuticular wax accumulation is associated with drought tolerance in wheat near-isogenic lines. *Front. Plant Sci.* 7:1809. doi: 10.3389/fpls.2016.01809

Hara, K., Kajita, R., Torii, K. U., Bergmann, D. C., and Kakimoto, T. (2007). The secretory peptide gene EPF1 enforces the stomatal one-cell-spacing rule. *Genes Dev.* 21, 1720–1725. doi: 10.1101/gad.1550707

Haworth, M., Elliott-Kingston, C., and McElwain, J. C. (2013). Co-ordination of physiological and morphological responses of stomata to elevated $[CO_2]$ in vascular plants. *Oecologia* 171, 71–82. doi: 10.1007/s00442-012-2406-9

Haworth, M., Killi, D., Materassi, A., Raschi, A., and Centritto, M. (2016). Impaired stomatal control is associated with reduced photosynthetic physiology in crop species grown at elevated $[CO_2]$. *Front. Plant Sci.* 7:1568. doi: 10.3389/fpls.2016.01568

Haworth, M., Scutt, C. P., Douthe, C., Marino, G., Gomes, M. T. G., Loreto, F., et al. (2018). Allocation of the epidermis to stomata relates to stomatal physiological control: stomatal factors involved in the evolutionary diversification of the angiosperms and development of amphistomaty. *Environ. Exp. Bot.* 151, 55–63. doi: 10.1016/j.envexpbot.2018.04.010

Hepworth, C., Caine, R. S., Harrison, E. L., Sloan, J., and Gray, J. E. (2018). Stomatal development: focusing on the grasses. *Curr. Opin. Plant Biol.* 41, 1–7. doi: 10.1016/J.PBI.2017.07.009

Hepworth, C., Doheny-Adams, T., Hunt, L., Cameron, D. D., and Gray, J. E. (2015). Manipulating stomatal density enhances drought tolerance without deleterious effect on nutrient uptake. *New Phytol.* 208, 336–341. doi: 10.1111/nph.13598

Hepworth, C., Turner, C., Landim, M. G., Cameron, D., and Gray, J. E. (2016). Balancing water uptake and loss through the coordinated regulation of stomatal and root development. *PLoS One* 11:e0156930. doi: 10.1371/journal.pone.0156930

Hetherington, A. M., and Woodward, F. I. (2003). The role of stomata in sensing and driving environmental change. *Nature* 424, 901–908. doi: 10.1038/nature01843

Howden, S. M., Soussana, J. -F., Tubiello, F. N., Chhetri, N., Dunlop, M., and Meinke, H. (2007). Adapting agriculture to climate change. *Proc. Natl. Acad. Sci. U. S. A.* 104, 19691–19696. doi: 10.1073/pnas.0701890104

Hughes, J., Hepworth, C., Dutton, C., Dunn, J. A., Hunt, L., Stephens, J., et al. (2017). Reducing stomatal density in barley improves drought tolerance without impacting on yield. *Plant Physiol.* 174, 776–787. doi: 10.1104/pp.16.01844

Hunt, L., Amsbury, S., Baillie, A., Movahedi, M., Mitchell, A., Afsharinafar, M., et al. (2017). Formation of the stomatal outer cuticular ledge requires a guard cell wall proline-rich protein. *Plant Physiol.* 174, 689–699. doi: 10.1104/pp.16.01715

Hunt, L., Bailey, K. J., and Gray, J. E. (2010). The signalling peptide EPFL9 is a positive regulator of stomatal development. *New Phytol.* 186, 609–614. doi: 10.1111/j.1469-8137.2010.03200.x

Hunt, L., and Gray, J. E. (2009). The signaling peptide EPF2 controls asymmetric cell divisions during stomatal development. *Curr. Biol.* 19, 864–869. doi: 10.1016/J.CUB.2009.03.069

Ichie, T., Inoue, Y., Takahashi, N., Kamiya, K., and Kenzo, T. (2016). Ecological distribution of leaf stomata and trichomes among tree species in a Malaysian lowland tropical rain forest. *J. Plant Res.* 129, 625–635. doi: 10.1007/s10265-016-0795-2

Iglesias, A., and Garrote, L. (2015). Adaptation strategies for agricultural water management under climate change in Europe. *Agric. Water Manag.* 155, 113–124. doi: 10.1016/J.AGWAT.2015.03.014

IPCC. (2014). Climate change 2014 synthesis report summary chapter for policymakers. IPCC 31.

Jordan, G. J., Carpenter, R. J., Koutoulis, A., Price, A., and Brodribb, T. J. (2015). Environmental adaptation in stomatal size independent of the effects of genome size. *New Phytol.* 205, 608–617. doi: 10.1111/nph.13076

Kardiman, R., and Raebild, A. (2017). Relationship between stomatal density, size and speed of opening in Sumatran rainforest species. *Tree Physiol.* 38, 696–705. doi: 10.1093/treephys/tpx149

Kollist, H., Nuhkat, M., and Roelfsema, M. R. G. (2014). Closing gaps: linking elements that control stomatal movement. *New Phytol.* 203, 44–62. doi: 10.1111/nph.12832

Kromdijk, J., Głowacka, K., Leonelli, L., Gabilly, S. T., Iwai, M., Niyogi, K. K., et al. (2016). Improving photosynthesis and crop productivity by accelerating recovery from photoprotection. *Science* 354, 857–861. doi: 10.1126/science.aai8878

Lake, J. A., Quick, W. P., Beerling, D. J., and Woodward, F. I. (2001). Plant development: signals from mature to new leaves. *Nature* 411:154. doi: 10.1038/35075660

Lawson, T., and Blatt, M. R. (2014). Stomatal size, speed, and responsiveness impact on photosynthesis and water use efficiency. *Plant Physiol.* 164, 1556–1570. doi: 10.1104/pp.114.237107

Lawson, T., and Vialet-Chabrand, S. (2019). Speedy stomata, photosynthesis and plant water use efficiency. *New Phytol.* 221, 93–98. doi: 10.1111/nph.15330

Lee, J. S., Hnilova, M., Maes, M., Lin, Y. -C. L., Putarjunan, A., Han, S. -K., et al. (2015). Competitive binding of antagonistic peptides fine-tunes stomatal patterning. *Nature* 522, 439–443. doi: 10.1038/nature14561

Lefebvre, S., Lawson, T., Zakhleniuk, O. V., Lloyd, J. C., Raines, C. A., and Fryer, M. (2005). Increased sedoheptulose-1,7-bisphosphatase activity in transgenic tobacco plants stimulates photosynthesis and growth from an early stage in development. *Plant Physiol.* 138, 451–460. doi: 10.1104/pp.104.055046

Liao, J. -X., Chang, J., and Wang, G. -X. (2005). Stomatal density and gas exchange in six wheat cultivars. *Cereal Res. Commun.* 33, 719–726. doi: 10.1556/CRC.33.2005.2-3.140

Lipper, L., Thornton, P., Campbell, B. M., Baedeker, T., Braimoh, A., Bwalya, M., et al. (2014). Climate-smart agriculture for food security. *Nat. Clim. Chang.* 4, 1068–1072. doi: 10.1038/nclimate2437

Liu, T., Ohashi-Ito, K., and Bergmann, D. C. (2009). Orthologs of *Arabidopsis thaliana* stomatal bHLH genes and regulation of stomatal development in grasses. *Development* 136, 2265–2276. doi: 10.1242/dev.032938. Available at: http://dev.biologists.org/content/136/13/2265.long (Accessed June 4, 2017).

Liu, Y., Qin, L., Han, L., Xiang, Y., and Zhao, D. (2015). Overexpression of maize SDD1 (ZmSDD1) improves drought resistance in *Zea mays* L. by reducing stomatal density. *Plant Cell Tissue Organ Cult.* 122, 147–159. doi: 10.1007/s11240-015-0757-8

Lobell, D. B., Schlenker, W., and Costa-Roberts, J. (2011). Climate trends and global crop production since 1980. *Science* 333, 616–620. doi: 10.1126/science.1204531

Lu, Z. -M. (1989). Ratio of stomatal resistance on two sides of wheat leaves as affected by soil water content. *Agric. For. Meteorol.* 49, 1–7. doi: 10.1016/0168-1923(89)90057-9

Lu, Z., Quiñones, M. A., and Zeiger, E. (1993). Abaxial and adaxial stomata from Pima cotton (*Gossypium barbadense* L.) differ in their pigment content and sensitivity to light quality. *Plant Cell Environ.* 16, 851–858. doi: 10.1111/j.1365-3040.1993.tb00507.x

MacAlister, C. A., Ohashi-Ito, K., and Bergmann, D. C. (2007). Transcription factor control of asymmetric cell divisions that establish the stomatal lineage. *Nature* 445, 537–540. doi: 10.1038/nature05491

McAdam, S. A. M., Sussmilch, F. C., and Brodribb, T. J. (2016). Stomatal responses to vapour pressure deficit are regulated by high speed gene expression in angiosperms. *Plant Cell Environ.* 39, 485–491. doi: 10.1111/pce.12633

McAusland, L., Vialet-Chabrand, S., Davey, P., Baker, N. R., Brendel, O., and Lawson, T. (2016). Effects of kinetics of light-induced stomatal responses on photosynthesis and water-use efficiency. *New Phytol.* 211, 1209–1220. doi: 10.1111/nph.14000

McElwain, J. C., Yiotis, C., and Lawson, T. (2016). Using modern plant trait relationships between observed and theoretical maximum stomatal conductance and vein density to examine patterns of plant macroevolution. *New Phytol.* 209, 94–103. doi: 10.1111/nph.13579

McKown, K. H., and Bergmann, D. C. (2018). Grass stomata. *Curr. Biol.* 28, R814–R816. doi: 10.1016/j.cub.2018.05.074

Medrano, H., Tomás, M., Martorell, S., Flexas, J., Hernández, E., Rosselló, J., et al. (2015). From leaf to whole-plant water use efficiency (WUE) in complex canopies: limitations of leaf WUE as a selection target. *Crop J.* 3, 220–228. doi: 10.1016/J.CJ.2015.04.002

Merilo, E., Jõesaar, I., Brosché, M., and Kollist, H. (2014). To open or to close: species-specific stomatal responses to simultaneously applied opposing environmental factors. *New Phytol.* 202, 499–508. doi: 10.1111/nph.12667

Miyazawa, S. -I., Livingston, N. J., and Turpin, D. H. (2006). Stomatal development in new leaves is related to the stomatal conductance of mature leaves in poplar (*Populus trichocarpa*×P. deltoides). *J. Exp. Bot.* 57, 373–380. doi: 10.1093/jxb/eri278

Monda, K., Araki, H., Kuhara, S., Ishigaki, G., Akashi, R., Negi, J., et al. (2016). Enhanced stomatal conductance by a spontaneous Arabidopsis tetraploid, Me-0, results from increased stomatal size and greater stomatal aperture. *Plant Physiol.* 170, 1435–1444. doi: 10.1104/pp.15.01450

Morales-Navarro, S., Pérez-Díaz, R., Ortega, A., de Marcos, A., Mena, M., Fenoll, C., et al. (2018). Overexpression of a SDD1-like gene from wild tomato decreases stomatal density and enhances dehydration avoidance in Arabidopsis and cultivated tomato. *Front. Plant Sci.* 9:940. doi: 10.3389/fpls.2018.00940

Mott, K. A. (2009). Opinion: stomatal responses to light and CO_2 depend on the mesophyll. *Plant Cell Environ.* 32, 1479–1486. doi: 10.1111/j.1365-3040.2009.02022.x

Müller, H. M., Schäfer, N., Bauer, H., Geiger, D., Lautner, S., Fromm, J., et al. (2017). The desert plant Phoenix dactylifera closes stomata via nitrate-regulated SLAC1 anion channel. *New Phytol.* 216, 150–162. doi: 10.1111/nph.14672

Mustilli, A. -C. (2002). Arabidopsis OST1 protein kinase mediates the regulation of stomatal aperture by abscisic acid and acts upstream of reactive oxygen species production. *Plant Cell (online)* 14, 3089–3099. doi: 10.1105/tpc.007906

Ohsumi, A., Kanemura, T., Homma, K., Horie, T., and Shiraiwa, T. (2007). Genotypic variation of stomatal conductance in relation to stomatal density and length in rice (*Oryza sativa* L.). *Plant Prod. Sci.* 10, 322–328. doi: 10.1626/pps.10.322

Ort, D. R., Merchant, S. S., Alric, J., Barkan, A., Blankenship, R. E., Bock, R., et al. (2015). Redesigning photosynthesis to sustainably meet global food and bioenergy demand. *Proc. Natl. Acad. Sci.* 112, 8529–8536. doi: 10.1073/pnas.1424031112

Ouyang, W., Struik, P. C., Yin, X., and Yang, J. (2017). Stomatal conductance, mesophyll conductance, and trans piration efficiency in relation to leaf anatomy in rice and wheat genotypes under drought. *J. Exp. Bot.* 68, 5191–5205. doi: 10.1093/jxb/erx314

Pillitteri, L. J., and Dong, J. (2013). Stomatal development in Arabidopsis. *Arab. B.* 11:e0162. doi: 10.1199/tab.0162

Pillitteri, L. J., and Torii, K. U. (2012). Mechanisms of stomatal development. *Annu. Rev. Plant Biol.* 63, 591–614. doi: 10.1146/annurev-arplant-042811-105451

Qi, X., and Torii, K. U. (2018). Hormonal and environmental signals guiding stomatal development. *BMC Biol.* 16:21. doi: 10.1186/s12915-018-0488-5

Raissig, M. T., Abrash, E., Bettadapur, A., Vogel, J. P., and Bergmann, D. C. (2016). Grasses use an alternatively wired bHLH transcription factor network to establish stomatal identity. *Proc. Natl. Acad. Sci.* 113, 8326–8331. doi: 10.1073/pnas.1606728113

Raissig, M. T., Matos, J. L., Gil, M. X. A., Kornfeld, A., Bettadapur, A., Abrash, E., et al. (2017). Mobile MUTE specifies subsidiary cells to build physiologically improved grass stomata. *Science* 355, 1215–1218. doi: 10.1126/science.aal3254

Raschke, K., and Fellows, M. P. (1971). Stomatal movement in Zea mays: shuttle of potassium and chloride between guard cells and subsidiary cells. *Planta* 101, 296–316. doi: 10.1007/BF00398116

Rudall, P. J., Chen, E. D., and Cullen, E. (2017). Evolution and development of monocot stomata. *Am. J. Bot.* 104, 1122–1141. doi: 10.3732/ajb.1700086

Rudall, P. J., Hilton, J., and Bateman, R. M. (2013). Several developmental and morphogenetic factors govern the evolution of stomatal patterning in land plants. *New Phytol.* 200, 598–614. doi: 10.1111/nph.12406

Sack, F. D. (1994). Structure of the stomatal complex of the monocot *Flagellaria indica*. *Am. J. Bot.* 81, 339–344. doi: 10.2307/2445461

Sack, L., and Buckley, T. N. (2016). The developmental basis of stomatal density and flux. *Plant Physiol.* 171, 2358–2363. doi: 10.1104/pp.16.00476

Schäfer, N., Maierhofer, T., Herrmann, J., Jørgensen, M. E., Lind, C., von Meyer, K., et al. (2018). A tandem amino acid residue motif in guard cell SLAC1 anion channel of grasses allows for the control of stomatal aperture by nitrate. *Curr. Biol.* 28, 1370–1379.e5. doi: 10.1016/J.CUB.2018.03.027

Schroeder, J. I., Allen, G. J., Hugouvieux, V., Kwak, J. M., and Waner, D. (2001). Guard cell signal transduction. *Annu. Rev. Plant Physiol. Plant Mol. Biol.* 52, 627–658. doi: 10.1146/annurev.arplant.52.1.627

Schuler, M. L., Sedelnikova, O. V., Walker, B. J., Westhoff, P., and Langdale, J. A. (2018). SHORTROOT-mediated increase in stomatal density has no impact on photosynthetic efficiency. *Plant Physiol.* 176, 757–772. doi: 10.1104/pp.17.01005

Sekiya, N., and Yano, K. (2008). Stomatal density of cowpea correlates with carbon isotope discrimination in different phosphorus, water and CO_2 environments. *New Phytol.* 179, 799–807. doi: 10.1111/j.1469-8137.2008.02518.x

Sherwood, S., and Fu, Q. (2014). Climate change. A drier future? *Science* 343, 737–739. doi: 10.1126/science.1247620

Sorrentino, G., Haworth, M., Wahbi, S., Mahmood, T., Zuomin, S., and Centritto, M. (2016). Abscisic acid induces rapid reductions in mesophyll conductance to carbon dioxide. *PLoS One* 11:e0148554. doi: 10.1371/journal.pone.0148554

Stebbins, G. L., and Shah, S. S. (1960). Developmental studies of cell differentiation in the epidermis of monocotyledons. *Dev. Biol.* 2, 477–500. doi: 10.1016/0012-1606(60)90050-6

Sugano, S. S., Shimada, T., Imai, Y., Okawa, K., Tamai, A., Mori, M., et al. (2010). Stomagen positively regulates stomatal density in Arabidopsis. *Nature* 463, 241–244. doi: 10.1038/nature08682

Sun, Y., Yan, F., Cui, X., and Liu, F. (2014). Plasticity in stomatal size and density of potato leaves under different irrigation and phosphorus regimes. *J. Plant Physiol.* 171, 1248–1255. doi: 10.1016/J.JPLPH.2014.06.002

Sutimantanapi, D., Pater, D., and Smith, L. G. (2014). Divergent roles for maize PAN1 and PAN2 receptor-like proteins in cytokinesis and cell morphogenesis. *Plant Physiol.* 164, 1905–1917. doi: 10.1104/pp.113.232660

Taylor, S. H., Franks, P. J., Hulme, S. P., Spriggs, E., Christin, P. A., Edwards, E. J., et al. (2012). Photosynthetic pathway and ecological adaptation explain stomatal trait diversity amongst grasses. *New Phytol.* 193, 387–396. doi: 10.1111/j.1469-8137.2011.03935.x

Taylor, S. H., Ripley, B. S., Woodward, F. I., and Osborne, C. P. (2011). Drought limitation of photosynthesis differs between C3 and C4 grass species in a comparative experiment. *Plant Cell Environ.* 34, 65–75. doi: 10.1111/j.1365-3040.2010.02226.x

Teare, I. D., Peterson, C. J., and Law, A. G. (1971). Size and frequency of leaf stomata in cultivars of *Triticum aestivum* and other triticum species 1. *Crop Sci.* 11, 496. doi: 10.2135/cropsci1971.0011183X001100040010x

Tombesi, S., Nardini, A., Frioni, T., Soccolini, M., Zadra, C., Farinelli, D., et al. (2015). Stomatal closure is induced by hydraulic signals and maintained by ABA in drought-stressed grapevine. *Sci. Rep.* 5, 12449. doi: 10.1038/srep12449

Varshney, R. K., Singh, V. K., Kumar, A., Powell, W., and Sorrells, M. E. (2018). Can genomics deliver climate-change ready crops? *Curr. Opin. Plant Biol.* 45, 205–211. doi: 10.1016/J.PBI.2018.03.007

Vatén, A., and Bergmann, D. C. (2012). Mechanisms of stomatal development: an evolutionary view. *EvoDevo* 3, 11. doi: 10.1186/2041-9139-3-11

Vico, G., Manzoni, S., Palmroth, S., and Katul, G. (2011). Effects of stomatal delays on the economics of leaf gas exchange under intermittent light regimes. *New Phytol.* 192, 640–652. doi: 10.1111/j.1469-8137.2011.03847.x

Von Groll, U., Berger, D., and Altmann, T. (2002). The subtilisin-like serine protease SDD1 mediates cell-to-cell signaling during Arabidopsis stomatal development. *Plant Cell* 14, 1527–1539. doi: 10.1105/tpc.001016

Wang, C., Liu, S., Dong, Y., Zhao, Y., Geng, A., Xia, X., et al. (2016). PdEPF1 regulates water-use efficiency and drought tolerance by modulating stomatal density in poplar. *Plant Biotechnol. J.* 14, 849–860. doi: 10.1111/pbi.12434

Willmer, C. M., and Fricker, M. D. (1996). Stomata. 2nd edition. London: Chapman & Hall. Available at: https://books.google.co.uk/books/about/Stomata.html?id=AXvwAAAAMAAJ&redir_esc=y (Accessed November 19, 2018).

Winter, D., Vinegar, B., Nahal, H., Ammar, R., Wilson, G. V., and Provart, N. J. (2007). An "electronic fluorescent pictograph" browser for exploring and analyzing large-scale biological data sets. *PLoS One* 2:e718. doi: 10.1371/journal.pone.0000718

Wong, S. C., Cowan, I. R., and Farquhar, G. D. (1979). Stomatal conductance correlates with photosynthetic capacity. *Nature* 282, 424–426. doi: 10.1038/282424a0

Woodward, F. I. (1987). Stomatal numbers are sensitive to increases in CO_2 from pre-industrial levels. *Nature* 327, 617–618. doi: 10.1038/327617a0

Xu, Z., and Zhou, G. (2008). Responses of leaf stomatal density to water status and its relationship with photosynthesis in a grass. *J. Exp. Bot.* 59, 3317–3325. doi: 10.1093/jxb/ern185

Yan, F., Sun, Y., Song, F., and Liu, F. (2012). Differential responses of stomatal morphology to partial root-zone drying and deficit irrigation in potato leaves under varied nitrogen rates. *Sci. Hortic.* 145, 76–83. doi: 10.1016/J.SCIENTA.2012.07.026

Yin, X., Biswal, A. K., Dionora, J., Perdigon, K. M., Balahadia, C. P., Mazumdar, S., et al. (2017). CRISPR-Cas9 and CRISPR-Cpf1 mediated targeting of a stomatal developmental gene EPFL9 in rice. *Plant Cell Rep.* 36, 745–757. doi: 10.1007/s00299-017-2118-z

Yoo, C. Y., Pence, H. E., Jin, J. B., Miura, K., Gosney, M. J., Hasegawa, P. M., et al. (2010). The Arabidopsis GTL1 transcription factor regulates water use efficiency and drought tolerance by modulating stomatal density via transrepression of SDD1. *Plant Cell* 22, 4128–4141. doi: 10.1105/tpc.110.078691

Yu, L., Chen, X., Wang, Z., Wang, S., Wang, Y., Zhu, Q., et al. (2013). Arabidopsis enhanced drought tolerance1/HOMEODOMAIN GLABROUS11 confers drought tolerance in transgenic rice without yield penalty. *Plant Physiol.* 162, 1378–1391. doi: 10.1104/pp.113.217596

Zeiger, E., Farquhar, G. D., and Cowan, I. R. (1987). *Stomatal function*. Stanford, California: Stanford University Press.

Zeisler-Diehl, V., Müller, Y., and Schreiber, L. (2018). Epicuticular wax on leaf cuticles does not establish the transpiration barrier, which is essentially formed by intracuticular wax. *J. Plant Physiol.* 227, 66–74. doi: 10.1016/j.jplph.2018.03.018

Zhang, X., Facette, M., Humphries, J. A., Shen, Z., Park, Y., Sutimantanapi, D., et al. (2012). Identification of PAN2 by quantitative proteomics as a leucine-rich repeat-receptor-like kinase acting upstream of PAN1 to polarize cell division in maize. *Plant Cell* 24, 4577–4589. doi: 10.1105/tpc.112.104125

Zhao, W., Sun, Y., Kjelgren, R., and Liu, X. (2015). Response of stomatal density and bound gas exchange in leaves of maize to soil water deficit. *Acta Physiol. Plant.* 37, 1704. doi: 10.1007/s11738-014-1704-8

Zhou, Y., Lam, H. M., and Zhang, J. (2007). Inhibition of photosynthesis and energy dissipation induced by water and high light stresses in rice. *J. Exp. Bot.* 58, 1207–1217. doi: 10.1093/jxb/erl291

Zoulias, N., Harrison, E. L., Casson, S. A., and Gray, J. E. (2018). Molecular control of stomatal development. *Biochem. J.* 475, 441–454. doi: 10.1042/BCJ20170413

Conflict of Interest Statement: The authors declare that the research was conducted in the absence of any commercial or financial relationships that could be construed as a potential conflict of interest.

frontiers in Plant Science

ORIGINAL RESEARCH
published: 28 February 2019
doi: 10.3389/fpls.2019.00160

Interactive Regimes of Reduced Irrigation and Salt Stress Depressed Tomato Water Use Efficiency at Leaf and Plant Scales by Affecting Leaf Physiology and Stem Sap Flow

Hui Yang[1], *Manoj K. Shukla*[2], *Xiaomin Mao*[1], *Shaozhong Kang*[1] *and Taisheng Du*[1]*

[1] Center for Agricultural Water Research in China, China Agricultural University, Beijing, China, [2] Plant and Environmental Sciences Department, New Mexico State University, Las Cruces, NM, United States

OPEN ACCESS

Edited by:
Bhabani S. Das,
Indian Institute of Technology Kharagpur, India

Reviewed by:
Alejandra Navarro,
Council for Agricultural and Economics Research, Italy
Marcella Michela Giuliani,
University of Foggia, Italy

***Correspondence:**
Taisheng Du
dutaisheng@cau.edu.cn

Specialty section:
This article was submitted to Plant Physiology, a section of the journal Frontiers in Plant Science

Received: *25 September 2018*
Accepted: *29 January 2019*
Published: *28 February 2019*

Citation:
Yang H, Shukla MK, Mao X, Kang S and Du T (2019) Interactive Regimes of Reduced Irrigation and Salt Stress Depressed Tomato Water Use Efficiency at Leaf and Plant Scales by Affecting Leaf Physiology and Stem Sap Flow. Front. Plant Sci. 10:160. doi: 10.3389/fpls.2019.00160

Interactive effects of reduced irrigation and salt stress on leaf physiological parameters, biomass accumulation, and water use efficiency (WUE) of tomato plants at leaf and whole plant scales were investigated in a field experiment during 2016 and a greenhouse experiment during 2017. Experiment utilized two irrigation regimes (full, 2/3 of full irrigation) and four soil salt regimes (0, 0.3, 0.6, 0.9% in 2016 season; and 0, 0.2, 0.3, 0.4% in 2017 season). Three salts, sodium chloride, magnesium sulfate, and calcium sulfate (mass ratio of 2:2:1), were homogeneously mixed with soil prior to packing into containers (0.024 m^3). Li-COR 6400 was used to measure tomato leaf physiological parameters. Instantaneous water use efficiency (WUE_{ins}, μmol $mmol^{-1}$) and intrinsic water use efficiency (WUE_{int}, μmol mol^{-1}) were determined at leaf scale, yield water use efficiency (WUE_Y, g L^{-1}), and dry biomass water use efficiency (WUE_{DM}, g L^{-1}) were determined at whole plant scale. Plants irrigated with 2/3 of full irrigation with zero soil-salt treatment had higher dry biomass and yield per plant, resulting in the highest WUE_{DM} and WUE_Y at whole plant scale. Increasing soil salinity decreased dry biomass and yield, leading to greater decreases in whole plant WUE_{DM} and WUE_Y under both irrigation treatments. At full irrigation, no decreases in stomatal conductance (g_s, mol m^{-2} s^{-1}) and slight increase in photosynthetic rate (P_n, μmol m^{-2} s^{-1}) led to higher WUE_{int} at leaf scale during both years. Under full and reduced irrigation, increasing soil salt content decreased P_n and transpiration rate (T_r, mmol m^{-2} s^{-1}) and led to reductions in WUE_{ins} at the leaf scale. However, compared to full irrigation, reduced irrigation improved WUE_{ins} with a significant decline in T_r in no salt and 0.3% soil-salt treatments during both years. For soil salt content of 0.6%, stomatal limitation due to salt stress resulted in higher WUE_{int}, but soil salt content of 0.9% decreased WUE_{int} due to non-stomatal limitation. Soil salt content significantly decreased sap flow, with the maximum variation of daily sap flow per plant of 7.96–31.37 g/h in 2016 and 12.52–36.02 g h^{-1} in 2017. Sap flow rate

was linearly related to air temperature (T_a, °C), solar radiation (R_s, W m^{-2}), and vapor pressure deficit (VPD, kPa). These results advance knowledge on tomato response to abiotic stresses and could improve management of tomato production in water- and salt-stressed areas.

Keywords: reduced irrigation, salt stress, tomato, water use efficiency, sap flow, soil moisture

INTRODUCTION

Appropriate water-saving irrigation regimes are needed to alleviate the threat of water shortage and severe drought on food security under increasing population worldwide (Wei et al., 2016), especially in ecologically fragile arid and semi-arid areas. More than 6% of the world's land is subject to salinity problems (Unesco Water Portal, 2007), and the use of water-saving strategies could exacerbate secondary salinization. Approximately 20% of irrigated land was affected by salinity where crop yields were notably reduced (Qadir et al., 2014). Therefore, soil salinity measurements must precede implementation of water-saving irrigation regimes (Reina-Sánchez et al., 2005). Increases in the duration of droughts have necessitated the use of lower quality groundwater to supplement irrigation in semi-arid regions (Flores et al., 2016, 2017; Baath et al., 2017). Understanding plant responses to coupled abiotic stresses of water and salinity, and the underlying mechanisms of improving WUE from leaf to whole plant scale, would be useful to stabilize crop performance and production under drought and saline conditions in a changing climate.

Salinity-induced morphological and physiological changes in plants are mostly identical to drought during osmotic stress phase (Munns, 2002). Drought and salinity stresses cause progressive reductions of water use, leaf growth, and yield via restriction on stomatal apertures to mediate leaf photochemistry and carbon metabolism (Negrão et al., 2017). Under salinity stress, plants could suffer due to salt-specific effects of ion toxicity (Deb et al., 2013; Farooq et al., 2015). Most of the experiments reported so far were conducted under simulated conditions of using either hydroponic culture with different gradients of nutritive solutions (Albaladejo et al., 2017) or soil irrigated with different levels of saline solutions of NaCl (Ahmed et al., 2013; Galli et al., 2016), NaCl and $CaCl_2$ (Katerji et al., 2011), or brackish groundwater (Flores et al., 2016; Baath et al., 2017).

It is more realistic for plant roots to be exposed to multiple salts simultaneously due to the specific ion effects as wells as competitions among ions (Farooq et al., 2015), but very few studies have been conducted in soil containing salt. Schiattone et al. (2017) mixed two salts (NaCl and $CaCl_2$) with soil to investigate water use and rocket crop performance under different salt-stressed conditions. The results showed that the increasing soil salt content decreased leaf size and numbers, water use, and yield. Faster uptake and transport from roots to the shoots of ions in solution caused symptoms to occur early in tomato leaves (Albaladejo et al., 2017). Na^+ interfered with K^+ uptake causing disturbance in stomatal regulations (Siddiqi et al., 2011) and also stimulated sulfate uptake of safflower plant (Patil, 2012).

Plant acclimation to water stress is the result of osmotic adjustment by chemical growth regulators in roots which maintain plants water status with little influence on photosynthetic rate (Martínez et al., 2007; Chaves et al., 2009; Du et al., 2015; Negrão et al., 2017). In addition, plant adaptation to salinity causes adjustments in ion uptake, extrusion, and sequestration as well as synthesis of compatible solutes to maintain cellular homeostasis (Chaves et al., 2009). Some salt-tolerant species are better able to maintain a longer greenness and photosynthetic process under high levels of Na^+ concentration in tissues (Flores et al., 2016; Negrão et al., 2017). However, response to individual stress factors cannot be isolated from plant response (Mittler, 2006).

Another challenge is linking changes in leaf physiology to WUE at leaf and whole plant scales. Reduced irrigation has been reported to improve WUE at plant scale by maintaining yield (Chen et al., 2013; Cosić et al., 2015; Yang et al., 2017). WUE at leaf scale is impacted by external factors, e.g., VPD and soil water content, and internal factors, e.g., stomatal conductance, leaf mesophyll conductance, and leaf water deficit (Chaves et al., 2009; Niu et al., 2011). Instantaneous water use efficiency (WUE_{ins}, μmol $mmol^{-1}$) is reported to decrease with increasing rainfall (Farquhar and Sharkey, 1982) while intrinsic water use efficiency (WUE_{int}, μmol mol^{-1}) is improved by sustaining P_n or decreasing g_s (Wang et al., 2010).

Tomato is moderately tolerant to salinity, with a threshold saturated paste EC of 1.3∼6 dS m^{-1} (Maggio et al., 2004). The marketable yield and dry matter of tomato decrease with salinity (Reina-Sánchez et al., 2005). Dry biomass water use efficiency (WUE_{DM}, g L^{-1}) of tomato plants did not differ at 35 and 70 mM NaCl compared to control (Romero-Aranda et al., 2001). In contrast, Reina-Sánchez et al. (2005) found that WUE_{DM} of four tomato cultivars slightly improved, while yield water use efficiency (WUE_Y, g L^{-1}) decreased with increasing salinity (Zhang et al., 2016). However, water use efficiency (WUE_{ins} and WUE_{int}) at leaf scale for tomato species under salt-stressed conditions are still unknown.

Generally, sap flow rate is affected by various internal and external factors. Internal factors refer to plant water status, i.e., canopy structure, stomatal aperture, stem hydraulic structure, and hydraulic conductivity of roots; and external factors including solar radiation (R_s, W m^{-2}) and VPD (De Swaef and Steppe, 2010; Liu et al., 2010). Only a few studies have documented that sap flow of tomato plants significantly decreased in deficit-irrigated treatments (Liu et al., 2010; Qiu et al., 2015; Mao et al., 2017).

Tomato is widely planted in northwest China. However, with increasing tomato consumption and decreasing water resources in northwest China, greenhouse tomato cultivation has shown a large potential. Therefore, in this study, one field experiment and one greenhouse experiment were conducted in 2016 and 2017, respectively. Our hypotheses were that reduced irrigation coupled with salt stress will decrease tomato sap flow rate and the WUE will improve under water stress with/without mild salt stress at leaf and plant levels. The objectives were to (1) investigate the influence of simultaneous water and salt stresses on WUE_{ins} and WUE_{int} at leaf and plant scale, (2) evaluate actual transpiration of tomato under different water and salt treatments, and (3) determine tomato WUE from leaf scale to plant scale under different water and salt stresses.

MATERIALS AND METHODS

Experimental Setup

Two experiments were carried out, one in a field and another in a solar greenhouse 200 m away from the field, at the Shiyanghe Experimental Station of Crop Water Use, Wuwei city of northwest China (37°52′N, 102°50′E, 1581 m above sea level). The field experiment was conducted from May to August 2016 (2016 season) and the greenhouse experiment from April to August 2017 (2017 season). The greenhouse was 76 × 8 m in size and made of a steel frame covered with 0.2-mm thick polyethylene, with no heating or cooling system. A narrow ventilation on the roof controled the interior daytime temperature in the summer.

The pink series tomato (*Lycopersicon esculentum*, cultivars "Nathen" and "Jinpeng") were grown in the 2016 and 2017 seasons; both are common indeterminate tomato cultivars widely used in local tomato production. During both field and greenhouse experiments, the seedlings were transplanted at the 3rd to 4th leaf stage into 7.8L plastic containers (35 cm top diameter, 30 cm bottom diameter, and 25 cm depth) filled with 16 kg air-dried sandy loam soil (<5 mm) with a bulk density of 1.3 ± 0.5 g cm^{-3}. During both years, cheesecloth and 1 kg of small gravel were packed at the bottom of the container to prevent soil loss. The containers were buried in the ground up to the top edge to maintain a soil temperature similar to the field. Soil surface of each container was covered with white polyethylene film to prevent soil water evaporation. The fertilizers applied were 200 mg kg^{-1} soil N (CH_4N_2O), 390 mg kg^{-1} soil P ($Ca(H_2PO_4)$, and 55 mg kg^{-1} soil K (KH_2PO_4). All three fertilizers were mixed homogeneously with soil before filling the containers to support plant growth during both years. The sandy loam soil had an average *in situ* bulk density of 1.52 g cm^{-3}, volumetric soil water content of 25.3% at pot water-holding capacity, electrical conductivity of 0.302 dS m^{-1}, and pH of 7.88 (**Table 1**). Considering the cultivars' characteristics of indetermination, tomato plants were pinched when the third truss of flowers came out.

Treatments

Two levels of irrigation, full irrigation (W1) and reduced irrigation (W2/3, 2/3 of W1), were applied with four soil salt regimes during two experiments. In the field experiment of 2016, four salt treatments created were S0 (no salt added), S3 (0.3%), S6 (0.6%), and S9 (0.9%), corresponding to the soil solution electrical conductivity (EC_s) of 0.205, 1.030, 1.932, and 2.597 dS m^{-1}. Salt content in parentheses represents the mass ratio of total salts to air-dried soil. Three salts, sodium chloride (NaCl), magnesium sulfate ($MgSO_4$), and calcium sulfate ($CaSO_4$), were homogeneously mixed with soil prior to packing into containers with the mass ratio of 2:2:1, respectively. In the greenhouse experiment of 2017, S6 and S9 salinity treatments were discontinued and replaced with S2 (0.2%) and S4 (0.4%) with EC_s of 0.814, and 1.326 dS m^{-1} because plants were almost dead under S6 and S9 treatments. The experiment design was a split plot with water treatments (two levels) as main plot and salt treatments (four levels) as sub-plot, each treatment has 10 and 20 containers in 2016 and 2017, respectively.

One tomato plant was transplanted to each container at the 3rd to 4th leaf stage on 9 May 2016 and 24 April 2017. Container spacing was 0.5 × 0.4 m, resulting in five plants per m^2. A drip arrow irrigation system was employed with two-drop arrow emitters in each container. For each treatment, the irrigation volume was controlled by a plastic bucket with scales installed at the head of the drip pipes, and sand and mesh filters were installed to prevent emitter clogging. Tap water with an electrical conductivity of 0.62 dS m^{-1} was used for irrigation. The irrigation treatments started on June 5th in 2016 at flowering stage, and on May 5th in 2017 in the middle of vegetative stage. Tomato plants were irrigated to 90% of pot water-holding capacity for the full irrigation treatment when its average soil water content (observed by 5TE sensors) decreased to 50 ± 2% of pot water-holding capacity. Irrigation amounts and times for each treatment are listed in **Table 2**.

The entire growth period of tomato was divided into three stages, i.e., vegetative stage (transplant to first blossom), flowering stage (first blossom to first fruit set), and fruit development and ripening stage (first fruit set to harvesting). Details of growth periods and irrigations are shown in **Table 2**.

Environmental Variables

The meteorological factors, solar radiation (R_s, W m^{-2}), relative humidity (RH, %), air temperature (T_a, °C), and vapor pressure deficit (VPD, kPa), for field and greenhouse experiments are shown in **Figure 1**. In the field experiment of 2016, meteorological data were recorded every 15 min from a weather station (Weather Hawk, Campbell Scientific, USA) 50 m away from the experiment field. In the greenhouse experiment of 2017, an automatic weather station (HOBO, Onset Computer Corp., USA) was installed in the middle of the greenhouse and data were collected every 15 min. VPD was calculated from RH and T_a (Norman, 1998). To measure soil water content (SWC, cm^3 cm^{-3}), one 5TE sensor (Decagon Devices, Inc., USA) was installed at the depth of 15 cm in three randomly selected containers in each treatment in both experiments. The data were collected every 30 min by an EM50 data logger (Decagon Devices, Inc., USA). Sensors were calibrated by optimizing gravimetrically and sensor-measured volumetric water contents.

TABLE 1 | Mean for some of the physiochemical properties of soil used for field experiment in 2016 and greenhouse experiment in 2017.

Season	Soil texture	% Sand	% Silt	% Clay	pH	Bulk density (g cm^{-3})	Field capacity (cm^3 cm^{-3})	Soil conductivity (dS m^{-1})
2016	Sandy loam	50	45	5	7.96	1.52	0.258	0.205
2017	Sandy loam	51	45	5	7.8	1.52	0.247	0.398

TABLE 2 | Details of irrigation treatment during tomato growth period during 2016–2017.

Year	Growth stage	Date (MM/DD)	Irrigation amount (L)		Irrigation times (No.)
			W2/3	W1	
2016	Vegetative	05/09–06/05	10.7	10.7	8
	Flowering	06/06–06/24	9.2	12.5	11
	Fruit development and ripening	06/25–08/11	22.7	32.5	22
	Whole	05/09–08/11	39.7	52.7	41
2017	Vegetative	04/24–05/24	6.9	8.2	8
	Flowering	05/25–06/13	10.1	14.4	10
	Fruit development and ripening	06/14–08/09	30.6	42.8	35
	Whole	04/24–08/09	47.6	62.4	53

W1, full irrigation; W2/3, deficit irrigation received 2/3 of full irrigation amount; vegetative stage, transplant to the first blossom; flowering stage, first blossom to first fruit set; fruit development and ripening stage, first fruit set to harvesting.

Leaf and Plant Measurements

Leaf gas exchange parameters, including photosynthesis rate (P_n, μmol m^{-2} s^{-1}), transpiration rate (T_r, mmol m^{-2} s^{-1}), stomatal conductance (g_s, mol m^{-2} s^{-1}), and the ratio of interacellular CO_2 concentration (C_i, μmol CO_2 mol^{-1}) to atmospheric CO_2 concentration (C_a, μmol CO_2 mol^{-1}) were determined on fully expanded upper leaves with three replications in each treatment using a Portable Photosynthesis System (LI-6400XT, LI-COR Corporation, USA). Measurements were conducted on random sunny days from 7:00 a.m. to 7:00 p.m. every 2 h on 22 July and 7 August in 2016 and 4 July, 11 July, and 9 August in 2017 at the fruit development and ripening stages. Instantaneous water use efficiency (WUE_{ins}, mmol mol^{-1}) was defined as the ratio of P_n to T_r and instrinsic water use efficiency (WUE_{int}, μmol mol^{-1}) as the ratio of P_n to g_s (Bierhuizen and Slatyer, 1965; Sinclair et al., 1984).

Sap flow rates of tomato plants were measured using dynagages (SGB9, SGB13, Dynamax, USA) during fruit development and ripening stages with Stem Heat Balance (SHB) method. In this method a stem is wrapped in a heater coil emitting a constant energy flux. The supplied energy is dissipated by convection along the stem by sap flow transport. Therefore, by measuring the convective heat fluxes and the energy supply, the rate of water flux along a stem can be calculated (Trambouze and Voltz, 2001). The dynagages were installed on the stems of plants between the third and fourth internode above the soil surface. Leaf branches beneath the fifth internode were removed and plastic film was placed to avoid stem transpiration. A CR1000 data logger (Campbell Scientific, USA) was used to collect data every 30 s and averaged every 15 min. Consequently, hourly sap flow rate per plant (Q_h, g h^{-1}) was obtained. Since the CR1000 had eight channels, two plants per treatment of W2/3 treatments were first randomly selected to monitor sap flow during 27 June to 6 July, and two plants per treatment of W1 treatments were then selected from 19 July to 28 July in the 2016 season. In 2017, one plant per treatment was selected for sap flow measurement between 25 June and 30 June.

Three tomato plants for each treatment were harvested on 11 August 2016 and 9 August 2017. All fresh fruits from the three plants in each treatment were collected and yield (Y, g per plant) was recorded using an electronic balance with accuracy of 0.01 g (ME2002E, Mettler Toledo, USA). Roots, stems, and leaves were seperately dried at 75 °C in the oven to the constant weight and dry matter weight was recorded. Water use efficiency at plant scale WUE_{DM} was calculated as the ratio of dry aboveground biomass to irrigation water per plant, and WUE_Y as fresh yield to irrigation water per plant.

Statistical Analyses

Two-way analysis of variance was performed using SPSS version 23.0 (IBM Statistics) by year to evaluate the effects of irrigation and salt regimes, as well as their interactions on tomato leaf physiology parameters and WUE at different scales. Duncan's multiple range test was used to assess differences between treatments at $P = 0.05$. Pearson correlation analysis was done for 13 parameters, including WUE_{DM}, WUE_Y, WUE_{int}, WUE_{ins}, P_n, T_r, g_s, C_i/C_a, yield, dry aboveground biomass, sap flow rate, irrigation amount, and SSC (**Table 4**). The values of leaf physiology parameters were daily averages of all measurements.

Principal component analysis (PCA) was used to evaluate the comprehensive WUE at different scales as affected by reduced irrigation and salt stress regimes. The standardized data included WUE_{DM}, WUE_Y, WUE_{int}, and WUE_{ins}. PCA was carried out using correlation matrix of SPSS version 23.0 after the KMO and Bartlett's test, and factors with eigenvalues >1 were retained. Using compute variables module in SPSS, PCs were determined and then maximum and minimum principal component for each treatment were calculated. Finally, a comprehensive score was determined for each treatment; the larger the score, the higher the performance of the treatment (Shukla et al., 2006; Wang et al., 2015).

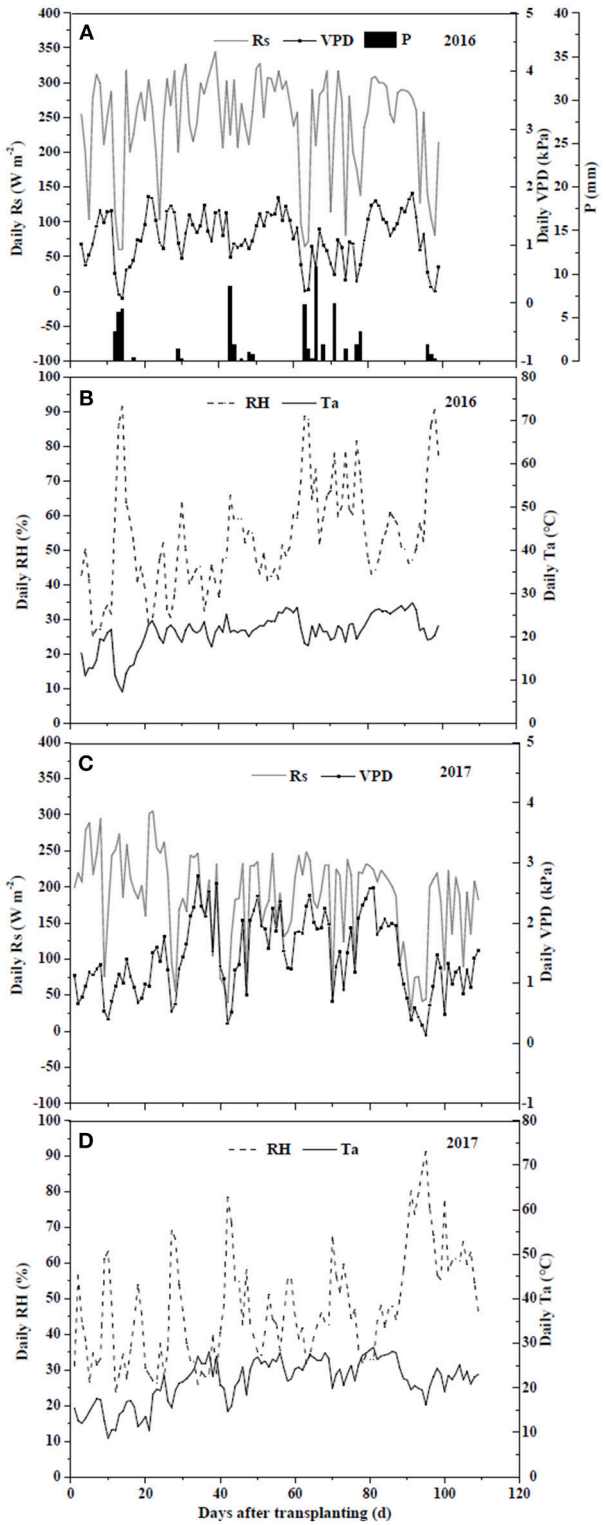

FIGURE 1 | Climate variances including daily solar radiation (R_S) **(A,C)**, relative humidity (RH) **(B,D)**, temperature (T_a) **(B,D)**, and vapor pressure deficit (VPD) **(A,C)** of field experiment in 2016 and greenhouse experiment in 2017.

RESULTS

Environmental Variables

In the field, R_s ranged from 59.7 W m^{-2} on cloudy or rainy days to 327.8 W m^{-2} on sunny days, with an average of 243.1 W m^{-2} (**Figure 1**). RH, Ta and VPD varied from 25.3 to 91.6%, from 7.2 to 27.8°C, and from 0.08 to 1.89 kPa, with the averages of 53.0%, 21.0°C and 1.14 kPa, respectively. In the greenhouse, R_s ranged from 28.2 to 305.1 W m^{-2}, with an average of 171.8 W m^{-2}. RH, Ta and VPD varied from 23.7 to 91.4%, from 8.7 to 29.1°C, and from 0.14 to 2.78 kPa, with the averages of 50.0%, 23.7°C and 1.56 kPa, respectively. Variations of daily average SWC in the 0–20 cm soil profile under different irrigation and salt stress treatments during field and greenhouse experiments are presented in **Figure 2**. In the field experiment of 2016, SWC under W1S9 treatment was higher than W1S6, W1S3, and W1S0 treatments during the whole growth season because plants were severely stressed and uptake was very low. Under reduced irrigation, the variation of SWC among S0, S3, and S6 treatments decreased compared to full irrigation (**Figures 2A,B**). In the greenhouse experiment of 2017, SWC increased with increasing soil salt content under both full and reduced irrigation (**Figures 2C,D**).

Yield and Dry Biomass Per Plant

In the field experiment of 2016, dry biomass per plant of stem, leaf, root, and total as well as root/shoot ratio were significantly affected by soil salt treatments, while water treatments and the interaction of water and salt had no significant effects. Fresh fruit yield of tomato per plant was influenced by water and salt treatments, and their interaction (**Table 3**). Increasing soil salt content caused more yield reductions under both irrigation treatments. In the field experiment of 2016, reduced irrigation (W2/3) treatments produced higher yields compared to W1 under S0 and S3 treatments, while W2/3 treatments exacerbated yield reductions under S6 and S9 treatments. In the greenhouse experiment of 2017, since the gradient of soil salt treatments was reduced, salt treatments didnot show significant effects on dry biomass of stem, leaf, root, and root/shoot ratio. Only leaf biomass was affected by water treatments and the interaction of water and salt, and root/shoot ratio was influenced by water treatments. The effect of salt treatments on total biomass per plant was also significant. Yields showed similar trends with those in the field experiment of 2016 under water and salt treatments (**Table 3**). The proportions of stem, leaf, and root dry matter were about 45.5, 42.9, and 13.4%, respectively (**Figure 3**).

Gas Exchange Parameters

All the gas exchange parameters P_n, T_r, g_s, and C_i/C_a were significantly affected by irrigation regimes, salt treatment, and their interactions in both experiments (**Table 3**). In 2016, P_n and T_r decreased with increasing soil salt stress under both W2/3 and W1 treatments. However, in the greenhouse experiment of 2017, plants grown in salt treatments of S2 and S3 had notably 35.5 and 49.4% higher P_n, respectively, than those grown in S0 treatment

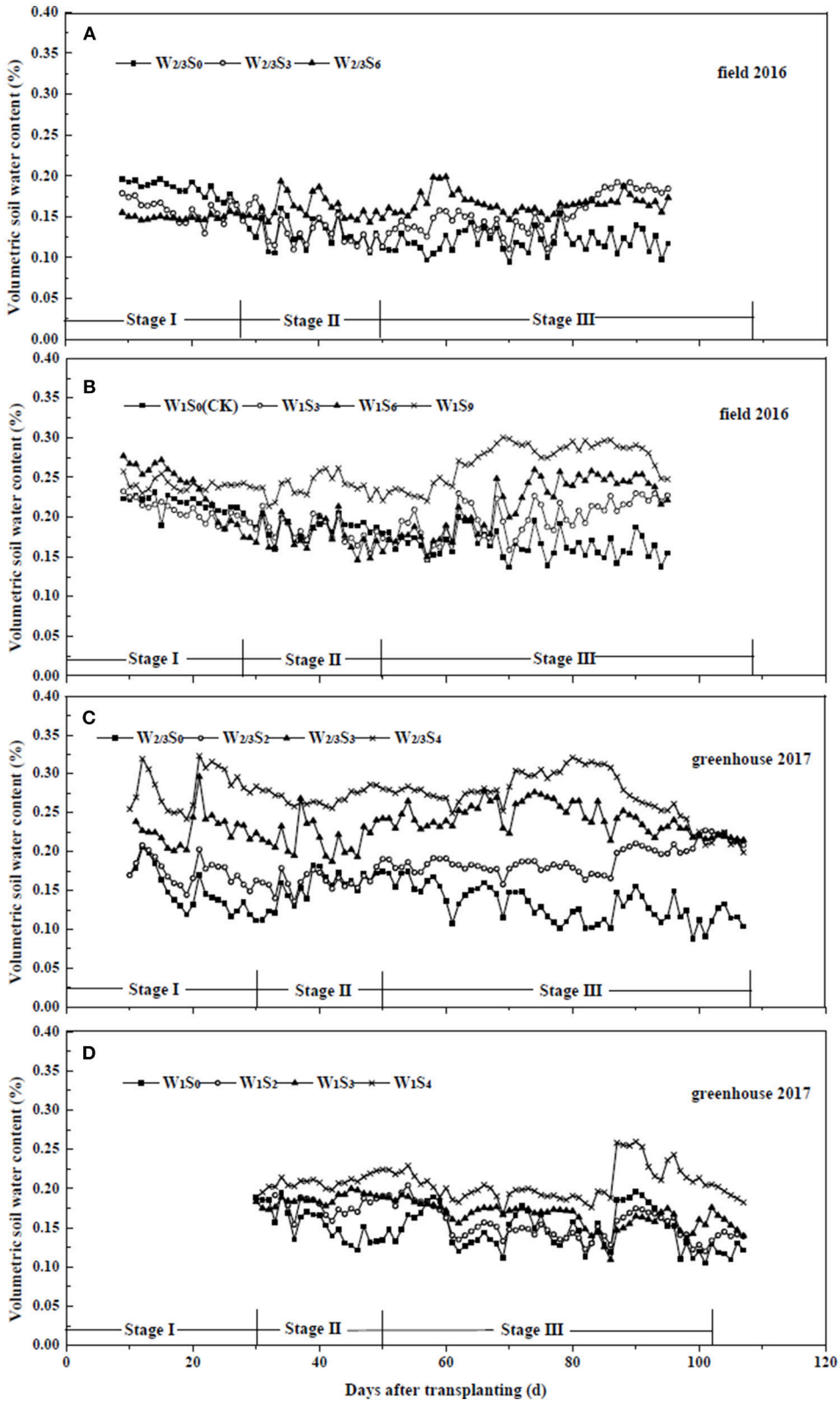

FIGURE 2 | Soil water content of tomato under different water and salt treatments in field experiment of 2016 **(A,B)** and greenhouse experiment of 2017 **(C,D)**. Stage I: vegetative stage, Stage II: flowering stage, Stage III: fruit development and ripening stage.

TABLE 3 | P_n, T_r, g_s, C_i/C_a, DM, Y, and WUE at different scale of tomato under water and salt treatments at fruit development and ripening stage during 2016–2017.

Year	Treatment	Pn (μmol m^{-2} s^{-1})	Tr (mmol $m^{-2}s^{-1}$)	gs (mol $m^{-2}s^{-1}$)	Ci/Ca	WUE_{ins} (μmol $mmol^{-1}$)	WUE_{int} (μmol mol^{-1})	SD (g $plant^{-1}$)	LD (g $plant^{-1}$)	RD (g $plant^{-1}$)	Root/ shoot	DM (g $plant^{-1}$)	Y (g $plant^{-1}$)	WUE_{DM} (g L^{-1})	WUE_Y (g L^{-1})
2016	**Water Treatments (w)**														
	W2/3	7.45	4.26	0.090	0.529	1.72	82.3	24.2	21.1	6.8	0.18	50.8	577.0	1.28	14.54
	W1	8.13	4.51	0.102	0.524	1.80	82.7	29.8	22.4	7.4	0.17	55.1	557.3	1.05	10.58
	Salt Treatments (s)														
	S0	11.46a	5.96a	0.148a	0.537b	1.93a	77.6d	47.0a	45.7a	10.1a	0.11b	102.7a	1036.4a	2.29a	23.17a
	S3	8.46b	4.95b	0.106b	0.523c	1.72c	80.9b	21.0b	16.9b	7.2b	0.19a	45.1b	753.0b	0.98b	16.64b
	S6	6.49c	3.70c	0.070c	0.481d	1.77b	93.4a	20.5b	16.3b	7.7b	0.21a	41.9b	334.5c	0.91b	7.30c
	S9	4.75d	2.95d	0.061d	0.565a	1.62d	78.3c	9.1c	8.1c	3.6c	0.20a	22.3c	144.7d	0.48c	3.13d
	w	**	**	**	**	**	**	ns	ns	ns	ns	ns	**	**	**
	s	**	**	**	**	**	**	**	**	**	**	**	**	**	**
	w×s	**	**	**	**	**	**	ns	ns	ns	ns	ns	**	**	**
2017	**Water Treatments (w)**														
	W2/3	10.69	8.91	0.275	0.790	1.21	40.3	18.9	19.7	5.7	0.15	45.4	774.1	0.95	16.26
	W1	11.86	10.31	0.332	0.749	1.16	36.7	20.7	21.5	5.4	0.14	48.8	771.5	0.94	14.90
	Salt Treatments (s)														
	S0	10.97b	9.55c	0.300c	0.865a	1.18a	39.4b	26.1a	27.1a	6.1a	0.12a	59.2a	1052.6a	1.08a	19.50a
	S2	12.11a	11.01a	0.353a	0.743c	1.12b	35.1d	21.5a	23.8a	6.4a	0.14a	54.0a	787.7b	0.98b	14.64b
	S3	11.01b	9.90b	0.309b	0.731d	1.11b	36.9c	20.4a	21.6a	5.4a	0.13a	47.4ab	694.2c	0.90ab	12.90c
	S4	9.08c	8.59d	0.228d	0.750b	1.06c	39.8a	16.6a	17.8a	4.7a	0.14a	33.8b	526.2d	0.61b	9.73d
	w	**	**	**	**	**	**	ns	*	ns	*	ns	*	ns	**
	s	**	**	**	**	**	**	ns	ns	ns	ns	**	**	**	**
	w×s	**	**	**	**	**	**	ns	*	ns	ns	*	ns	*	**

P_n, photosynthetic rate; T_r, transpiration rate; g_s, stomatal conductance; C_i, intercellular CO_2 concentration; C_a, atmospheric CO_2 concentration; WUE_{ins}, instantaneous water use efficiency at leaf scale; WUE_{int}, intrinsic water use efficiency at leaf scale; SD, stem biomass per plant; LD, leaf biomass per plant; RD, root biomass per plant; DM, dry aboveground biomass per plant; Y, fresh yield per plant; WUE_{DM}, water use efficiency at dry biomass level; WUE_Y, water use efficiency at yield scale. The values are the averages of the two water treatments W2/3 and W1 and the same for salt treatments (S0, S3, S6, and S9). The gas exchange values (except DM, Y, WUE_{DM}, and WUE_Y) represent the daily mean of sample measurements on 07/22 and 08/07 in 2016 and 07/04, 07/11, and 08/09 in 2017. Differences due to treatments were determined using analyses of variance for each season, w, water effect; s, salt effect; w×s, interactive effect of water and salt. *Significant differences for $P < 0.05$; **Significant differences for $P < 0.01$; ns, no significant.

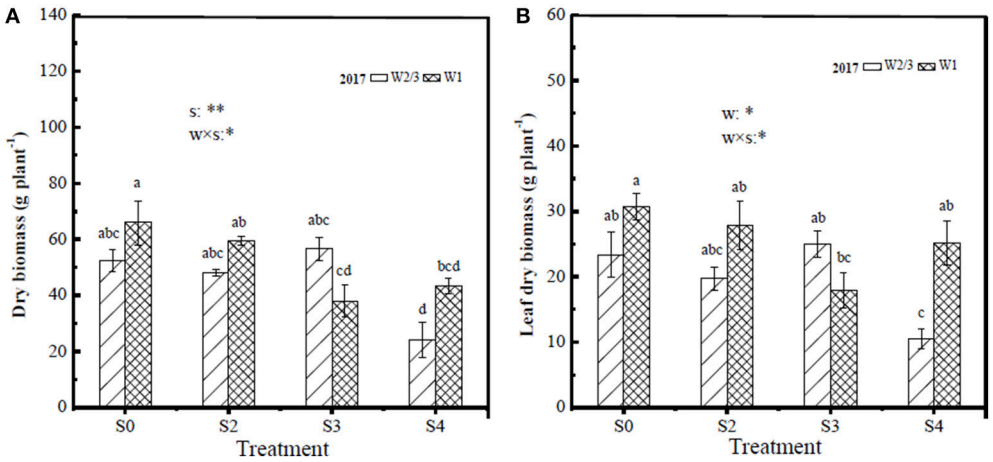

FIGURE 3 | Tomato dry biomass of whole plant **(A)** and leaf dry biomass **(B)** under different water and salt treatments at harvest in 2017. Only the positive effects of the interactions (w×s) are showed in the figure, w, water treatments; s, salt treatments, *significant differences for $P < 0.05$; **significant differences for $P < 0.01$.

TABLE 4 | Pearson correlation coefficients between WUE at leaf and plant scales and irrigation amount, soil salt content, sap flow rate, leaf physiological parameters, dry matter per plant, and fresh yield per plant.

Index	WUE_{ins} (μmol $mmol^{-1}$)	WUE_{int} (μmol mol^{-1})	WUE_{DM} (g L^{-1})	WUE_Y (g L^{-1})	I (L)	SSC (%)	P_n (μmol m^{-2} s^{-1})	T_r (mmol m^{-2} s^{-1})	g_s (mol m^{-2} s^{-1})	C_i/C_a	DM (g $plant^{-1}$)	Y (g $plant^{-1}$)
WUE_{int} (μmol mol^{-1})	0.934**											
WUE_{DM} (g L^{-1})	0.454	0.185										
WUE_Y (g L^{-1})	0.130	−0.139	0.803**									
Irrigation amount (L)	−0.569*	−0.558*	−0.265	−0.192								
Soil salt content (%)	0.169	0.423	−0.639**	−0.882**	−0.213							
P_n (μmol m^{-2} s^{-1})	−0.390	−0.648**	−0.467	0.620*	0.365	−0.827**						
T_r (mmol m^{-2} s^{-1})	−0.801**	−0.918**	0.030	0.279	0.597*	−0.586*	0.850**					
g_s (mol m^{-2} s^{-1})	−0.766**	−0.896**	0.033	0.260	0.543*	−0.540*	0.846**	0.986**				
C_i/C_a	−0.841**	−0.892**	−0.190	0.206	0.417	−0.430	0.462	0.730**	0.716**			
DM (g $plant^{-1}$)	0.298	0.011	0.939**	0.764**	0.047	−0.752**	0.638**	0.239	0.233	−0.055		
Y (g $plant^{-1}$)	−0.098	−0.366	0.686**	0.930**	0.150	−0.981**	0.782**	0.521*	0.490	0.393	0.771**	
Sap flow rate (g h^{-1})	0.175	−0.042	0.480	0.396	0.489	−0.577*	0.526	0.258	0.252	0.031	0.684**	0.581*

P_n, photosynthetic rate; T_r, transpiration rate; g_s, stomatal conductance; C_i, intracellular CO_2 concentration; C_a, atmospheric CO_2 concentration; I, irrigation amount; SSC, soil salt content; DM, dry aboveground biomass per plant; Y, fresh yield per plant; WUE_{ins}, instantaneous water use efficiency at leaf scale; WUE_{int}, intrinsic water use efficiency at leaf scale; WUE_{DM}, water use efficiency at dry biomass level; WUE_Y, water use efficiency at yield scale. The values of all parameters used for analyzing were daily averages (except I, SSC, DM, and Y) collected during 2016–2017.

**Significant differences for $P < 0.05$; **Significant differences for $P < 0.01$.*

under reduced irrigation regime (W2/3). For W1 treatment, highest P_n of 13.30 μmol m^{-2} s^{-1} was for S0 treatment (**Table 3**). Moreover, T_r was significantly positively correlated with P_n and g_s and was also notably correlated with P_n and T_r (**Table 4**). Although irrigation amount and soil salt content notably affected C_i/C_a (**Table 3**), Pearson correlation coefficients between C_i/C_a, irrigation amount and soil salt content were not significant; C_i/C_a had significant positive correlation with T_r and g_s (**Table 4**).

In 2016, diurnal variations of P_n and g_s in S0 treatment under W2/3 and W1 regimes initially showed an increase from 7:00 to 9:00 a.m. and a decrease until 3:00 p.m.; however, multiple peaks were observed around 5:00 p.m., compensation of mild salt stress (S3) in P_n was more obvious than that of S0 (**Figures 4A,B,E, F**). In 2017, the diurnal variations of g_s under various water and salt treatments showed a single-peak curve with the peak occurring at 10:00 a.m. (**Figures 5E,F**), and T_r remained relatively high between 10:00 a.m. and 2:00 p.m. (**Figures 5C,D**), which was consistent with the results in the field experiment during 2016 (**Figures 4C,D**).

Sap Flow Variation

The daily variations of sap flow rate per plant under irrigation and salt treatments varied diurnally. Sap flow increased significantly from early morning (7:00 a.m.), reached the

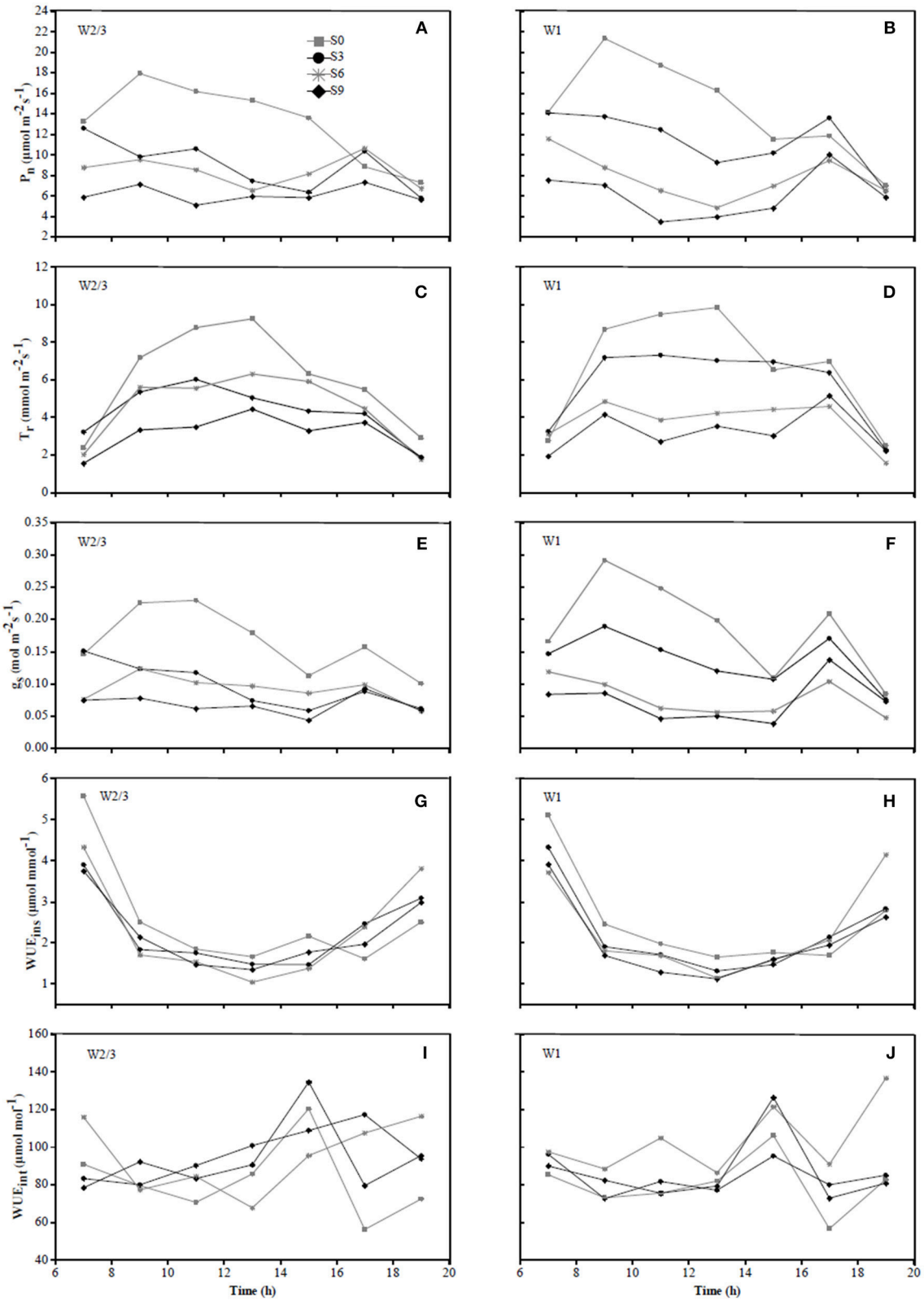

FIGURE 4 | Diurnal variations in photosynthetic rate (P_n) **(A,B)**, transpiration rate (T_r) **(C,D)**, stomatal conductance (g_s) **(E,F)**, instantaneous water use efficiency (WUE_{ins}) **(G,H)**, and intrinsic water use efficiency (WUE_{int}) **(I,J)** of tomato under different water treatments at fruit ripening stage (date 07/22) in 2016.

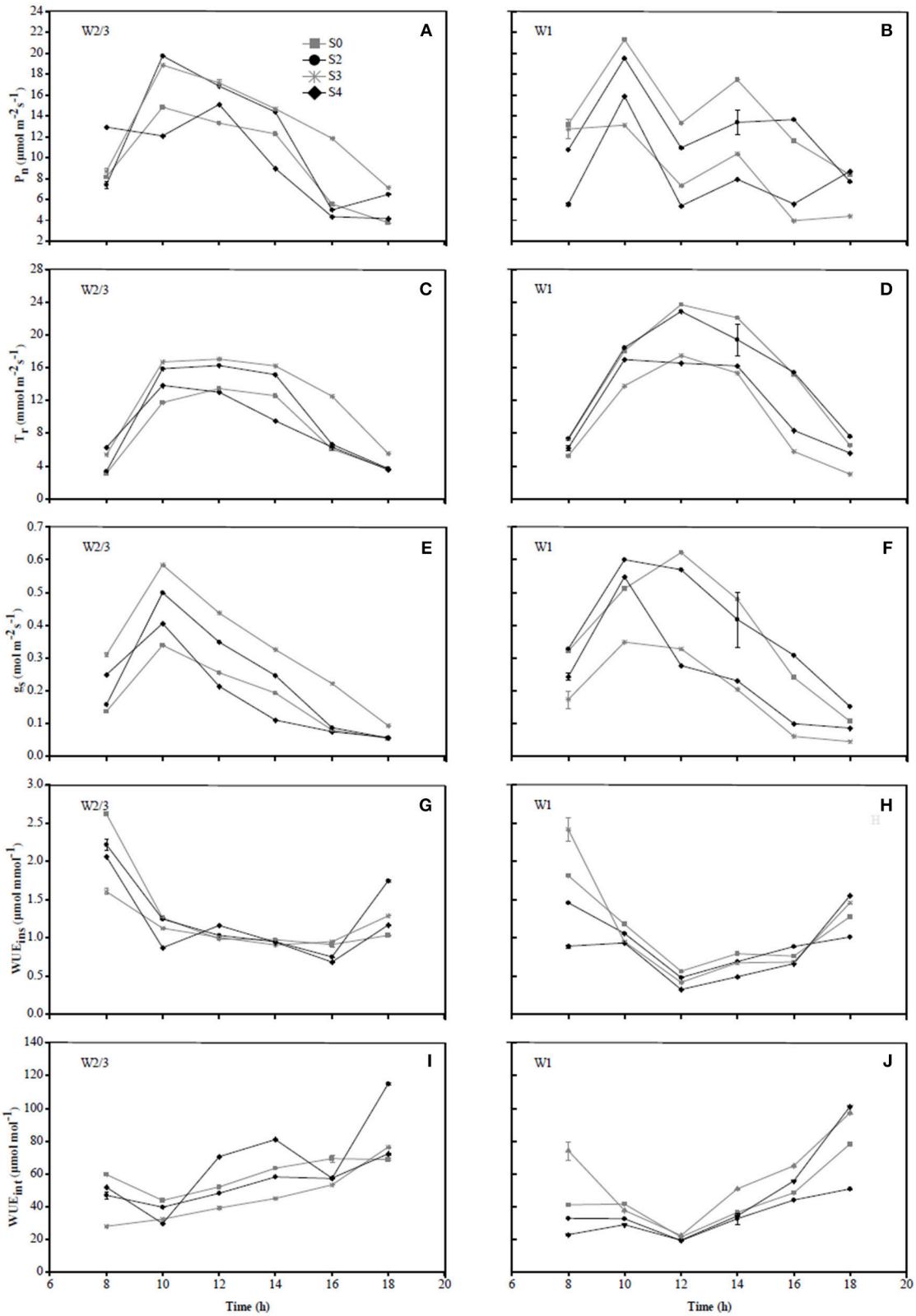

FIGURE 5 | Diurnal variations in photosynthetic rate (P_n) **(A,B)**, transpiration rate (T_r) **(C,D)**, stomatal conductance (g_s) **(E,F)**, instantaneous water use efficiency (WUE_{ins}) **(G,H)**, and intrinsic water use efficiency (WUE_{int}) **(I,J)** of tomato under different water treatments at fruit ripening stage (date 07/11) in 2017.

maximum around noon, but notably decreased after 4:00 p.m., with no sap flow measured at 9:00 p.m. (**Figures 6**, **7**) in both experiments. In the field experiment, increases in sap flow in the morning were significantly delayed with increasing soil salt content, maximum sap flow was much lower than that in S0, and sap flow stopped earlier in the night (**Figures 6C,D**). The diurnal variations in sap flow under various water and salt treatments showed a single-peak curve, and sap flow rate was smaller throughout the day with increasing soil salt content under both W2/3 and W1 treatments (**Figures 6C,D,G,H**). In the greenhouse experiment, however, diurnal variations in sap flow showed a peak around noon, and another small peak was observed at 6:00 p.m. W1S2 treatment showed a relatively higher sap flow throughout the day, following the W1S3 and W2/3S0 treatments. Soil salt content significantly decreased daily sap flow (**Table 4**). The daily variation of sap flow rate per plant ranged from 7.96 to 31.37 g h^{-1} in the field experiment and from 12.52 to 36.02 g h^{-1} in the greenhouse experiment among various salt stresses.

The relationships between sap flow rates and climate variables under different irrigation and salt treatments at fruit development and ripening stage were established in the field and greenhouse experiments. The significant level of regression coefficients was less than 0.01, and the most of correlation coefficients (R^2) were higher than 0.5 (**Table 5**). In 2016, sap flow rate under W2/3 treatments increased linearly with increasing R_s, T_a, and VPD ($R^2 > 0.5$). In 2017, sap flow also showed a positive correlation with R_s, T_a, and VPD under various water and salt treatments except W2/3S4 treatment ($R^2 = 0.41$ for T_a and 0.46 for VPD) (**Table 5**). The different regression equations indicated that the sensitivity of sap flow rates to climate variables varied with the irrigation regimes and salt treatments. In both experiments, the slopes of regression equations in no salt treatments (W2/3S0 and W1S0) were higher than those in salt stress treatments. The average R^2 between T_a and VPD were lower due to the lagging effects on sap flow rates (**Figures 6**, **7**). The climate variables affecting sap flow rates were ranked as R_s >VPD>T_a.

Water Use Efficiency (WUE) at Leaf and Plant Scales

Irrigation and soil salt treatments, and their interactive effects on tomato WUE_{ins} and WUE_{int} at leaf scale, were significant during both field and greenhouse experiments (**Table 4**). In the field experiment of 2016, WUE_{ins} ranged from 1.50 to 1.95 μmol $mmol^{-1}$, while WUE_{int} ranged from 74.5 to 98.9 μmol mol^{-1} under different water and salt treatments. Under full and reduced irrigation, increasing salt stress decreased P_n and T_r and led to the reductions in WUE_{ins} at the leaf scale. However, compared to full irrigation, reduced irrigation (W2/3) improved WUE_{ins} with a significant decline in g_s and T_r under no salt and 0.3% soil salt treatments. Under soil salt content of 0.6% and 0.9%, a slight increase in P_n and decline in T_r resulted in higher WUE_{ins} in the full irrigation treatment. Significant reduction in g_s led to increasing WUE_{int} under S3 and S6 treatments compared to S0 treatment under both irrigations; however, further increases in soil salt content to 0.9% decreased the WUE_{int}.

In the greenhouse experiment of 2017, WUE_{ins} and WUE_{int} varied from 0.95 to 1.28 μmol $mmol^{-1}$ and from 30.3 to 46.7 μmol mol^{-1}, respectively. Compared to full irrigation, WUE_{int} under reduced irrigation was higher under no salt and 0.2% soil salt treatment in 2016, and WUE_{DM} and WUE_Y of tomato at whole plant scale were also significantly affected by irrigation regime, soil salt content, and their interaction in 2016 (**Table 4**), while in 2017, the effect of irrigation regime on WUE_{DM} was not significant. In the field experiment of 2016, increasing soil salt content decreased plant dry biomass and yield, and resulted in greater decreases in whole plant WUE_{DM} and WUE_Y under both irrigation treatments. Compared to full irrigation, reduced irrigation increased both WUE_{DM} and WUE_Y under 0 and 0.3% soil salt treatments. In the greenhouse experiment of 2017, WUE_{DM} in W2/3S4 treatment was significantly lower than that in W2/3S0 treatment. WUE_Y decreased with increasing soil salt content under both irrigation treatments. WUE_Y under reduced irrigation was higher compared to full irrigation under 0, 0.2, 0.3, and 0.4% soil salt treatments.

PCA for Comprehensive Evaluation of WUE

The results of PCA evaluation of tomato WUE at leaf and plant scales among all the treatments in the field and greenhouse experiments are shown in **Figure 8**. The index y_i^* represents closeness of principal component of the treatment to the maximum principal; the larger the index value, the better the performance of the treatment. The PCA analysis showed that plants grown under both full and reduced irrigation with zero soil salt content (W2/3S0 and W1S0) had optimal comprehensive WUE with the highest y_i^* values of 0.743 and 0.569 in the field experiment of 2016. W2/3S0 and W2/3S2 treatments ranked first and second in the greenhouse experiment of 2017, with y_i^* values of 0.953 and 0.670, respectively.

DISCUSSION

It has been suggested that high soil salt content reduces plant water uptake (Reina-Sánchez et al., 2005; Machado and Serralheiro, 2017; Phogat et al., 2018), which supported our result where root zone soil water content remained higher in containers with higher soil salt content in both reduced and full irrigation treatments during both years (**Figure 2**). Our results were also consistent with Reina-Sánchez et al. (2005) who reported that tomato plants grown under 75 mM NaCl consumed 40% less water than plants under non-saline condition. Several mechanisms are responsible for this decrease, including modulation of underlying growth mechanisms. Saline growth medium adversely affects plant growth due to low soil osmotic potential (high osmotic stress), resulting in lower leaf and root water potentials, relative water content, and plant dehydration (Ashraf, 2004; Maggio et al., 2004). Salinity-induced ion toxicity, macro and micro nutrient deficiency (such as N, Ca, K, P, Fe, and Zn), as well as oxidative stresses on plants also limit water uptake from soil (Shrivastava and Kumar, 2015).

In this study, dry aboveground tomato biomass per plant was prominently affected by soil salt content, while the effect of irrigation was non-significant in both field and greenhouse experiments (**Table 3**). These results contrasted with those of

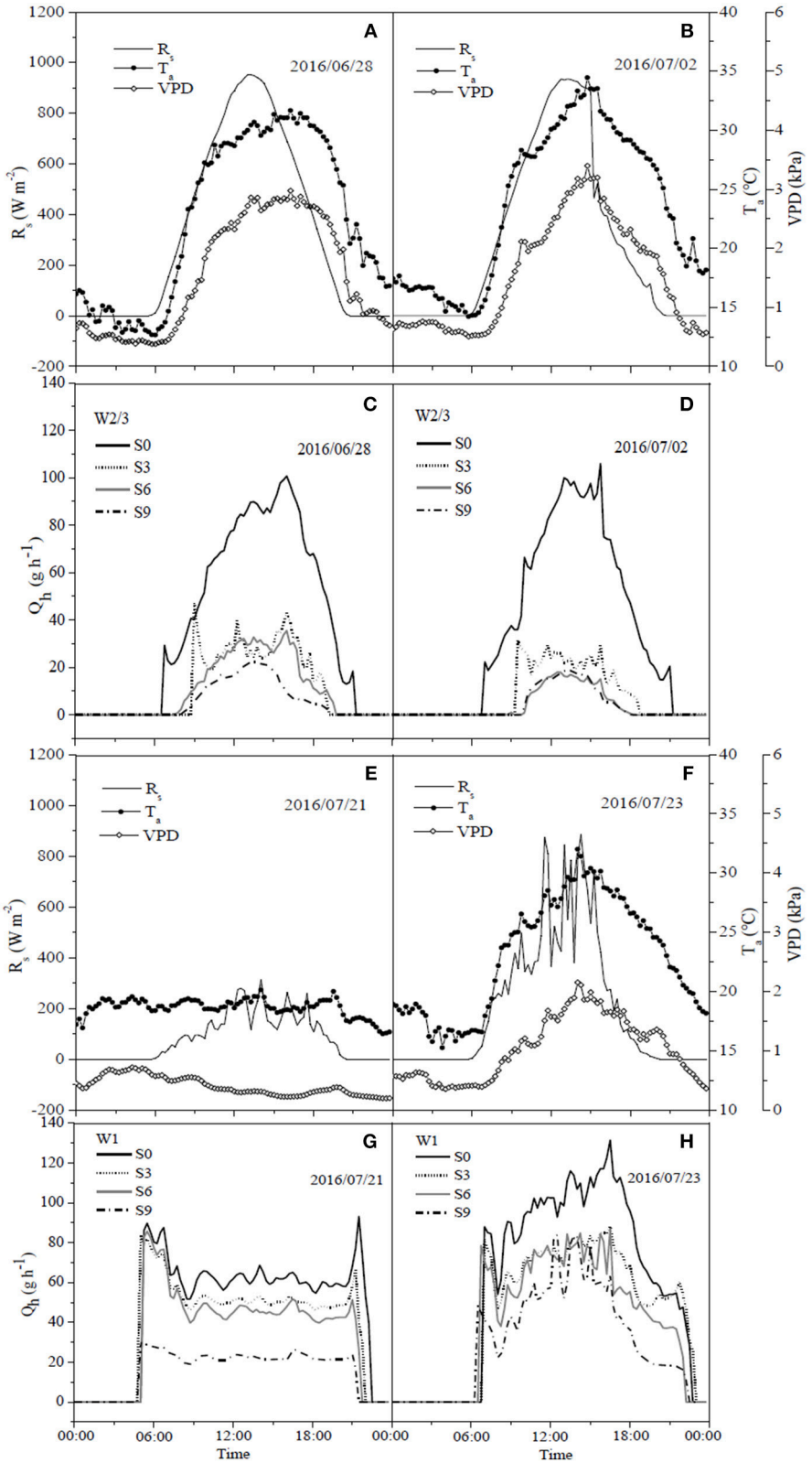

FIGURE 6 | Diurnal dynamics of hourly sap flow rate per plant (Q_h) **(C,D,G,H)** in tomato and corresponding solar radiation (R_s), air temperature (T_a) and vapor pressure deficit (VPD) **(A,B,E,F)** under different water and salt treatments in 2016.

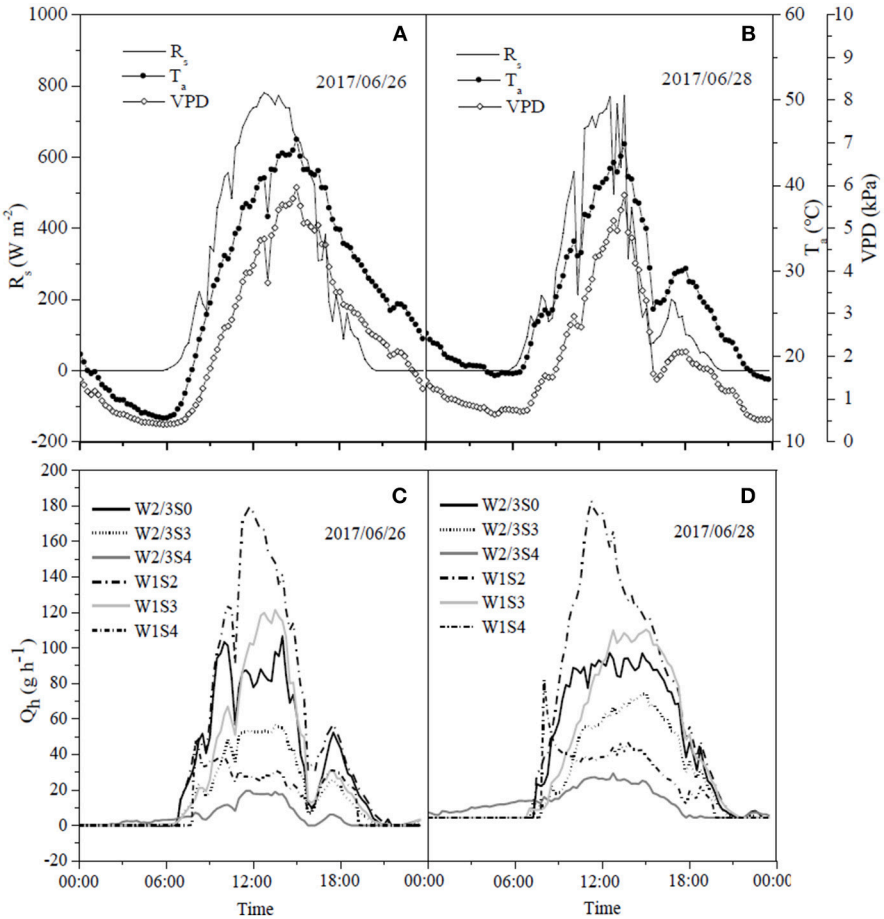

FIGURE 7 | Diurnal dynamics of hourly sap flow rate per plant (Q_h) **(C,D)** in tomato and corresponding solar radiation (R_s), air temperature (T_a), and vapor pressure deficit (VPD) **(A,B)** under different water and salt treatments in 2017.

Álvarez et al. (2018). A likely explanation is that the Álvarez et al. (2018) experiments were conducted under simulated conditions of soil cultivation and were irrigated with different levels of saline solutions. Uptake and transport rates of saline ions from root to shoot differ when plants are subjected to nutritive solution and multiple salts (Albaladejo et al., 2017) due to the competition among ions (i.e., K^+, Ca^{2+}, NO_3^- Na^+, Cl^-, and SO_4^{2-}) (Hu and Schmidhalter, 2005; Hussain et al., 2016). Most vegetable crops, including tomato, had a salinity threshold of 2.5 dS m^{-1} (Machado and Serralheiro, 2017). However, in this study, 32.9 and 20.7% yield reductions were observed at the EC of 1.03 dS m^{-1} for soil salt content of 0.3% under 2/3 of full irrigation and full irrigation, respectively, in the field experiment, and 23.6 and 26.7% at the EC of 0.81 dS m^{-1} for soil salt content of 0.2% under 2/3 of full irrigation and full irrigation, respectively, in the greenhouse experiment. Thus, the salinity threshold in this study was at or below 0.81 dS m^{-1}. This difference could result from species and different saline ions in solution and in the soil, suggesting that multiple salts in soil could further aggravate the adverse effect of salt stress on plants.

Previous studies have observed that reduced irrigation could enhance plant water use efficiency because of only slight decreases in yield but moderate declines in water application as compared to full irrigation (Kang et al., 2002, 2017; Du et al., 2010; Patanè et al., 2011; Yang et al., 2017). This study clearly illustrated that reduced irrigation improved plant yield and dry biomass WUE (WUE_Y and WUE_{DM}) under low soil salt content (SSC $\leq$ 0.3%) in both experiments (**Table 3**). However, in 2016, WUE_Y and WUE_{DM} decreased with further increases in soil salt content (SSC $\geq$ 0.9%) due to the significant reduction of yield and dry biomass. Khataar et al. (2018) results for wheat WUE were similar to this study under low salinities (EC $\leq$ 8 dS m^{-1}). However, Khataar et al. (2018) reported that bean WUE increased with increasing water and salt stresses and contradicted our results for tomato at higher soil salt content.

Tomato P_n, yield, dry biomass, WUE_Y, and WUE_{DM} decreased with increasing soil salt content under both full and reduced irrigation during the field experiment (**Table 3**), indicating the source-sink relationships in which the source organ (leaves) gained the assimilation product through photosynthesis and delivered it to the sink organ (fruits) (Liu

TABLE 5 | Relationships between sap flow rates (Q_h, g h^{-1}) every 15 min and corresponding solar radiation (R_s, W m^{-2}), air temperature (T_a, °C), and vapor pressure (VPD, kPa) deficit under different irrigation and salt stress treatments during 2016 and 2017 seasons.

Growth season	Treatment	N	R_s		T_a		VPD	
			Regression equation	R^2	Regression equation	R^2	Regression equation	R^2
2016	W2/3S0	192	$Q_h = (0.097 \pm 0.003)R_s+5.63$	0.86	$Q_h = (4.91 \pm 0.16)T_a$-77.25	0.83	$Q_h = (36.49 \pm 0.98)$VPD−20.31	0.88
	W2/3S3	192	$Q_h = (0.032 \pm 0.001)R_s$-0.26	0.76	$Q_h = (1.47 \pm 0.09)T_a$-23.99	0.59	$Q_h = (11.03 \pm 0.53)$VPD−7.671	0.70
	W2/3S6	192	$Q_h = (0.026 \pm 0.001)R_s$-0.92	0.76	$Q_h = (1.08 \pm 0.08)T_a$-17.80	0.49	$Q_h = (8.44 \pm 0.52)$VPD−5.86	0.58
	W2/3S9	192	$Q_h = (0.019 \pm 0.001)R_s$-1.112	0.87	$Q_h = (0.753 \pm 0.05)T_a$-12.5	0.51	$Q_h = (5.83 \pm 0.35)$VPD−4.14	0.59
	W1S0	96	$Q_h = (0.048 \pm 0.01)R_s+36.5$	0.16	$Q_h = (3.29 \pm 0.54)T_a$-29.65	0.28	$Q_h = (28.2 \pm 5.04)$VPD+17.21	0.24
	W1S3	96	$Q_h = (0.039 \pm 0.01)R_s+30.24$	0.14	$Q_h = (2.42 \pm 0.49)T_a$-17.54	0.20	$Q_h = (20.54 \pm 4.55)$VPD+17.06	0.17
	W1S6	96	$Q_h = (0.037 \pm 0.01)R_s+26.35$	0.14	$Q_h = (2.19 \pm 0.47)T_a$-16.59	0.18	$Q_h = (18.49 \pm 4.41)$VPD+14.87	0.15
	W1S9	96	$Q_h = (1.262 \pm 0.19)R_s$-13.22	0.31	$Q_h = (1.26 \pm 0.19)T_a$-13.2	0.31	$Q_h = (10.81 \pm 1.79)$VPD+4.71	0.27
2017	W2/3S0	192	$Q_h = (0.127 \pm 0.004)R_s+6.53$	0.86	$Q_h = (3.50 \pm 0.13)T_a$-61.12	0.78	$Q_h = (19.97 \pm 0.87)$VPD−10.99	0.73
	W2/3S3	192	$Q_h = (0.08 \pm 0.002)R_s+2.84$	0.88	$Q_h = (2.31 \pm 0.07)T_a$-42.59	0.86	$Q_h = (13.72 \pm 0.38)$VPD−10.52	0.87
	W2/3S4	192	$Q_h = (0.024 \pm 0.001)R_s+1.94$	0.83	$Q_h = (0.50 \pm 0.04)T_a$-6.44	0.41	$Q_h = (3.13 \pm 0.25)$VPD−10.15	0.46
	W1S2	192	$Q_h = (0.209 \pm 0.005)R_s+5.69$	0.91	$Q_h = (5.45 \pm 0.24)T_a$-97.5	0.74	$Q_h = (31.25 \pm 1.48)$VPD−19.56	0.70
	W1S3	192	$Q_h = (0.137 \pm 0.004)R_s+3.13$	0.86	$Q_h = (3.96 \pm 0.12)T_a-74.82$	0.86	$Q_h = (23.81 \pm 0.59)$VPD−20.75	0.90
	W1S4	192	$Q_h = (0.049 \pm 0.002)R_s+3.63$	0.69	$Q_h = (1.30 \pm 0.08)T_a$-21.32	0.58	$Q_h = (7.08 \pm 0.51)$VPD−1.97	0.50

N, sample number; the significance of regression coefficients is less than 0.01.

et al., 2017). Inverse relationships between P_n and increasing salt stress are also reported by other researchers (Netondo et al., 2004; Chaves et al., 2009; Senguttuvel et al., 2014; Das et al., 2015; Negrão et al., 2017).

Stomata control, both water losses and CO_2 assimilation, is a vital mechnism for plant acclimation to varying environments. Abiotic stress could suppress cell growth and photosynthesis (Wilkinson and Davies, 2002; Liu et al., 2006; Zhang et al., 2015; Álvarez et al., 2018). On the other hand, Galmés et al. (2007) reported that limited recovery of leaf hydraulic conductivity of some species after re-watering could also cause down-regulation of stomatal conductance. In addition, sodium, which was added to soil in this study, disturbs stomatal regulation by interfering with potassium uptake and transport (Farooq et al., 2015). Photosynthesis is affected by changes in stomatal conductance through the pathways noted above. All these are in good agreement with the present study, which found that g_s was significantly positively correlated to P_n as well as T_r (**Table 4**) under various water and salinity conditions.

Wei et al. (2018) reported that reduced irrigation improved WUE_{ins} and WUE_{int} of tomato with significant decrease in gs and Tr at leaf scale. However, the effects of salt stress and the interaction of water and salt stresses on tomato WUE at leaf scale are still unknown. In the present study, salt stress reduced WUE_{ins} under both irrigation treatments; WUE_{ins} and WUE_{int} improved under reduced irrigation compared to full ittigation when soil salt content was less than 0.4%. Both water and salt treatments together with their interaction had significant effects on WUE_{ins} and WUE_{int} in both experiments (**Table 3**). In the field experiment of 2016, WUE_{ins} and WUE_{int} of tomato increased under S6 and S9 salt treatments compared to S0 and S3 treatments only when full irrigation was applied, indicating that g_s and T_r were more sensitive to drought and salinity than P_n. Diurnal variation of WUE_{ins} in **Figures 4**, **5** showed that WUE_{ins} in various water regimes and soil salt contents were relatively high in the morning and late afternoon, while it remained low from 10:00 a.m. until 4:00 p.m. during both years. In contrast, diurnal variation of WUE_{int} remained inconsistent during 2016 as well as 2017. The ratio of C_i to C_a is characteristically near 0.7 for non-stressed C_3 plants (Farquhar et al., 1989). Lower C_i:C_a ratios resulting from either lower stomatal conductance or higher photosynthetic capacity could improve plant WUE_{int} (Condon et al., 2002). Our study found that the value of C_i:C_a ranged from 0.5 to 0.6 in 2016, whereas it was near 0.7 in 2017 (except W2/3S0 treatment) (**Table 3**). Lower C_i:C_a ratios were in accord with positive correlations with T_r and g_s.

Liu et al. (2010) reported that on sunny days sap flow showed a single-peaked curve starting at 6:00 a.m., rapidly increased to the maximum at 1:00 p.m. with increasing R_s and VPD, and decreased after 2:00 p.m. On cloudy days, sap flow exhibited a multimodal curve corresponding to the variation of R_s, and there was no flow during the night. In our field experiment, the sap flow also began at 6:00 a.m., but the maximum was reached at around 3:00 p.m. (**Figures 6C,D**). Differences in these studies are mostly due to the different atmospheric conditions (R_s, VPD, and T_a). In the greenhouse experiment, sap flow exhibited a double-peaked curve with the maximum around 12:00 a.m., and the second small peak appeared at 5:30 p.m. (**Figures 7C,D**), which was affected by the variation of daily R_s, T_a, and VPD (**Figures 7A,B**). R_s, VPD, and T_a had positive linear relationships with sap flow, and the three variables affecting sap flow were ranked as R_s >VPD>T_a (**Table 5**) in both experiments, which was in good agreement with Liu et al. (2010) for tomato and Jiang et al. (2016) for maize.

The sap flow in our study also showed a multimodal curve on cloudy days (**Figure 6G**). It has been reported that reduced

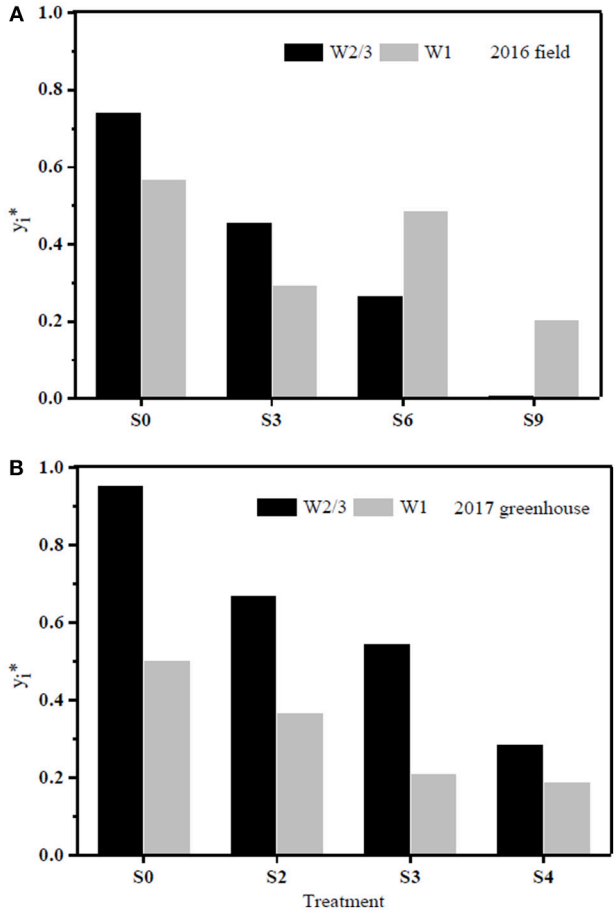

FIGURE 8 | PCA evaluation of tomato water use efficiency (WUE) at leaf and plant scales (four parameters: WUE_{ins}, WUE_{int}, WUE_{DM}, and WUE_Y) among all the treatments during 2016 **(A)** and 2017 **(B)**, respectively. y_i^* represents closeness of principal component of each treatment to the maximum principal.

irrigation restricted tomato sap flow (Liu et al., 2010; Qiu et al., 2015; Mao et al., 2017), whereas our study found that sap flow was significantly related to soil salt content, and salt stress prominently decreased sap flow rate and delayed start in the morning (**Table 4** and **Figures 6C,D**). The daily variation of sap flow was possibly caused by decreasing plant size and leaf area with increasing salt stress. This result was supported by the significant positive Pearson correlation between daily sap flow rate, dry matter, and fresh yield per plant (**Table 4**). PCA approach is an effective tool for simplifying data sources, which can realize the accurate and comprehensive assessment of variance source after the feature extraction and dimensionality reduction. In the present study, the PCA appraisement of integrated WUE attributes of tomato grown under water and salt stress included four parameters (WUE_{ins} and WUE_{int} at leaf level and WUE_Y and WUE_{DM} at plant level). Reduced irrigation in the absence of salt stress (W2/3S0 treatments) achieved the highest comprehensive WUE among all the treatments both in 2016 and 2017; in addition, 2/3 of full irrigation combined with mild salt stress (soil salt content of 0.2%) showed a relative higher integrated WUE in 2017 (**Figure 8**).

CONCLUSION

This study is important for regulating water-saving strategies for saline soil environments and improving water use efficiency at various scales 2/3 of full irrigation coupled with low soil salt contents (SSC $\leq$ 0.3%) improved WUE_Y and WUE_{DM} at the plant level, but WUE_Y and WUE_{DM} decreased under the salt stress of 0.6 and 0.9%. Plants irrigated with full irrigation compensated for salt stress and maintained yield and dry biomass. 2/3 of full irrigation in the absence of salt stress improved P_n and reduced T_r, leading to the highest WUE_{ins} at leaf level. Moderate salt stress (SSC $\leq$ 0.6%) improved WUE_{int} at leaf level under both irrigation regimes. The PCA analysis showed that 2/3 of full irrigation without salt stress possessed the highest integrated WUE among all the treatments in both years; reduced irrigation coupled with mild salt stress (SSC = 0.2%) also achieved a relative higher comprehensive WUE in 2017. Soil salt content threshold for tomato caused by multiple salts was found to be below 0.2% and is lower than thresholds reported for nutrient solution.

AUTHOR CONTRIBUTIONS

HY carried out the experiments and finished the first manuscript. MS and TD supervised the work. XM and SK helped to edit the manuscript.

FUNDING

This research received grants from the National Natural Science Foundation of China (51725904, 51621061, 51861125103), and the Discipline Innovative Engineering Plan (111 Program, B14002).

ACKNOWLEDGMENTS

The authors thank New Mexico State University Agricultural Experiment Station. The authors also thank Mr. Franklin Sholedice of New Mexico State University for editing the manuscript.

REFERENCES

Ahmed, I. M., Dai, H., Zheng, W., Cao, F., Zhang, G., Sun, D., et al. (2013). Genotypic differences in physiological characteristics in the tolerance to drought and salinity combined stress between Tibetan wild and cultivated barley. *Plant Physiol. Biochem.* 63, 49–60. doi: 10.1016/j.plaphy.2012.11.004

Albaladejo, I., Meco, V., Plasencia, F., Flores, F. B., Bolarin, M. C., and Egea, I. (2017). Unravelling the strategies used by the wild tomato species *Solanum pennellii* to confront salt stress: from leaf anatomical adaptations to molecular

responses. *Environ. Exp. Bot*. 135, 1–12. doi: 10.1016/j.envexpbot.2016.12.003

Álvarez, S., Rodríguez, P., Broetto, F., and Sánchez-Blanco, M. J. (2018). Long term response and adaptive strategies of *Pistacia Lentiscus* under moderate and severe deficit irrigation and salinity: osmotic and elastic adjustment, growth, ion uptake and photosynthetic activity. *Agric. Water Manage*. 202, 253–262. doi: 10.1016/j.agwat.2018.01.006

Ashraf, M. (2004). Some important physiological selection criteria for salt tolerance in plants. *Flora* 199, 361–376. doi: 10.1078/0367-2530-00165

Baath, G. S., Shukla, M. K., Bosland, P. W., Steiner, R. L., and Walker, S. J. (2017). Irrigation water salinity influences at various growth stages of *Capsicum annuum*. *Agric. Water Manage*. 179, 246–253. doi: 10.1016/j.agwat.2016.05.028

Bierhuizen, J. F., and Slatyer, R. O. (1965). Effect of atmospheric concentration of water vapour and CO_2 in determining transpiration-photosynthesis relationships of cotton leaves. *Agric. Meteorol*. 2, 259–270. doi: 10.1016/0002-1571(65)90012-9

Chaves, M. M., Flexas, J., and Pinheiro, C. (2009). Photosynthesis under drought and salt stress: regulation mechanisms from whole plant to cell. *Ann. Bot*. 103, 551–560. doi: 10.1093/aob/mcn125

Chen, J. L., Kang, S. Z., Du, T. S., Qiu, R. J., Guo, P., and Chen, R. Q. (2013). Quantitative response of greenhouse tomato yield and quality to water deficit at different growth stages. *Agric. Water Manage*. 129, 152–162. doi: 10.1016/j.agwat.2013.07.011

Condon, A. G., Richards, R. A., Rebetzke, G. J., and Farquhar, G. D. (2002). Improving intrinsic water use efficiency and crop yield. *Crop Sci*. 42, 122–131. doi: 10.2135/cropsci2002.1220

Cosić, M., Djurović, N., Todorović, M., Maletić, R., Zećević, B., and Stričević, R. (2015). Effect of irrigation regime and application of kaolin on yield, quality and water use efficiency of sweet pepper. *Agric. Water Manage*. 159, 139–147. doi: 10.1016/j.agwat.2015.05.014

Das, P., Nutan, K. K., Singla-Pareek, S. L., and Pareek, A. (2015). Understanding salinity responses and adopting 'omics-based' approaches to generate salinity tolerant cultivars of rice. *Front. Plant Sci*. 6:712. doi: 10.3389/fpls.2015.00712

De Swaef, T., and Steppe, K. (2010). Linking stem diameter variations to sap flow, turgor and water potential in tomato. *Funct. Plant Biol*. 37, 429–438. doi: 10.1071/FP09233

Deb, S. K., Sharma, P., Shukla, M. K., and Sammis, T. W. (2013). Drip-irrigated pecan seedling response to irrigation water salinity. *Hortscience* 48, 1548–1555. doi: 10.21273/HORTSCI.48.12.1548

Du, T. S., Kang, S. Z., Sun, J. S., Zhang, X. Y., and Zhang, J. H. (2010). An improved water use efficiency of cereals under temporal and spatial deficit irrigation in north China. *Agric. Water Manage*. 97, 66–74. doi: 10.1016/j.agwat.2009.08.011

Du, T. S., Kang, S. Z., Zhang, J. H., and Davies, W. (2015). Deficit irrigation and sustainable water-resource strategies in agriculture for China's food security. *J. Exp. Bot*. 66, 2253–2269. doi: 10.1093/jxb/erv034

Farooq, M., Hussain, M., Wakeel, A., and Siddique, K. H. M. (2015). Salt stress in maize: effects, resistance mechanisms, and management. A review. *Agron. Sustain. Dev*. 35, 461–4811. doi: 10.1007/s13593-015-0287-0

Farquhar, G. D., Ehleringer, J. R., and Hubick, K. T. (1989). Carbon isotope discrimination and photosynthesis. *Annu. Rev. Plant Physiol. Plant Mol. Biol*. 40, 503–537. doi: 10.1146/annurev.pp.40.060189.002443

Farquhar, G. D., and Sharkey, T. D. (1982). Stomatal conductance and photosynthesis. *Annu. Rev. Plant Physiol*. 33, 317–345. doi: 10.1146/annurev.pp.33.060182.001533

Flores, A., Shukla, M. K., Daniel, D., Ulery, A., Schutte, B., Pichionni, G., et al. (2016). Evapotranspiration changes with irrigation using saline groundwater and RO concentrate. *J. Arid Environ*. 131, 35–45. doi: 10.1016/j.jaridenv.2016.04.003

Flores, A., Shukla, M. K., Schutte, B., Picchioni, G., and Daniel, D. (2017). Physiologic response of six plant species grown in two contrasting soils and irrigated with brackish groundwater and RO concentrate. *Arid Land Res. Manage*. 31, 182–203. doi: 10.1080/15324982.2016.1275068

Galli, V., Messias, R. D. S., Perin, E. C., Borowski, J. M., Bamberg, A. L., and Rombaldi, C. V. (2016). Mild salt stress improves strawberry fruit quality. *LWT* 73, 693–699. doi: 10.1016/j.lwt.2016.07.001

Galmés, J., Flexas, J., Savé, R., and Medrano, H. (2007). Water relations and stomatal characteristics of Mediterranean plants with different growth forms and leaf habits: responses to water stress and recovery. *Plant Soil* 290, 139–155. doi: 10.1007/s11104-006-9148-6

Hu, Y., and Schmidhalter, U. (2005). Drought and salinity: a comparison of their effects on mineral nutrition of plants. *J. Plant Nutr. Soil Sci*. 168, 541–549. doi: 10.1002/jpln.200420516

Hussain, M. I., Lyra, D. A., Farooq, M., Nikoloudakis, N., and Khalid, N. (2016). Salt and drought stresses in safflower: a review. *Agron. Sustain. Dev*. 36:4. doi: 10.1007/s13593-015-0344-8

Jiang, X. L., Kang, S. Z., Li, F. S., Du, T. S., Tong, L., and Comas, L. (2016). Evapotranspiration partitioning and variation of sap flow in female and male parents of maize for hybrid seed production in arid region. *Agric. Water Manage*. 176, 132–141. doi: 10.1016/j.agwat.2016.05.022

Kang, S. Z., Hao, X. M., Du, T. S., Tong, L., Su, X. L., Lu, H. N., et al. (2017). Improved agricultural water productivity to ensure food security in China under changing environment: from research to practice. *Agric. Water Manage*. 179, 5–17. doi: 10.1016/j.agwat.2016.05.007

Kang, S. Z., Zhang, L., Liang, Y. L., Hu, X. T., Cai, H. J., and Gu, B. J. (2002). Effects of limited irrigation on yield and water use efficiency of water wheat in the Loess Plateau of China. *Agric. Water Manage*. 55, 203–216. doi: 10.1016/S0378-3774(01)00180-9

Katerji, N., Mastrorilli, M., Lahmer, F. Z., Maalouf, F., and Oweis, T. (2011). Faba bean productivity in saline-drought conditions. *Eur. J. Agron*. 35, 2–12. doi: 10.1016/j.eja.2011.03.001

Khataar, M., Mohhamadi, M. H., and Shabani, F. (2018). Soil salinity and matric potential interaction on water use, water use efficiency and yield response factor of bean and wheat. *Sci. Rep*. 8:2679. doi: 10.1038/s41598-018-20968-z

Liu, F. L., Shahnazari, A., Andersen, M. N., Jacobsen, S. E., and Jensen, C. R. (2006). Physiological response of potato (*Solanum tuberosum* L.) to partial root-zone drying: ABA signaling, leaf gas exchange, and water use efficiency. *J. Exp. Bot*. 57, 3727–3735. doi: 10.1093/jxb/erl131

Liu, H., Sun, J. S., Duan, A. W., Liu, Z. G., and Liang, Y. Y. (2010). Experiments on variation of tomato sap flow under drip irrigation conditions in greenhouse. *Trans. CSAE* 26, 77–82. doi: 10.3969/j.issn.1002-6819.2010.10.012

Liu, Y., Li, P., Xu, G. C., Xiao, L., Ren, Z. P., and Li, Z. B. (2017). Growth, morphological, and physiological responses to drought stress in *bothriochloa ischaemum*. *Front. Plant Sci*. 8:230. doi: 10.3389/fpls.2017.00230

Machado, R. M. A., and Serralheiro, R. P. (2017). Soil Salinity: effect on vegetable crop growth. Management practices to prevent and mitigate soil salinization. *Horticulturae* 3:30. doi: 10.3390/horticulturae3020030

Maggio, A., De Pascale, S., Angelino, G., Ruggiero, C., and Barbieri, G. (2004). Physiological response of tomato to saline irrigation in long-term salinized soils. *Eur. J. Agron*. 21, 149–159. doi: 10.1016/S1161-0301(03)00092-3

Mao, H. P., Ikram, U., Ni, J. H., Qaiser, J., and Ahmad, A. (2017). Estimating tomato water consumption by sap flow measurement in response to water stress under greenhouse conditions. *J. Plant Interact*. 12, 402–413. doi: 10.1080/17429145.2017.1373869

Martínez, J. P., Silva, H., Ledent, J. F., and Pinto, M. (2007). Effect of drought stress on the osmotic adjustment, cell wall elasticity and cell volume of six cultivars of common beans (*Phaseolus vulgaris* L.). *Eur. J. Agron*. 26, 30–38. doi: 10.1016/j.eja.2006.08.003

Mittler, R. (2006). Abiotic stress, the field environment and stress combination. *Trends Plant Sci*. 11, 15–19. doi: 10.1016/j.tplants.2005.11.002

Munns, R. (2002). Comparative physiology of salt and water stress. *Plant Cell Environ*. 25, 239–250. doi: 10.1046/j.0016-8025.2001.00808.x

Negrão, S., Schmöckel, S. M., and Tester, M. (2017). Evaluating physiological response of plants to salinity. *Ann. Bot*. 119, 1–11. doi: 10.1093/aob/mcw191

Netondo, G. W., Onyango, J. C., and Beck, E. (2004). Sorghum and Salinity: II. Gas exchange and chlorophyll fluorescence of sorghum under salt stress. *Crop Sci*. 44, 806–811. doi: 10.2135/cropsci2004.8060

Niu, S. L., Xing, X. R., Zhang, Z., Xia, J. Y., Zhou, X. H., Song, B., et al. (2011). Water use efficiency in response to climate change: from leaf to ecosystem in a temperate steppe. *Glob. Change Biol*. 17, 1073–1082. doi: 10.1111/j.1365-2486.2010.02280. x

Norman, J. M. (1998). *An Introduction to Environmental Biophysics*. New York, NY: Springer-Verlag.

Patanè, C., Tringali, S., and Sortino, O. (2011). Effects of deficit irrigation on biomass, yield, water productivity and fruit quality of processing tomato

under semi-arid Mediterranean climate conditions. *Sci. Hortic.* 129, 590–596. doi: 10.1016/j.scienta.2011.04.030

Patil, N. M. (2012). Adaptations in response to salinity in Safflower Cv. Bhima. *Asian J. Crop Sci.* 4, 50–62. doi: 10.3923/ajcs.2012.50.62

Phogat, V., Pitt, T., Cox, J. W., Šimunek, J., and Skewes, M. A. (2018). Soil water and salinity dynamics under sprinkler irrigated almond exposed to a varied salinity stress at different growth stages. *Agric. Water Manage.* 201, 70–82. doi: 10.1016/j.agwat.2018.01.018

Qadir, M., Quillérou, E., Nangia, V., Murtaza, G., Singh, M., Thomas, R. J., et al. (2014). Economics of salt-induced land degradation and restoration. *Nat. Resour. Forum* 38, 282–295. doi: 10.1111/1477-8947.12054

Qiu, R. J., Du, T. S., Kang, S. Z., Chen, R. Q., and Wu, L. S. (2015). Influence of water and nitrogen stress on stem sap flow of tomato grown in a solar greenhouse. *J. Am. Soc. Hortic. Sci.* 140, 111–119. doi: 10.21273/JASHS.140.2.111

Reina-Sánchez, A., Romero-Aranda, R., and Cuartero, J. (2005). Plant water uptake and water use efficiency of greenhouse tomato cultivars irrigated with saline water. *Agric. Water Manage.* 78, 54–66. doi: 10.1016/j.agwat.2005.04.021

Romero-Aranda, R., Soria, T., and Cuartero, J. (2001). Tomato plant-water uptake and plant-water relationships under saline growth conditions. *Plant Sci.* 160, 265–272. doi: 10.1016/S0168-9452(00)00388-5

Schiattone, M. I., Candido, V., Cantore, V., Montesano, F. F., and Boari, F. (2017). Water use and crop performance of two wild rocket genotypes under salinity conditions. *Agric. Water Manage.* 194, 214–221. doi: 10.1016/j.agwat.2017.09.009

Senguttuvel, P., Vijayalakshmi, C., Thiyagarajan, K., Kannanbapu, J. R., Kota, S., Padmavathi, G., et al. (2014). Changes in photosynthesis, chlorophyll fluorescence, gas exchange parameters and osmotic potential to salt stress during early seedling stage in rice (*Oryza sativa* L.). *SABRAO J. Breed. Genet.* 46, 120–135.

Shrivastava, P., and Kumar, R. (2015). Soil Salinity: a serious environmental issue and plant growth promoting bacteria as one of the tools for its alleviation. *Saudi J. Biol. Sci.* 22, 123–131. doi: 10.1016/j.sjbs.2014.12.001

Shukla, M. K., Lal, R., and Ebinger, M. (2006). Determining soil quality indicators by factor analysis. *Soil Tillage Res.* 87, 194–204. doi: 10.1016/j.still.2005.03.011

Siddiqi, E. H., Ashraf, M., Al-Qurainy, F., and Akram, N. A. (2011). Salt-induced modulation in inorganic nutrients, antioxidant enzymes, proline content and seed oil composition in safflower (*Carthamus tinctorius* L.). *J. Sci. Food Agric.* 91, 2785–2793. doi: 10.1002/jsfa.4522

Sinclair, T. R., Tanner, C. B., and Bennett, J. M. (1984). Water use efficiency in crop production. *AIBS* 34, 36–40. doi: 10.2307/1309424

Trambouze, W., and Voltz, M. (2001). Measurement and modeling of the transpiration of a Mediterranean vineyard. *Agric. Water Manage.* 107, 153–166. doi: 10.1016/S0168-1923(00)00226-4

Unesco Water Portal (2007). Available online at: http://www.unesco.org/water (Accessed October 25, 2007).

Wang, C. X., Gu, F., Chen, J. L., Yang, H., Jiang, J. J., Du, T. S., et al. (2015). Assessing the response of yield and comprehensive fruit quality of tomato grown in greenhouse to deficit irrigation and nitrogen application strategies. *Agric. Water Manage.* 161, 9–19. doi: 10.1016/j.agwat.2015.07.010

Wang, Y. S., Liu, F. L., Andersen, M. N., and Jensen, C. R. (2010). Improved plant nitrogen nutrition contributes to higher water use efficiency in tomatoes under alternate partial root-zone irrigation. *Funct. Plant Biol.* 37, 175–182. doi: 10.1071/FP09181

Wei, Z. H., Du, T. S., Li, X. N., Fang, L., and Liu, F. L. (2018). Interactive effects of CO_2 concentration elevation and nitrogen fertilization on water and nitrogen use efficiency of tomato grown under reduced irrigation regimes. *Agric. Water Manage.* 202, 174–182. doi: 10.1016/j.agwat.2018.02.027

Wei, Z. H., Du, T. S., Zhang, J., Xu, S. J., Cambre, P. J., and Davies, W. J. (2016). Carbon isotope discrimination shows a higher water use efficiency under alternate partial root-zone irrigation of field-grown tomato. *Agric. Water Manage.* 165, 33–43. doi: 10.1016/j.agwat.2015.11.009

Wilkinson, S., and Davies, W. J. (2002). ABA-based chemical signaling: the co-ordination of responses to stress in plants. *Plant Cell Environ.* 25, 195–210. doi: 10.1046/j.0016-8025.200.00824.x

Yang, H., Du, T. S., Qiu, R. J., Chen, J. L., Li, Y., Wang, C. X., et al. (2017). Improved water use efficiency and fruit quality of greenhouse crops under regulated deficit irrigation in northwest China. *Agric. Water Manage.* 179, 193–204. doi: 10.1016/j.agwat.2016.05.029

Zhang, P., Senge, M., and Dai, Y. (2016). Effects of salinity stress on growth, yield, fruit quality and water use efficiency of tomato under hydroponics system. *Rev. Agric. Sci.* 4, 46–55. doi: 10.7831/ras.4.46

Zhang, X. Z., Ervin, E. H., Liu, Y. M., Hu, G. F., Shang, C., Fukao, T., et al. (2015). Differential response of antioxidants, abscisic acid, and auxin to deficit irrigation in two perennial ryegrass cultivars contrasting in drought tolerance. *J. Am. Soc. Hortic. Sci.* 140, 562–572. doi: 10.21273/JASHS.140.6.562

Conflict of Interest Statement: The authors declare that the research was conducted in the absence of any commercial or financial relationships that could be construed as a potential conflict of interest.

frontiers in Plant Science

REVIEW
published: 19 February 2019
doi: 10.3389/fpls.2019.00103

Water-Use Efficiency: Advances and Challenges in a Changing Climate

Jerry L. Hatfield and Christian Dold*

National Laboratory for Agriculture and the Environment, Agricultural Research Service, United States Department of Agriculture, Ames, IA, United States

Water use efficiency (WUE) is defined as the amount of carbon assimilated as biomass or grain produced per unit of water used by the crop. One of the primary questions being asked is how plants will respond to a changing climate with changes in temperature, precipitation, and carbon dioxide (CO_2) that affect their WUE At the leaf level, increasing CO_2 increases WUE until the leaf is exposed to temperatures exceeded the optimum for growth (i.e., heat stress) and then WUE begins to decline. Leaves subjected to water deficits (i.e., drought stress) show varying responses in WUE. The response of WUE at the leaf level is directly related to the physiological processes controlling the gradients of CO_2 and H_2O, e.g., leaf:air vapor pressure deficits, between the leaf and air surrounding the leaf. There a variety of methods available to screen genetic material for enhanced WUE under scenarios of climate change. When we extend from the leaf to the canopy, then the dynamics of crop water use and biomass accumulation have to consider soil water evaporation rate, transpiration from the leaves, and the growth pattern of the crop. Enhancing WUE at the canopy level can be achieved by adopting practices that reduce the soil water evaporation component and divert more water into transpiration which can be through crop residue management, mulching, row spacing, and irrigation. Climate change will affect plant growth, but we have opportunities to enhance WUE through crop selection and cultural practices to offset the impact of a changing climate.

Keywords: transpiration, energy balance, carbon dioxide, photosynthesis, agronomic practices, temperature, carbon dioxide–analysis, biomass

OPEN ACCESS

Edited by:
Stuart Anthony Casson, The University of Sheffield, United Kingdom

Reviewed by:
John Chandler Cushman, University of Nevada, Reno, United States
Chan Yul Yoo, University of California, Riverside, United States

****Correspondence:***
Jerry L. Hatfield
jerry.hatfield@ars.usda.gov

Specialty section:
This article was submitted to Plant Physiology, a section of the journal Frontiers in Plant Science

Received: *10 October 2018*
Accepted: *23 January 2019*
Published: *19 February 2019*

Citation:
Hatfield JL and Dold C (2019) Water-Use Efficiency: Advances and Challenges in a Changing Climate. Front. Plant Sci. 10:103. doi: 10.3389/fpls.2019.00103

INTRODUCTION

Water use efficiency (WUE) is a concept introduced 100 years ago by Briggs and Shantz (1913) showing a relationship between plant productivity and water use. They introduced the term, WUE, as a measure of the amount of biomass produced per unit of water used by a plant. Since that time, there have been countless original papers and reviews written on the topic with the most recent one by Basso and Ritchie (2018) demonstrating that maize (*Zea mays* L.) productivity could be increased with no change in water use rate and result in increased WUE. This is a critical observation because the prevailing hypothesis for WUE (**Figure 1**) is based on plant productivity increasing with increasing water use and in order to increase WUE will require increased crop water use. To understand how WUE could be affected by a changing climate it will be necessary to determine how climate change will impact plant growth and water use of the plant. To achieve

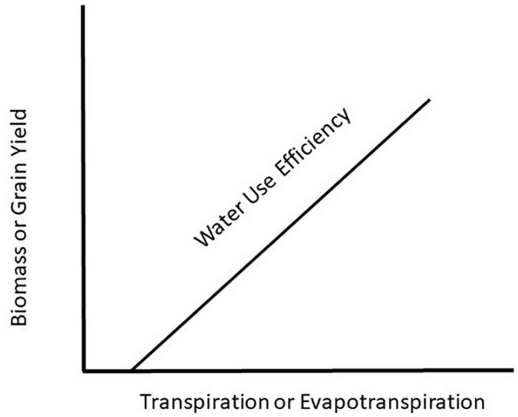

FIGURE 1 | Generalized view of water use efficiency as a function of the water use by a crop relative to biomass or grain production.

this understanding requires we examine WUE at the leaf, plant, and canopy level in response to a changing climate.

Throughout this review we will address the potential changes in WUE at multiple levels of plants to determine where potential improvements could be made in WUE. If we examine concept of water use by the plant there is a difference among the processes that occur at the leaf level compared to the canopy level. At the leaf level, water use is controlled by the available energy impinging on the leaf, vapor pressure deficit, and aerodynamic exchange, but, regulated by stomatal conductance (g_s). While at the canopy level, the processes involve energy exchange at the soil surface and the plant canopy and water loss is a combination of evaporation from the soil surface and transpiration from the plant canopy. The combination of evaporation and transpiration is referred to as evapotranspiration (ET) and in the literature on WUE of plants, there is extensive use of crop water use as the metric for WUE. These specific terms need to be carefully evaluated when interpreting the results obtained from different studies or comparing among studies.

CHANGING CLIMATE

There are four factors changing in the climate that will affect water use by plants. These factors are: increasing carbon dioxide (CO_2) concentrations, increasing temperatures, more variable precipitation, and variations in humidity. Projections of climate change are a result of a combined set of simulation models using various scenarios of changes in carbon dioxide (CO_2) concentrations and the associated forcing functions (Collins et al., 2013). The current CO_2 concentrations are nearly 400 ppm in 2018 and projected to increase to a range of 794–1142 ppm by 2100 without any abatement scenarios (Collins et al., 2013). These findings have been summarized based from the reports by Trenberth (2011) and Collins et al. (2013) as:

(1) Global mean temperatures will increase throughout the 21st century if CO_2 concentrations continue to increase and under the highest CO_2 emission scenario increases range from 2.6 to 4.8°C.
(2) Temperatures changes will not be uniform across regions with land surfaces warming more than over the oceans.
(3) Increasing global temperatures will result in more hot extremes and fewer cold extremes at both daily and seasonal time scales.
(4) Precipitation will increase with increases in global mean surface temperature and could increase 1–3% $°C^{-1}$; however, there will be substantial spatial variation in these changes.
(5) The water holding capacity of air increases by 7% $°C^{-1}$. The air can take up more water, and water vapor inclines. That leads to higher intensity of precipitation, i.e., higher amount of rainfall per rain event.
(6) Annual surface evaporation will increase with temperatures increases; however, over land, evaporation will be linked to precipitation.

These changes in climate will increase atmospheric water demand by crops and increase the potential for limitations in soil water availability, because of the increased variation in precipitation during the growing season and even more so in soils with limited water holding capacity. For example, Xiao et al. (2013) observed that the spatial patterns in carbon and water fluxes were dependent upon annual temperatures, precipitation, and growing season length when they compared these fluxes across a range of latitudes using eddy covariance flux systems. These types of comparisons identify the factors related to WUE of different ecosystems, and they found WUE was related to annual precipitation, gross primary productivity (GPP), and growing season length (Xiao et al., 2013). In their comparison, forests and coastal wetlands had a higher WUE than grasslands and croplands. Guoju et al. (2013a) found that in China, WUE of maize (*Z. mays* L.), wheat (*Triticum aestivum* L.), and potato (*Solanum tuberosum* L.) increased over the past 50 years that they attributed to an increase in temperature and a decrease in precipitation. Projected changes in climate are expected to increase the areas subjected to drought around the world (Dai, 2013; Feng and Fu, 2013; Fu and Feng, 2014; Huang et al., 2015). The effect of increasing drought on net primary productivity has been seen by Zhao and Running (2009) where they found a reduction of 55 petagrams of carbon due to drought. Drought will impact productivity and throughout this paper, we will explore the mechanisms of avenues to increase WUE of agricultural systems to take advantage of a limited water supply.

LEAF LEVEL PROCESSES

One way to explore the impact of a changing climate on WUE is to begin at the leaf level. The interactions of a changing CO_2 and water and temperature regimes will be most evident at the leaf level because there are not the confounding effects of canopy architecture or the interactions of the soil environment on WUE. There have been two ways proposed to calculated leaf level WUE. The instantaneous WUE is calculated as the net photosynthetic

rate (A_n) divided by transpiration rate (E). Another measure is the intrinsic WUE, which is calculated as A_n divided by g_s.

Leaf level WUE has a distinctive pattern depending on the carboxylation pathway, i.e., C_3 photosynthesis, C_4 photosynthesis, and Crassulacean acid metabolism (CAM). C_4 plants have higher intrinsic WUE than C_3 plants, owing to higher A_n and lower g_s (Taylor et al., 2010). A comparison of C_3 and C_4 plants with Crassulacean acid metabolism (CAM) reveals a completely different pattern of stomatal response to environmental conditions. Males and Griffiths (2017) provide an overview of the stomatal processes in CAM plants and the advantages in arid environments. Bartlett et al. (2014) proposed a model to describe the storage of malic acid in CAM plants and how this responded to rubisco dynamics in the leaf carbon assimilation model. The WUE of CAM plants is quite high compared to C_3 and C_4 plants because of this unique cycle of carbon fixation and storage during the diurnal cycle. Yang et al. (2015) proposed a series of potential studies to enhance the understanding of the potential utilization of CAM plants as part of the food security pathways under a changing climate.

Heat and Water-Deficit Stress, and Radiation Limitations

Climatic changes may induce or ameliorate abiotic stress to the plant, that is (1) water-deficit stress and (2) heat stress. The combined effect of heat and water-deficit stress on plant productivity have been summarized by Hatfield et al. (2011) for crops and Izaurralde et al. (2011) for range and pasture plants. Hatfield et al. (2018) in evaluating the cause for yield reductions in the Midwest found a combination of high temperatures during the pollination and grain-filling period coupled with water-deficit stress induced by below normal precipitation during the grain-filling period explained yield variation among years. Water-deficit stress may be induced by changes in available water and vapor pressure deficit (VPD). Heat stress may be induced by increased ambient air temperature and in the absence of water-deficit stress will decrease productivity (Hatfield, 2016).

There have been numerous assessment of the effects of increased temperatures or drought on the productivity of crops (Long and Ort, 2010; Lobell et al., 2011, 2013, 2014). A novel observation by Vanzo et al. (2015) showed a difference in the isoprene emissions from poplar (*Populus* spp.) and found differences between emitting (IE) and non-emitting (NE) isoprene plants. When exposed to hot, dry conditions, the chloroplastidic electron transport rate of NE plants became impaired, while IE plants maintained values similar to unstressed controls. During recovery from hot, dry exposures, IE plants reached higher daily net CO_2 assimilation rates compared with NE genotypes. Examining the changes in volatile emissions from plants coupled with observations on the enzymatic activity may begin to reveal the differences among plants in their response to high temperatures, water deficits, as well as fluctuating light regimes. Leaf level responses are complex because of the internal changes in enzymatic activity in response to the environment. Illustrative of this is the recent observations by Slattery et al. (2018) in which they observed Rubisco, Rubisco activase (Rca), glyceraldehyde-3-phosphate dehydrogenase (GAPDH), Fru-1,6-bisphosphatase (FBPase), sedoheptulose-1,7-bisphosphatase (SBPase), and phosphoribulokinase (PRK) where changed in response to changing light. These abiotic stresses are connected and additionally interact with increasing CO_2.

Increase of Ambient CO_2 Concentration

The sole effect of increasing CO_2 on A_n and WUE is generally positive because the gradient between the ambient air and the intercellular spaces is increased and in the presence of light, CO_2 within the leaf is rapidly converted to carbohydrates. If we adopt the kinetic model described by Charles-Edwards (1971) as redrawn in **Figure 2** then the linkages between CO_2 uptake and water loss by a leaf become apparent. The governing factors in this kinetic model are the diffusion coefficient, which is analogous to g_s. When we compare the exchange processes of CO_2 within the leaf and H_2O vapor then the dynamics of the exchange processes are controlled by g_s for water vapor and g_s and mesophyll conductance (g_m) for photosynthesis (Lawson and Blatt (2014). This is also why WUE increases under water-deficit stressed conditions – the reduction in A_n is less than the reduction of E or g_s. Earl (2002) found no significant difference in A_n, but lower g_s in soybean genotypes with higher WUE. Bierhuizen and Slatyer (1965) were among the first to explain the relationship observed between E and A_n for different species due the change in saturation deficit and CO_2 concentration. They showed there was an increase in WUE of cotton (*Gossypium hirsutum* L.) with increasing CO_2 levels across all light levels impinging on the leaf (**Figure 3**). However, there is a different response to rising CO_2 among C_3 photosynthesis and C_4 photosynthesis plants. A beneficial effect is observed in C_3 plants because CO_2 is a limiting factor owing to the functioning of the carboxylation pathway. C_4 plants show little effect on increased CO_2 under optimal soil water conditions; only under drought stress high CO_2 levels is beneficial owing to partial stomate closure thus reducing transpiration, and the ability of C_4 plants to assimilate carbon even when stomates are closed (Lopes et al., 2011).

Leaf Level Interactions Among Climatic Parameters and CO_2

Yoo et al. (2009) provided an overview of the role of changing transpiration on crop water use and understanding the combined response of climate impacts on carbon assimilation and water use will be key to quantifying the effects of a changing climate. It is therefore significant to observe the interactions of CO_2, temperature and water regime to understand WUE in a changing climate.

While increased CO_2 can ameliorate water-deficit stress, it cannot offset the increase in heat stress, and may even be adverse, because E decreases and leaf temperature increases (Lopes et al., 2011). Allen et al. (2003) used soybean [*Glycine max* (L.) Merr.] to evaluate the effect of CO_2 and temperature on WUE, foliage temperature, and canopy conductance. They used a combination of air temperatures in small chambers to expose soybean leaves to a range of temperatures, VPDs, and CO_2

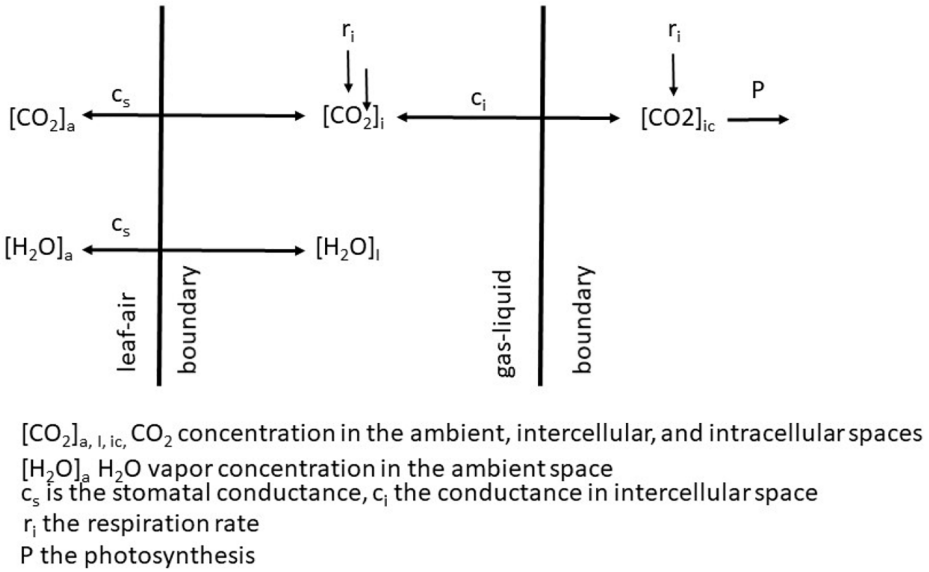

FIGURE 2 | Schematic of the exchange of CO_2 and H_2O vapor across from the ambient air to the intercellular spaces of a leaf.

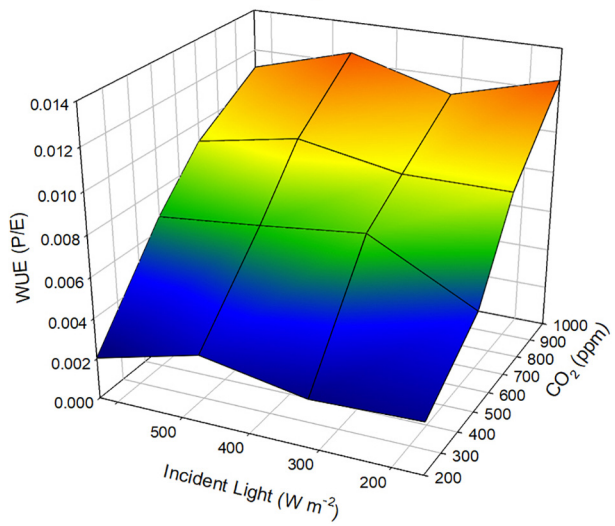

FIGURE 3 | Response of water use efficiency in cotton leaves as a function of changing CO_2 and incident light levels at a constant wind speed of 2.4 cm sec^{-1}. Data redrawn from Bierhuizen and Slatyer (1965).

concentrations. Leaf conductance did not show any response to increasing CO_2 but were affected by temperature with the lower conductance evident with the higher temperatures. Water use was not affected by increasing CO_2 but was increased with the higher temperatures. The overall result was the WUE decreased with the increasing temperatures but increased with increasing CO_2 at each temperature regime.

Another complicating factor in this type of experiment is the changing VPD of the air with changing temperature and the feedback effect on leaf temperature. The change in the air temperature surrounding the leaf will change leaf temperature and directly affect the gradient of water vapor between the leaf and the atmosphere. This gradient is affected by the internal leaf water vapor pressure (e; kPa) which is coupled to leaf temperature (T; °C) and can be calculated from Tetens' equation (Monteith and Unsworth, 2013):

$$e = 0.61078^{*} exp\left[17.269^{*} T/(T + 237.3)\right] \quad (1)$$

Atmospheric factors affecting the energy balance and leaf or canopy temperature drive internal water vapor pressure and ultimately water use. Increases in air temperature will directly increase crop canopy temperature, leaf water vapor pressure, and transpiration. The response shown in **Figure 3** would be expected at the leaf level because the uptake of CO_2 is controlled more by the concentration gradient from the leaf to the air than g_s or the diffusion coefficient. The CO_2 concentration gradient is large because the internal concentration at the mesophyll is near zero creating a large gradient from the ambient air into leaf. This is in contrast to the H_2O vapor gradient, which is at saturation just inside of the stomatal guard cell and a water vapor concentration dictated by air temperature and specific humidity. The differences in these two gradients reveal that leaves would be more efficient in the photosynthetic process than the transpiration process and would exhibit a preferential shift toward greater WUE at the leaf level because A_n would be affected more than *E*. El-Sharkawy and Cock (1984) compared different cassava (*Manihot esculenta* Crantz) cultivars and found WUE decreased with increasing VPD. If we extend this across species and climate change scenarios, then humidity of air in response to changing temperatures will have a significant impact on WUE. One has to be cautious of the older literature because the effect of a rapidly changing CO_2 was not part of the research

assessments and water availability, temperature, and humidity were the main variables.

Genetic Response to WUE

The concept of WUE, alongside with other parameters, had been proposed in plant breeding to identify water use efficient genotypes under changing climate regimes, heat and water-deficit stress, and interactions among them. Variation among genotypes for WUE has been found in a number of crop species, including barley (Hubick and Farquhar, 1989), cowpea [*Vigna unguiculata* (L.) Walp.] (Ismail and Hall, 1992; Ashok et al., 1999), peanut (*Arachis hypogaea* L.) (Hubick et al., 1988; Wright et al., 1994), sorghum [*Sorghum bicolor* (L.) Moench.] (Donatelli et al., 1992), soybean (Mian et al., 1996; Hufstetler et al., 2007), upland cotton and pima cotton (*G. barbadense* L.) (Quisenberry and McMichael, 1991; Saranga et al., 2004; Fish and Earl, 2009), and wheat (Ehdaie and Waines, 1993; Van Den Boogaard et al., 1997; Siahpoosh et al., 2011; Siahpoosh and Dehghanian, 2012). In a recent meta-analysis, Gago et al. (2014) found that WUE at the leaf level is a complex trait dependent upon physiological responses that link g_m and g_s with the key variable being the factors that affect the photosynthetic process at the leaf scale. Flexas et al. (2014) had proposed the ratio of g_m/g_s as the key variables related to uptake of CO_2 by the leaf. Gago et al. (2014) found that respiration rates were a key factor in WUE because increasing respiration decreased the net uptake of carbon (C) by the leaf. They proposed that genetic screening of plants for characteristics directly related to photosynthetic efficiency or reduced respiration would lead to insights in the potential impacts of climate change on WUE. Peng and Krieg (1992) in comparing genotypes of grain sorghum found that differences in WUE among genotypes was related to A_n and leaf area because there was little difference among genotypes in their water use. In peanut (*A. hypogaea* L.), Craufurd et al. (1999) found WUE was affected by specific leaf area (leaf thickness) and carbon isotope discrimination with differences between Virginia peanut (*A. hypogaea* L. spp. fastigiata) and Spanish peanut (*A. hypogaea* L. spp. hypogaea) genotypes. In these experiments, there was an interaction between WUE and high temperatures because of the effect on specific leaf area and proposed that specific leaf area could be a parameter useful for screening among genotypes for WUE. While Ismail and Hall (1992) proposed that carbon isotope discrimination was a good selection criteria in cowpea [*V. unguiculata* (L.) Walp.]. In their study comparing these genotypes, they found a 19% variation under wet conditions and a 23% variation under dry conditions. Ramirez Builes et al. (2011) compared six genotypes of common bean under water-deficit stress conditions in the greenhouse and found differences in transpiration efficiency and WUE and were able to extend these results to show differences in WUE when beans were grown in the field environment. Similar results were found by Siahpoosh et al. (2011) for bread wheats with WUE ranging from 5.092 and 7.296 kg ha^{-1} mm^{-1} depending upon the level of water-deficit stress imposed on the cultivars. They proposed that total biomass produced and cultivar ET during the season was a valuable screening tool (Siahpoosh et al., 2011). Hufstetler et al. (2007) and Fish and Earl (2009) used epidermal conductance of dark adapted soybean and cotton leaves as a phenotypic trait related to WUE and found a negative relationship between epidermal conductance and WUE. Kromdijk et al. (2016) found under fluctuating light conditions that the interconversion of violaxanthin and zeaxanthin in the xanthophyll cycle led to increasing productivity by 15% and suggests that screening for plant response under variable light may provide insights into increasing the photosynthetic efficiency. Being able to identify traits related to WUE will aid in being able to screen across genetic material for their response under a changing climate. Comparisons among species and within species is not new, Brown and Simmons (1979) demonstrated that apparent photosynthesis and transpiration under water-deficit conditions were related to WUE and could be used as tools to assess genetic material. Gebrekirstos et al. (2011) used wood carbon isotope composition as a proxy for WUE in tree species for ∼30 years. The authors identified different drought strategies among species, which could help to draw conclusions on future climate change adaption. Song et al. (2015) could show that WUE changes with tree age using the carbon isotope method on Mongolian pine (*Pinus sylvestris* var. *mongolica*).

There has also been criticism of using leaf level WUE to identify water efficient plants. One drawback is the difficulty to upscale from leaf to canopy level (see also section below). Medrano et al. (2015) cautioned against using leaf measurements of WUE to scale to whole canopy WUE because of the potential confounding effect of leaf position relative to the photosynthetically active radiation (PAR) regime and water demand on the leaf. The microclimate surrounding an individual leaf will determine the WUE which suggests that if leaves are being used to relate to canopy level responses then a composite of leaves be used that would more closely represent the canopy. Blum (2009) dismissed the WUE-concept for plant breeding because genotypes can only increase leaf level WUE by activating plant traits responsible for reducing E, not by increasing A_n. This would eventually lead to genotypes with reduced yield and drought tolerance. Instead, the author proposed to evaluate the Effective Use of Water (EUW) which focuses on genotypes, which are capable to maximize soil moisture capture for transpiration. There continue to be advances in our understanding of plant response to a changing CO_2 environment, one of these responses is a change in the stomatal density as observed by Caine et al. (2019) in rice and the evolution toward changes in stomatal density from C_3 to C_4 plants (Way et al., 2014). The use of more advanced techniques, e.g., carbon isotope discrimination (Cernusak, 2018; Gao et al., 2018a) or molecular genetics (Avramova et al., 2018) promise to offer new insights into understanding these linkages.

PLANT AND CANOPY LEVEL RESPONSES

Each plant species has a unique arrangement of a set of single leaves and canopies consist of an arrangement of plants according to a specific cultural practice, e.g., row spacing. The arrangement of plants creates a diverse exposure to solar radiation, i.e.,

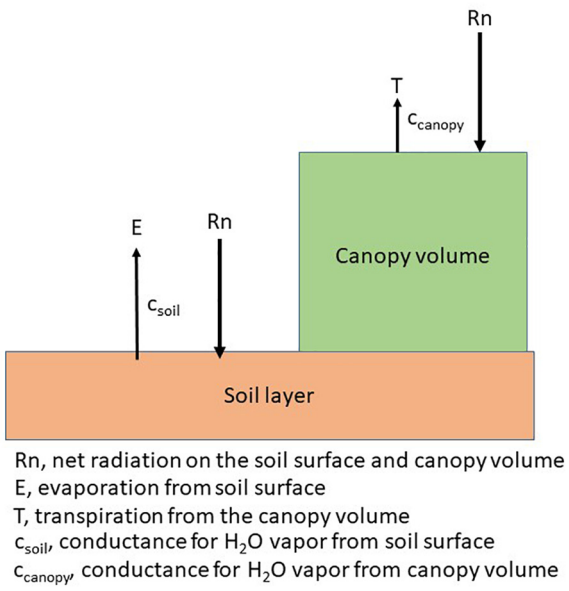

FIGURE 4 | Schematic of the energy distribution on the plant and soil surface and the canopy level conductances for a canopy arranged in rows.

PAR regimes on the leaves of the plant and on the soil as shown in the following diagram (**Figure 4**). Plant water use, or transpiration will be governed by a combination of physiological and morphological characteristics (Kimball, 2007) while soil water evaporation is dependent upon the energy at the soil surface (Ritchie, 1972). Photosynthesis and ultimately, dry matter production, will be impacted by the interception of PAR by the canopy. In annual crops, this creates a series of unique microclimates within the canopy throughout the growing season while in perennial crops, the changes throughout the growing season may not be as large because of the more constant canopy size.

As the plant canopy develops during the growing season, the increases in leaf area are proportional to the growth rate and transpiration increases linearly with leaf area (Ritchie, 1972). As the leaf area index (LAI) of the canopy approaches 4, *E* increases at a slower rate because there is complete light interception by the canopy. Total canopy photosynthesis exhibits a similar response with a diminishing rate of canopy photosynthesis at LAI > 4. At this point in growth and development, A_n and *E* are directly related to the energy available to the canopy. Mutual shading and interference among leaves become dominant factors in determining the rate of change in photosynthesis and transpiration and there is an uncoupling of these responses from changes in LAI above 4 (Ritchie, 1972; Villalobos and Fereres, 1990; Sau et al., 2004).

Carbon and Water Dynamics on a Canopy Level

Growth of plants and the accumulation of C into plant material on a canopy and ecosystem level is described by GPP and net ecosystem productivity (NEP). The GPP in terrestrial ecosystems is defined as the total amount of C assimilated by photosynthetic activity of plants. High GPP in the Northern Hemisphere is generated in the United States Corn Belt due to the large-scale cultivation of maize, which is a C_4 plant (Guanter et al., 2014). Although maize is often grown in rotation with soybean to utilize the nitrogen remaining by the legume crop, Dold et al. (2017) found that maize had a positive carbon balance while soybean showed a negative balance. The net primary production (NPP) is the sum of GPP and C losses by autotrophic respiration (i.e., plant respiration; RA) (Noble et al., 2000):

$$GPP = NPP - RA \quad (2)$$

Note the sign convention; fluxes from the atmosphere to the biosphere are positive, and *vice versa*. Hence, minimum GPP and maximum RA is zero, while NPP can be positive or negative. There have been alternative sign conventions and thresholds proposed (Roxburgh et al., 2005). The global NPP is estimated to 60 Gt C yr^{-1}, meaning that about half of C assimilated is lost by autotrophic respiration (Noble et al., 2000). The net ecosystem production (NEP) is calculated as the sum of GPP and ecosystem respiration (RE) (e.g., Dold et al., 2017):

$$GPP = NEP - RE \quad (3)$$

The RE is defined as the sum of RA and heterotrophic respiration, that is the soil mineralization from the edaphon and decomposition of dead organic material. The global NEP is estimated to 10 Gt C yr^{-1}. The Net Biome Production (NBP) is the amount of C stored in a biome or an ecosystem and can be calculated as the difference between NEP and the amount of C introduced in the biome (e.g., organic fertilizer), and leaving the system (e.g., yield, dissolved carbon in water, fire). The NBP varies among biomes and is approximated globally to ±1 Gt yr^{-1} globally (Noble et al., 2000).

One of the most used methods for quantifying crop water use has been through the Penman–Monteith equation (Allen et al., 1998, 2005):

$$\lambda ET = \frac{\Delta * (R_n - G) + p_a * C_p * \frac{VPD}{r_a}}{\Delta + \gamma * \left(1 + \frac{r_s}{r_a}\right)} \quad (4)$$

Where: λET = Latent heat flux (MJ m^{-2} s^{-1}), R_n = net radiation (MJ m^{-2} s^{-1}), G = soil heat flux (MJ m^{-2} s^{-1}), p_a = mean air density at constant pressure (kg m^{-3}), C_p = specific heat of air (MJ kg^{-1} $°C^{-1}$), Δ = slope of saturation vapor pressure – temperature relationship (kPa $°C^{-1}$), VPD = vapor pressure deficit (kPa), γ = psychrometric constant (kPa $°C^{-1}$), r_s = surface resistance (s m^{-1}), r_a = aerodynamic resistance (s m^{-1}).

Total crop water use can be separated into the soil water evaporation component and the transpiration component and when combined represent ET or typically what is referred to as crop water use. As we begin to examine WUE at the canopy scale, it becomes important to understand how climate affects each of these components in the soil-plant-atmosphere continuum.

At the leaf level there is a direct relationship to WUE induced by increasing CO_2 because of the concurrent increase in A_n and reduction in g_s. Extending from the leaf to canopy level,

the direct relationships between WUE and changes in climate parameters are less obvious and often not detectable (Polley, 2002). The primary reason for this lack of response is related to the temperature response of a given species and the relationship of growth response to a change in temperature and water use rate by the plant canopy (Polley, 2002). To estimate WUE at the canopy level requires a methodology to quantify the accumulation of dry matter and the water use by the canopy. One way to estimate WUE is to divide the GPP by ET, by that incorporating H_2O and CO_2 exchange at both, the soil surface and the plant canopy. Beer et al. (2009) tried to couple WUE to the plant canopy by multiplying canopy level WUE with daylight VPD as a proxy for canopy conductance and called it the inherent water use efficiency (IWUE*). Another WUE method is the ratio of biomass accumulated or yield produced to water used (e.g., Monteith et al., 1991; Droppelmann et al., 2000; Bai et al., 2016). Bai et al. (2016) also used the Water Equivalent Ratio (WER) to estimate WUE in mixed cropping systems.

$$WER = \frac{WUE_{int,A}}{WUE_{mono,A}} + \frac{WUE_{int,B}}{WUE_{mono,B}} \quad (5)$$

Where: WUE_{mono} is the monocropped WUE, and WUE_{int} is the intercropped WUE of crop A and B, respectively.

A WER > 1 would indicate that water use was lower in the mixed stand compared to the sole crop and *vice versa*.

Impact of Elevated Atmospheric CO_2 on Plant Water Use

The effect of increased CO_2 on seasonal crop water use was observed by Bernacchi et al. (2007) when they found the control plots extracted the available soil water and the crop become water limited. In contrast, in the elevated CO_2 plots the stomata remained open and the plants continued to transpire because of the water conservation induced by the elevated CO_2. Soybean grown under elevated CO_2 continued to photosynthesize and grow longer while the control plants ceased growth. Under rain-fed agriculture, which often experiences short periods of drought, the net impact of elevated concentrations of CO_2 would enable soil water conservation, thus sustaining crop productivity for more days than under current CO_2 concentrations.

Growth of C_3 species with a doubling of atmospheric CO_2 above present-day levels will increase growth nearly 30% under optimum temperature and water availability (e.g., Kimball, 1983, 2007; Kimball and Idso, 1983; Kimball et al., 2002). With a doubling of CO_2 in soybean, g_s decreased about 40% (Ainsworth et al., 2002; Ainsworth and Rogers, 2007). Ainsworth and Long (2005) utilized free-air CO_2 enrichment studies to evaluate the response of two C_3 and C_4 species to increased CO_2 concentrations from present to 550–600 μmol mol^{-1} and found no significant differences between species with an average reduction in g_s of 20%. As the g_s decreases there is a concurrent decrease in water lost to the atmosphere. The expected changes in CO_2 over the remainder of this century would decrease transpiration and have a positive impact on plant WUE directly related to g_s changes.

Given the fact that T is closely linked with crop growth and reaches a maximum after canopy closure (LAI > 4), we can expect the effects of CO_2 on leaf area changes to be relatively small. The most significant factor is the duration of green leaf area of the plant canopy because water use will be in direct relationship to how long the leaf area persists during the growing season. However, as summarized by Hatfield et al. (2011) and Hatfield and Prueger (2015) increasing temperatures will increase the rate of development. This effect is extremely evident during the reproductive stage of crops when exposure to high temperatures hastens the rate of maturity and this is in the crop growth cycle with the maximum water use (Hatfield, 2016). The net result of increasing temperatures would be a reduction in the seasonal water use because of the shorten duration of leaf area and shortened growth cycle. A shift toward crops with a longer growing season or perennial crops would increase the seasonal crop water use because of the longer leaf area duration. Any of these crops, when exposed to increased CO_2 exhibits decreased g_s (Kimball and Idso, 1983; Morison, 1987; Wand et al., 1999; Allen et al., 2003).

Canopy Level Interactions of Elevated CO_2 and ET

At the leaf scale, increasing CO_2 results in water conservation; however, at the whole plant, canopy, or ecosystem scale these responses have diminished because of the factors that affect ET become more dominant than conductance (Field et al., 1995; Polley, 2002). The results have been variable across a range of crops on the change in ET with changing CO_2, these results are dependent upon whether the experiments were conducted in controlled versus field environments. Hui et al. (2001) observed an increase in ET with increasing CO_2 levels. Jones et al. (1985) observed a 12% reduction in seasonal transpiration and 51% increase in WUE when grown in ambient and doubled CO_2. Observations in wheat (*T. aestivum* L.) by André and Du Cloux (1993) showed an 8% decrease in transpiration to doubled CO_2, while Hunsaker et al. (1996, 2000) found a 4% reduction in ET with a 200 μmol mol^{-1} CO_2 increase in a free air CO_2 studies when water and N were limiting. In contrast, cotton (*G. hirsutum* L.) showed no change in ET in a similar experiment (Hunsaker et al., 1994) that they attributed to the greater growth response in cotton. However, Reddy et al. (2000) found transpiration in cotton decreased by 8% with a doubling of CO_2. Free –air CO_2 experiments conducted in Illinois on soybean grown at 375 and 550 μmol mol^{-1} revealed an ET decrease of 9–16% with the differences caused variation in temperature among the growing seasons (Bernacchi et al., 2007).

Water deficit conditions are likely to occur under increasing variation of precipitation and will increase the importance of understanding the interactions of CO_2 enrichment with climatic factors of water supply and evaporative demand. An advantage of elevated CO_2 will be evident first on reduced g_s which in turn leads to enhanced soil water conservation and less water-deficit stress detectable when crops are grown under conditions with periodic soil water deficit or under high evaporative demand. Reducing water-deficit stress has a positive impact on

photosynthesis, growth, and yield and that has been documented for wheat (Wall et al., 2006) and sorghum (Ottman et al., 2001; Wall et al., 2001; Triggs et al., 2004). Under water deficit conditions, sorghum showed a positive biomass and grain yield response to the CO_2 increases; however, the CO_2 effect was not observed when the crop was grown under full irrigation (Ottman et al., 2001). The g_s of the sorghum plant was reduced by 32–37% (Wall et al., 2001) with a concurrent decrease in ET of 13% (Triggs et al., 2004).

Impact of Ambient Air Temperature

Exposure to higher temperatures from both experimental evidence and simulation models shows the CO_2–induced benefit to conductance diminishes as temperatures increase. Observations of leaf temperatures in controlled environment chambers with a twofold increase in CO_2 showed soybean foliage temperatures increased 1–2°C, dry bean (*Phaseolus vulgaris* L.) by 1.5°C, and sorghum by 2°C (Pan, 1996; Prasad et al., 2002, 2006; Allen et al., 2003). Wand et al. (1999) conducted a meta-analysis on wild C_3 and C_4 grass species, grown with no stress, and observed that elevated CO_2 reduced g_s by 39% in C_3 and 29% in C_4 species. The g_s to combinations of CO_2, temperature, and VPD has been evaluated using crop simulation models (Allen, 1990). In these simulations, increasing CO_2 from 330 to 800 μmol mol^{-1}, increased foliage temperature by nearly 1°C with low air VPD, but showed an increase of 2.5–4°C with air VPD in the range of 1.5 and 3 kPa. Experimental observations on soybean showed canopies increased their conductance when exposed to progressively larger VPD (associated with higher temperature).

Increasing air temperatures will negate the positive effects of CO_2 on plant growth, in soybean there was a 9% decrease in ET at 28/18°C but no reduction at 40/30°C (Allen et al., 2003), while in rice (*Oryza sativa* L.) there was a 15% reduction in ET at 26°C but an increase at 29.5°C (Horie et al., 2000). In general, increasing CO_2 at moderate temperatures will create increased WUE; however, the positive effect diminishes as the temperature increases above the optimum temperature for the species.

There are offsetting effects between the increases in canopy temperature from the increased air temperature and the increased leaf area caused by the increase in CO_2 resulting in very small changes in ET (Allen et al., 2003). An examination of Eq. 4 provides an assessment of the impact of a changing climate on crop ET. Kimball (2007) utilized data from Maricopa, Arizona to assess changes in temperature on alfalfa (*Medicago sativa* L.) ET and found only changing temperature, the reference ET increased 3.4% $°C^{-1}$. When a constant relative humidity was evaluated, and temperature increased, annual ET increased 2.1% $°C^{-1}$. With a change in absolute humidity, potentially caused by precipitation changes there was a decrease in ET by −0.2% per % change in absolute humidity. The feedbacks between transpiration and leaf temperature under changing CO_2 have been evaluated by Boote et al. (1997) using a soybean growth model to show seasonal transpiration decreased 11–16% under irrigated conditions and 7% for rainfed environments, while ET decreased by 6–8% in the irrigated site and 4% for the rainfed conditions. The simulated WUE showed an increase between 53 and 61% and was attributed to prolonged use of soil water in the rainfed environments. These studies highlight the need to understand the interactions of soil water, CO_2, and temperature during the growing season in or to develop more effective management strategies to cope with the changing climate.

Solar Radiation

One component of the changing climate that is often overlooked, but extremely critical for growth is the solar radiation regime. A changing climate will increase clouds and potentially aerosols causing an increase in diffuse solar and PAR. Stanhill and Cohen (2001) found that over time there was a "solar dimming" in agricultural areas caused by the increasing presence to clouds and water vapor in the atmosphere. There have been reviews on this topic, (e.g., Ruimy et al., 1995; Kanniah et al., 2012, 2013) and revealed that changes in the solar radiation regime would affect photosynthesis and GPP. In a recent study, Gao et al. (2018b) evaluated the effect of clouds and aerosols on maize GPP and WUE and found that both RUE and WUE decreased linearly with increasing clearness, i.e., more direct PAR. Kromdijk et al. (2016) observed that the fluctuating light would actually increase productivity in plants because of the effects on photoprotection mechanisms while Slattery et al. (2018) found that C_4 plants are most sensitive than C_3 plants to fluctuating light conditions. They attributed this difference to changes in enzyme activities during light fluctuations. While in C_4 plants, there was a greater sensitivity to variable light due to linkage between the bundle sheath C_3 cycles and the mesophyll C_4 cycles. Drewry et al. (2014) showed that changes in canopy architecture would have positive benefits on the overall productivity of crops and should be considered as a component in addressing future cropping systems. Changes in the radiation environment to more diffuse radiation increased both radiation-use efficiency (RUE) and WUE because of the more uniform light environment on the maize canopy. Changes in the solar radiation environment under climate change needs to be considered when evaluating the effects of temperature and precipitation.

CROPPING SYSTEM IMPACTS ON WATER USE EFFICIENCY

Cropping systems interact with climate with changes in phenology, growth, yield, and water use (Hatfield et al., 2011). The changes that are occurring and will occur under climate change will impact the efficiency of radiation capture (radiation use efficiency, RUE) and WUE. These two metrics are related through the dynamics of plant growth; however, if we examine WUE in response to climate variation, we must be aware that the efficiency of a plant canopy to intercept light will be affected by those same variables. These variables are not the only ones that affect WUE, earlier studies, e.g., alfalfa in response to ozone (O_3) and water-deficit stress showed the interaction between these factors (Temple and Benoit, 1988). Increasing O_3 reduced WUE because of the effect on leaf senescence and maintenance of leaf area of the alfalfa canopy. This illustrates that climate change

impacts could arise from many different parameters that would affect WUE.

Over the recent years, studies on the impact of climate change and WUE have made use of historical observations of the growing season conditions coupled with physiological responses of different crops to temperature and CO_2 (Guoju et al., 2013a,b). On potato (*S. tuberosum* L.), Guoju et al. (2013b) used controlled experiments to manipulate temperatures to define the relationship between temperature and WUE. They found WUE increased as temperatures increased to 1.5°C above normal and then began to decrease. Interestingly, they found that WUE began to decrease linearly with increases in annual precipitation above 310 mm. They proposed that the combination of increased temperatures and precipitation affected the respiration rate of potato which directly influenced the productivity of the plant. This concept was proposed by Reichstein et al. (2002) for evergreen trees demonstrates that agriculturalists focus on the climate effects on respiration as a factor contributing to WUE. In a similar study conducted in the semi-arid of northwest China, Guoju et al. (2013a) found for wheat, potato, and maize there was an increase of 1.6°C in the period from 1990 to 2009 compared to 1960–1969 and a decrease in annual precipitation of 105.6 mm. They showed that WUE increased in the 1990–2009 period in wheat by 0.0011 mm m^{-2} yr^{-1}, potatoes by 0.00045 mm m^{-2} yr^{-1}, and maize by 0.0012 mm m^{-2} yr^{-1} compared to the previous values. This response could be expected, if the temperatures during the growing season were not above the optimum for the specific crop.

CULTURAL PRACTICES AT THE CANOPY SCALE

Fertilizer Application and Mulching

Climate change can extend beyond the direct impacts on photosynthesis and water use by canopies to the indirect impacts related to changes in cultural practices that would affect how crop canopies respond to climate variation. The framework for these changes can be shown in **Figure 4**, when we separate the soil and plant components in water use. For example, Li et al. (2018) evaluated plastic and straw mulch on WUE of potato and found plastic mulch increased productivity by 24% and straw mulch by 16%. This resulted in an increase of WUE of potato by 29% under a plastic mulch and 6% under the straw mulch. The effectiveness of the mulching practices on WUE were increased when precipitation was less than 400 mm and decreased when precipitation was above 400 mm. They found WUE of potato was affected by seasonal air temperature, precipitation, baseline soil fertility, and fertilizer management. Seasonal temperatures between 15 and 20°C showed the highest WUE but declined when temperatures were above or below this range (Li et al., 2018). In a study that combined plastic mulch with plant density on maize, Liu et al. (2014) found that different mulches did not affect WUE, but plastic mulch increased WUE compared to no mulch and this additional water saved because of the reduced soil water evaporation was able to support a higher plant population. The effects of mulch on WUE was reviewed by Zhang et al. (2017) and overall, mulch increased WUE by 61% because of the change in the water balance and the increased productivity of the maize crop.

Adding crop residue to the soil surface has shown benefits in decreasing soil water evaporation and increasing WUE in semi-arid regions. Ali et al. (2018) evaluated different soil management practices and found adding wheat residue at 5 t ha^{-1} coupled with an irrigation of 350 mm increased soil water availability compared to no residue and increased grain yield by 62% and WUE by 35%. They found that the presence of the wheat residue increased rainfall-use efficiency by 50% because of the reduced soil water evaporation. Wang et al. (2014) evaluated planting pattern and irrigation on wheat in the North China Plain and found a combination of furrow ridge planting combined with 135 mm of irrigation increased WUE by nearly 14% and suggested that this strategy would provide a more efficient production system in water-limited environments. Ibrahim et al. (2015) showed that mulching and micro-dosing of NPK fertilizer increases WUE in low-input agriculture in a semi-arid climate.

In tall fescue (*Festuca arundinacea* Schreb.), Kunrath et al. (2018) found that limiting nitrogen to the crop had a negative effect on WUE because the transpiration decreased relative to soil water evaporation. Similar results for alfalfa when plant stands were decreased, WUE decreased because of the increased soil water evaporation component (Kunrath et al., 2018). They suggested that understanding the interactions between nitrogen status and water deficits would be necessary to improve WUE.

Irrigation

Another manipulation of the microclimate of the crop is to apply irrigation as a water supply to overcome water deficits. The impact on WUE could be substantial, if, the amount of water applied greatly improved the production compared to the amount of water use by the crop. Fan et al. (2018) conducted a meta-analysis on 49 experiments of irrigated wheat and cotton throughout China under furrow and micro-irrigation systems to determine the optimum water use level to achieve maximum WUE. If the goal is to maximize WUE rather than yield, across these studies, water use for wheat could be reduced by 30% with a grain yield decrease of only 15%; however, in cotton water use of 51% was linked with a yield reduction of 52%. The adoption of micro-irrigation was able to reduce wheat water use by 23% and increase yield by 37%, while in cotton this practice reduced water use by 37% and decreased yield by 21%. Adoption of micro-irrigation system reduces the soil water evaporation from between the plant rows early in the season and limits almost all the evaporation component from the canopy. These changes have a positive effect on WUE in areas with irrigated crops and demonstrates that WUE can be changed by water management of the system.

Crop Arrangement

Manipulation of row spacing will affect the partitioning of the soil water evaporation and the transpiration of the canopy. Narrow rows would reduce the time the soil is not covered

(**Figure 4**) and in theory would increase WUE. Barbieri et al. (2012) compared 35 and 70 cm rows of maize and found there was no difference in seasonal totals of ET because differences between row spacing diminished as the maize plant developed; however, the narrow row spacing increased WUE by 17% with significant effects when the crop was nitrogen and water limited but had no effect if the crop was irrigated and well-fertilized (Barbieri et al., 2012). As a climate adaptation strategy, reducing row spacing would increase WUE in water limited environments or under rainfed environments with increasing variability of rainfall during the growing season. Gregory et al. (2000) showed using simulation models, reduction of row width was an effective strategy in rainfed production regions of the world because of the effect on soil water evaporation. They showed that changing row spacing was most effective in areas with clay soils with frequent rain events and low atmospheric demand and would least effective in sandy soils with variable rain events and high evaporative demand.

Crop Rotations and Mixed Crop Stands

To cope with climate change, one adaptive strategy would be to diversify the crop rotation to increase the resilience of the overall cropping system. Álvaro-Fuentes et al. (2009) compared four rotations in northeastern Spain to determine if adding a more diverse rotation of wheat and barley (*Hordeum vulgare* L.) would increase WUE. They used four rotations over a 6-year period, a wheat monoculture, a barley monoculture, wheat-barley-rapeseed (*Brassica napus* L.), and wheat-barley-vetch (*Vicia sativa* L.). Rainfall variation among growing seasons was the main determinate of water use and WUE. There was a failure of the rapeseed and vetch to produce a crop in several of the years, that impacted the WUE of the overall rotation system compared to the monoculture systems (Álvaro-Fuentes et al., 2009). Franco et al. (2018) examined an intercropping system consisting of peanut, watermelon [*Citrullus lanatus* (Thunb.) Matsum. & Nakai], okra [*Abelmoschus esculentus* (L.) Moench], cowpea, and pepper (*Capsicum annuum* L.) planted alone or in various intercropping combinations. In a low fertilizer input system in Texas. Peanut showed an increased WUE from 0.00015 kg plant^{-1} mm^{-1} when grown in monoculture to 0.00022 kg plant^{-1} mm^{-1} when grown in an intercropping system, watermelon and okra both showed similar positive responses to intercropping. They suggested that intercropping system would offer advantages for more efficient water use in water-limited environments.

Agroforestry

Another strategy is to utilize agroforestry systems (AFS), where woody perennials (i.e., trees or shrubs) or perennial forbs are grown with annual crops on the same parcel of land and during same or different time periods. AFS systems comprise silvopastures, alley cropping, riparian buffers, windbreaks, parklands, home gardens, and fallow systems, among many others (Sauer and Hernandez-Ramirez, 2011; Nair et al., 2017). One theory is that the AFS annuals and perennials utilize different resource pools, i.e., there is a spatial complementarity. The roots of the tree component reach deeper soil layers than the annual crops, thus exploiting unused water and nutrient resources. At the same time the upper tree canopy provides shade to crops, which reduces evaporative water loss and water stress by generating a favorable micro-climate. The opposite would be the spatial competition, where the different AFS components compete for the same resources. Tree roots exploit the same soil layers than annual crops, the tree canopy reduces incoming PAR, and negatively affects rainfall distribution (Monteith et al., 1991; Ong et al., 1991). Both, spatial complementarity and competition, can occur and may change over time. For example, trees may cause a decrease of the groundwater table, which may lead to tree dieback under extreme climatic conditions (Song et al., 2015). Adverse effects can be partly ameliorated with additional management efforts such as tree root barriers, tree canopy pruning, use of different tree species, tree density and spatial arrangement, and effective use of run-off water (e.g., Ong et al., 1991; Droppelmann et al., 2000; Muthuri et al., 2009). These interactions eventually alter WUE. However, studies on WUE in AFS are scarce to fully understand all interactions and implications to WUE in the different types of AFS. Droppelmann et al. (2000) showed higher and lower WUE values among two seasons in sorghum and cowpea planted in an *Acacia saligna* (Labill.) H. Wendl. alley cropping system in semi-arid Kenya compared to monocrop annuals. Eastham et al. (1990) found that WUE in silvopastures of both, forage and trees, changed with tree density, but the authors did not compare WUE with single pasture systems. Muthuri et al. (2009) found higher chlorophyll content in monocrop maize than in AFS maize in Kenya, and that WUE and chlorophyll content are correlated. Perhaps a better way to look at WUE in AFS is the WER (see above). Bai et al. (2016) found in a semi-arid climate in northeast China consistently higher WUE in monocropping systems of sweet potato [*Ipomoea batatas* (L.) Lam.], peanut, and millet [*Setaria italica* (L.) P. Beauvois] compared to intercropped with apricot trees. However, overall WER was greater than 1 owing to the similar WUE of apricot in AFS and monocrop settings, indicating that overall yield to water use ratio was improved in AFS. Despite the need to further investigate WUE in AFS, there are promising results indicating that under good management practices AFS may ameliorate water use in water-limited environments, such as in sub-humid – arid climates, or during the dry season in the humid tropics.

WATER USE EFFICIENCY TRENDS

Basso and Ritchie (2018) suggested that WUE has increased over time because the grain yields have increased while water use has remained relatively constant. Nagore et al. (2017) compared an older maize hybrid with more recently released hybrids and found the more recent hybrids had a WUE of 25.1 kg ha^{-1} mm^{-1} compared to 23.1 kg ha^{-1} mm^{-1} for the older hybrid. The more recent hybrids also showed a greater advantage in WUE all at soil water contents over the course of this study. The plant parameter that showed the advantage to increasing WUE was kernels per plant. The resilience of genetic material to stress, e.g., temperature

or water, will provide the newer genetic material with greater WUE.

Increasing WUE under climate change will result from two fronts. First, being able to identify genotypes that have high assimilation rates under temperature and water-deficit stress. There are a range of techniques that can be used at both the leaf and canopy level and development of tools oriented toward phenotypic screening relative to WUE would pay dividends in terms of advancing our knowledge. We still face the challenge of being able to quantify the differences among plants in their response to temperatures above the optimum, water deficits, and increasing CO_2 and more importantly the interactions among these three factors. Second, we need to realize that there are a range of management practices we can adopt that will reduce soil water evaporation and shift the water use by the crop to more transpiration to limit the exposure of the plant to water-deficit stress and maintain productivity at the highest level possible. We can cope with climate change by understanding the physical and biological factors that interact to create a high WUE.

AUTHOR CONTRIBUTIONS

All authors listed have made a substantial, direct and intellectual contribution to the work, and approved it for publication.

FUNDING

This research was conducted under project 5030-11610-005-00D funded by the United States Department of Agriculture-Agricultural Research Service.

ACKNOWLEDGMENTS

This research was partially supported by USDA NIFA Project 2015-68007-23133, Developing and promoting water-, nutrient-, and climatesmart technologies to help agricultural systems adapt to climate and societal changes.

REFERENCES

Ainsworth, E. A., Davey, P. A., Bernacchi, C. J., Dermody, O. C., Heaton, E. A., Moore, D. J., et al. (2002). A meta-analysis of elevated [CO2] effects on soybean (*Glycine max*) physiology, growth and yield. *Global Change Biol.* 8, 695–709. doi: 10.1046/j.1365-2486.2002.00498.x

Ainsworth, E. A., and Long, S. P. (2005). What have we learned from 15 years of free-air CO2 enrichment (FACE)? A meta-analytic review of the responses of photosynthesis, canopy properties and plant production to rising CO2. *New Phytol.* 165, 351–372. doi: 10.1111/j.1469-8137.2004.01224.x

Ainsworth, E. A., and Rogers, A. (2007). The response of photosynthesis and stomatal conductance to rising [CO2]: mechanisms and environmental interactions. *Plant Cell Environ.* 30, 258–270. doi: 10.1111/j.1365-3040.2007.01641.x

Ali, S., Manzoor, A. J., Sohail, A., Khan, A., Khan, M. I., Khan, M. I., et al. (2018). Soil amendments strategies to improve water-use efficiency and productivity of maize under different irrigation conditions. *Agric. Water Manage.* 210, 88–95. doi: 10.1016/j.agwat.2018.08.009

Allen, L. H. (1990). Plant responses to rising carbon dioxide and potential interactions with air pollutants. *J. Environ. Qual.* 19, 15–34. doi: 10.2134/jeq1990.00472425001900010002x

Allen, L. H., Pan, D., Boote, K. J., Pickering, N. B., and Jones, J. W. (2003). Carbon dioxide and temperature effects on evapotranspiration and water use efficiency of soybean. *Agron. J.* 95, 1071–1081. doi: 10.2134/agronj2003.1071

Allen, R. G., Pereira, L. S., Raes D., and Smith, M. (1998). *Crop Evapotranspiration – Guidelines for Computing Crop Water Requirements – FAO Irrigation and Drainage Paper 56*. Rome: FAO, 174.

Allen, R., Walter, I., Elliott, R., Howell, T., Itenfisu, D., Jensen, M., et al. (2005). "The ASCE standardized reference evapotranspiration equation," in *Technical Committee report to the Environmental and Water Resources Institute of the American Society of Civil Engineers from the Task Committee on Standardization of Reference Evapotranspiration* (Reston, VA: ASCE), 58.

Álvaro-Fuentes, J., Lampurlanés, J., and Cantero-Martínez, C. (2009). Alternative crop rotations under Mediterranean no-tillage conditions: biomass, grain yield, and water-use efficiency. *Agron. J.* 101, 1227–1233. doi: 10.2134/agronj2009.0077

André, M., and Du Cloux, H. (1993). Interaction of CO2 enrichment and water limitations on photosynthesis and water efficiency in wheat. *Plant Physiol. Biochem.* 31, 103–112.

Ashok, I. S. A., Prasad, T. G., Wright, G. C., Kumar M. U., and Rao, R. C., N. (1999). Variation in transpiration efficiency and carbon isotope discrimination in cowpea. *Funct. Plant Biol.* 26, 503–510. doi: 10.1071/PP98097

Avramova, V., Meziane, A., Bauer, E., Blankenagel, S., Eggels, S., Gresset, S., et al. (2018). Carbon isotope composition, water use efficiency, and drought sensitivity are controlled by a common genomic segment in maize. *Theor. Appl. Genet.* 132, 53–63. doi: 10.1007/s00122-018-3193-4

Bai, W., Sun, Z., Zheng, J., Du, G., Feng, L., Cai, Q., et al. (2016). Mixing trees and crops increases land and water use efficiencies in a semi-arid area. *Agric. Water Manage.* 178, 281–290. doi: 10.1016/j.agwat.2016.10.007

Barbieri, P., Echarte, L., Della Maggiora, A., Sadras, V. O., Echeverria, H., and Andrade, F. H. (2012). Maize evapotranspiration and water-use efficiency in response to row spacing. *Agron. J.* 104, 939–944. doi: 10.2134/agronj2012.0014

Bartlett, M. S., Vico, G., and Porporato, A. (2014). Coupled carbon and water fluxes in CAM photosynthesis: modeling quantification of water use efficiency and productivity. *Plant Soil* 383, 111–138. doi: 10.1007/s11104-014-2064-2

Basso, B., and Ritchie, J. T. (2018). Evapotranspiration in high-yielding maize and under increased vapor pressure deficit in the US Midwest. *Agric. Environ. Lett.* 3:170039. doi: 10.2134/ael2017.11.0039

Beer, C., Ciais, P., Reichstein, M., Baldocchi, D., Law, B., Papale, D., et al. (2009). Temporal and among-site variability of inherent water use efficiency at the ecosystem level. *Global Biogeochem. Cycles* 23, 1–13.

Bernacchi, C. J., Kimball, B. A., Quarles, D. R., Long, S. P., and Ort, D. R. (2007). Decreases in stomatal conductance of soybean under open-air elevation of [CO_2] are closely coupled with decreases in ecosystem evapotranspiration. *Plant Physiol.* 143, 134–144. doi: 10.1104/pp.106.089557

Bierhuizen, J. F., and Slatyer, R. O. (1965). Effect of atmospheric concentration of water vapour and CO_2 in determining transpiration-photosynthesis relationships of cotton leaves. *Agric. Meteorol.* 2, 259–270. doi: 10.1016/0002-1571(65)90012-9

Blum, A. (2009). Effective use of water (EUW) and not water-use efficiency (WUE) is the target of crop yield improvement under drought stress. *Field Crops Res.* 112, 119–123. doi: 10.1016/j.fcr.2009.03.009

Boote, K. J., Pickering, N. B., and Allen, L. H. (1997). "Plant modeling: advances and gaps in our capability to predict future crop growth and yield in response to global climate change," in *Advances in Carbon Dioxide Effects Research*, eds L. H. Allen, M. B., Kirkham, D. M., Olszyk and C. E. Whitman (Madison, WI: American Society of Agronomy, Crop Science Society of America, Soil Science Society of America), 179–228.

Briggs, L. J., and Shantz, H. L. (1913). "The water requirement of plants," in *Bureau of Plant Industry Bulletin* (Washington, DC: US Department of Agriculture), 282–285.

Brown, R. H., and Simmons, R. E. (1979). Photosynthesis of grass species differing in CO2 fixation pathways. I. Water-use efficiency. *Crop Sci.* 19, 375–379. doi: 10.2135/cropsci1979.0011183X001900030025x

Caine, R. S., Yin, X., Sloan, J., Harrison, E. L., Mohammed, U., Fulton, T. A., et al. (2019). Rice with reduced stomatal density conserves water and has improved drought tolerance under future climate conditions. *New Phytol.* 221, 371–384. doi: 10.1111/nph.15344

Cernusak, L. A. (2018). Gas exchange and water use efficiency in plant canopies. *Plant Biol*. doi: 10.1111/plb.12939 [Epub ahead of print].

Charles-Edwards, D. A. (1971). A simple kinetic model for leaf photosynthesis and respiration. *Planta* 101, 43–50. doi: 10.1007/bf00387689

Collins, M., Knutti, R., Arblaster, J., Dufresne, J.-L., Fichefet, T., Friedlingstein, P., et al. (2013). "Long-term climate change: projections, commitments and irreversibility," in *Climate Change 2013: The Physical Science Basis. Contribution of Working Group I to the Fifth Assessment Report of the Intergovernmental Panel on Climate Change*, eds T. F. Stocker, D. Qin, G.-K. Plattner, M. Tignor, S. K. Allen (Cambridge: Cambridge University Press).

Craufurd, P. Q., Wheeler, T. R., Ellis, R. H., Summerfield, R. J., and Williams, J. H. (1999). Effect of temperature and water deficit on water-use efficiency, carbon isotope discrimination, and specific leaf area in peanut. *Crop Sci.* 39, 136–142. doi: 10.2135/cropsci1999.0011183X003900010022x

Dai, A. (2013). Increasing drought under global warming in observations and models. *Nat. Clim. Change* 3, 52–58. doi: 10.1038/nclimate1811

Dold, C., Büyükcangaz, H., Rondinelli, W., Prueger, J., Sauer, T., and Hatfield, J. (2017). Long-term carbon uptake of agro-ecosystems in the Midwest. *Agric. For. Meteorol.* 232, 128–140.

Donatelli, M., Hammer, G. L., and Vanderlip, R. L. (1992). Genotype and water limitation effects on phenology, growth, and transpiration efficiency in grain sorghum. *Crop Sci.* 32, 781–786. doi: 10.2135/cropsci1992.0011183X003200030041x

Drewry, D., Kumar, P., and Long, S. (2014). Simultaneous improvement in productivity, water use, and albedo through crop structural modification. *Global Change Biol.* 20, 1955–1967. doi: 10.1111/gcb.12567

Droppelmann, K. J., Lehmann, J., Ephrath, J. E., and Berliner, P. R. (2000). Water use efficiency and uptake patterns in a runoff agroforestry system in an arid environment. *Agroforest. Syst.* 49, 223–243. doi: 10.1023/a:1006352623333

Earl, H. J. (2002). Stomatal and non-stomatal restrictions to carbon assimilation in soybean (*Glycine max*) lines differing in water use efficiency. *Environ. Exp. Bot.* 48, 237–246. doi: 10.1016/S0098-8472(02)00041-2

Eastham, J., Rose, C. W., Cameron, D. M., Rance, S. J., Talsma, T., and Charlesedwards, D. A. (1990). Tree/pasture interactions at a range of tree densities in an agroforestry experiment. III. Water uptake in relation to soil hydraulic conductivity and rooting patterns. *Aust. J. Agric. Res.* 41, 709–718. doi: 10.1071/AR9900709

Ehdaie, B., and Waines, J. G. (1993). Variation in water-use efficiency and its components in wheat: I. Well-watered pot experiment. *Crop Sci.* 33, 294–299. doi: 10.2135/cropsci1993.0011183X003300020016x

El-Sharkawy, M. A., and Cock, J. H. (1984). Water use efficiency of cassava. I. Effects of air humidity and water stress on stomatal conductance and gas exchange. *Crop Sci.* 24, 497–502. doi: 10.2135/cropsci1984.0011183X002400030017x

Fan, Y., Wang, C., and Nan, Z. (2018). Determining water use efficiency of wheat and cotton: a meta-regression analysis. *Agric. Water Manage.* 199, 48–60. doi: 10.1016/j.agwat.2017.12.006

Feng, S., and Fu, Q. (2013). Expansion of global drylands under a warming climate. *Atmos. Chem. Phys.* 13, 10081–10094. doi: 10.5194/acp-13-10081-2013

Field, C. B., Jackson, R. B., and Mooney, H. A. (1995). Stomatal responses to increased CO2: implications from the plant to the globl scale. *Plant Cell Environ*. 18, 1214–1225. doi: 10.1111/j.1365-3040.1995.tb00630.x

Fish, D. A., and Earl, H. J. (2009). Water-use efficiency is negatively correlated with leaf epidermal conductance in cotton (*Gossypium* spp.). *Crop Sci.* 49, 1409–1415. doi: 10.2135/cropsci2008.08.0490

Flexas, J., Diaz-Espejo, A., Gago, J., Gallé, A., Galmés, J., Gulías, J., et al. (2014). Photosynthetic limitations in Mediterranean plants: a review. *Environ. Exp. Bot.* 103, 12–23. doi: 10.1016/j.envexpbot.2013.09.002

Franco, J. G., King, S. R., and Volder, A. (2018). Component crop physiology and water use efficiency in response to intercropping. *Eur. J. Agron.* 93, 27–39. doi: 10.1016/j.eja.2017.11.005

Fu, Q., and Feng, S. (2014). Responses of terrestrial aridity to global warming. *J. Geophys. Res. Atmos.* 119, 7863–7875. doi: 10.1002/2014D021608

Gago, J., Douthe, C., Florez-Sarasa, I., Escalona, J. M., Galmes, J., Fernie, A. R., et al. (2014). Opportunities for improving leaf water use efficiency under climate change conditions. *Plant Sci.* 226, 108–119. doi: 10.1016/j.plantsci.2014.04.007

Gao, Q., Sun, J., Tong, H., Wang, W., Zhang, Y., Zhang, G., et al. (2018a). Evaluation of rice drought stress response using carbon isotope discrimination. *Plant Physiol. Biochem.* 132, 80–88. doi: 10.1016/j.plaphy.2018.08.030

Gao, X., Gu, F., Mei, X., Hao, W., Li, H., Gong, D., et al. (2018b). Light and water use efficiency as influenced by clouds and/or aerosols in a rainfed spring maize cropland on the loess plateau. *Crop Sci.* 58, 853–862. doi: 10.2135/cropsci2017.06.0341

Gebrekirstos, A., van Noordwijk, M., Neufeldt, H., and Mitlöhner, R. (2011). Relationships of stable carbon isotopes, plant water potential and growth: an approach to asses water use efficiency and growth strategies of dry land agroforestry species. *Trees* 25, 95–102. doi: 10.1007/s00468-010-0467-0

Gregory, P. J., Simmonds, L. P., and Pilbeam, C. J. (2000). Soil type, climatic regime, and the response of water use efficiency to crop management. *Agron. J.* 92, 814–820. doi: 10.2134/agronj2000.925814x

Guanter, L., Zhang, Y., Jung, M., Joiner, J., Voigt, M., Berry, J. A., et al. (2014). Global and time-resolved monitoring of crop photosynthesis with chlorophyll fluorescence. *Proc. Natl. Acad. Sci. U.S.A.* 111, E1327–E1333.

Guoju, X., Fengju, Z., Zhengji, Q., and Yubi, Y. (2013a). Impact of climate change on water use efficiency by wheat, potato and corn in semiarid areas of China. *Agric. Ecosyst. Environ.* 181, 108–114. doi: 10.1016/j.agee.2013.09.019

Guoju, X., Fengju, Z., Zhengji, Q., Yubi, Y., Runyuan, W., and Juying, H. (2013b). Response to climate change for potato water use efficiency in semi-arid areas of China. *Agric. Water Manage.* 127, 119–123. doi: 10.1016/j.agwat.2013.06.004

Hatfield, J. L. (2016). Increased temperatures have dramatic effects on growth and grain yield of three maize hybrids. *Agric. Environ. Lett.* 1:150006. doi: 10.2134/ael2015.10.0006

Hatfield, J. L., and Prueger, J. H. (2015). Temperature extremes: effect on plant growth and development. *Weather Clim. Extrem.* 10, 4–10. doi: 10.1016/j.wace.2015.08.001

Hatfield, J. L., Boote, K. J., Kimball, B. A., Ziska, L. H., Izaurralde, R. C., Ort, D., et al. (2011). Climate impacts on agriculture: implications for crop production. *Agron. J.* 103, 351–370. doi: 10.2134/agronj2010.0303

Hatfield, J. L., Wright-Morton, L., and Hall, B. (2018). Vulnerability of grain crops and croplands in the Midwest to climatic variability and adaptation strategies. *Clim. Change* 146, 263–275. doi: 10:1007/s10584-017-1997-x

Horie, T., Baker, J., Nakagawa, H., Matsui T., and Kim, H. (2000). "Crop ecosystem responses to climatic change: rice," in *Climate Change and Global Crop Productivity,* eds K. R. Reddy and H. F. Hodges (Wallingford: CAB International), 81–106.

Huang, J., Yu, H., Guan, X., and Guo, R. (2015). Accelerated dryand expansion under climate change. *Nat. Clim. Change* 6, 166–171. doi: 10.1038/nclimate2837

Hubick, K., and Farquhar, G. D. (1989). Carbon isotope discrimination and the ratio of carbon gained to water lost in barley cultivars. *Plant Cell Environ.* 12, 795–804. doi: 10.1111/j.1365-3040.1989.tb01641.x

Hubick, K., Shorter, R., and Farquhar, G. (1988). Heritability and genotype x environment interactions of carbon isotope discrimination and transpiration efficiency in peanut (*Arachis hypogaea* L.). *Funct. Plant Biol.* 15, 799–813. doi: 10.1071/PP9880799

Hufstetler, E. V., Boerma, H. R., Carter, T. E., and Earl, H. J. (2007). Genotypic variation for three physiological traits affecting drought tolerance in soybean. *Crop Sci.* 47, 25–35. doi: 10.2135/cropsci2006.04.0243

Hui, D., Luo, Y., Cheng, W., Coleman, J. S., and Johnson, D. W. (2001). Canopy radiation- and water-use efficiencies as affected by elevated [CO_2]. *Global Change Biol.* 7, 75–91. doi: 10.1046/j.1365-2486.2001.00391.x

Hunsaker, D. J., Hendrey, G. R., Kimball, B. A., Lewin, K. F., Mauney, J. R., and Nagy, J. (1994). Cotton evapotranspiration under field conditions with CO2 enrichment and variable soil moisture regimes. *Agric. For. Meteorol.* 70, 247–258. doi: 10.1016/0168-1923(94)90061-2

Hunsaker, D. J., Kimball, B. A., Pinter, P. J. Jr., LaMorte, R. L., and Wall, G. W. (1996). Carbon dioxide enrichment and irrigation effects on wheat evapotranspiration and water use efficiency. *Trans. ASAE* 39, 1345–1355. doi: 10.13031/2013.27626

Hunsaker, D. J., Kimball, B. A., Pinter, P. J., Wall, G. W., LaMorte, R. L., Adamsen, F. J., et al. (2000). CO2 enrichment and soil nitrogen effects on wheat

evapotranspiration and water use efficiency. *Agric. For. Meteorol.* 104, 85–105. doi: 10.1016/S0168-1923(00)00157-X

Ibrahim, A., Abaidoo, R. C., Fatondji, D., and Opoku, A. (2015). Integrated use of fertilizer micro-dosing and *Acacia tumida* mulching increases millet yield and water use efficiency in Sahelian semi-arid environment. *Nutr. Cycl. Agroecosyst.* 103, 375–388. doi: 10.1007/s10705-015-9752-z

Ismail, A. M., and Hall, A. E. (1992). Correlation between water-use efficiency and carbon isotope discrimination in diverse cowpea genotypes and isogenic lines. *Crop Sci.* 32, 7–12. doi: 10.2135/cropsci1992.0011183X003200010003x

Izaurralde, R. C., Thomson, A. M., Morgan, J. A., Fay, P. A., Polley, H. W., and Hatfield, J. L. (2011). Climate impacts on agriculture: implications for forage and rangeland production. *Agron. J.* 103, 371–380. doi: 10.2134/agronj2010.0304

Jones, P., Jones, J. W., and Allen, L. H. Jr. (1985). Seasonal carbon and water balances of soybeans grown under stress treatments in sunlit chambers. *Trans. ASAE* 28, 2021–2028. doi: 10.13031/2013.32559

Kanniah, K. D., Beringer, J., and Hutley, L. (2013). Exploring the link between clouds, radiation, and canopy productivity of tropical savannas. *Agric. For. Meteorol.* 18, 304–313. doi: 10.1016/j.agrformet.2013.06.010

Kanniah, K. D., Beringer, J., North, P., and Hutley, L. (2012). Control of atmospheric particles on diffuse radiation and terrestrial plant productivity: a review. *Prog. Phys. Geogr.* 36, 209–237. doi: 10.1177/0309133311434244

Kimball, B. A. (1983). Carbon dioxide and agricultural yield: an assemblage and analysis of 430 prior observations. *Agron. J.* 75, 779–788. doi: 10.2134/agronj1983.00021962007500050014x

Kimball, B. A., and Idso, S. B. (1983). Increasing atmospheric CO2: effects on crop yield, water use and climate. *Agric. Water Manage.* 7, 55–72. doi: 10.1016/0378-3774(83)90075-6

Kimball, B. A. (2007). "Global change and water resources," in *Irrigation of Agricultural Crops Monograph*, eds R. J. Lascano and R. E. Sojka (Madison, WI: ASA-CSSA-SSSA), 627–653.

Kimball, B. A., Kobayashi, K., and Bindi, M. (2002). "Responses of agricultural crops to free-air CO2 enrichment," in *Advances in Agronomy*, ed. D. L. Sparks (Cambridge, MA: Academic Press), 293–368.

Kromdijk, J., Głowacka, K., Leonelli, L., Gabilly, S. T., Iwai, M., Niyogi, K. K., and Long, S. P. (2016). Improving photosynthesis and crop productivity by accelerating recovery from photoprotection. *Science* 354, 857–861. doi: 10.1126/science.aai8878

Kunrath, T. R., Lemaire, G., Sadras, V. O., and Gastal, F. (2018). Water use efficiency in perennial forage species: interactions between nitrogen nutrition and water deficit. *Field Crops Res.* 222, 1–11. doi: 10.1016/j.fcr.2018.02.031

Lawson, T., and Blatt, M. R. (2014). Stomatal size, speed, and responsiveness impact on photosynthesis and water use efficiency. *Plant Physiol.* 164, 1556–1570.

Li, Q., Li, H., Zhang, L., Zhang, S., and Chen, Y. (2018). Mulching improves yield and water-use efficiency of potato cropping in China: a meta-analysis. *Field Crops Res.* 221, 50–60. doi: 10.1016/j.fcr.2018.02.017

Liu, J., Bu, L., Zhu, L., Luo, S., Chen, X., and Li, S. (2014). Optimizing plant density and plastic film mulch to increase maize productivity and water-use efficiency in semiarid areas. *Agron. J.* 106, 1138–1146. doi: 10.2134/agronj13.0582

Lobell, D., Schlenker, W., and Costa-Roberts, J. (2011). Climate trends and global crop production since 1980. *Science* 333, 616–620. doi: 10.1126/science.1204531

Lobell, D., Hammer, G., McLean, G., Messina, C., Roberts, M., and Schlenker, W. (2013). The critical role of extreme heat for maize poduction in the United States. *Nat. Clim. Change* 3, 497–501. doi: 10.1038/nclimate1832

Lobell, D., Roberts, M., Schlenker, W., Braun, N., Little, B., Rejesis, R., and Hammer, G. (2014). Greater sensitivity to drought accompanies Maize yield increase in the U.S. Midwest. *Science* 344, 516–519. doi: 10.1126/science.1251423

Long, S., and Ort, D. (2010). More than taking the heat: crops and global change. *Curr. Opin. Plant Biol.* 13, 241–248. doi: 10.1016/j.pbi.2010.04.008

Lopes, M. S., Araus, J. L., van Heerden, P. D. R., and Foyer, C. H. (2011). Enhancing drought tolerance in C4 crops. *J. Exp. Bot.* 62, 3135–3153. doi: 10.1093/jxb/err105

Males, J., and Griffiths, H. (2017). Stomatal biology of CAM plants. *Plant Physiol.* 174, 550–560.

Medrano, H., Tomás, M., Martorell, S., Flexas, J., Hernández, E., Rosselló, J., et al. (2015). From leaf to whole-plant water use efficiency (WUE) in complex canopies: limitations of leaf WUE as a selection target. *Crop J.* 3, 220–228. doi: 10.1016/j.cj.2015.04.002

Mian, M. A. R., Bailey, M. A., Ashley, D. A., Wells, R., Carter, T. E., Parrott, W. A., et al. (1996). Molecular markers associated with water use efficiency and leaf ash in soybean. *Crop Sci.* 36, 1252–1257. doi: 10.2135/cropsci1996.0011183X003600050030x

Monteith, J., and Unsworth, M. (2013). *Principles of Environmental Physics: Plants, Animals, and the Atmosphere*, 4th Edn. Cambridge, MA: Academic Press, 440.

Monteith, J. L., Ong, C. K., and Corlett, J. E. (1991). Microclimatic interactions in agroforestry systems. *For. Ecol. Manage.* 45, 31–44. doi: 10.1016/0378-1127(91)90204-9

Morison, J. I. L. (1987). "Intercellular CO2 concentration and stomatal response to CO2," in eds *Stomatal function*, eds E. Zeiger, G. D. Farquhar, and I. R. Cowan (Palo Alto, CA: Stanford University Press).

Muthuri, C. W., Ong, C. K., Craigon, J., Mati, B. M., Ngumi, V. W., and Black, C. R. (2009). Gas exchange and water use efficiency of trees and crops in agroforestry systems in semi-arid Kenya. *Agric. Ecosyst. Environ.* 129, 497–507.

Nagore, M. L., Della Maggiora, A., Andrade, F. H., and Echarte, L. (2017). Water use efficiency for grain yield in an old and two more recent maize hybrids. *Field Crops Res.* 214, 185–193. doi: 10.1016/j.fcr.2017.09.013

Nair, P. K., Viswanath, S., and Lubina, P. A. (2017). Cinderella agroforestry systems. *Agroforest. Syst.* 91, 901–917. doi: 10.1007/s10457-016-9966-3

Noble, I., Bolin, B., Ravindranath, N., Verardo, D., and Dokken, D. (2000). *Land use, Land Use Change, and Forestry*. Cambridge: Cambridge University Press.

Ong, C. K., Corlett, J. E., Singh, R. P., and Black, C. R. (1991). Above and below ground interactions in agroforestry systems. *For. Ecol. Manage.* 45, 45–57. doi: 10.1016/0378-1127(91)90205-A

Ottman, M. J., Kimball, B. A., Pinter, P. J., Wall, G. W., Vanderlip, R. L., Leavitt, S. W., et al. (2001). Elevated CO2 increases sorghum biomass under drought conditions. *New Phytol.* 150, 261–273. doi: 10.1046/j.1469-8137.2001.00110.x

Pan, D. (1996). *Soybean Responses to Elevated Temperature and Doubled CO2*. Ph.D, Dissertation, University of Florida, Gainesville, FL, USA.

Peng, S., and Krieg, D. R. (1992). Gas exchange traits and their relationship to water use efficiency of grain sorghum. *Crop Sci.* 32, 386–391. doi: 10.2135/cropsci1992.0011183X003200020022x

Polley, H. W. (2002). Implications of atmospheric and climatic change for crop yield and water use. *Crop Sci.* 42, 131–140. doi: 10.2135/cropsci2002.1310

Prasad, P. V. V., Boote, K. J., Allen, L. H., and Thomas, J. M. G. (2002). Effects of elevated temperature and carbon dioxide on seed-set and yield of kidney bean (*Phaseolus vulgaris* L.). *Global Change Biol.* 8, 710–721. doi: 10.1046/j.1365-2486.2002.00508.x

Prasad, P. V. V., Boote, K. J., and Allen, L. H. (2006). Adverse high temperature effects on pollen viability, seed-set, seed yield and harvest index of grain-sorghum [*Sorghum bicolor* (L.) Moench] are more severe at elevated carbon dioxide due to higher tissue temperatures. *Agric. For. Meteorol.* 139, 237–251. doi: 10.1016/j.agrformet.2006.07.003

Quisenberry, J. E., and McMichael, B. L. (1991). Genetic variation among cotton germplasm for water-use efficiency. *Environ. Exp. Bot.* 31, 453–460. doi: 10.1016/0098-8472(91)90044-O

Ramirez Builes, V. H., Porch, T. G., and Harmsen, E. W. (2011). Genotypic differences in water use efficiency of common bean under drought stress. *Agron. J.* 103, 1206–1215. doi: 10.2134/agronj2010.0370

Reichstein, M., Tenhunen, J. D., Roupsard, O., Ourcival, J.-M., Rambal, S., Miglietta, F., et al. (2002). Severe drought effects on ecosystem CO2 and H2O fluxes at three Mediterranean evergreen sites: revision of current hypotheses? *Global Change Biol.* 8, 999–1017. doi: 10.1046/j.1365-2486.2002.00530.x

Reddy, K. R., Hodges, H. F. and Kimball, B. A. (2000). "Crop ecosystem responses to global climate change: cotton," in *Climate Change and Global Crop Productivity*, eds K. R. Reddy and H. F. Hodges (Wallingford: CAB International), 162–187.

Ritchie, J. T. (1972). Model for predicting evaporation from a row crop with incomplete cover. *Water Resour. Res.* 8, 1204–1213. doi: 10.1029/WR008i005p01204

Roxburgh, S., Berry, S., Buckley, T., Barnes, B., and Roderick, M. (2005). What is NPP? Inconsistent accounting of respiratory fluxes in the definition of net primary production. *Funct. Ecol.* 19, 378–382.

Ruimy, A., Jarvis, P. G., Baldocchi, D. D., and Saugier, B. (1995). "CO_2 fluxes over plant canopies and solar radiation: a review," in *Advances in Ecological Research*, eds M. Begon and A. H. Fitter (Cambridge, MA: Academic Press), 1–68.

Saranga, Y., Jiang, C. X., Wright, R. J., Yakir, D., and Paterson, A. H. (2004). Genetic dissection of cotton physiological responses to arid conditions and their inter-relationships with productivity. *Plant Cell Environ.* 27, 263–277. doi: 10.1111/j.1365-3040.2003.01134.x

Sau, F., Boote, K. J., Bostick, W. M., Jones, J. W., and Mínguez, M. I. (2004). Testing and improving evapotranspiration and soil water balance of the DSSAT crop models. *Agron. J.* 96, 1243–1257. doi: 10.2134/agronj2004.1243

Sauer, T. J., and Hernandez-Ramirez, G. (2011). "Agroforestry," in *Soil Management: Building a Stable Base for Agriculture*, eds J. L. Hatfield and T. J. Sauer (Madison, WI: Soil Science Society of America), 351–370.

Siahpoosh, M. R., and Dehghanian, E. (2012). Water use efficiency, transpiration efficiency, and uptake efficiency of wheat during drought. *Agron. J.* 104, 1238–1243. doi: 10.2134/agronj2011.0320

Siahpoosh, M. R., Dehghanian, E., and Kamgar, A. (2011). Drought tolerance evaluation of bread wheat genotypes using water use efficiency, evapotranspiration efficiency, and drought susceptibility index. *Crop Sci.* 51, 1198–1204. doi: 10.2135/cropsci2010.05.0243

Slattery, R. A., Walker, B. J. Weber, A. P. M., and Ort, D. R. (2018). The impacts of fluctuating light on crop performance. *Plant Physiol.* 176, 990–1003.

Song, L., Zhu, J., Yan, Q., Li, M., and Yu, G. (2015). Comparison of intrinsic water use efficiency between different aged *Pinus sylvestris* var. mongolica wide windbreaks in semiarid sandy land of northern China. *Agroforest. Syst.* 89, 477–489. doi: 10.1007/s10457-014-9784-4

Stanhill, G., and Cohen, S. (2001). Global dimming: a review of the evidence for a widespread and significant reduction in global radiation with discussion of its probable causes and possible agricultural consequences. *Agric. For. Meteorol.* 107, 255–278. doi: 10.1016/S0168-1923(00)00241-0

Taylor, S. H., Hulme, S. P., Rees, M., Ripley, B. S., Ian Woodward, F., and Osborne, C. P. (2010). Ecophysiological traits in C3 and C4 grasses: a phylogenetically controlled screening experiment. *New Phytol.* 185, 780–791. doi: 10.1111/j.1469-8137.2009.03102.x

Temple, P. J., and Benoit, L. F. (1988). Effects of ozone and water stress on canopy temperature, water use, and water use efficiency of alfalfa. *Agron. J.* 80, 439–447. doi: 10.2134/agronj1988.00021962008000030011x

Trenberth, K. E. (2011). Changes in precipitation with climate change. *Clim. Res.* 47, 123–138.

Triggs, J. M., Kimball, B. A., Pinter, P. J., Wall, G. W., Conley, M. M., Brooks, T. J., et al. (2004). Free-air CO2 enrichment effects on the energy balance and evapotranspiration of sorghum. *Agric. For. Meteorol.* 124, 63–79. doi: 10.1016/j.agrformet.2004.01.005

Van Den Boogaard, R., Alewijnse, D., Veneklaas, E. J., and Lambers, H. (1997). Growth and water-use efficiency of 10 *Triticum aestivum* cultivars at different water availability in relation to allocation of biomass. *Plant Cell Environ.* 20, 200–210. doi: 10.1046/j.1365-3040.1997.d01-60.x

Vanzo, E., Jud, W., Li, Z., Albert, A., Domagalska, M. A., Ghirardo, A., et al. (2015). Facing the future: effects of short-term climate extremes on isoprene-emitting and nonemitting Poplar. *Plant Phsyiol.* 169, 560–575.

Villalobos, F. J., and Fereres, E. (1990). Evaporation measurements beneath corn, cotton, and sunflower canopies. *Agron. J.* 82, 1153–1159. doi: 10.2134/agronj1990.00021962008200060026x

Wall, G. W., Brooks, T. J., Adam, N. R., Cousins, A. B., Kimball, B. A., Pinter, P. J., et al. (2001). Elevated atmospheric CO2 improved *Sorghum* plant water status by ameliorating the adverse effects of drought. *New Phytol.* 152, 231–248. doi: 10.1046/j.0028-646X.2001.00260.x

Wall, G. W., Garcia, R. L., Kimball, B. A., Hunsaker, D. J., Pinter, P. J., Long, S. P., et al. (2006). Interactive effects of elevated carbon dioxide and drought on wheat. *Agron. J.* 98, 354–381. doi: 10.2134/agronj2004.0089

Wand, S. J., E., Midgley, G. F., Jones, M. H., and Curtis, P. S. (1999). Responses of wild C4 and C3 grass (*Poaceae*) species to elevated atmospheric CO2 concentration: a meta-analytic test of current theories and perceptions. *Global Change Biol.* 5, 723–741. doi: 10.1046/j.1365-2486.1999.00265.x

Wang, G. Y., Han, Y. Y., Zhou, X. B., Chen, Y. H., and Ouyang, Z. (2014). Planting pattern and irrigation effects on water-use efficiency of winter wheat. *Crop Sci.* 54, 1166–1174. doi: 10.2135/cropsci2013.06.0363

Way, D. A., Katul, G. G., Manzoni, S., and Vico, G. (2014). Increasing water use efficiency along the C3 to C4 evolutionary pathway: a stomatal optimization perspective. *J. Exp. Bot.* 65, 3683–3693. doi: 10.1093/jxb/eru205

Wright, G. C., Rao, R. C. N., and Farquhar, G. D. (1994). Water-use efficiency and carbon isotope discrimination in peanut under water deficit conditions. *Crop Sci.* 34, 92–97. doi: 10.2135/cropsci1994.0011183X003400010016x

Xiao, J., Sun, G., Chen, J., Chen, H., Chen, S., Dong, G., et al. (2013). Carbon fluxes, evapotranspiration, and water use efficiency of terrestrial ecosystems in China. *Agric. For. Meteorol.* 18, 76–90. doi: 10.1016/j.agrformet.2013.08.007

Yang, X., Cushman, J. C., Borland, A. M., Edwards, E. J., Wullschleger, S. D., Tuskan, G. A., et al. (2015). A roadmap for research on crassulacean acid metabolism (CAM) to enhance sustainable food and bioenergy production in a hotter, drier world. *New Phytol.* 207, 491–504.

Yoo, C. Y., Pence, H. E., Hasegawa, P. M., and Mickelbart, M. V. (2009). Regulation of transpiration to improve crop water use. *Crit. Rev. Plant Sci.* 28, 410–431. doi: 10.1080/07352680903173175

Zhang, Q., Wang, Z., Miao, F., and Wang, G. (2017). Dryland maize yield and water-use efficiency responses to mulching and tillage practices. *Agron. J.* 109, 1196–1209. doi: 10.2134/agronj2016.10.0593

Zhao, M., and Running, S. W. (2009). Drought-induced reduction in global terrestrial net primary production from 2000 through 2009. *Science* 329, 940–943. doi: 10.1126/science.1192666

Conflict of Interest Statement: The authors declare that the research was conducted in the absence of any commercial or financial relationships that could be construed as a potential conflict of interest.

frontiers in Plant Science

ORIGINAL RESEARCH
published: 25 January 2019
doi: 10.3389/fpls.2019.00015

Can High Throughput Phenotyping Help Food Security in the Mediterranean Area?

Donatella Danzi[1†], Nunzio Briglia[2†], Angelo Petrozza[3], Stephan Summerer[3], Giovanni Povero[4], Alberto Stivaletta[4], Francesco Cellini[3], Domenico Pignone[1,5], Domenico De Paola[1] and Michela Janni[1,6]*

[1] Institute of Biosciences and Bioresources, National Research Council, Bari, Italy, [2] Dipartimento delle Culture Europee e del Mediterraneo: Architettura, Ambiente, Patrimoni Culturali, Università degli Studi della Basilicata, Matera, Italy, [3] ALSIA Centro Ricerche Metapontum Agrobios, Metaponto, Italy, [4] Valagro SpA, Atessa, Italy, [5] Institute for Veterinary and AgriFood Bioethics, Fiumicino, Italy, [6] Institute of Materials for Electronics and Magnetism, National Research Council, Parma, Italy

OPEN ACCESS

Edited by:
Stuart Anthony Casson,
University of Sheffield,
United Kingdom

Reviewed by:
Robert David Hall,
Wageningen University & Research,
Netherlands
Radmila Stikic,
University of Belgrade, Serbia

***Correspondence:**
Michela Janni
michela.janni@ibbr.cnr.it

[†] These authors have contributed equally to this work

Specialty section:
This article was submitted to Plant Physiology, a section of the journal Frontiers in Plant Science

Received: 30 October 2018
Accepted: 07 January 2019
Published: 25 January 2019

Citation:
Danzi D, Briglia N, Petrozza A, Summerer S, Povero G, Stivaletta A, Cellini F, Pignone D, De Paola D and Janni M (2019) Can High Throughput Phenotyping Help Food Security in the Mediterranean Area? Front. Plant Sci. 10:15. doi: 10.3389/fpls.2019.00015

According to the IPCC 2014 report the Mediterranean region will be affected by strong climatic changes, both in terms of average temperature and of precipitations regime. This area hosts some half a billion people and the impact on food production will be severe. To implement a climate smart agriculture paradigm and a sustainable increase of agricultural productivity different approaches can be deployed. Agriculture alone consumes 70% of the entire water available on the planet, thus the observed reduction of useful rainfall and growing costs for irrigation water may severely constrain food security. In our work we focused on two typical Mediterranean crops: durum wheat, a rainfed crop, and tomato, an irrigated one. In wheat we explored the possibility of identifying genotypes resilient to water stress for future breeding aims, while in tomato we explored the possibility of using biostimulants to increase the plant capacity of using water. In order to achieve these targets, we used high throughput phenotyping (HTP). Two traits were considered: digital biovolume, a measure based on imaging techniques in the RGB domain, and Water Use Efficiency index as calculated semi-automatically on the basis of evaporation measurements resulting in a high throughput, non-destructive, non-invasive approach, as opposed to destructive and time consuming traditional methods. Our results clearly indicate that HTP is able to discriminate genotypes and biostimulant treatments that allow plants to use soil water more efficiently. In addition, these methods based on RGB quality images can easily be scaled to field phenotyping structure USVs or UAVs.

Keywords: high throughput phenotyping, digital biovolume, water use efficiency, biostimulants, genetic resources, durum wheat, tomato

INTRODUCTION

The agricultural sector is going to face enormous challenges in order to feed the 9.6 billion people that are going to inhabit the planet by 2050 (Elbehri, 2015). This goal has to be achieved in spite of limited availability of arable lands, of increasing need for irrigation water (agriculture consumes 70% of the world's fresh water supply) and of the severe impact of climate change. It impacts

on agriculture mostly through three drivers: water, heat and pests. Water plays an important role, due to its use for agriculture and also for most human activities. Drought affects a significant proportion of the global population, particularly those living in semi-arid and arid zones of the world, by increasing frequency, severity and duration of the adverse events (Steduto et al., 2012). The Mediterranean region has been indicated as one of the most prominent hotspots where the oncoming climate change will strike harder, with unpredictable impact on crop production in this area (Araus and Cairns, 2014; Reynolds et al., 2016). Recent years events in this region have demonstrated that drought stress (DS) severely impacts on wheat yield when occurring at grain filling stage (Berger et al., 2010) or during flowering and fruit enlargement in tomato (Jangid and Dwivedi, 2016). Periods of drought vary in timing and intensity and water is not used with equal efficiency during all crop stages (Reynolds et al., 2016). Drought hampers crop production and food security altering the photosynthetic efficiency, the nutrient uptake and the efficiency plants use water. Effects on plant growth under drought conditions are due to impaired enzyme activities, loss of turgor, and decrease in energy supply (Farooq et al., 2012). Climate change threats on wheat cultivation is even intensified by the great genetic uniformity of this crop in developed countries. In fact, wheat production for industrial food making generally relies on few cultivated varieties closely related to each other and genetically uniform (Lopes et al., 2015). These occurrences have increased the efforts of using in breeding schemes, the reservoir genetic diversity present in germplasm collection to identify traits able to mitigate the effects of climate change on crop production (Pignone and Hammer, 2013; Pignone et al., 2015). Recently climate smart agriculture (CSA) has been proposed as a further approach for developing actions needed to transform and reorient agricultural systems to effectively support development and ensure food security under climate change (du Jardin, 2015). Innovative agricultural practices are estimated to mitigate drought effects on crops and among them, a promising approach is the application of biostimulants at proper plant developmental stages (du Jardin, 2015); some experiences have in fact demonstrated the increase of plant tolerance to DS after biostimulant application (Petrozza et al., 2014; Rouphael et al., 2018) by improving leaf pigmentation, photosynthetic efficiency, leaf number and area, shoot and root biomass, as well as fruit number and/or mean weight, especially under adverse environmental conditions (Ertani et al., 2013, 2014; Petrozza et al., 2014; Colla and Rouphael, 2015; Lucini et al., 2015; Rouphael et al., 2018). In both approaches (plant breeding or new agricultural practices), intense experimental plant phenotyping is required to study and assess plant resilience to stresses.

While genomic tools are in place for major crop species giving a huge amount of data, the systematic quantification of phenotypic traits or components remains a big challenge (Chen et al., 2014). Thus, bridging the gap from genotype to the phenotype is one of the most important problems in modern plant science (Ubbens and Stavness, 2017). High-throughput phenotyping (HTP) has unlocked new perspectives for non-destructive phenotyping of large populations over time (Singh et al., 2016). It employs the acquisition of digital phenotypic traits by means of sensors, typically in the visible spectrum, as well in the near infrared, and in the induced fluorescence domain (Tardieu et al., 2017), to monitor the plants photosynthetic activity (Li et al., 2014; Fahlgren et al., 2015; Perez-Sanz et al., 2017), growth status (Pieruschka and Poorter, 2012; Petrozza et al., 2014) and the overall water content (Chen et al., 2014) as main components of plant response to limited water availability and heat stress (Comastri et al., 2018).

This paper aims at discussing two case studies, to demonstrate how high throughput phenotyping techniques may help promote the food security giving a special attention to the Mediterranean area by: (a) selecting new drought tolerant wheat genotypes from germplasm collections, and (b) increasing the understanding of the physiological mechanisms activated by the application of new biostimulant molecules able to improve water use in crops.

MATERIALS AND METHODS

Plant Material, Growth Conditions, and Treatments

Wheat

A selection of durum wheat genotypes was grown in the Greenhouse at the Research Center Metapontum Agrobios (ALSIA). The germplasm panel comprised a set of 36 durum wheat genotypes, selected from a core set of 452, named SSD collection, produced by single seed descent from a worldwide durum wheat germplasm collection (Pignone et al., 2015). In recent years, the whole core set had been analyzed based on a set of morphometric parameters recorded in the RGB (Red, Green, Blue) domain and elaborated for morphological convolution. This analysis led to the identification of the 36 genotypes used in the present study that are highly representative of the variation of response to DS in the entire SSD collection. Three reference Italian varieties (Svevo, Saragolla, and Cappelli) were used as controls, considering their different response to drought (**Table 1**).

Seeds were germinated at room temperature for maximum of 4 days on moist filter paper in Petri dishes and then transplanted into polystyrene plateaus. The plateaus were then stored at 4°C for 2 weeks in order to synchronize the plantlets growth. Individual plants were then transferred into two liter pots filled with a 1:1(v/v) mixture of river sand and peat moss until a total weight of 1200 g. Then plants were grown in glasshouse under natural light conditions, and environmental conditions were monitored every 30 min using a datalogger (Watchdog Model 450, Spectrum Tecnologies, Inc.).

Three treated and three control replicates of each accession were randomly distributed in greenhouse to minimize through spatial distribution the possible establishment of microclimatic variation in the greenhouse. To identify each single pot a barcode was applied in proper position to allow automatic reading of the plant identifier.

Wheat plants were manually kept fully irrigated up to the booting stage (Z45, 104 days after sowing, DAS), then DS was imposed for 43 days (up to 147 DAS) by maintaining the amounts

TABLE 1 | SSD entry names and origins of the durum wheat genotypes used in the study.

SSD Entry	Origin
35	Algeria
44	Tunisia
64	Morocco
69	Morocco
92	USA- North Dakota
96	Azerbaijan
99	Ethiopia
109	Iraq
112	Iraq
116	Iraq
122	USA- North Dakota
135	Turkey
171	Peru
178	France
195	Saudi Arabia
231	Ethiopia
244	Ethiopia
253	Cyprus
269	Iran
278	Bulgaria
322	Turkey
325	Syria
335	Iraq
343	Iran
397	Crete
409	Greece
415	Crete
416	Greece
441	Crete
451	Iraq
459	USA
467	Greece
477	Italy
487	Greece
494	Greece
511	Lybia
Cappelli	Italy
Saragolla	Italy
Svevo	Italy

of water in the soil around 50% field capacity (FC) through manual irrigation following pot weighting (**Figure 1A**).

Tomato

Thirty five tomato plants (*cv*. Ikram) were cultivated in 3 L pots filled with 1800 g of a substrate consisting of a 1:1(v/v) mixture of peat moss and river sand. The tomato plants were grown in glasshouse under natural light conditions. The environmental conditions were monitored every 30 min using a datalogger (Watchdog Model 450, Spectrum Tecnologies, Inc.).

At the moment of transplanting the plants were fertilized with 20 units of nitrogen, 40 units of phosphate (P_2O_5) and 20 units of potassium oxide (K_2O) per pot.

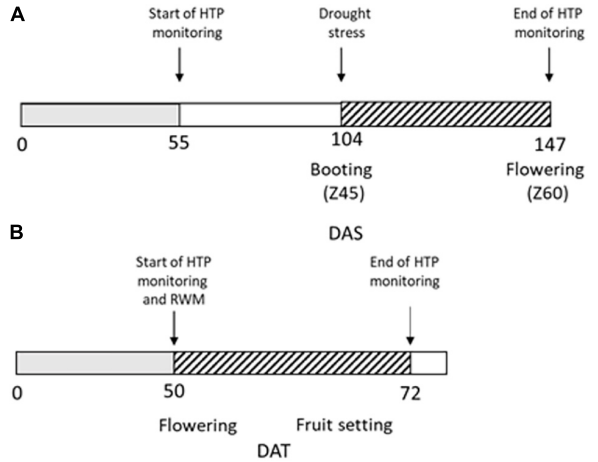

FIGURE 1 | Experimental design of the high throughput phenotyping (HTP) experiment. **(A)** Durum wheat plants were regularly irrigated up to 104 DAS (days after sowing, gray box); drought stress (dashed box) was then imposed for 43 days from 104 to 147 DAS. RGB images for HTP were acquired from 55 DAS to 147 DAS; **(B)** Tomato plants were regularly irrigated up to 50 days from transplant (gray box) when reduced water management (RWM) was performed and biostimulants were applied three times in the 22 days indicated with the dashed box.

Fifty days after transplanting, tomato plants were subjected to a reduced water management for 22 days (**Figure 1B**): the group of control plants UTC(70) was watered to restore 70% of the field capacity (FC), while another group of plants was kept at the same water regime and treated with six different natural biostimulant formulations (blindly identified as n. prototypes: 2148, 2197, 2219, 2220, 2221, and 2390). Biostimulant treatments were supplied in three applications by drenching, at the rate of 20 L/ha. Such biostimulants were particularly conceived (Valagro SpA) to improve water use efficiency (WUE) in different crops, including tomato. Their composition is proprietary, and the different formulation codes were provided by Valagro SpA for testing.

As control, 10 pots filled with the same soil mixture but without plants were randomly loaded on the conveyor belt LemnaTec system in order to estimate the daily water evaporation from bare soil.

Phenotyping Analysis

Images in the RGB domain (white light) for HTP were captured every other day according to Petrozza et al. (2014), by using a Scanalyzer 3D system (LemnaTec GmbH, Aachen, Germany) held in the Phen-Italy platform located in ALSIA Metapontum Agrobios (Metaponto).

Several traits can be recorded by using the RGB module of the 3D Scanalyzer; each plant is imaged sequentially employing different wavelengths in the visible and non-visible spectrum even if for this investigation only the visible wavelength have been considered.

The imaging involving three mutually orthogonal vantage points was used to evaluate morphometric parameters of the plant, such as height, width, or biomass (Petrozza et al., 2014).

The digital biovolume (DB), was calculated from the three orthogonal images of the same plant according to the formula

$$\sum pixelsideview0^{\circ} + \sum pixelsideview90^{\circ} + \log\left(\sum \frac{pixeltopview}{3}\right) \quad (1)$$

(Eberius and Lima-Guerra, 2009) and is assumed to be proportional to the aerial mass of the plant (Poiré et al., 2014). The Digital Biovolume Ratio was calculated as (biovolume of treated plants/biovolume of control plants). Wheat plants were monitored applying image acquisition at 2-day intervals from 55 DAS up to 147 DAS for a total of 92 days, while tomato plants were monitor applying the same interval for a total of 22 days.

Water Use Efficiency Estimation

Water use efficiency was determined for tomato plants and for all wheat genotypes using the following formula:

$$\mathrm{WUE} = \frac{\mathrm{DB}_{t_n} - \mathrm{DB}_{t_0}}{\sum_{t_0}^{t_n}(\mathrm{Tr})} \quad (2)$$

where DB_{t_n} is the DB at a specific time point, DB_{t_0} is the DB at 0 DAT for both experiments and the denominator corresponds to the sum of the quantity of water consumed (i.e., transpiration) during the corresponding growth period (Richards, 1991).

The volume of water evapotranspirated by individual plants was calculated as the difference between the weight measurement at field capacity and the current weight.

The WUE ratio index was calculated dividing the WUE of drought stressed plants by WUE of control plants for each genotype throughout the experiment. On the basis of this index, a heatmap chart was generated including each genotype using the R package ggplot2 (Wickham, 2009).

The green color indicates a higher WUE ratio and refers to values ranging between 1.32 and 1, red color indicates a lower WUE ratio including values raging between 1 and 0.52.

Statistical Analysis

Descriptive statistical parameters for DB and WUE were calculated on wheat phenotyping data, ANOVA analysis was performed with SigmaPlot ver.13 (Systat Software Inc.). The *F* test statistic, calculated as the ratio between estimated population variance between groups and estimated population variance within groups, was determined. To demonstrate the correlation between DB and fresh weight biomass harvested a Linear Correlation Analysis was performed (SigmaPlot ver.13, Systat Software Inc.). Phenotyping data from the tomato trial were analyzed using one-way analysis of variance (ANOVA), and the means were compared using the Duncan's New Multiple Range Test (MRT; $p < 0.05$) employing the R package agricolae (Mendiburu, 2016).

Data Availability

Phenotyping raw data and images are available upon request to the authors. Tables containing data used for the analyses but non-included in the text, are reported in the **Supplementary Material**.

RESULTS

RGB High Throughput Phenotyping Image Analyses to Monitor Plant Stress Response

The RGB imaging index DB was used to monitor the phenotypic response to DS in wheat and to assess the benefits brought by the application of biostimulants in tomato plants under reduced water conditions. The effectiveness of this digital parameter as indicator of the plant biomass variation during plant growth has been previously described (Poiré et al., 2014).

Wheat and tomato plants were monitored over a period of 13 and 3 weeks, respectively, through a non-invasive, non-destructive, high throughput phenotyping platform. The activity regarded plants used as controls and others grown under drought/water limiting stress conditions.

Assessing Durum Wheat Landraces Response to Drought

The RGB index was chosen to monitor and evaluate the differences in growth limitation following DS in the set of durum wheat landraces was DB. No significant difference in the DB was observed between treated and untreated plants in the period from 55 to 104 DAS, corresponding to the well-watered cultivation period; in this same period differences in DB could only be observed among the analyzed genotypes as expected.

The evaluation of the DB in control and drought stressed plants, showed that this index is significantly affected in plants subjected to drought starting at 8 days after the imposition of the stress (104–112 DAS, $F178.181$; $P < 0.001$; **Figure 2A** and **Table 2**), then it remained quite steady for 12 days, to drop significantly in the last 12 days of the withholding of water (124–147 DAS) reaching the minimum value recorded. The highest difference observed between the treatments was at 139 DAS ($F351.417$; $P < 0.001$, **Figures 2A,B** and **Table 2**).

Generally, all the analyzed genotypes were affected by DS as variation in the DB. Nevertheless, the differences between the control and stressed lots of the same genotype changed significantly in the period of stress administration (104–147 DAS). Some genotypes were more affected by water limitation, while others appeared to be way more tolerant to the stress. In particular genotypes 44, 195, 269, 322, 409, 416, and 447 showed a smaller reduction in the DB during the entire stress period of the experiment (**Table 3**). Similar behavior was observed for the variety Svevo, generally considered a standard for tolerance to DS under Mediterranean agro-climatic condition, and the variety Cappelli, identified as source of drought resistance traits (Aprile et al., 2013).

Exploitation of Genetic Resources to Increase Water Use Efficiency

The WUE trend was studied in order to rank the genotypes according to their WUE, and to correlate this index with DS resilience. WUE was calculated as the above-ground biomass

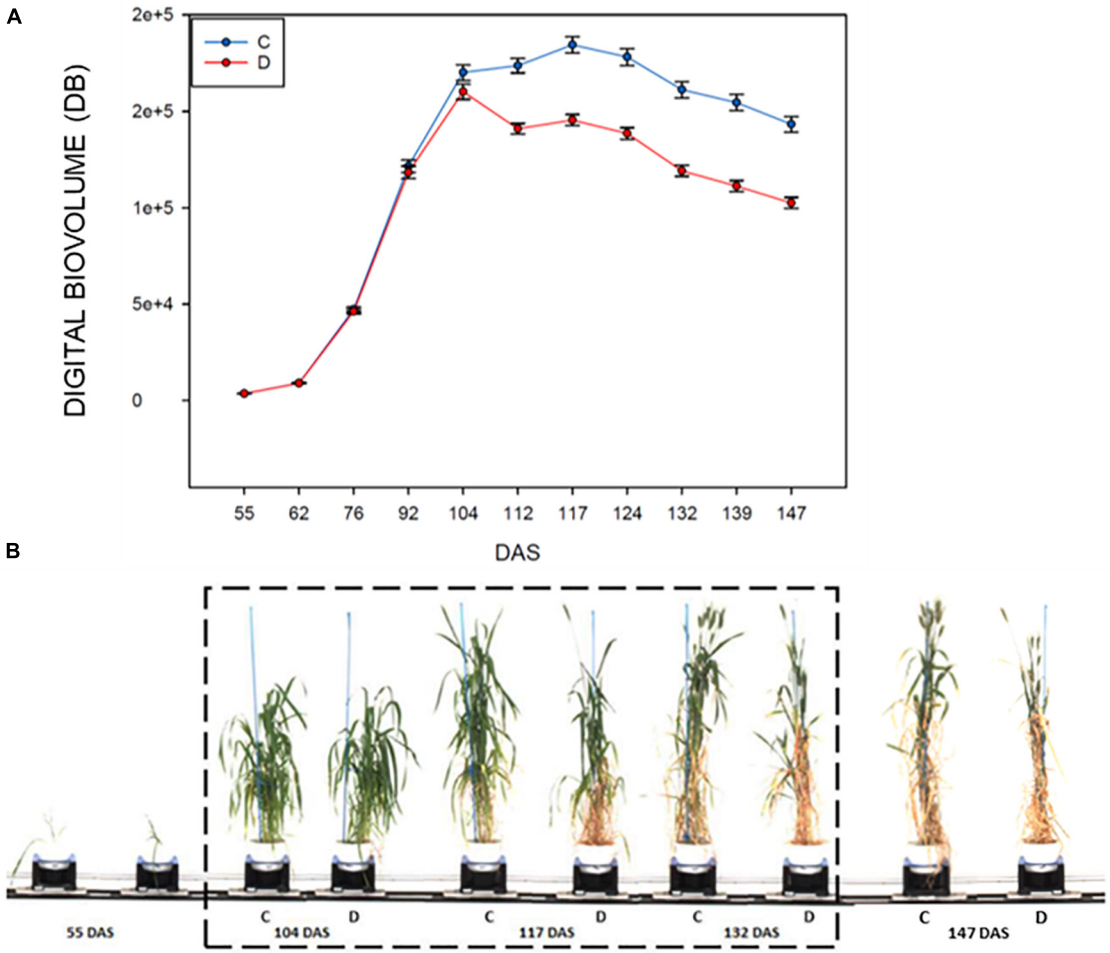

FIGURE 2 | RGB HTP analyses for control and drought-stressed plants in the period 55–147 DAS, measured using a Lemnatec Scanalyzer 3D. **(A)** Mean value of the Digital biovolume (DB): C, control plant; D, drought stressed plants. **(B)** Example of the acquired RGB Images of a representative durum wheat genotype, showing the effects of drought stress on plant growth. The drought stress interval is indicated with dashed box.

TABLE 2 | Digital biovolume average values of all the control and drought stressed SSD plants analyzed by HTP and results of the ANOVA test.

DAS	Digital biovolume		Treatment	Genotype	G × T
	C plants*	DS plants**			
55	3545.83	3594.66	$F = 1.319$; $p = 0.253$	$F = 7.403$; $p < 0.001$	$F = 0.889$; $p = 0.655$
62	9009.33	8876.71	$F = 0.0472$; $p = 0.828$	$F = 14.366$; $p < 0.001$	$F = 1.023$; $p = 0.445$
76	47345.44	46197.58	$F = 1.935$; $p = 0.166$	$F = 18.241$; $p < 0.001$	$F = 1.296$; $p = 0.140$
92	121543.46	118389.87	$F = 3.708$; $p = 0.056$	$F = 20.059$; $p < 0.001$	$F = 1.915$; $p = 0.004$
104	171139.38	160179.77	$F = 10.299$; $p = 0.002$	$F = 18.862$; $p < 0.001$	$F = 0.824$; $p = 0.751$
112	173693.21	140974.00	$F = 178.181$; $p < 0.001$	$F = 17.754$; $p < 0.001$	$F = 1.333$; $p = 0.117$
117	184458.11	145476.21	$F = 242.848$; $p < 0.001$	$F = 21.295$; $p < 0.001$	$F = 1.675$; $p = 0.016$
124	178176.04	138575.22	$F = 235.265$; $p < 0.001$	$F = 22.406$; $p < 0.001$	$F = 2.071$; $p = 0.001$
132	161236.76	119183.28	$F = 301.286$; $p < 0.001$	$F = 24.497$; $p < 0.001$	$F = 2.736$; $p < 0.001$
139	154549.81	111244.18	$F = 351.417$; $p < 0.001$	$F = 26.295$; $p < 0.001$	$F = 2.645$; $p < 0.001$
147	143304.76	102564.49	$F = 303.089$; $p < 0.001$	$F = 22.379$; $p < 0.001$	$F = 2.369$; $p < 0.001$

*F statistic represents the ratio between estimated population variance between groups and estimated population variance within groups. *C plants: control plants; **DS plants Drought Stressed plants.*

TABLE 3 | Digital Biovolume Ratio (DBR) calculated for all SSD genotypes tested and control varieties for the entire experiment length.

SSD	DAS										
	55	62	72	92	104	112	117	124	132	139	147
35	1.23	1.12	0.85	1.04	1.12	0.78	0.74	0.78	0.75	0.73	0.69
44	1.03	0.93	0.93	1.31	0.84	0.80	0.84	0.82	0.84	0.84	0.81
64	1.06	0.97	0.95	0.98	0.81	0.90	0.83	0.90	0.83	0.72	0.67
69	0.97	1.10	1.15	1.09	1.07	0.88	0.82	0.81	0.76	0.77	0.67
92	1.08	0.93	1.14	0.93	0.83	0.74	0.73	0.74	0.76	0.79	0.72
96	0.86	0.98	1.00	0.79	1.12	0.73	0.72	0.81	0.76	0.73	0.69
99	1.11	1.03	0.95	1.15	1.10	0.96	0.70	0.69	0.61	0.52	0.52
109	1.03	1.08	1.24	1.16	0.96	0.86	0.87	0.82	0.79	0.73	0.74
112	1.16	0.99	0.99	1.07	0.86	0.73	0.68	0.68	0.64	0.63	0.66
116	0.92	1.01	0.97	0.98	0.86	0.87	0.77	0.77	0.78	0.83	0.80
122	1.04	0.85	0.81	0.90	0.79	0.80	0.76	0.71	0.78	0.75	0.68
135	0.94	0.85	0.79	0.70	0.79	0.66	0.67	0.63	0.58	0.55	0.53
171	0.93	0.95	0.87	0.93	0.89	0.69	0.71	0.71	0.67	0.76	0.75
178	1.03	0.76	0.83	0.78	0.92	0.77	0.76	0.74	0.68	0.58	0.56
195	1.13	1.19	1.08	1.43	0.96	0.99	0.94	0.94	0.95	0.89	0.93
231	0.97	0.92	0.89	0.97	0.91	0.76	0.82	0.79	0.78	0.68	0.80
244	1.04	0.97	0.81	0.96	0.80	0.80	0.73	0.78	0.70	0.70	0.72
253	0.92	0.90	0.96	0.97	0.92	0.76	0.79	0.74	0.71	0.68	0.62
269	0.98	0.84	0.78	0.86	0.96	0.89	0.88	0.87	0.85	0.88	0.89
278	1.24	1.19	1.34	1.06	1.13	0.79	0.74	0.67	0.59	0.62	0.64
322	1.48	1.17	1.04	1.00	0.94	0.89	0.88	0.87	0.89	0.79	0.83
325	1.07	1.02	0.96	0.95	0.99	0.80	0.78	0.72	0.65	0.63	0.62
335	1.09	1.12	0.97	1.10	0.88	0.79	0.82	0.83	0.72	0.67	0.69
343	0.89	0.93	0.91	0.75	0.85	0.83	0.89	0.98	0.90	0.80	0.94
397	1.31	1.09	1.08	0.86	1.00	0.81	0.82	0.84	0.75	0.68	0.69
409	1.01	1.05	1.01	1.04	0.90	0.97	0.95	0.91	0.94	0.96	0.97
415	0.92	0.97	1.03	0.98	0.99	0.73	0.69	0.73	0.73	0.78	0.71
416	1.17	1.17	1.07	0.96	1.02	0.82	0.88	0.86	0.90	0.88	0.89
441	1.41	1.30	1.23	0.93	0.97	0.89	0.90	0.91	0.73	0.72	0.69
451	1.05	1.04	1.19	1.11	0.96	0.81	0.75	0.74	0.73	0.79	0.79
459	0.98	0.84	0.92	0.83	0.88	0.78	0.80	0.77	0.70	0.60	0.56
467	1.11	0.87	0.99	1.04	1.03	0.86	0.85	0.73	0.76	0.78	0.79
477	1.32	1.09	1.08	1.08	1.03	0.83	0.87	0.86	0.89	0.88	0.86
487	0.86	1.01	1.01	0.97	0.94	0.79	0.79	0.81	0.76	0.74	0.76
494	1.10	1.00	1.07	0.96	0.98	0.85	0.84	0.83	0.81	0.81	0.76
511	0.99	0.79	0.96	0.77	1.01	0.86	0.76	0.75	0.70	0.62	0.64
Cappelli	1.00	1.08	1.02	0.93	0.99	0.99	0.99	1.00	0.98	0.95	0.97
Saragolla	0.91	1.09	0.98	1.08	0.97	0.77	0.69	0.64	0.63	0.61	0.60
Svevo	0.89	0.89	0.88	0.69	0.93	0.93	1.03	1.01	0.97	0.90	0.88

Digital biovolume ratio is calculated as: biovolume of drought stresses plants/biovolume control plants.

produced per mass of water consumed, including evaporation and transpiration (Richards, 1991) in the set of plants under measurement.

As expected WUE was strongly affected by DS in all genotypes (**Figure 3A**) and significantly decreased immediately after the beginning of the stress at 104 DAS (F121.141; $p < 0.001$) (**Figure 3A**). It reached a minimum at 139 DAS (F231.910; $p < 0.001$) and remained constant till the end of the measurements (**Supplementary Table 1**). This result lead to hypothesize a direct correlation between the reduction of WUE in the plants and their reduction in biovolume as a consequence of the reduction of evapotranspiration in the stressed samples. The strong correlation ($R^2 = 0.96$, $P \leq 0.001$) observed between DB and WUE observed at 139 DAS (**Figure 3B**) supports this hypothesis (**Figure 3B**) and proves the efficacy of the DB as strong indicator of the plant health status.

The WUE indicator also provides a measure of the different abilities to recover among different genotypes. To this purpose the WUE ratio (WUE drought/WUE controls) was estimated (Pandey, 2017) (**Figure 4**). As expected, a difference in the WUE ratio was observed among the genotypes due to the

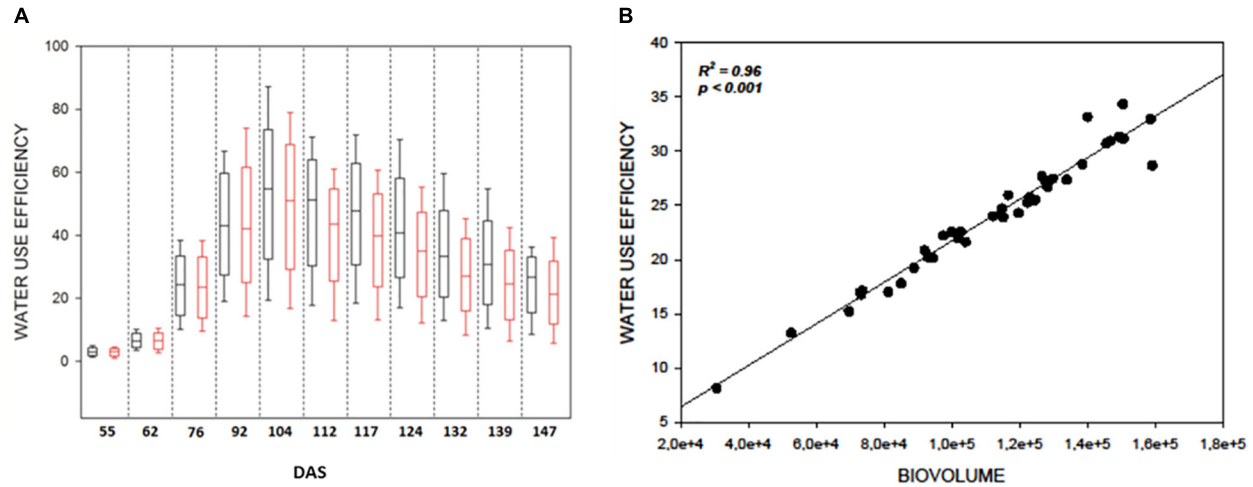

FIGURE 3 | (A) Boxplots showing the distribution of WUE values during the experiment. Black boxes are control plants, red boxes the water stressed lot. Drought stress was imposed at 104 DAS; **(B)** Correlation plot between WUE index and digital biovolume acquired by Scanalyzer at 139 DAS.

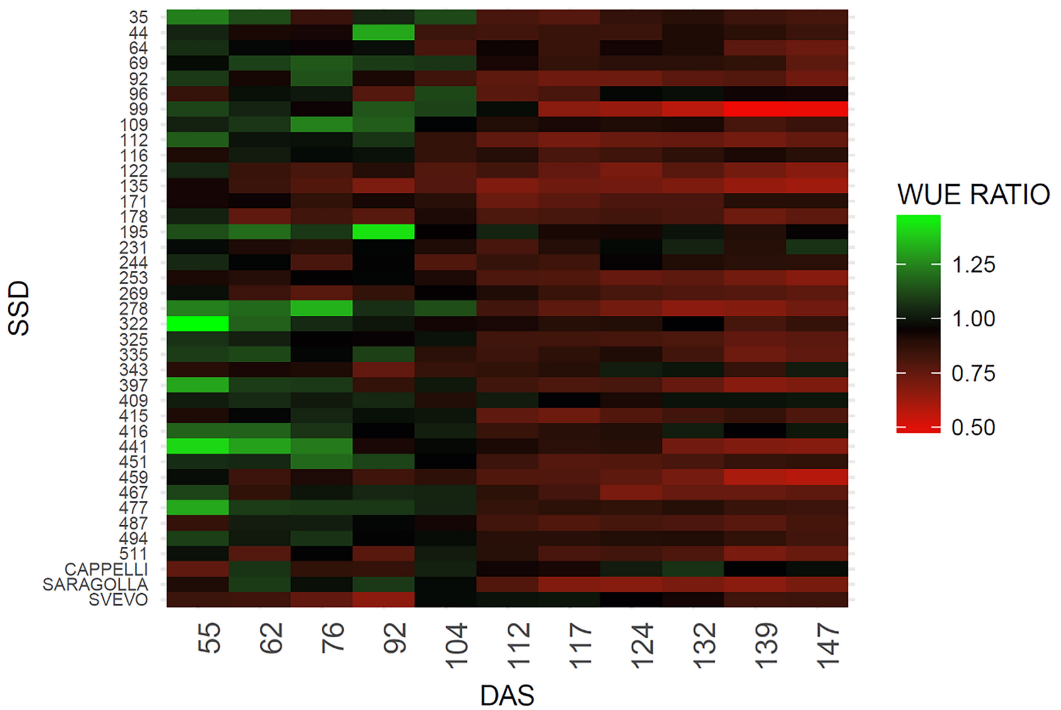

FIGURE 4 | Heatmap of WUE ratio for the analyzed genotypes. The green color indicates a higher WUE ratio, red color a lower WUE ratio. WUE ratio is calculated as WUE of drought stresses plants/WUE control plants.

genetic variability posed in the collection. An overall reduction in the WUE was observed, however, SSD lines 69, 109, 195, 231, 244, 322, 343, 409, and 416 maintain similar values of WUE under stress condition for the entire set of measurements (**Figure 4**). The reliability of the measure is also supported by the observation that similar behavior is shown by the variety Cappelli reported to be drought resistant (Aprile et al., 2013). In contrast, SSD lines 99, 135, 253, 278, 397 and the Italian variety Saragolla showed a marked decrease in the WUE ratios immediately after the stress imposition (112 DAS), which remains of same entity for the entire experiment (**Figure 4** and **Supplementary Table 2**). A high variability between SSDs was expected due to the high genetic diversity present in the material, however a certain range of variation in the WUE is also described by the heatmap before the stress imposition; this probably

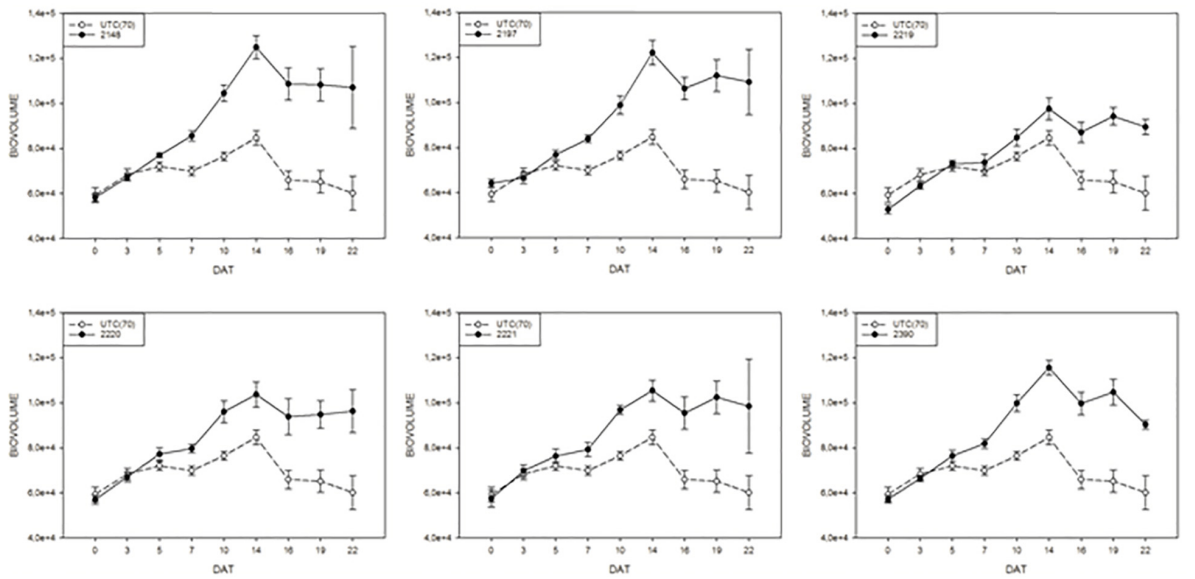

FIGURE 5 | Digital biovolume (DB) measurements on tomato plants exposed to different biostimulant prototypes: UTC(70) refers to the Untreated Control thesis where plants were irrigated with 70% FC, indicated with a dashed line. Tomato plants under reduced water condition (70% FC) and treated with the biostimulant prototypes are indicated with the solid line.

occurred for an operational bias in the manual watering procedures, thus confirming the high sensitivity of this method in fine recording small variation of WUE during the plant growth.

Impact of the Application of Natural Biostimulants on Digital Biovolume and Water Use Efficiency in Tomato Plants

In order to monitor the effect of biostimulants on tomato plants grown under limiting water availability, the variation of the digital biomass based on RGB imaging was used. The differences in DB value between the UTC(70) and biostimulants-treated plants were observed. Interestingly, all prototype formulations exerted a consistent increase in DB in comparison with UTC(70). In particular, prototypes 2148, 2197, and 2390 were the most effective (**Figure 5**); the observed increase in DB was consistent and significant already from 7 Days After Treatment (DAT, **Figure 5**) and reached a peak at 14 DAT, when the maximum difference between treated and untreated plants was recorded. The observed increase in DB values in the biostimulant-treated plants indicates an overall benefit of such formulations on plant growth and development, in particular under limited water management (**Figure 5**).

A closer look at the 14 DAT time-point, when the highest difference in DB was observed between biostimulants-treated and UTC(70), allowed a ranking of biostimulant prototypes efficacy. To better express biostimulant performance, the digital biovolume ratio (DBR) was used. The ranking showed (Duncan's MRT; $p < 0.05$) that prototype 2148 formulation was the most effective in increasing DBR (**Figure 6**).

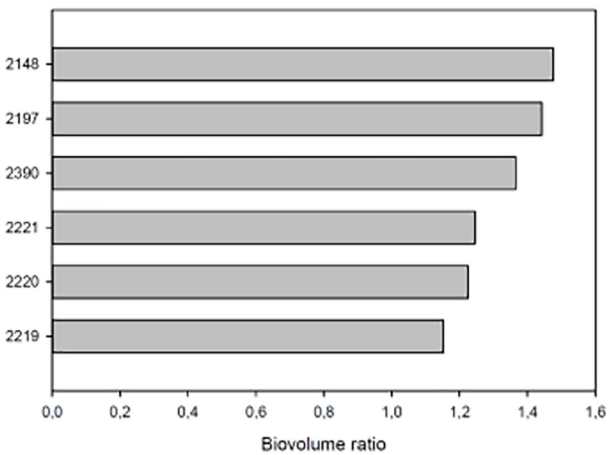

FIGURE 6 | DBR at 14 DAT of tomato plants exposed to different water limiting conditions. The UTC(70) plants were used as reference. On the *Y* axis each bar is identified by the number of the prototype formulation used to treat tomato plants. On the *X* axis the biovolume ratio. All plants were growth at 70% of the field capacity (FC) and treated with the relative prototype as indicated in Section "Materials and Methods."

Water use efficiency of tomato plants treated with biostimulants compared to UTC(70) control plants was also evaluated. Considering this parameter, an overall positive effect of the application of biostimulant prototypes was observed for all prototypes (**Figure 7**), in line with the observations on DBR. Prototype 2148 (Talete®), which was the most effective in increasing DB, was also able to increase consistently the WUE of plants under limiting water conditions, thus confirming

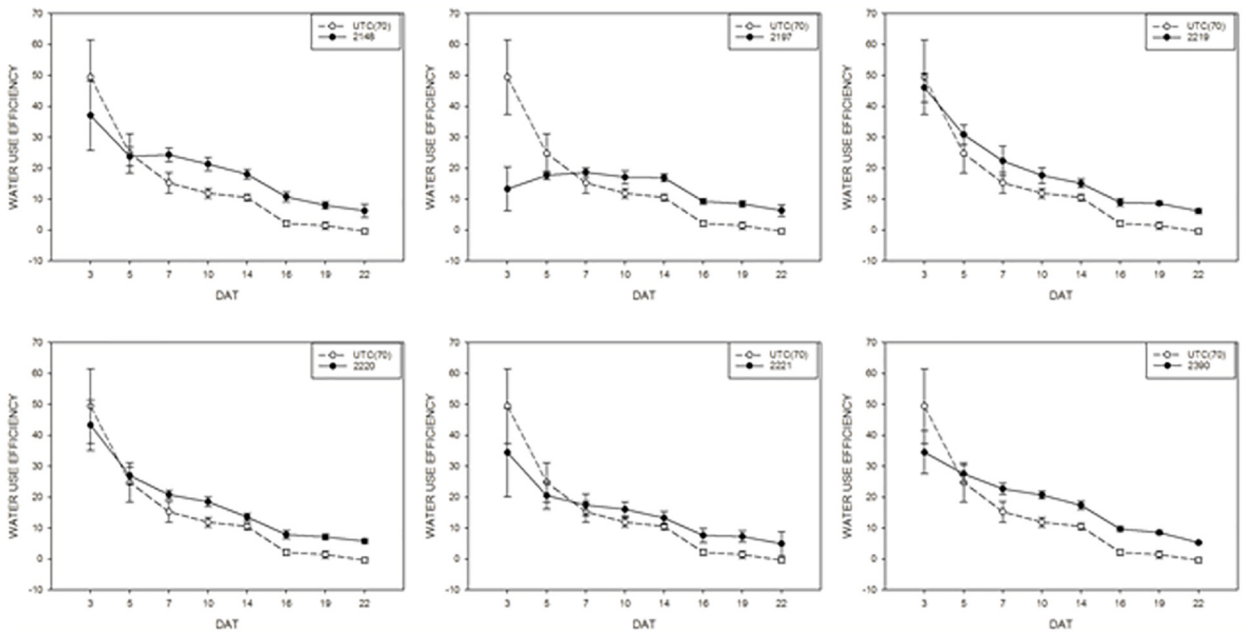

FIGURE 7 | Water use efficiency mean values of tomato plants exposed to different watering conditions: UTC(70) refers to the Untreated Control thesis where plants were irrigated with 70% FC, indicated with a dashed line. Tomato plants under reduced water condition (70% FC) and treated with the biostimulant prototypes are indicated with the solid line.

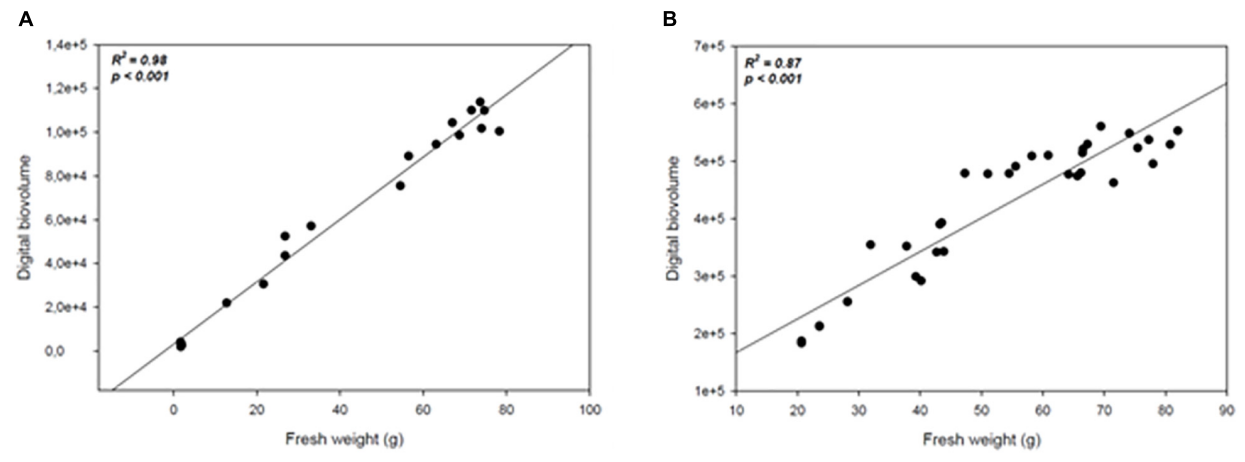

FIGURE 8 | Scatter plots of the automated (digital biovolume) and manual (fresh weight) measurements in Wheat **(A)** and Tomato **(B)**. The scatter plots and linear regressions displayed in **(A,B)** indicate a strong correlation between the estimated and the manually measured parameters in wheat and tomato plants, with correlation coefficients of 0.98 and 0.87 respectively to the plants' fresh weight.

this prototype as the best candidate for further commercial development.

Is the Imaging Based Digital Biovolume Efficient in Determining Plant Growth and Biomass?

In order to assess whether the image acquisition system provided a reliable representation of plants growth under drought conditions or upon treatment with biostimulants under reduced water availability, a measurement of plant biomass using traditional destructive methods was performed for both crops: at 147 DAS for wheat, and every 4 days throughout the experiment for tomato. The manually measured fresh weight was compared with the automated DB value previously acquired at the same time point. A high positive correlation (R^2 = 0.98; $P < 0.0001$; R^2 = 0.87; $P < 0.0001$) was recorded between the automated DB and the manual fresh weight in both wheat and tomato plants (**Figures 8A,B**). Our results are in agreement with previous reports (Poiré et al., 2014) thus validating the

DB as an effective plant biomass predictive tool. It could be used in germplasm selection aimed at pre-breeding and breeding programs or in evaluating the effect of agricultural practices on plant growth.

Taken all together these results support the efficacy of the DB as a strong phenomic indicator of the overall health status of the plant following limiting growth conditions in both crops. The characteristic of being non-destructive, scalable and applicable to many crops plants enrich its applicability for both basic and applied research.

DISCUSSION

Recently the concept of Climate-smart agriculture (CSA) was proposed to increase the sustainability of agricultural systems, by reorienting the agricultural development to face the treats of climate change (Lipper et al., 2014). CSA aims at effectively supporting development and ensuring food security, particularly in those areas where climate change strikes, by achieving three main objectives: increasing sustainable agricultural productivity; adapting and building resilience to climate change; and adopting techniques that reduce greenhouse gas emissions (Food and Agriculture Organization [FAO], 2017). Most of the impacts of climate change on agricultural systems are expected to result from changes in the water cycle impacting on both rainfed and irrigated crops as a consequence of: increased evapotranspiration, changes in the amount and regime of rainfall, and variations in water availability from both surface and ground sources. Our paper focused on Mediterranean agriculture and two key crops of this region characterized by different water management: durum wheat, a rainfed crop that represents the principal food grain of the Mediterranean, and tomato, an irrigated crop being a key element of the Mediterranean diet and a cash crop of the area.

Two different climate smart strategies for the two crops have been identified: digging into the vast genetic pool of durum wheat in order to identify resilience traits for the next generation of varieties, and identifying agricultural practices aimed at improving the utilization of irrigation water in tomato.

To tackle these strategies, we have explored the potential of high throughput phenotyping technologies. Until recent, phenotyping has been hampered by the huge amount of human work needed to collect enough data. The recent introduction of high throughput phenotyping facilities has brought to researchers, breeders, and agriculturalist a bunch of new techniques to collect a paramount mass of data in a continuous, non-invasive, non-destructive way. The aim of this paper was to verify the possibility of utilizing a high throughput phenotyping infrastructure, located in Metaponto (Matera, Italy), to contribute to maintain food security notwithstanding the effects of climate change in the Mediterranean area.

We have used high resolution RGB images, taken in three projections by the platform, and elaborated through proper algorithms, in order to evaluate two parameters considered related to resilience to DS: DB and WUE. Both these parameters have been based on data recorded in a non-destructive manner, which allows to examine one and the same plant over the time.

The information on plants phenotype collected by RGB cameras provide a huge amount of high quality data, thanks to the high resolution of these images. The use of an RGB high quality camera has some advantages over multi- or hyper-spectral sensors. In fact, if on the one side vegetation indices formulated using RGB images have a more limited spectral range and color resolution (only broad bands within the visible region) with respect to the equivalent indices formulated by spectral sensors, on the other side RGB images have generally a much higher spatial resolution than spectral imagers. In this kind of analyses, high spectral resolution can be worthwhile substituted by high spatial resolution with equal or even better results (Araus and Kefauver, 2018).

In the present study we have exploit a digital biomass index as predictive of physical measurement of the plant biomass. The latter method, the traditional one, is based on weighing the cut plant and recording its fresh weight. This is a destructive method. High Throughput Phenotyping, on the contrary, is based on non-destructive methods since they allow the analysis of a single and the same plant over time, thus reducing the possible bias introduced by small individual variation. Moreover, this timescale phenotyping approach can even be used to unveil genetic traits that could not be otherwise analyzed using traditional methods (Busemeyer et al., 2013).

Water use efficiency based on an automatable process expressing the amount of water used by the plant from that evaporated from the soil was also evaluated. The effective measure of WUE is based on isotopic discrimination of Carbon (Seibt et al., 2008) which is a complicated and time consuming process. In this paper we use a digital extrapolated WUE with the idea that this is a parameter able to provide indication on drought resilience. In the Mediterranean region rainfed agriculture is facing unpredictable seasonal rainfall. Under these conditions the ability to use at best the soil moisture is a crucial component of drought resistance (Blum, 2005).

Further statistical analyses, such as regression analysis, support the efficacy of high throughput phenotyping in monitoring plants WUE, and highlight how DB can be used as an index to perform quality testing on the efficacy of biostimulant formulations in improving plant performance under reduced irrigation regimes. The latter observation is in line with the view of the European Biostimulant Industry Council (EBIC, 2018), that promotes the use of plant biostimulants to foster plant growth and development throughout the crop life cycle in a number of demonstrated ways, including the improvements of WUE (EBIC, 2018).

The development of effective HTP platforms, especially open field HTP facilities, is a bottleneck for future breeding progress (Araus and Cairns, 2014). The test of analytical approaches under controlled conditions is essential to devise and implement technologies to be transferred to the field.

So far, HTP platforms employ a variety of imaging methodologies to collect data for quantitative studies of complex traits related to growth, yield and adaptation to biotic or abiotic stress (Li et al., 2014). Conventional digital RGB cameras have been widely used in plant phenotyping platforms since allowing a wide range of phenotyping applications

(Araus and Kefauver, 2018). One of the main advantages is the wide versatility of the data (information) collected by RGB cameras, which is essentially linked to the high resolution of these images and the general high quality of factory color calibration. RGB devices have excellent spatial and temporal resolution; they can produce a very large number of images in very short periods, they are portable, and there are many software tools to perform image processing (Perez-Sanz et al., 2017). Although, limitations in RGB-derived information may arise in standardizing the light conditions, the potential impact of light conditions is not necessarily an overwhelming problem because it is often less relevant than expected (e.g., for wheat and barley assessed under Mediterranean conditions; Araus and Kefauver, 2018).

Our work proves that the use of RGB images for the detection of the DB is an effective tool for evaluating the resilience of durum wheat plants to chronic water stress or the effect of biostimulants in supporting tomato plants under water shortage, thus supporting the application of RGB not only for canopy measurements but also for the evaluation of more complex traits. Since this is a parameter easily recordable using RGB images it is possible to implement this instrument in simple field phenotyping platforms or even in UAVs fitted with high quality cameras, provided that solutions for high quality color calibration tools are implemented in an environment with often erratic light quality (Andrade-Sanchez et al., 2014).

Our approach performed under a controlled environment and using a HTP platform has proven to be an excellent approach to select durum wheat genotypes for resilience to water stress.

By using this approach, we have succeeded in identifying a number of genotypes within the landraces collection with potentially increased reliance to DS. Exotic germplasm such as landraces and wild relatives possess high levels of genetic diversity for valuable traits, including adaptation to stressful environments (Wang et al., 2017) traditionally grown and used in the centers of origin and domestication located for durum wheat around the Fertile crescent, and centers of diversification in N. Africa and in the highlands of Ethiopia characterized by challenging environment and water availability (Janni et al., 2018). Finally, our phenomic investigation on tomato plants revealed the ability of different biostimulant prototypes to increase DB and WUE.

This is in accordance with the documented ability of biostimulants to modify physiological processes in plants in a way that provides potential benefits to growth, development or stress response is widely recognised (du Jardin, 2015; Lucini et al., 2015; Povero et al., 2016).

The positive effects of biostimulants on tomato growth, yield and quality have been also considered resulting in a high stability of yields under reduced fertilizers application and upon drought treatment (Petrozza et al., 2014; Koleška et al., 2017), moreover several effects have been proposed (du Jardin, 2015). However, in case of low water regimes the main action feature of biostimulants resides in their high content of aminoacid (Koleška et al., 2017). Furthermore, a strong modification in the gene expression profile and correlated with increased drought adaptation have been demonstrated (Petrozza et al., 2014).

This approach allowed for the selection of 2148 as the most effective prototype, that can be proposed as a new solution able to modulate plant physiology so that plants require less water per unit of yield, and induce optimal plant response under reduced water availability. Such biostimulant-based approach can be adopted to reduce unproductive water losses and maintain healthy, vigorously growing crops for both irrigated and rainfed cropping systems. This should be associated with the choice of well-adapted crop types, together with the optimized management of water, nutrient and agronomic practices. Effective biostimulants like the ones investigated in this study would also allow to reduce the use of irrigation especially in hot, dry environments, where irrigation is most wasteful, in that it produces the least yield per unit of water, as a result of high evaporation rates.

This work provides new evidence in the suitability of RGB images as tool for assessing the WUE for genotype selection as well as and the effects of new biostimulant formulations in limiting environment condition in controlled environment, open also new perspective for its application also in field conditions. The results obtained in our work can be easily exploited in different cultivation systems and transferred to several crops outside the Mediterranean area. The phenomic approach and the proxies identified for physiological response to drought tolerance and biostimulant application to improve water use in crops, can be widely adopted and are of global interest for agriculture sustainability.

AUTHOR CONTRIBUTIONS

MJ and DP drafted the manuscript. DD and NB carried out the experiments of growth, treatments and phenotyping activities, and contribute to the data analyses. SS and AP carried out the image analyses and performed the data analyses and interpretations. DDP provided technical assistance. FC, GP, and AS edited the manuscript. MJ and DP coordinated the wheat experiments. GP planned the biostimulants experiments. AS realized the biostimulants formulations. All authors have read and approved the final manuscript.

FUNDING

The authors acknowledge the RGV FAO DM 10271 program for financially supporting part of the research described here. The research conducted on tomato plants was funded by Valagro SpA, which provided biostimulant prototypes that were blindly identified by a numbered code to avoid any conflict of interest in the data production. The prototypes were named only at the end of the experiments.

SUPPLEMENTARY MATERIAL

The Supplementary Material for this article can be found online at: https://www.frontiersin.org/articles/10.3389/fpls.2019.00015/full#supplementary-material

REFERENCES

Andrade-Sanchez, P., Gore, M. A., Heun, J. T., Thorp, K. R., Carmo-Silva, A. E., French, A. N., et al. (2014). Development and evaluation of a field-based high-throughput phenotyping platform. *Funct. Plant Biol.* 41, 68–79. doi: 10.1071/FP13126

Aprile, A., Havlickova, L., Panna, R., Marè, C., Borrelli, G. M., Marone, D., et al. (2013). Different stress responsive strategies to drought and heat in two durum wheat cultivars with contrasting water use efficiency. *BMC Genomics* 14:821. doi: 10.1186/1471-2164-14-821

Araus, J. L., and Cairns, J. E. (2014). Field high-throughput phenotyping: the new crop breeding frontier. *Trends Plant Sci.* 19, 52–61. doi: 10.1016/j.tplants.2013.09.008

Araus, J. L., and Kefauver, S. C. (2018). Breeding to adapt agriculture to climate change: affordable phenotyping solutions. *Curr. Opin. Plant Biol.* 45(Pt B), 237–247. doi: 10.1016/j.pbi.2018.05.003

Berger, B., Parent, B., and Tester, M. (2010). High-throughput shoot imaging to study drought responses. *J. Exp. Bot.* 61, 3519–3528. doi: 10.1093/jxb/erq201

Blum, A. (2005). Drought resistance, water-use efficiency, and yield potential—are they compatible, dissonant, or mutually exclusive? *Aust. J. Agric. Res.* 56, 1159–1168. doi: 10.1071/AR05069

Busemeyer, L., Ruckelshausen, A., Möller, K., Melchinger, A. E., Alheit, K. V., Maurer, H. P., et al. (2013). Precision phenotyping of biomass accumulation in triticale reveals temporal genetic patterns of regulation. *Sci. Rep.* 3:2442. doi: 10.1038/srep02442

Chen, D., Neumann, K., Friedel, S., Kilian, B., Chen, M., Altmann, T., et al. (2014). Dissecting the phenotypic components of crop plant growth and drought responses based on high-throughput image analysis. *Plant Cell* 26, 4636–4655. doi: 10.1105/tpc.114.129601

Colla, G., and Rouphael, Y. (2015). Biostimulants in horticulture. *Sci. Hortic.* 196, 1–2. doi: 10.1016/j.scienta.2015.10.044

Comastri, A., Janni, M., Simmonds, J., Uauy, C., Pignone, D., Nguyen, H. T., et al. (2018). Heat in wheat: exploit reverse genetic techniques to discover new alleles within the *Triticum durum* sHsp26 family. *Front. Plant Sci.* 9:1337. doi: 10.3389/fpls.2018.01337

du Jardin, P. (2015). Plant biostimulants: definition, concept, main categories and regulation. *Sci. Hortic.* 196, 3–14. doi: 10.1016/j.scienta.2015.09.021

Eberius, M., and Lima-Guerra, J. (2009). High-throughput plant phenotyping – data acquisition, transformation, and analysis. *Bioinformatics* 7, 259–278. doi: 10.1007/978-0-387-92738-1_13

EBIC (2018). *Promoting the Biostimulant Industry and the Role of Plant Biostimulants in Making Agriculture More Sustainable*. Available at: http://www.biostimulants.eu/

Elbehri, A. (2015). *Climate Change and Food Systems: Global Assessments and Implications for Food Security and Trade*. Available at: http://www.fao.org/3/a-i4332e/index.html [accessed February 6, 2018].

Ertani, A., Pizzeghello, D., Francioso, O., Sambo, P., Sanchez-Cortes, S., and Nardi, S. (2014). *Capsicum chinensis* L. growth and nutraceutical properties are enhanced by biostimulants in a long-term period: chemical and metabolomic approaches. *Front. Plant Sci.* 5:375. doi: 10.3389/fpls.2014.00375

Ertani, A., Schiavon, M., Muscolo, A., and Nardi, S. (2013). Alfalfa plant-derived biostimulant stimulate short-term growth of salt stressed *Zea mays* L. plants. *Plant Soil* 364, 145–158. doi: 10.1007/s11104-012-1335-z

Fahlgren, N., Gehan, M. A., and Baxter, I. (2015). Lights, camera, action: high-throughput plant phenotyping is ready for a close-up. *Curr. Opin. Plant Biol.* 24, 93–99. doi: 10.1016/j.pbi.2015.02.006

Farooq, M., Hussain, M., Wahid, A., and Siddique, K. H. M. (2012). "Drought stress in plants: an overview," in *Plant Responses to Drought Stress*, ed. R. Aroca (Berlin: Springer), 1–33. doi: 10.1007/978-3-642-32653-0_1

Food and Agriculture Organization [FAO] (2017). *Climate-Smart Agriculture Sourcebook Summary*, 2nd Edn. Rome: Food and Agriculture Organization of the United Nations.

Jangid, K. K., and Dwivedi, P. (2016). Physiological responses of drought stress in tomato: a review. *Int. J. Agric. Environ. Biotechnol.* 9, 53–61. doi: 10.5958/2230-732X.2016.00009.7

Janni, M., Cadonici, S., Bonas, U., Grasso, A., Dahab, A. A. D., Visioli, G., et al. (2018). Gene-ecology of durum wheat HMW glutenin reflects their diffusion from the center of origin. *Sci. Rep.* 8:16929. doi: 10.1038/s41598-018-35251-4

Koleška, I., Hasanagić, D., Todorović, V., Murtić, S., Klokić, I., Parađiković, N., et al. (2017). Biostimulant prevents yield loss and reduces oxidative damage in tomato plants grown on reduced NPK nutrition. *J. Plant Interact.* 12, 209–218. doi: 10.1080/17429145.2017.1319503

Li, L., Zhang, Q., and Huang, D. (2014). A review of imaging techniques for plant phenotyping. *Sensors* 14, 20078–20111. doi: 10.3390/s141120078

Lipper, L., Thornton, P., Campbell, B. M., Baedeker, T., Braimoh, A., Bwalya, M., et al. (2014). Climate-smart agriculture for food security. *Nat. Clim. Change* 4, 1068–1072. doi: 10.1038/nclimate2437

Lopes, M. S., El-Basyoni, I., Baenziger, P. S., Singh, S., Royo, C., Ozbek, K., et al. (2015). Exploiting genetic diversity from landraces in wheat breeding for adaptation to climate change. *J. Exp. Bot.* 66, 3477–3486. doi: 10.1093/jxb/erv122

Lucini, L., Rouphael, Y., Cardarelli, M., Canaguier, R., Kumar, P., and Colla, G. (2015). The effect of a plant-derived biostimulant on metabolic profiling and crop performance of lettuce grown under saline conditions. *Sci. Hortic.* 182, 124–133. doi: 10.1016/j.scienta.2014.11.022

Mendiburu, F. D. (2016). *agricolae: Statistical Procedures for Agricultural Research. R package version 1.2-4*. Available at: http://CRAN.R-project.org/package=agricolae

Pandey, P. (2017). *High Throughput Phenotyping of Sorghum for the Study of Growth Rate, Water Use Efficiency, and Chemical Composition*. Available at: http://digitalcommons.unl.edu/biosysengdiss/74

Perez-Sanz, F., Navarro, P. J., and Egea-Cortines, M. (2017). Plant phenomics: an overview of image acquisition technologies and image data analysis algorithms. *Gigascience* 6, 1–18. doi: 10.1093/gigascience/gix092

Petrozza, A., Santaniello, A., Summerer, S., Di Tommaso, G., Di Tommaso, D., Paparelli, E., et al. (2014). Physiological responses to Megafol® treatments in tomato plants under drought stress: a phenomic and molecular approach. *Sci. Hortic.* 174, 185–192. doi: 10.1016/j.scienta.2014.05.023

Pieruschka, R., and Poorter, H. (2012). Phenotyping plants: genes, phenes and machines. *Funct. Plant Biol.* 39:813. doi: 10.1071/FPv39n11_IN

Pignone, D., De Paola, D., Rapanà, N., and Janni, M. (2015). Single seed descent: a tool to exploit durum wheat (*Triticum durum* Desf.) genetic resources. *Genet. Resour. Crop Evol.* 62, 1029–1035. doi: 10.1007/s10722-014-0206-2

Pignone, D., and Hammer, K. (2013). "Conservation, evaluation, and utilization of biodiversity," in *Genomics and Breeding for Climate-Resilient Crops: Concepts and Strategies*, Vol. 1, ed. C. Kole (Berlin: Springer), 9–26. doi: 10.1007/978-3-642-37045-8_2

Poiré, R., Chochois, V., Sirault, X. R. R., Vogel, J. P., Watt, M., and Furbank, R. T. (2014). Digital imaging approaches for phenotyping whole plant nitrogen and phosphorus response in *Brachypodium distachyon*. *J. Integr. Plant Biol.* 56, 781–796. doi: 10.1111/jipb.12198

Povero, G., Mejia, J. F., Di Tommaso, D., Piaggesi, A., and Warrior, P. (2016). A systematic approach to discover and characterize natural plant biostimulants. *Front. Plant Sci.* 7:435. doi: 10.3389/fpls.2016.00435

Reynolds, M. P., Quilligan, E., Aggarwal, P. K., Bansal, K. C., Cavalieri, A. J., Chapman, S. C., et al. (2016). An integrated approach to maintaining cereal productivity under climate change. *Glob. Food Secur.* 8, 9–18. doi: 10.1016/j.gfs.2016.02.002

Richards, R. A. (1991). Crop improvement for temperate Australia: future opportunities. *Field Crops Res.* 26, 141–169. doi: 10.1016/0378-4290(91)90033-R

Rouphael, Y., Spíchal, L., Panzarová, K., Casa, R., and Colla, G. (2018). High-throughput plant phenotyping for developing novel biostimulants: from lab to field or from field to lab? *Front. Plant Sci.* 9:1197. doi: 10.3389/fpls.2018.01197

Seibt, U., Rajabi, A., Griffiths, H., and Berry, J. A. (2008). Carbon isotopes and water use efficiency: sense and sensitivity. *Oecologia* 155, 441–454. doi: 10.1007/s00442-007-0932-7

Singh, A., Ganapathysubramanian, B., Singh, A. K., and Sarkar, S. (2016). Machine learning for high-throughput stress phenotyping in plants. *Trends Plant Sci.* 21, 110–124. doi: 10.1016/j.tplants.2015.10.015

Steduto, P., Faurès, J.-M., Hoogeveen, J., Winpenny, J. T., and Burke, J. J. (eds). (2012). *Coping with Water Scarcity: an Action Framework for Agriculture and Food Security*. Rome: Food and Agriculture Organization of the United Nations.

Tardieu, F., Cabrera-Bosquet, L., Pridmore, T., and Bennett, M. (2017). Plant phenomics, from sensors to knowledge. *Curr. Biol.* 27, R770–R783. doi: 10.1016/j.cub.2017.05.055

Ubbens, J. R., and Stavness, I. (2017). Deep plant phenomics: a deep learning platform for complex plant phenotyping tasks. *Front. Plant Sci.* 8:1190. doi: 10.3389/fpls.2017.01190

Wang, C., Hu, S., Gardner, C., and Lübberstedt, T. (2017). Emerging avenues for utilization of exotic germplasm. *Trends Plant Sci.* 22, 624–637. doi: 10.1016/j.tplants.2017.04.002

Wickham, H. (2009). *ggplot2: Elegant Graphics for Data Analysis*. New York, NY: Springer-Verlag. doi: 10.1007/978-0-387-98141-3

Conflict of Interest Statement: The authors declare that the research was conducted in the absence of any commercial or financial relationships that could be construed as a potential conflict of interest.

frontiers in Plant Science

CORRECTION
published: 31 May 2019
doi: 10.3389/fpls.2019.00737

Corrigendum: Can High Throughput Phenotyping Help Food Security in the Mediterranean Area?

Donatella Danzi[1†], Nunzio Briglia[2†], Angelo Petrozza[3], Stephan Summerer[3], Giovanni Povero[4], Alberto Stivaletta[4], Francesco Cellini[3], Domenico Pignone[1,5], Domenico De Paola[1] and Michela Janni[1,6]*

[1] Institute of Biosciences and Bioresources, National Research Council, Bari, Italy, [2] Dipartimento delle Culture Europee e del Mediterraneo: Architettura, Ambiente, Patrimoni Culturali, Università degli Studi della Basilicata, Matera, Italy, [3] ALSIA Centro Ricerche Metapontum Agrobios, Metaponto, Italy, [4] Valagro SpA, Atessa, Italy, [5] Institute for Veterinary and AgriFood Bioethics, Fiumicino, Italy, [6] Institute of Materials for Electronics and Magnetism, National Research Council, Parma, Italy

Keywords: high throughput phenotyping, digital biovolume, water use efficiency, biostimulants, genetic resources, durum wheat, tomato

OPEN ACCESS

Approved by:
Frontiers Editorial Office, Frontiers Media SA, Switzerland

***Correspondence:**
Michela Janni
michela.janni@ibbr.cnr.it

†These authors have contributed equally to this work

Specialty section:
This article was submitted to Plant Physiology, a section of the journal Frontiers in Plant Science

Received: *13 May 2019*
Accepted: *16 May 2019*
Published: *31 May 2019*

Citation:
Danzi D, Briglia N, Petrozza A, Summerer S, Povero G, Stivaletta A, Cellini F, Pignone D, De Paola D and Janni M (2019) Corrigendum: Can High Throughput Phenotyping Help Food Security in the Mediterranean Area? Front. Plant Sci. 10:737. doi: 10.3389/fpls.2019.00737

A Corrigendum on

Can High Throughput Phenotyping Help Food Security in the Mediterranean Area?
by Danzi, D., Briglia, N., Petrozza, A., Summerer, S., Povero, G., Stivaletta, A., et al. (2019) Front. Plant Sci. 10:15. doi: 10.3389/fpls.2019.00015

In the original article, the reference for the "European Biostimulant Industry Council" was incorrectly written as "(Electron-Beam-Induced Current [EBIC, 2018])". It should be "(EBIC, 2018)."

The authors apologize for this error and state that this does not change the scientific conclusions of the article in any way. The original article has been updated.

REFERENCES

EBIC (2018). *Promoting the Biostimulant Industry and the Role of Plant Biostimulants in Making Agriculture More Sustainable*. Available online at: http://www.biostimulants.eu/

frontiers in Plant Science

ORIGINAL RESEARCH
published: 12 November 2018
doi: 10.3389/fpls.2018.01540

Whole-Plant Water Use in Field Grown Grapevine: Seasonal and Environmental Effects on Water and Carbon Balance

*Cyril Douthe[1], Hipólito Medrano[1], Ignacio Tortosa[1], Jose Mariano Escalona[1], Esther Hernández-Montes[2†] and Alicia Pou[2]**

[1] Research Group on Plant Biology Under Mediterranean Conditions, INAGEA, Department of Biology, University of the Balearic Islands, Palma, Spain, [2] Instituto de Ciencias de la Vid y del Vino, Logroño, Spain

OPEN ACCESS

Edited by:
Manoj Menon,
University of Sheffield,
United Kingdom

Reviewed by:
Claudio Lovisolo,
Università degli Studi di Torino, Italy
Walter Chitarra,
Consiglio per la Ricerca in Agricoltura e l'Analisi dell'Economia Agraria (CREA), Italy

***Correspondence:**
Alicia Pou
alicia.pou.81@gmail.com

†Present address:
Esther Hernández-Montes,
Department of Horticulture and Landscape Architecture, Irrigated Agriculture Research and Extension Center, Washington State University, Prosser, WA, United States

Specialty section:
This article was submitted to Plant Physiology, a section of the journal Frontiers in Plant Science

Received: 14 August 2018
Accepted: 02 October 2018
Published: 12 November 2018

Citation:
Douthe C, Medrano H, Tortosa I, Escalona JM, Hernández-Montes E and Pou A (2018) Whole-Plant Water Use in Field Grown Grapevine: Seasonal and Environmental Effects on Water and Carbon Balance. Front. Plant Sci. 9:1540. doi: 10.3389/fpls.2018.01540

Water scarcity is a main challenge in vineyards sustainability in most of the grapevine areas now and even more in near future due to climatic change perspectives. In consequence, water use efficiency (WUE) measurements are of the highest interest to improve the sustainability of this crop. The vast majority of WUE measurements relays on measurements of leaf carbon and water fluxes at leaf-level. However, less data are available at the whole-plant level, and for the moment those data are not totally coincident with conclusions reached at leaf scale. In this study, we used whole-plant chambers able to enclose an entire plant of 12 years old to measure at the same time water and carbon fluxes under realistic field grown conditions. The main objectives were to identify the technical issues interfering the whole-plant measurements and track the environmental and other abiotic factors that can affect water and carbon balance, i.e., WUE at the whole-plant scale. To achieve those objectives, we measured whole-plant water and carbon fluxes in grapevine exposed to two different water regimes at three phenological stages [pea size (July), ripening (August), and harvest (September)]. In September, measurements were repeated under high CO_2 to also check its effect at the whole-plant scale. The results indicate that water and carbon fluxes are well coordinated under both water availability treatments. Under drought conditions, both fluxes were drastically reduced, but surprisingly the estimated WUE resulted not improved but decreased, contrarily to what is shown at the leaf scale. The phenology (September) also strongly decreased both water and carbon fluxes when compared to measurements in July. We hypostatized that harvest load respiration rates could have an important weight on the whole-plant net carbon exchange (NCE). Finally, high CO_2 measurements, after correction for leaks, indicated an increase of whole-plant NCE as well as increased whole-plant WUE, as expected. Several technical issues were identified, like 1/instability of [CO_2] during the night period that prevent robust estimation of whole-plant respiration and 2/condensation during last night and sun-rise hours which may affect the estimation of daily plant transpiration.

Keywords: grapevine, water use efficiency, whole plant chambers, water stress, carbon balance

INTRODUCTION

Water use efficiency (WUE) refers to the ratio of water used in plant carbon assimilation (photosynthesis; A_N) or in biomass production to water lost by the plant through transpiration (E) and it has become an important parameter to take into account in agricultural systems to increase yield production in semi-arid areas to get more crop per drop. Either A_N or E are commonly recorded on single leaves by using portable infrared gas analyzers (IRGAs). However, in canopies such as grapevine and other crops, it has been shown that leaf-level photosynthesis measurements are largely dependent on leaf position (Escalona et al., 2003) so that typical single-leaf measurements can provide incomplete information if extrapolated to quantify photosynthesis at the whole-plant level. On the other hand, whole-vine photosynthesis expressed on a leaf area basis usually results below than expected extrapolating values from single-leaf measurements (Edson et al., 1993; Intrieri et al., 1997; Poni et al., 2009). Factors such as leaf light exposure and position on the shoot, leaf aging and the presence of organs like fruits, shoots, and trunks in a given canopy makes difficult to scaling up from single-leaf to whole-canopy photosynthesis (Alleweldt et al., 1982; Schultz, 1993; Intrieri et al., 1997; Poni et al., 1997; Petrie et al., 2000; Escalona et al., 2003). Moreover, other processes such as nocturnal water loss and respiration (Escalona et al., 2012, 2013) or possible changes in dry matter partitioning among different sinks (Tomàs et al., 2014) may explain a frequently reported lack of correlation between WUEi and WUE expressed as biomass accumulation per unit of water lost.

Scaling up to the whole canopy by using meteorological methods such as eddy correlation or covariance (Field et al., 1989; Long and Hällgren, 1989; Garcia et al., 1990), or by enclosing methods in open system flow-through chambers in which water vapor and CO_2 fluxes are measured using an IRGA (Garcia et al., 1990; Poni et al., 1997) has been explored as a way to achieve a reliable measurement of the whole-plant gas-exchange measurement. Moreover, it has become an interesting tool to assess whole-plant responses to climatic change conditions, e.g., high CO_2, water stress, high temperatures, etc. But on the other hand, one of scientist's current concerns is to design a good enclosure system to minimize disturbance of the plant natural environment (Intrieri et al., 1997; Poni et al., 1997; Perez Peña and Tarara, 2004), i.e., to diminish errors associated with the "chamber effect." Hence, even with a highly transparent cover, an enclosure increases air temperature and reduces incident radiation intensity in the canopy as well as gas exchange between the plant and the atmosphere (Perez Peña and Tarara, 2004) and, contrarily of what it happened when measuring WUE at the leaf-level, these studies reported that WUE at the whole-plant level was not higher on a daily basis in deficit-irrigated vines in comparison with well-watered plants, likely due to their higher respiration rates (Pagay, 2016).

On the other hand, studies about the quantification of the CO_2 flows from different organs such as stems, roots and fruits along the vine vegetative cycle and the grapevine's leaves maturity effects on the whole-plant carbon budgets are important but rather scarce. Several previous studies showed the contribution of grapevine clusters to the total carbon balance (Ollat and Gaudillère, 2000; Palliotti and Cartechini, 2001; Escalona et al., 2012; Hernández-Montes et al. unpublished data) and they reported a contribution of 10 and 18% to the carbon required for fruit development obtained by fruit photosynthesis and by the whole berry respiration, respectively. In this sense, it would be expected that a high rate of respiration during fruit ripening would greatly reduce daily net CO_2 exchange rate (NCER). Miller et al. (1997) stated a rapid decrease of the NCER rate from, through harvest, in sharp contrast to the broadleaf chamber which showed no change in A_N rate per unit leaf area over the same period. Thus, to quantify the CO_2 flows from each organ may contribute to calculate more accurately total plant carbon balances.

In this work, we have used an open framed, open-top, flow through chamber, according to Perez Peña and Tarara (2004) as has been previously reported in Escalona et al. (2016). A detailed evaluation of the daily whole-canopy NCERs and whole-canopy transpiration rates (E) have been done. Parameters such as nocturnal transpiration (E_{night}) and canopy dark respiration (R_d), were also considered to evaluate the whole-canopy WUE and to point out potential problems of integrating this data.

The goals of this study were: (i) to asses about leaks and difficulties encountered when measuring daily NCER and E to identify improvements needed for a more accurate estimation rates, (ii) measure daily whole-plant WUE for grapevines as affected by different irrigation treatments and high CO_2, and (iii) to estimate the contribution of the grapevine's leaves age and berry development to the total plant carbon balance along the vine phenology.

MATERIALS AND METHODS

Plant Material and Site of Study

Measurements were conducted in summer 2017 in an experimental vineyard planted in 2009 with Grenache vines grafted in 110-Richter rootstocks, at the University of Balearic Islands. Vines were planted with 2.5 m between rows and 1 m between vines in a N–S orientation, and were submitted to two water regimes: (i) a moderate water irrigation (I) applying a crop coefficient of 0.5 of potential evapotranspiration calculated using Penman–Monteith equation, and (ii) non-irrigation (NI) (see Escalona et al., 2016 for details). Plants were irrigated twice a week from June to September with drips delivering 2 L h^{-1} placed at 0.6 m from each other.

Measurements were carried-out in two representative plants for each phenological stage [pea size, irrigation (July); ripening, non-irrigation (August) and harvest, irrigation and high CO_2 (September)]. The corresponding meteorological data is shown in **Figure 1**. The same irrigated plants were measured in July and September, while other two non-irrigated plants were measured in August. Thus, for pure phenological effect, sessions of July

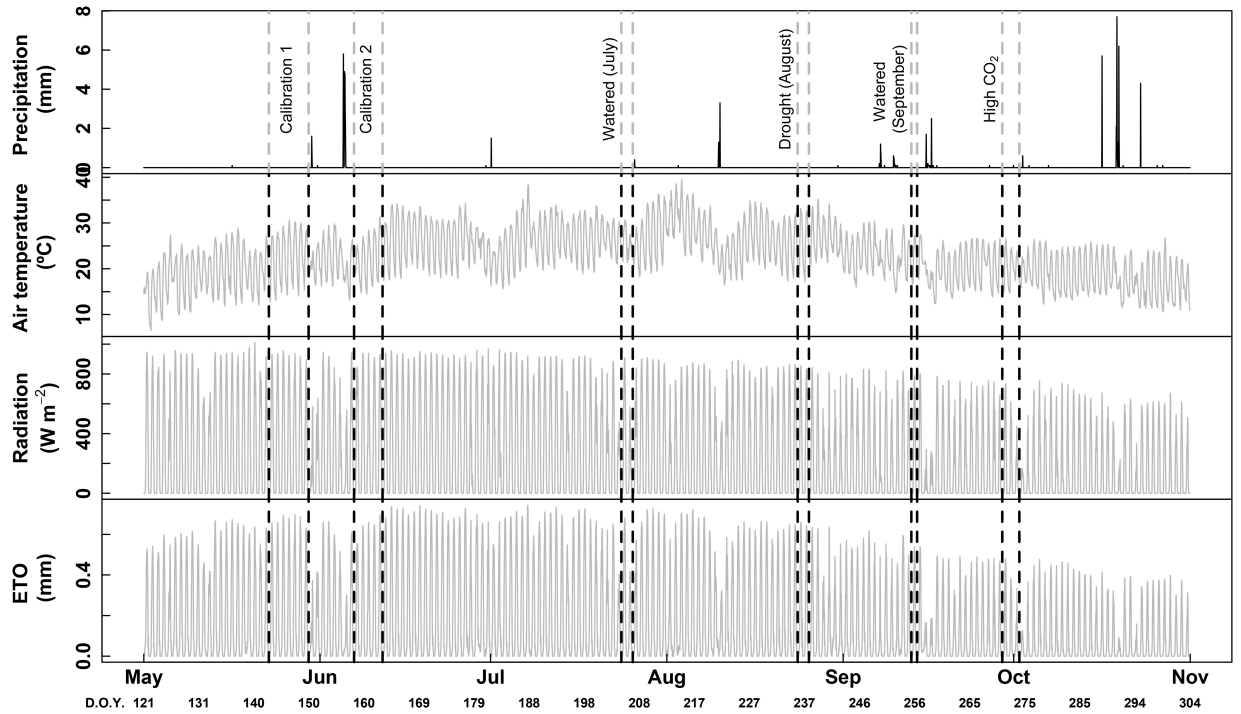

FIGURE 1 | Hourly raw data of precipitation, air temperature, radiation and ET_0 (potential evapotranspiration). Vertical dotted lines indicate dates of each session of measurements performed in this study, with the corresponding treatments. D.O.Y. for day of the year.

and September can be directly compared (same plants and both in watered conditions). For drought effects, sessions of August and September can be compared, since only 20 days separated the two measurements. For each session, plants remained inside the chambers 2 or 3 days before the measurements were taken to avoid the disturbing effect of the chamber installation. Afterward the chambers were removed and plants were grown outside the chambers until the next period of measurements (1 month between each period). Each measuring session (for each phenological stage) last two or three consecutive days. Concerning the data treatment, all data were averaged from 1 h.

Meteorological Condition During the Experiment

Weather information was recorded using an automatic meteorological station located in the experimental vineyard (Meteodata, 3000, Geonica) (see **Table 1** and **Figure 1**). Effective rainfall was <5 mm in July and August with similar mean diurnal temperatures (29.5°C) and relative humidity (46–48%), while measurements in September were performed with more rainfall (11.5 mm), lower mean diurnal temperatures (23.8°C) and higher relative humidity (67.1%).

Whole-Plant Gas Exchange Chambers

Whole-plant net carbon exchange (NCE) and transpiration were measured using two open-top chambers (3.36 m^3 each) covered with plastic film (RX 140-Propafilm^{TM}). An air flow (Series 641 Air Velocity Transmitter, Dwyer, IN, United States) through the chamber of 278 mol min^{-1} (F) was maintained for all measurements, delivered by a constant speed turbine (S & P 500) fed by a Ø = 165 mm pipe taking the atmospheric air at 3 m above ground. Air entering and leaving the chamber was pumped (TD4x2 type NA; Braislford Pumps, United States) at a flow of 0.5–1 L min^{-1} to feed a calibrated gas analyzer (Li-840, Li-Cor, Inc., Lincoln, NE, United States). The air flow entering

TABLE 1 | Average values of air temperature (T_{air}, °C), relative humidity (RH, %), wind speed (m s^{-1}), cumulative precipitations (Precip.), average radiation (Rad, W m^{-2}) and cumulative evapotranspiration (ET_0, mm) for each month of measurement and separated for day/night time.

Month	Daytime	T_{air}	RH	Wind speed	Precip.	Rad	ETO
May	Day	23.23	46.83	1.43	2.6	541.21	136.62
June	Day	27.84	45.37	1.42	13.4	567.07	152.53
July	Day	29.49	46.65	1.37	0.4	531.70	152.53
August	Day	29.73	48.17	1.22	3.5	451.41	132.26
September	Day	23.78	67.10	1.14	8.1	353.73	88.28
October	Day	21.01	79.50	0.64	20.9	266.04	61.93
May	Night	15.62	75.25	0.23	0	0	0
June	Night	20.58	70.74	0.20	15.5	0	0
July	Night	22.50	71.00	0.18	1.5	0	0
August	Night	23.27	72.38	0.26	3.6	0	0
September	Night	18.42	88.41	0.19	3.4	0	0
October	Night	15.23	98.20	0.04	15.5	0	0

and outgoing the chamber was measured during five consecutive minutes each, alternatively. The four first minutes of data were eliminated to ensure a complete turn-over of the gas in the measuring circuit. [CO_2] and [H_2O] were used to estimate plant NCE and transpiration (E) with:

$$NCE = F\,(C_e - C_o)/L_a$$

$$E = F\,(W_o - W_e)/L_a$$

where F is the air flow through the chamber, C_e and W_e the [CO_2] and [H_2O] entering the chamber, C_o and W_o the [CO_2] and [H_2O] outgoing the chamber and L_a the total leaf area of the plant. Plant leaf area was estimated in each one of the measured plants at harvest using the methodology proposed by Sánchez-de-Miguel et al. (2010).

Air temperature was measured with type K thermocouple (RoHS, Model TP-01), and placed in the top-center of the chamber. The atmospheric air temperature was recorded with a meteorological station (see above) situated at 50 m from the chambers. The difference in temperature inside/outside the chamber was comprised between 4 and 5°C, with some punctual peaks at 10°C during august. Some of these variations come from the fact that the thermocouple was directly exposed to sun (not shaded), which could increase the estimated temperature from the real one.

Validation of the Gas Exchange Measurements

We intended to confirm the reliability of the gas-exchange measurements with an external estimation of the plant transpiration. For these measurements, we placed one potted vine in each chamber (total plant leaf area around 0.5 m^2), placed on a balance (Baxtran, equipped with Giropes module L6E) to measure Transpiration by the loss of weight through 4 days. Chambers were equipped with the gas-exchange system described just above (except the 3 m chimney that was not placed for the calibration), and transpiration via gravimetry and gas-exchange were compared.

Statistical Analysis

All the data analysis was performed using R (R Core Team, 2016), Foundation for Statistical Computing, Vienna, Austria).

RESULTS

Conditions During the Study

The **Figure 1** shows the meteorological conditions all along the experiment as well as the location of each session of calibration and measurement.

Climate conditions during the experiment (May–September 2017) were typical for Mediterranean regions, with daytime temperatures above 25°C, night temperatures above 20°C and diurnal radiation frequently reaching 800 W m^{-2} (**Figure 1**). Peak photosynthetic photon flux density (PPFD) at midday was usually 1500–1700 μmol m^{-2} s^{-1} (not shown).

Comparison Between Gas-Exchange and Gravimetry

To validate the gas-exchange measurements, a potted plant on a balance was placed in each chamber. The weight of each plant was monitored continuously during 24 h for five consecutive days. The calibration procedure was carried-out two times in May and June 2017 (see **Figure 1**). The resulted correlation between both estimations of the plant transpiration for chamber 1 and chamber 2 were R^2 = 0.54 and 0.65 (both $p < 0.001$), respectively (**Figure 2**). We observed that gravimetry and gas-exchange data were sometimes noisy (irregular peaks). Such peaks were not related to plant transpiration dynamics but to 1/noise measurement form the device and 2/some possible condensation inside the plant chamber. Diurnal cycles were treated with a spline to eliminate such non-biological noise (**Figures 2C,D**). The resultant correlations were improved for both chambers (**Figure 2B**), with R^2 = 0.75 and 0.73 (both $p < 0.001$) for chamber 1 and 2, respectively. We also observed a progressive decrease of the maximum transpiration rate along the calibration session (5 days), since plants were not watered while being inside the chamber.

Technical Limitations for the Measurements

We identified some of the limits encountered when using whole-plant chambers. First, the atmospheric (entering air flow) [CO_2] was instable during the night (**Figure 3**, right). While the day [CO_2] was around 380 μmol mol^{-1} and presented very low hourly variations along the day (∼5 μmol mol^{-1}), [CO_2] used to increase up to 430 μmol mol^{-1} during the night, with 20–30 μmol mol^{-1} variation between two consecutive hours. The same variation pattern was observed for both chambers, and for each daily cycle measured during the session of September (harvest), but these variations were less pronounced than during the other two sessions. In parallel, we observed that NCE estimates during the night were very noisy; meanwhile during the day they were much more robust. We also observed that this gas-exchange system was able to pick the effect of sun-flecks on NCE. Indeed, PAR variations between 700 and 1,500 μmol photons m^{-2} s^{-1} within 30 min—1 h (punctual clouds) could induce variations of NCE between 6 and 8 μmol CO_2 m^{-2} s^{-1} (**Figure 3**, left).

The whole-plant gas-exchange system also allowed us to detect condensation at the sun-rise. This was demonstrated by negative transpiration, systematically occurring between 6 and 9 h in the morning. This phenomenon was observed either by gravimetry (**Figure 4**), and gas exchange (not shown).

Carbon and Water Balance Through Different Phenological and Environmental Conditions

Gas-exchange rate was clearly affected by phenological period of the plant, as expected. When measured in July (pea size, irrigated plants), plant NCE described a classical Gauss curve along the day

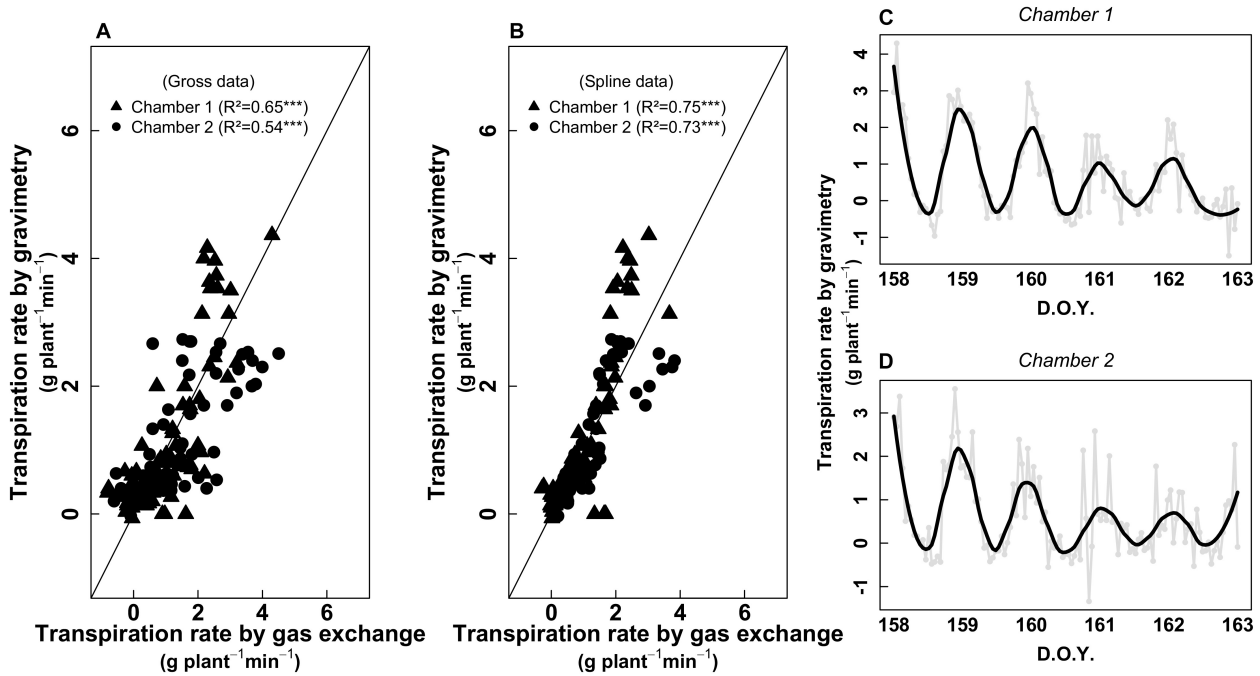

FIGURE 2 | (A) Relationship between Transpiration rate (g H_2O $plant^{-1}$ min^{-1}) estimated from gravimetry and gas exchange (whole-plant chamber). The continuous line represents the 1:1 relationship. **(B)** Same relationship but with data treated with a spline. The continuous line represents the 1:1 relationship. **(C,D)** gross data of gravimetry [gray circles and lines, same as presented in **(A)**] for chambers 1 and 2, respectively. The black lines represent the data treated with a spline in order to remove non-biological noise, as presented in **(B)**. The data in **(A,B)** come from two sampling sessions (first session: from D.O.Y. 143–150; second session: from D.O.Y. 158–163; see **Figure 1**).

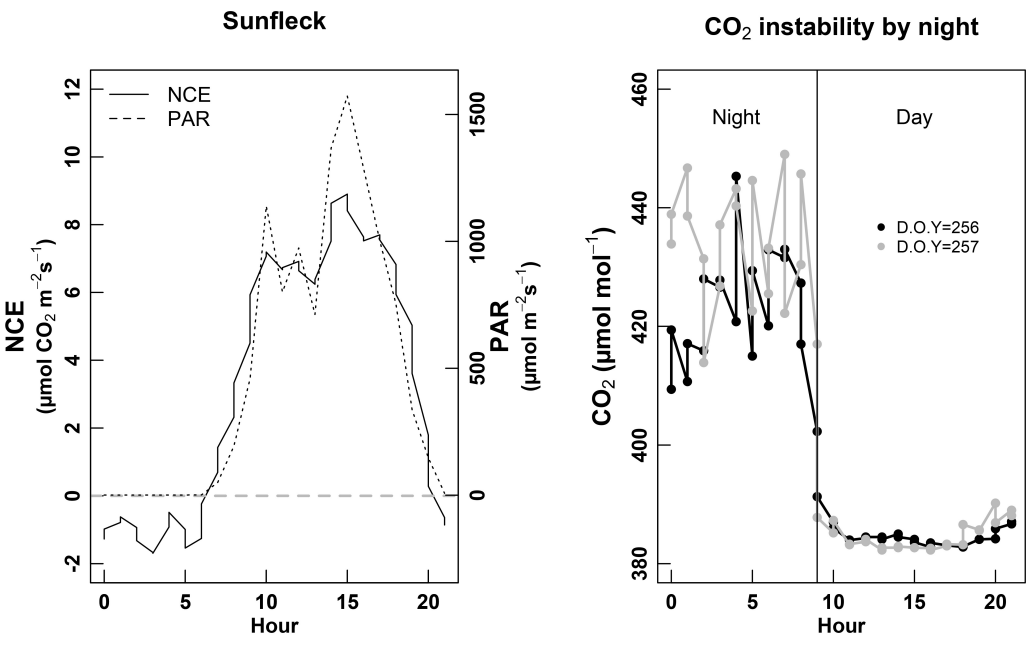

FIGURE 3 | Left panel: example of sun fleck (PAR, discontinuous line) effect on the NCE (net carbon exchange of the whole-plant, continuous line). Right panel: monitoring of the [CO_2] entering the chamber (atmospheric [CO_2]) over a complete 24 h cycle, during two consecutive days (D.O.Y. 256 black line and D.O.Y. 257 gray line). The vertical continuous black line denotes the day/night limit.

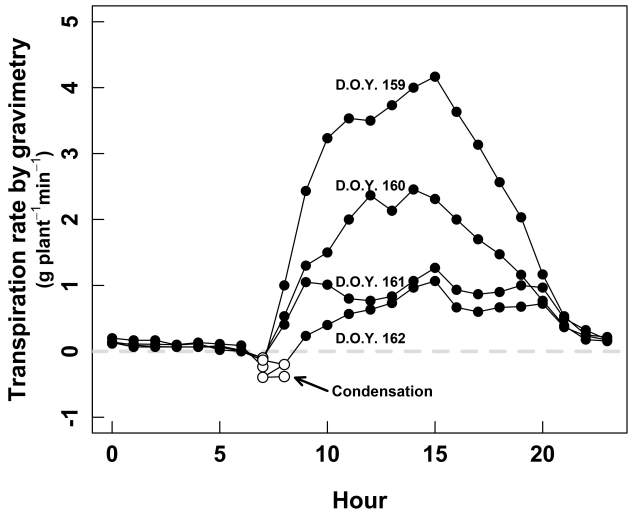

FIGURE 4 | Daily course of the whole-plant transpiration measured by gravimetry during the second calibration session (D.O.Y. 158 to D.O.Y. 162). The black dots denote positive transpiration, while the white dots denote negative transpiration, interpreted as condensation during the earlier hours of the day.

(**Figure 5**, left), with the maximum peak reached at 12 h and NCE values of 10 μmol m^{-2} s^{-1}. The whole-plant transpiration (E) described the same type of variations, with maximum values of 2.5–3 mmol H_2O m^{-2} s^{-1}, coordinately with the peak of NCE (**Figure 5**, right).

When measured during the ripening (August, non-irrigated conditions), vines described a different daily cycle, with the maximum NCE of 1–2 μmol m^{-2} s^{-1} around 8–9 h in the morning, then decreasing slowly during the day (**Figure 5**, left). E was also strongly decreased, with maximum values of 0.5 mmol m^{-2} s^{-1} around 12–13 h (**Figure 5**, right). We observed that the non-irrigation conditions in August provoked a dramatic decrease in absolute values of both NCE and E, but with a strong asymmetry along the day for NCE (taking advantage of the early morning) but not for E.

During the harvest period (irrigated conditions, before harvesting the fruits), both NCE and E described the same shape of daily cycle than under non-irrigated condition (August, i.e., with an asymmetric for NCE, not for E), with clearly lower values than for the measurements during July (irrigated conditions), but higher than in August. The night respiration was much more erratic and higher (more negative values) during the harvest (September, irrigated conditions, with higher fruits load) than during previous periods. Finally, we checked whether NCE values of our study were concordant with values previously measured by Pou et al. (2014, unpublished), using the same gas-exchange system, in watered conditions and for same grape cultivar (Grenache). Absolute values and shape of both NCE and E along the day were identical with the measurements of this previous study. The only differences were shown for night respiration, higher (more negative) for Pou et al., 2014, unpublished) than this study. No relationship was found between temperature and night NCE (not shown).

Light Intensity and Carbon and Water Balance Under Different Phenological and Environmental Conditions

The measurements performed during full daily cycles, enabled to perform a comparison of photosynthesis and transpiration dependency from incoming light. This allowed to establish light response curves of NCE and E under different phenological and environmental conditions.

During the pea-size period (July, irrigated conditions), both NCE and E described a positive relationship with the increase in light through the day. NCE followed a clearly saturating shape at high light (after ∼1,000 μmol m^{-2} s^{-1}), while E described a less saturated response (**Figure 6**, left and middle).

The NCE and E response to light showed lower values under non-irrigated conditions (August, ripening). NCE showed an asymmetric response, with maximum values reached at ∼500 μmol m^{-2} s^{-1} and with a clear decrease at highest light intensity. The E response in August was not asymmetric, with a classical saturated response to light (**Figure 6**, middle). Again, we observed that during the harvest (September, irrigated conditions), NCE and E showed the same shape of daily cycle as under non-irrigated conditions (August), but with slightly higher absolute values.

The WUE described a decreasing curvilinear tendency with increasing light, with high variations at low light, corresponding to sunrise and sunset (**Figure 6**, right). In both irrigated conditions (especially in July, with well performing plants), the WUE was higher than under non-irrigated plants (see inset in **Figure 6**, right).

Response to High CO_2 Conditions

At the end of the measurement session of September 2017 (in watered condition and pre-harvest period, see **Figure 1**), instead of removing the plants from the chambers, they were kept inside and [CO_2] entering the chamber was increased until a level of 500 μmol m^{-2} s^{-1} (**Figure 7**, left). Plants were kept 5 days in high CO_2 conditions before taking measurements. Calibration curves were also performed before analyzing the raw data (**Figure 7**, right). After this pretreatment, the whole-plant CO_2 response was studied increasing steep by steep the CO_2 concentrations inside the chamber (from 400 to 900 ppm).

Each chamber showed a different response of apparent NCE to [CO_2], likely due to different intensity of leaks (see **Figure 7**, right). Nevertheless, the total pool of NCE data showed a continuous relationship to [CO_2] when plotted against corrected-NCE (**Figure 8**, left).

Under high CO_2, the NCE along the day was clearly higher than under ambient [CO_2], measured 5–6 days before (**Figure 8**, left). While plants in ambient [CO_2] showed a strong decrease at highest PAR intensities, under high [CO_2] they maintained a high NCE (∼10 μmol m^{-2} s^{-1}) along the whole day. The chamber 2 showed slightly higher values than chamber 1, but keeping in the same range, and recovering both the values of watered condition

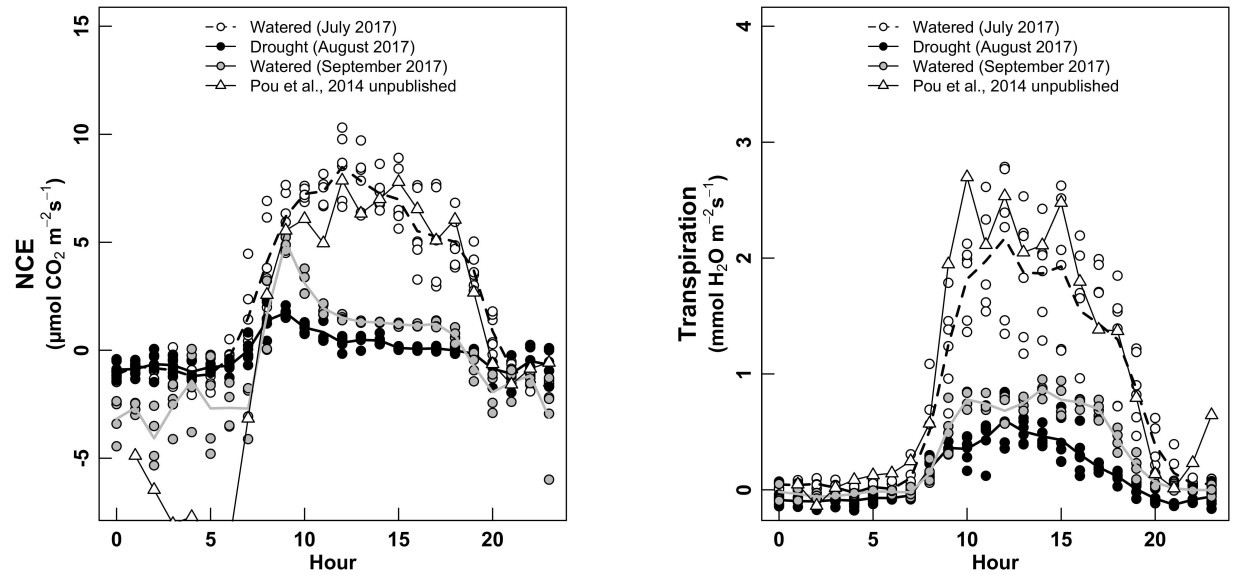

FIGURE 5 | Daily cycle of NCE—whole-plant net carbon exchange (left panel, µmol m^{-2} s^{-1}) and whole-plant Transpiration (right, mmol m^{-2} s^{-1}), for three water treatments: white dots for "Watered" (measured in July 2017); black dots for "Drought" (measured in August 2017); gray dots for "Watered" (measured in September 2017). The white triangles are measurements performed in 2015 (Pou et al., 2014, unpublished), using the same chamber and experimental set-up in watered conditions.

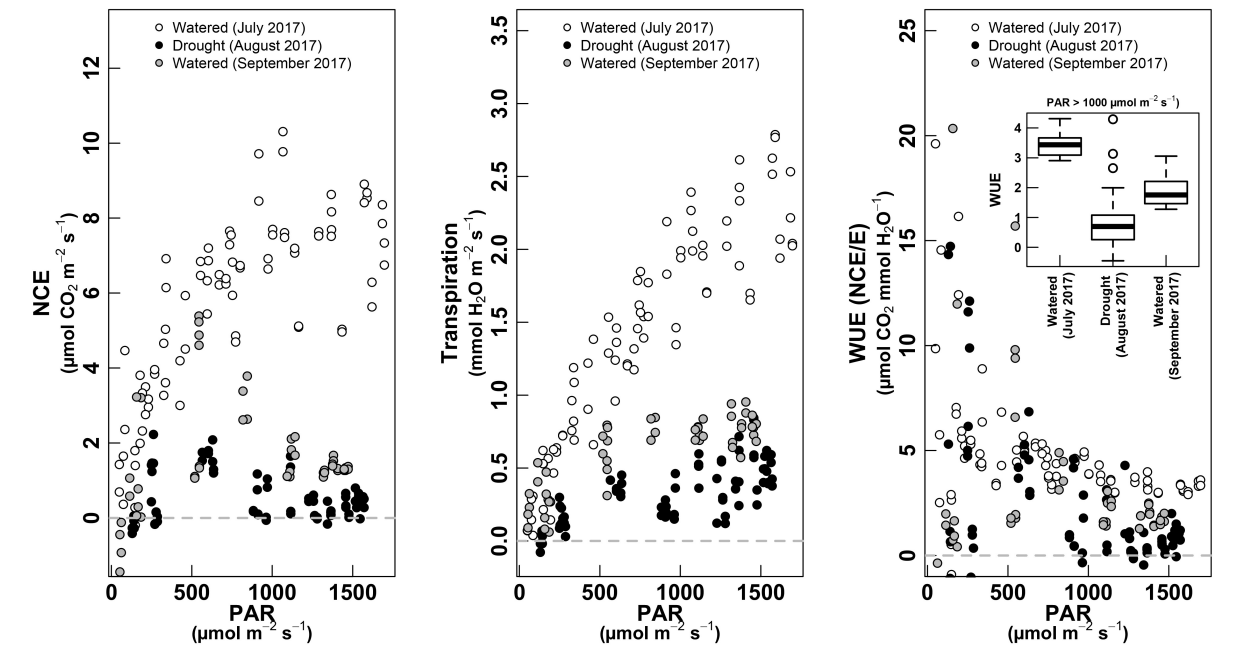

FIGURE 6 | PAR response curves for NCE—whole-plant net carbon exchange (left panel, µmol m^{-2} s^{-1}), whole-plant Transpiration (middle panel, mmol m^{-2} s^{-1}) and WUE as NCE/E (right panel, µmol CO_2 $mmol^{-1}$ H_2O). The relationship is shown for the three water treatments: white dots for "Watered" (measured in July 2017); black dots for "Drought" (measured in August 2017); gray dots for "Watered" (measured in September 2017). The boxplot inset in the right panel shows values of WUE for each treatment when PAR is >1,000 µmol m^{-2} s^{-1}. Only data with PAR >50 µmol m^{-2} s^{-1} are shown.

in July. Surprisingly, the values of transpiration increased under high CO_2 when compared to previous values of watered conditions in September, but fitted very well with *E*-values of July, in watered conditions (**Figure 6**, middle). The WUE was clearly increased under high CO_2 (**Figure 6**, middle), four by eightfold when compared to September in watered conditions, and by twofold when compared to July, watered conditions (see inset **Figure 8**, right).

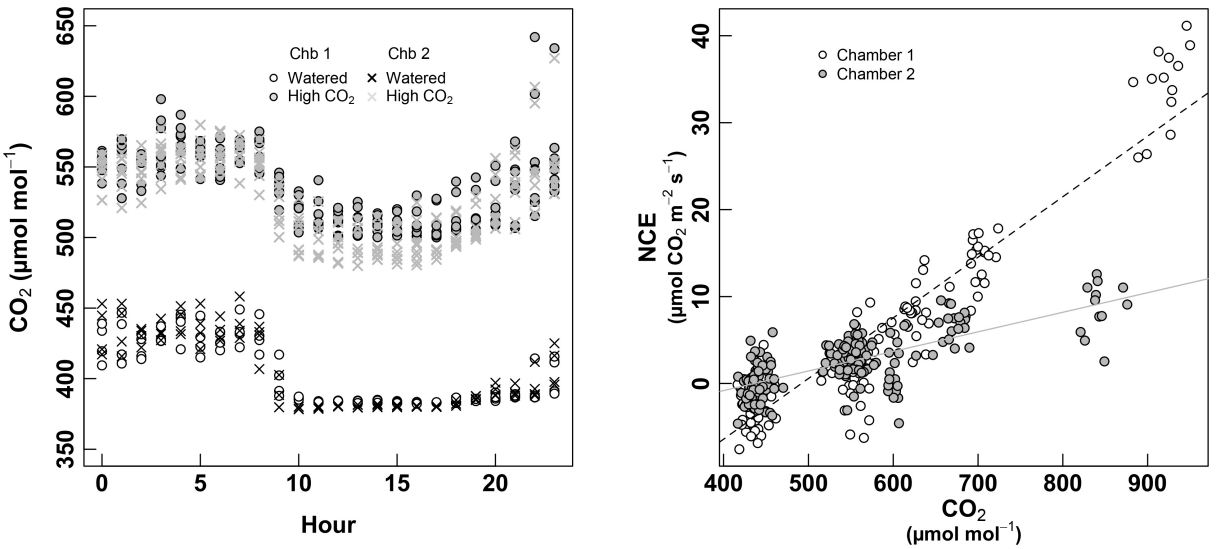

FIGURE 7 | Left panel: monitoring of the [CO_2] entering the chamber over cycles of 24 h. White dots denote the second "Watered" session (September 2017) for the chamber 1, and the black crosses for the chamber 2, both of them at ambient (atmospheric) CO_2. Gray circles and gray crosses denote the "High CO_2" treatment (September 2017) for chambers 1 and 2, respectively. Right panel: calibration curves used to correct the estimated NCE during the "High CO_2" experiment. White dots are for the chamber 1, and gray dots for the chamber 2. Measurements where carried-out during the night to avoid photosynthetic processes to influence the measurements (and considering the night-respiration as negligible), then [CO_2] was increased by steps from 400 µmol mol^{-1} to approximately 900 µmol mol^{-1} in order to obtain a calibration curve. This curve was then subtracted to the row-data obtained under high CO_2 conditions.

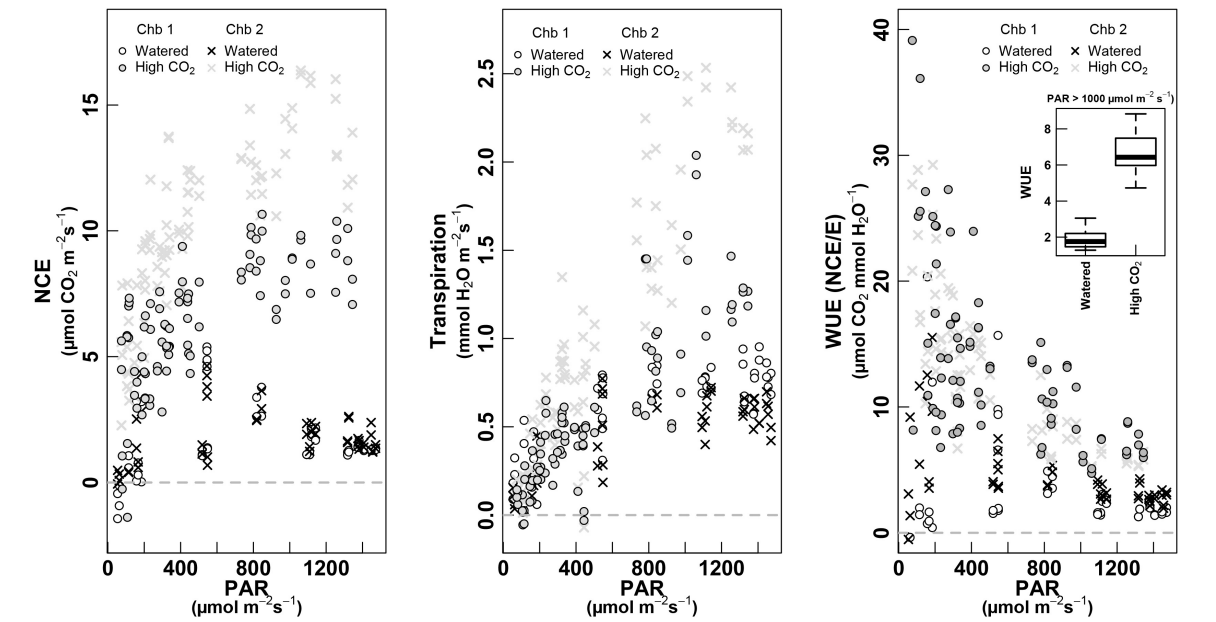

FIGURE 8 | PAR response curves for NCE—whole-plant net carbon exchange (left, µmol m^{-2} s^{-1}), whole-plant Transpiration (mmol m^{-2} s^{-1}, middle) and WUE as NCE/E (µmol CO_2 mmol^{-1} H_2O, right). The relationship is shown for the two treatments: white dots for "Watered" of chamber 1 and crosses for chamber 2; gray dots for "High CO_2" for chamber 1 and gray crosses for the chamber 2 (both treatments were measured in September 2017, on the same plant). The boxplot inset in the right panel shows values of WUE for each treatment when PAR is >1,000 µmol m^{-2} s^{-1}. Only data with PAR >50 µmol m^{-2} s^{-1} are shown.

DISCUSSION

A better understanding of Carbon and water fluxes at the whole-plant scale is needed to improve the natural ecosystems and crops water management. But this must be done firstly by improving the knowledge of the relationship between whole-plant and single-leaf gas exchange, and their occasional discrepancy when they are directly compared

(Medrano et al., 2012; Tomàs et al., 2012). In particular, when talking about WUE, the variability of leaf to leaf environmental conditions and plant gas-exchange regulation could lead to some contradictory results (Poni et al., 2009; Tarara et al., 2011; Escalona et al., 2016). To understand why intensive leaf-level measurements do not always completely reflect the whole-plant physiology, an exhaustive array of data was gathered using entire enclosed plants. To ensure reliability of the data from the whole-plant gas-exchange system, a preliminary calibration was set in order to calibrate chamber-derived transpiration rates by comparing gas exchange versus gravimetric vine water loss. The resulted correlations between both estimations of the plant transpiration were sometimes noisy and apparently not related to plant transpiration dynamics. Thus, diurnal cycles were treated with a spline to eliminate such non-biological noise leading to close linear relationships (R^2 = 0.75 and 0.73; both $p < 0.001$ in chamber 1 and 2, respectively). This resulted in a successful validation of the chamber-derived vine transpiration, in agreement with findings previously reported by Poni et al. (1999, 2014). These noisy measurements faced two large problems. The first one was probably due to the absence of the 3.5 m metal pipe during the calibration process, usually added to minimize fluctuations in ambient CO_2 (Perez Peña and Tarara, 2004), emphasizing the importance of having a proper buffer volume during measurements. The second was likely derived from a detected condensation, both by gravimetry and by gas exchange, which systematically occurred between 6 and 9 h a.m., when the temperature of the inner surface of the chamber was surely below the dew point. Maintaining a minimum temperature increase in the chamber and improving air circulation inside whole-plant chambers is therefore necessary to avoid condensation when calculating daily transpiration rates.

Moreover, tracking the whole-plant carbon balance during the vine growing cycle was attempted to be verified by firstly checking the flux of [CO_2] during night periods (i.e., nocturnal NCE or night respiration, R_d). Surprisingly, [CO_2] measurements at night stand out for their instability, which were especially high during harvest period and not dependent of wind speed or other environmental factors. Such [CO_2] instability has been previously described by Patil et al. (2014), who attributed the pronounced CO_2 peaks to the absence of solar radiation and accumulation of CO_2 in unstable boundary layer. Thus, these noisy measurements may lead to unreliable night respiration estimations, again reinforcing the idea that proper buffer volumes are necessary when large plant chambers are used.

Carbon and Water Balance Through Different Phenology and Environmental Conditions

Instantaneous rates of NCE showed reliable and stable values, and varied with irradiance, temperature and elapsed time, as expected. Over the course of the day, NCE highly correlates with canopy light interception, as also have been reported by Petrie et al. (2009) and Poni et al. (1997). Daily cycles of NCE were very similar for the two water regimes and the two different phenology stages in early morning and late afternoon when sunlight was largely diffuse. Conversely, canopy NCE trends started to differentiate and showed maximum difference from about 9 till 16 h when canopies were subjected to a higher proportion of direct light. Thus, we stressed that the daily NCE measurements were affected by the applied water regime, both pre- and post-véraison, obtaining different shapes when comparing between irrigation treatments (July vs. August) and between different phenological times (different aging) (July vs. September), even being under the same water regime. NCE for watered plants (in July) followed the sinusoidal pattern of irradiance. By contrast, in August (for stressed plants) and September (for watered plants), instantaneous NCE reflected a morning maximum (8 h) peak of about 5 and 2 μmol m^{-2} s^{-1}, respectively, and then declined steadily after 12 h. Most of the higher CO_2 fixation rates during the entire day in watered plants in July could be due to the faster canopy development (high proportion of fully expanded leaves) rather than a higher average photosynthetic rate per leaf, as it has been previously described by Poni et al. (2000). On the other hand, instantaneous rates of NCE in August reflected a combined effect of water stress (no irrigation delivery), similarly of what has been previously observed in Tarara et al. (2011). However, a different trend was observed by Pagay (2016), who did not show differences in diurnal NCE patterns pre-veraison under different water regimes. This was likely because vines did not have a sufficiently long period without irrigation to experience water deficit.

Interestingly, R_d-values in the present study showed slight decreases between pea size (in July) vs. pre-harvest (in September), within the same irrigation level. The dearth of information on R_d as affected by water stress and leaf aging makes comparisons with the present study difficult. On one side, Pagay (2016) described higher R_d-values for deficit-irrigated vines, however, in our experiment, the system sensitivity might not be sufficient to highlight early-season differences in respiration with respect to different irrigation regime mainly due to the obtained high nocturnal CO_2 fluctuations and the impossibility of adjusting flow rates at night. On the other side, Zufferey (2016) and Hernández-Montes et al. (2018) showed that during the rapid plant growth phase, young leaves presented the highest R_d rates compared to the mature ones. However, once the vegetative growth had stopped, the effect of the leaf age on R_d was less noticeable. At this stage (i.e., when the vegetative growing phase stops), we can hypothesized that the contribution of grapevine clusters to the total carbon balance by the whole berry respiration, might be highly enough to greatly reduce the daily NCE. Accordingly, Miller et al. (1997) stated a rapid decrease of the NCE rate from veraison through harvest.

Moreover, recent results showed that bunches respiration at veraison and ripening are the main component of plant respiration (Hernández-Montes, 2017), so that this component can be an important part of the NCE rates of the whole canopy during those months reducing significantly the net carbon uptake. On the basis of this important CO_2 flux, a more detailed study of the influence of the grapevine clusters to the total NCE is necessary to better understand the whole-plant carbon fluxes.

Patterns of canopy transpiration (E) followed a similar outline than VPD and PAR (data not shown). In accordance to Tarara

and Pena (2015), similar patterns of E were obtained between irrigation regimes, and between time points. However, it is noticeable here, that all along the entire experiment, different absolute values of E and E_{night} (nocturnal water loss) varied following both, different water regimes and the leaf aging of the plant. On the one hand, either at leaf and whole-canopy level, it is well documented that the most important environmental factors affecting transpiration are humidity, temperature, light intensity, wind, and the soil water content (Escalona et al., 2003; Medrano et al., 2003; Merli et al., 2015; Pagay et al., 2016). However, on the other hand, less attention has been given to the evolution of whole-plant transpiration throughout the vine vegetative cycle. Boyer et al. (1997) described the importance of leaf aging in the E levels, mainly because of a great reduction of the cuticular transpiration. So, at the whole-plant level and during the harvest stage, it was expected to have decreased E-values, as it happens here (**Figure 5B**). It can be also hypothesized that the decrease of photosynthetic capacity due to leaf ontology through the season goes along a decrease in E.

Responses to Light

Over the course of the day, studies have found that patterns of NCE correlates highly with canopy light interception (Poni et al., 1997; Petrie et al., 2009). Pooling data gathered throughout the different treatments permitted to obtain different light response curves for NCE and E. The obtained curves were similar to that known for the light dependence of CO_2 assimilation (Harbinson and Foyer, 1991). However, compared with single-leaf light response curves, whole-canopy photosynthesis in well-watered plants showed a much more gradual gain in NCE with increasing PAR and lack of a clear saturation plateau (Corelli-Grappadelli and Magnanini, 1997; Intrieri et al., 1997; Poni et al., 2003).

At low light intensities, below 500 μmol photons m^{-2} s^{-1}, similar values of NCE and E were observed for the two watered treatments (July and September data) but at high light intensities the maximum values decreased with leaf aging. Indeed, since light intensity is coupled to the energy balance of leaves, the light response curves of photosynthesis are modulated by leaf age through differences in the stomatal sensitivity, and also boundary layer conditions (Field and Mooney, 1983; Zufferey et al., 2000; Poni et al., 2003), likely leading to obtain such differences on a seasonal basis. Additionally, because high light intensity hours are in coincidence with high temperatures, their effect on whole-plant respiration and mainly clusters respiration surely influence the observed light curve shape.

The light response curves of photosynthesis became distinctly flatter with increasing water scarcity. In this case, there was a significant treatment effect starting at low irradiance. Moreover there was a lack of a sharp saturation threshold in the trends of E, which continued to increase even after NCE had started to decrease.

Regardless of the amount of the water supplied and the leaf aging effect, canopy WUE exhibited decreasing trends and flattened out from approximately 500 μmol photons m^{-2} s^{-1}. Contrarily to the expected, canopy WUE was distinctly higher in the well-watered treatment than under water stress. This scenario differed from that which might derive from traditional single-leaf assessment and some other estimates on the basis of single-leaf measurements made in the entire canopy (Escalona et al., 2003; Medrano et al., 2012). However, these results are in line with most of studies which have tackled the combination of both, leaf and whole-canopy gas exchange (Poni et al., 2009, 2014; Tarara et al., 2011; Merli et al., 2015). Only Palliotti et al. (2014) reported that drought vines exhibited increased WUE at both the single-leaf and whole-canopy levels on *Vitis vinifera* cv. Sangiovese. Supporting our results, Intrieri et al. (1998) has shown that shaded or partially shaded leaves usually show lower WUE than well-exposed ones since low light limits photosynthesis more than water loss. So, in this case, scaling up WUE readings from leaves to whole-plant, lead to a disappointingly low correlation, mainly because of the obvious differences that a whole canopy may present in terms of leaf exposure and the dynamics of light interception during the day. Moreover, the recent results on the respiration rate of bunches throughout this period (véraison-ripening), could contribute to better understand the discrepancy among single-leaf and whole-canopy results. So, the overall carbon gain is ultimately regulating total plant growth and thus, the study of respiration and photosynthesis of intact whole clusters under field conditions can led us to gain important new knowledge about the real contribution of fruit to the total vine carbon balance.

Responses to High CO_2

Increases of atmospheric CO_2 concentrations are rising year by year at a rate that has been shown to affect photosynthetic rates in C3 plants (Gerhart and Ward, 2010). There is no doubt that growth at elevated [CO_2] stimulates NCE in C3 plants (Drake et al., 1997; Norby et al., 1999; Nowak et al., 2004; Ainsworth and Long, 2005; Ainsworth and Rogers, 2007). We conducted different response curves of NCE to increasing [CO_2], and as predicted, there were significant and marked increases in NCE with increasing [CO_2]. However, the relative rises in NCE were steeper at low irradiance probably because ATP concentration responds more steeply to increasing CO_2 supply when photosynthesis is limited by RuBP regeneration (Buckley et al., 2003).

When comparing between the two analyzed plants for the same treatment, we have obtained similar shapes of NCE to the increasing [CO_2] values, however, at high CO_2, curves were shifted to higher NCE values for chamber 2. This difference would not be explained by the "chamber effect," as similar [CO_2] was entering in both chambers (**Figure 7**), so, a much further effect to high CO_2 may be suggested in this case for the enclosed plant 2.

Concerning the PAR response curves for transpiration to rises in [CO_2], and contrary of what was expected (Long et al., 2004) increasing transpiration values in response to increasing [CO_2] have been obtained for the two enclosed plants. We may argue that other direct effects on water loss by transpiration such as ambient temperature, VPD or other driving forces for exchange of the water vapor from the leaf surface to the surrounding atmosphere may even dominate over the stomatal conductance,

but also a differential CO_2 effect on g_s for the shaded canopy leaves. Also, plants were subjected to high [CO_2] during 3–4 days before taking the measurements, while the single-leaf CO_2 response are always performed at the minute scale. A medium-term stomatal adjustment could also explain this higher *E* under high [CO_2] conditions. However, a complication for the correct estimation of the effect of elevated [CO_2] on transpiration is that experiments have been performed in environmentally controlled and generally well mixed and ventilated experimental set-up (open-top chambers), where the indirect effects may not show up so prominently as in a real and outside future climate (Unsworth et al., 1984; Leuning and Foster, 1990).

CONCLUSION

Whole-plant chambers were developed as a mean to measure gas-exchange rates in grapevines growing in the field, thus becoming a valuable way to handle the daily variations of carbon and water fluxes in the whole-plant under variable environmental conditions [i.e., water regimes, (CO_2), etc.], and leaf aging.

These results clearly show marked differences in daily NCE and *E* all along the vine vegetative growing cycle as well as when comparing between irrigation treatments.

Water scarcity and leaf aging were shown to significantly decrease daily water use but at expenses of lower NCE, but reducing WUE and confirming the lack of correlation between WUEi and whole-canopy WUE. At late stages (i.e., when the vegetative growing phase stops), we suggest that the contribution of grapevine clusters to the total carbon balance by the whole berry respiration, might be high enough to greatly reduce the daily NCE, and thus to ultimately regulate total plant WUE.

Future studies in this area should address to measure the specific contribution of grapevine clusters to the whole-plant NCE as it may explain the reported discrepancy between WUEi and whole-canopy WUE.

AUTHOR CONTRIBUTIONS

All authors contributed to the experiments, data collection, and results evaluation. HM supervised and discussed the manuscript.

FUNDING

This work has been developed with financial support from the Spanish Ministry of Science and Technology (project AGL-2014-54201-C4-1R AEI/FEDER, UE) and by the UE project ERA-NET COFOUNMD FACCE SURPLUS, (Ref: 652615). We would like to thank Mr. Miquel Mas and collaborators of the UIB Experimental Field and Greenhouses which are supported by the UIBGrant 15/2015.

REFERENCES

Ainsworth, E. A., and Long, S. P. (2005). What have we learned from 15 years of free-air CO2 enrichment (FACE)? A meta-analytic review of the responses of photosynthesis, canopy properties and plant production to rising CO2. *New Phytol.* 165, 351–372. doi: 10.1111/j.1469-8137.2004.01224.x

Ainsworth, E. A., and Rogers, A. (2007). The response of photosynthesis and stomatal conductance to rising [CO2]: mechanisms and environmental interactions. *Plant Cell Environ.* 30, 258–270. doi: 10.1111/j.1365-3040.2007.01641.x

Alleweldt, G., Eibach, R., and Ruhl, E. (1982). Investigations on gas exchange in grapevine. I. Influence of temperature, leaf age and time of day on net photosynthesis and transpiration. *Vitis* 21, 93–100.

Boyer, J. S., Wong, S. C., and Farquhar, G. D. (1997). CO2, and water vapor exchange across leaf cuticle (epidermis) at various water potentials. *Plant Physiol.* 114, 185–191. doi: 10.1104/pp.114.1.185

Buckley, T. N., Mott, K. A., and Farquhar, G. D. (2003). A hydromechanical and biochemical model of stomatal conductance. *Plant Cell Environ.* 26, 1767–1785. doi: 10.1104/pp.17.00666

Corelli-Grappadelli, L., and Magnanini, E. (1997). Whole-tree gas exchanges: can we do it cheaper? *Acta Horticult.* 451, 279–285. doi: 10.17660/ActaHortic.1997.451.32

Drake, B. G., Gonzalez-Meler, M. A., and Long, S. P. (1997). More efficient plants: a consequence of rising atmospheric CO2? *Annu. Rev. Plant Physiol. Plant Mol. Biol.* 48, 609–639. doi: 10.1146/annurev.arplant.48.1.609

Edson, C. E., Howell, G. S., and Flore, J. A. (1993). Influence of crop load on photosynthesis and dry matter partitioning of Seyval grape-vines. I. Single leaf and whole vine response pre- and post-harvest. *Am. J. Enol. Vitic.* 44, 139–147.

Escalona, J. M., Flexas, J., Bota, J., and Medrano, H. (2003). Distribution of leaf photosynthesis and transpiration within grapevine canopies under different drought conditions. *Vitis* 42, 57–64.

Escalona, J. M., Fuentes, S., Tomàs, M., Martorell, S., Flexas, J., and Medrano, H. (2013). Responses of leaf night transpiration to drought stress in *Vitis vinifera* L. *Agric. Water Manag.* 118, 50–58. doi: 10.1016/j.agwat.2012.11.018

Escalona, J. M., Pou, A., Tortosa, I., Hernández-Montes, E., Tomás, M., Martorell, S., et al. (2016). Using whole-plant chambers to estimate carbon and water fluxes in field-grown grapevines. *Theor. Exp. Plant Physiol.* 28, 241–254. doi: 10.1007/s40626-016-0073-7

Escalona, J. M., Tomas, M., Martorell, S., Medrano, H., Ribas-carbo, M., and Flexas, J. (2012). Carbon balance in grapevines under different soil water supply: importance of whole plant respiration. *Aust. J. Grape Wine Res.* 18, 308–318. doi: 10.1111/j.1755-0238.2012.00193.x

Field, C., and Mooney, H. A. (1983). Leaf age and seasonal effects on light, water, and nitrogen use efficiency in a California shrub. *Oecologia* 56, 348–355. doi: 10.1007/BF00379711

Field, C. B., Ball, J. T., and Berry, J. A. (1989). "Photosynthesis: Principles and field techniques, 209-253," in *Plant Physiological Ecology. Field Methods and Instrumentation*, eds R. W. Pearcy, J. Ehleringer, H. A. Mooney, and P. W. Rundel (New York, NY: Chapman and Hall Ltd.).

Garcia, R., Norman, J. M., and Mc Dermitt, D. K. (1990). Measurements of canopy gas exchange using an open chamber system. *Remote Sensing Rev.* 5, 141–162. doi: 10.1080/02757259009532126

Gerhart, L. M., and Ward, J. K. (2010). Plant responses to low [CO2] of the past. *New Phytol.* 188, 674–695. doi: 10.1111/j.1469-8137.2010.03441.x

Harbinson, J., and Foyer, C. H. (1991). Relationship between the efficiencies of Photosystem I and Photosystem II and stromal redox state in CO2 free air–evidence for cyclic electron flow in vivo. *Plant Physiol.* 97, 41–49. doi: /10.1104/pp.97.1.41

Hernández-Montes, E. (2017). *Respiratory Processes and Carbon Balance in Grapevines: Environmental and Genotype Effects*. Master's thesis. Spain: University of the Balearic Islands.

Hernández-Montes, E., Tomás, M., Escalona, J. M., Bota, J., and Medrano, H. (2018). Leaf growth rate and nitrogen content determine respiratory costs during leaf expansion in grapevines. *Physiol. Plant.* doi: 10.1111/ppl.12769 [Epub ahead of print].

Intrieri, C., Poni, S., Rebucci, B., and Magnanini, E. (1997). Effects of canopy manipulations on whole-vine photosynthesis: Results from pot and field experiments. *Vitis* 36, 167–173.

Intrieri, C., Poni, S., Rebucci, B., and Magnanini, E. (1998). Row orientation effects on whole-canopy gas exchange of potted and field grown grapevines. *Vitis* 37, 147–154.

Leuning, R., and Foster, L. J. (1990). Estimation of transpiration by single trees: comparison of a ventilated chamber, leaf energy budgets and a combination equation. *Agric. For. Meteorol.* 51, 63–68. doi: 10.1016/0168-1923(90)90042-5

Long, S. P., Ainsworth, E. A., Rogers, A., and Ort, D. R. (2004). Rising atmospheric carbon dioxide: plants FACE the Future. *Annu Rev. Plant Biol.* 55, 591–628. doi: 10.1146/annurev.arplant.55.031903.141610

Long, S. P., and Hällgren, J. E. (1989). "Measurement of CO2 assimilation by plants in the field and the laboratory, 62-94," in *Techniques in Bioproductivity and Photosynthesis*, eds J. Coombs, D. O. Hall, S. P. Long, and J. M. Scurlock (Oxford: Pergamon Press).

Medrano, H., Escalona, J. M., Cifre, J., Bota, J., and Flexas, J. (2003). A ten-year study on the physiology of two Spanish grapevine cultivars under field conditions: effects of water availability from leaf photosynthesis to grape yield and quality. *Funct. Plant Biol.* 30, 607–619. doi: 10.1071/FP02110

Medrano, H., Pou, A., Tomás, M., Martorell, S., Gulias, J., Flexas, J., et al. (2012). Average daily light interception determines leaf water use efficiency among different canopy locations in grapevine. *Agric. Water Manage.* 114, 4–10. doi: 10.1016/j.agwat.2012.06.025

Merli, M. C., Gatti, M., Galbignani, M., Bernizzoni, F., Magnanini, E., and Poni, S. (2015). Water use efficiency in Sangiovese grapes (*Vitis vinifera* L.) subjected to water stress before veraison: different levels of assessment lead to different conclusions. *Funct. Plant Biol.* 42, 198–208. doi: 10.1071/FP14112

Miller, D. P., Howell, G. S., and Flore, J. A. (1997). Influence of shoot number and crop load on potted Chambourcin grapevines: Whole-vine vs. single-leaf photosynthesis. *Vitis* 36, 109–114.

Norby, R. J., Wullschleger, S. D., Gunderson, C. A., Johnson, D. W., and Ceulemans, R. (1999). Tree responses to rising CO2 in field experiments: implications for the future forest. *Plant Cell Environ.* 22, 683–714. doi: 10.1046/j.1365-3040.1999.00391.x

Nowak, R. S., Ellsworth, D. S., and Smith, S. D. (2004). Functional responses of plants to elevated atmospheric CO2-do photosynthetic and productivity data from FACE experiments support early predictions? *New Phytol.* 162, 253–280. doi: 10.1111/j.1469-8137.2004.01033.x

Ollat, N., and Gaudillère, J. P. (2000). Carbon balance in developing grapevine berries. *Acta Horticult.* 526, 345–350. doi: 10.17660/ActaHortic.2000.526.37

Pagay, V. (2016). Effects of irrigation regime on canopy water use and dry matter production of Tempranillo grapevines in the semi-arid climate of Southern Oregon. *U.S.A. Agric. Water Manag.* 178, 271–280. doi: 10.1016/j.agwat.2016.10.014

Pagay, V., Zufferey, V., and Lakso, A. N. (2016). The influence of water stress on grapevine (*Vitis vinifera* L.) shoots in a cool humid climate: growth, gas exchange and hydraulics. *Funct. Plant Biol.* 43, 827–837. doi: 10.1071/FP16017

Palliotti, A., and Cartechini, A. (2001). Developmental changes in gas exchange activity in flowers, berries and tendrils of field-grown cabernet sauvignon. *Am. J. Enol. Viticult.* 4, 317–323.

Palliotti, A., Tombesi, S., Frioni, T., Famiani, F., Silvestroni, O., Zamboni, M., et al. (2014). Morpho-structural and physiological response of container-grown Sangiovese and Montepulciano cv. (*Vitis vinifera*) to re-watering after a pre-veraison limiting water deficit. *Funct. Plant Biol.* 41, 634–647. doi: 10.1071/FP13271

Patil, M. N., Dharmaraj, T., Waghmare, R. T., Prabha, T. V., and Kulkarni, J. R. (2014). Measurements of carbon dioxide and heat fluxes during monsoon-2011 season over rural site of India by eddy covariance technique. *J. Earth Syst. Sci.* 123, 177–185. doi: 10.1007/s12040-013-0374-z

Perez Peña, J. P., and Tarara, J. M. (2004). A portable whole canopy gas exchange system for several mature field-grown grapevines. *Vitis* 43, 7–14.

Petrie, P. R., Trought, C. T., and Howell, G. S. (2000). Influence of leaf aging, leaf area and crop load on photosynthesis, stomatal conductance and senescence of grapevines (*Vitis vinifera* L. cv. *Pinot noir)* leaves. *Vitis* 39, 31–36.

Petrie, P. R., Trought, M. C., Howell, G. S., Buchan, G. D., and Palmer, J. W. (2009). Whole-canopy gas exchange and light interception of vertically trained *Vitis vinifera* L. under direct and diffuse light. *Am. J. Enol. Vitic* 60, 173–182.

Poni, S., Bernizzonia, F., Civardia, S., Gattia, M., Porro, D., and Caminc, F. (2009). Performance and water-use efficiency (single-leaf vs. whole-canopy) of well-watered and half-stressed split-root *Lambrusco grapevines* grown in Po Valley (Italy). *Agric. Ecosyst. Environ.* 129, 97–106. doi: 10.1016/j.agee.2008.07.009

Poni, S., Intrieri, C., and Magnani, E. (1999). Set-up, calibration and testing of a custom-built system for measuring whole-canopy transpiration in grapevine. *Acta Hortic.* 493, 149–160. doi: 10.17660/ActaHortic.1999.493.14

Poni, S., Intrieri, C., and Magnani, E. (2000). Seasonal growth and gas exchange of conventionally and minimally pruned Chardonnay canopies. *Vitis* 39, 13–18.

Poni, S., Magnanini, E., and Rebucci, B. (1997). An automated chamber system for measurements of whole-vine gas exchange. *HortScience* 32, 64–67.

Poni, S., Magnanini, E., and Bernizzoni, F. (2003). Degree of correlation between total light interception and whole-canopy net CO2 exchange rate in two grapevine growth systems. *Aust. J Grape Wine Res.* 9, 2–11.

Poni, S., Merli, M. C., Magnanini, E., Galbignani, M., Bernizzoni, F., Vercesi, A., et al. (2014). An Improved multi chamber gas exchange system for determining whole-canopy water-use. *Am. J. Enol. Vitic.* 65, 268–276. doi: 10.5344/ajev.2014.13117

R Core Team (2016). *R: A Language and Environment for Statistical Computing*. Vienna: R Foundation for Statistical Computing. Available at: https://www.R-project.org/

Sánchez-de-Miguel, P., Baeza, P., Junquera, P., and Lissarrague, J. R. (2010). "Vegetative development: total leaf area and surface area indexes," in *Methodologies and Results in Grapevine Research*, eds S. Delrot, H. Medrano, L. Bavaresco, and S. Grando (Amsterdam: Springer), 31–44.

Schultz, H. R. (1993). Photosynthesis of sun and shade leaves of field grown grapevines (*Vitis vinifera* L) in relation to leaf age. Suitability for the plastochron concept for the expression of physiological age. *Vitis* 32, 197–205.

Tarara, J. M., and Pena, J. E. P. (2015). Moderate water stress from regulated deficitirrigation decreases transpiration similarly to net carbon exchange ingrapevine canopies. *J. Am. Soc. Horticult. Sci.* 140, 413–426.

Tarara, J. M., Peña, J. E. P., Keller, M., Schreiner, R. P., and Smithyman, R. P. (2011). Net carbon exchange in grapevine canopies responds rapidly to timing and extent of regulated deficit irrigation. *Funct. Plant Biol.* 38, 386–400. doi: 10.1071/FP10221

Tomàs, M., Medrano, H., Escalona, J. M., Martorell, S., Pou, A., Ribas-Carbó, M., et al. (2014). Variability of water use efficiency in grapevines. *Environ. Exp. Bot.* 103, 148–157. doi: 10.1016/j.envexpbot.2013.09.003

Tomàs, M., Medrano, H., Pou, A., Escalona, J. M., Martorell, S., Ribas-Carbó, M., et al. (2012). Water-use efficiency in grapevine cultivars grown under controlled conditions: effects of water stress at the leaf and whole-plant level. *Austr. J. Grape Wine Res.* 18, 164–172. doi: 10.1111/j.1755-0238.2012.00184.x

Unsworth, M. H., Heagle, A. S., and Heck, W. W. (1984). Gas exchange in open top field chambers. I. Measurement and analysis of atmospheric resistances. *Atmosph. Environ.* 18, 373–380. doi: 10.1016/0004-6981(84)90111-2

Zufferey, V. (2016). Leaf respiration in grapevine (*Vitis vinifera* 'Chasselas') in relation to environmental and plant factors. *J. Grapevine Res.* 72, 65–72.

Zufferey, V., Murisier, F., and Schultz, H. R. (2000). A model analysis of the photosynthetic response of *Vitis vinifera* L. *cvs* Riesling and Chasselas leaves in the field. I. Interaction of age, light and temperature. *Vitis* 39, 19–26.

Conflict of Interest Statement: The authors declare that the research was conducted in the absence of any commercial or financial relationships that could be construed as a potential conflict of interest.

frontiers in Plant Science

PERSPECTIVE
published: 28 September 2018
doi: 10.3389/fpls.2018.01442

Effective Water Use Required for Improving Crop Growth Rather Than Transpiration Efficiency

*Thomas R. Sinclair**

Department of Crop and Soil Sciences, North Carolina State University, Raleigh, NC, United States

The phenomenological expression showing crop yield to be directly dependent on crop transpiration use efficiency (TE) has encouraged continued focus on TE as a viable approach to increasing crop yields. The difficulty in the phenomenological perspective is that research tends not to match up with the underlying mechanistic variables defining TE. Experimental evidence and the mechanistic derivation of TE by Tanner and Sinclair showed that the common focus on increasing the intrinsic ratio of leaf CO_2/H_2O exchange has limited opportunities for improvement. On the other hand, the derivation showed that daily vapor pressure deficit (VPD) weighted for the daily cycle of transpiration rate has a large, direct impact on TE. While VPD is often viewed as an environmental variable, daily weighted VPD can be under plant control as a result of partial stomatal closure during the midday. A critical feature of the partial stomatal closure is that transpiration rate is decreased resulting in conservation of soil water. The conserved soil water allows late-season, sustained physiological activity during subsequent periods of developing water deficits, which can be especially beneficial during reproductive development. The shift in the temporal dynamics of water use by water conservations traits has been shown in simulation studies to result in substantial yield increases. It is suggested from this analysis that *effective water use* through the growing season is more important for increasing crop yield than attempts focused on improving the static, intrinsic TE ratio.

Keywords: crop growth, effective water use, stomatal conductance, transpiration, vapor pressure deficit

OPEN ACCESS

Edited by:
Michael Vincent Mickelbart,
Purdue University, United States

Reviewed by:
Trevor Garnett,
The University of Adelaide, Australia
Albino Maggio,
Università degli Studi di Napoli Federico II, Italy

***Correspondence:**
Thomas R. Sinclair
trsincla@ncsu.edu

Specialty section:
This article was submitted to Plant Physiology, a section of the journal Frontiers in Plant Science

Received: *07 July 2018*
Accepted: *11 September 2018*
Published: *28 September 2018*

Citation:
Sinclair TR (2018) Effective Water Use Required for Improving Crop Growth Rather Than Transpiration Efficiency. Front. Plant Sci. 9:1442. doi: 10.3389/fpls.2018.01442

INTRODUCTION

There continues to be great interest in increasing crop transpiration efficiency (TE), which is often defined as crop mass production per unit of crop transpiration. This interest seems to be sustained in spite of the fact that more than a century of research has shown little progress in improving basic TE. This was pointed out by Tanner and Sinclair (1983) in their review of much of the research beginning early in the last century showed little evidence in progress toward increasing TE. The one noted exception has been the development from carbon isotope discrimination observations of the wheat cultivar 'Drysdale' in Australia for rainfed conditions (Rebetzke et al., 2002). However, the carbon isotope discrimination approach in itself did not resolve the exact physiological advantage of this variety. The percent yield increase of Drysdale was found to be less than 11% at a base yield of about 1 t ha^{-1} (i.e., yield improvement of 0.11 t ha^{-1}) and the percent yield increase declined linearly with higher base yields.

Stability in TE was fully illustrated in the analysis of C.T. deWit (1958) in which results from experiments worldwide were combined and plotted for each species as growth vs. transpiration normalized by evaporation from an open water surface. These data within a species represented a range of cultivars, soil fertility, soil water conditions, and environments. As shown in **Figure 1**, within in each species these straightforward graphs resulted in highly linear relationships. The slopes varied among species but within species the slopes were extremely stable across the wide range of experimental conditions.

Given the historical experience of little variation within a species for improvement in the ratio of growth to normalized transpiration, why is there such a continuing interest in improving crop TE? Likely one major reason is the intuitive view that increasing TE will result in increased crop yield. This view was illustrated in the phenomenological equation presented by Passioura (1977).

$$Y = HI \times TE \times W, \quad (1)$$

where Y = grain yield,

HI = harvest index,
W = transpired soil water.

A central feature of Eq. [1] is the TE variable, and this indicates that Y would be increased by increasing TE. The difficulty is that the Eq. [1] is not a *mechanistic* equation. As discussed below, TE is dependent on a large number of physical and physiological variables that make it very difficult to resolve TE in attempts at genetic comparisons and improvements.

A MECHANISTIC VIEW

Rather than the ambiguity in the phenomenological description of TE in Eq. [1], an improved understanding of canopy water use is obtained by examining a mechanistic description of TE. Such a mechanistic derivation was presented more than 30 years ago by Tanner and Sinclair (1983). In their derivation, the relationship between canopy mass accumulation and water loss was developed from the basic relation between carbon dioxide and water vapor exchange at the leaf level. The resultant expression resulted in the following deceptively simple expression for daily canopy TE.

$$TE = \int(k_d/VPD)dt/\int dt, \quad (2)$$

where

k_d = mechanistic coefficient accounting for physical and physiological characteristics (Pa),
VPD = vapor pressure deficit (Pa).

If TE is to be calculated on a daily time step, then the daily value of VPD to be used in Eq. [2] must be weighted to reflect the daily pattern of transpiration rate. That is, the weighted VPD value needs to be skewed for the times of the day when transpiration rate is high. Therefore, a simple mean daily VPD even if based only on daytime values is an inappropriate calculation for daily VPD. Tanner and Sinclair (1983) proposed that VPD is equal to 0.75 of the difference between maximum daily vapor pressure and minimum daily vapor pressure. Abbate et al. (2004) subsequently concluded that the weighting coefficient in the calculation of VPD for Argentine environments was 0.72.

The terms that define the parameter k_d in Eq. [2] is critical to understanding the nature of TE. The derivation of Tanner and Sinclair (1983) gave the following explicit definition of k_d.

$$k_d = (a \times b \times c/1.5) \times (C_a/(\rho \times \varepsilon)) \times L_D/L_T, \quad (3)$$

where

a = molecular weight ratio $[CH_2O]/[CO_2] = 0.68$,
b = conversion fraction to plant mass from hexose,
$c = (1-C_i/C_a)$, where C_i is leaf internal CO_2 partial pressure and C_a is atmospheric CO_2 partial pressure,
1.5 = accounting for diffusion difference between water vapor and CO_2,
ρ = air density,
ε = ratio of mole weight of water vapor to air (18/28.8 = 0.625),
L_D = leaf area index exposed to direct radiation (for nearly closed canopies ∼1.4),
LT = effective transpiring leaf area index (for nearly closed canopies ∼2.2).

In comparing k_d among crop species, the two key variables that result in differences in k_d are parameters b and c. The value of b ranges from about 0.75 for species producing high carbohydrate plant products to about 0.42 for species producing high energy products containing high amounts of oil and protein. The value of c depends on the photosynthetic pathway of a species with maximum values of about 0.7 for C4 species and about 0.3 for C3 species. Therefore, k_d can range from about 9–10 Pa for carbohydrate-producing C4 species to about 4 Pa for energy-rich C3 species.

Based on the derived definition of k_d, predicted k_d could be expected to be fairly stable within species. This conclusion is fully consistent with the stability in the slope in **Figure 1** from the analysis of deWit (1958). Further, the values of the slopes found by deWit reflect species differences in k_d. That is, the species with the highest slope in **Figure 1** is sorghum, which is predicted to have a high slope because it is a C4 species producing low energy vegetative mass and seeds. The next lower slope is wheat, which is a C3 species producing high carbohydrate plant material. The lowest slope is for alfalfa, which is a C3 species producing high protein concentration in the plant.

The definition of k_d indicates some possibility of increasing TE by decreasing C_i. There are two approaches to achieve decreased C_i: lower stomatal conductance allowing C_i to be taken to a low value by photosynthetic consumption of CO_2, or high leaf photosynthetic activity that results in the ready assimilation of CO_2 and low C_i. However, in the context of crop production neither approach seems likely to offer major opportunities for increases in TE. Low stomatal conductance will result in low leaf photosynthetic rates, which might result in a direct limitation on crop growth and yield. High leaf photosynthetic activity would

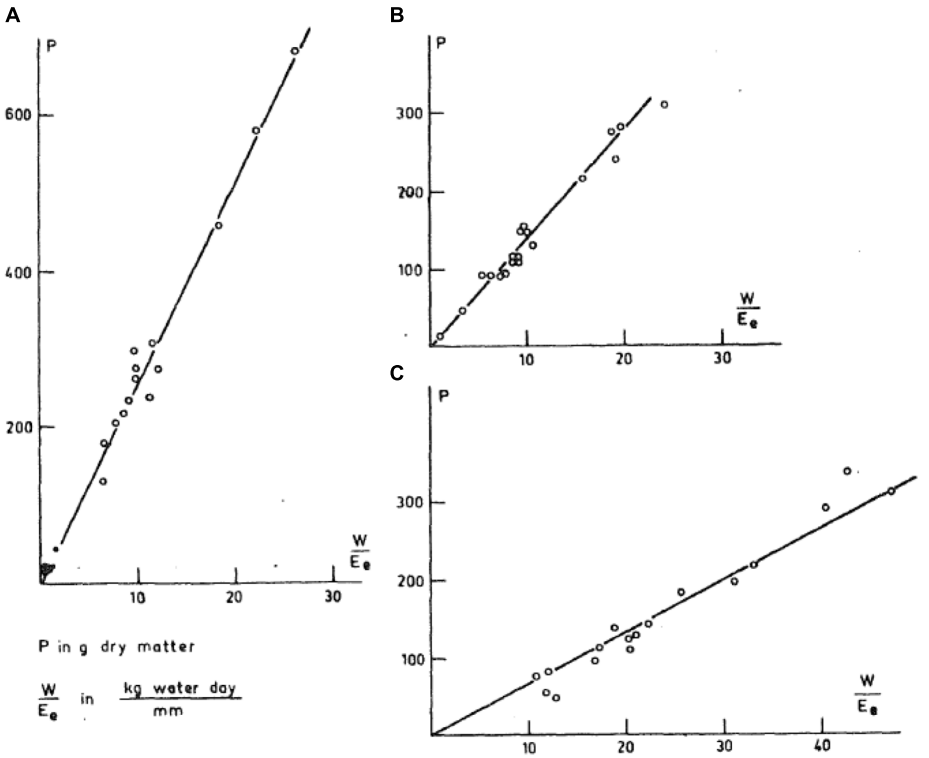

FIGURE 1 | Graph of plant mass production plotted against transpiration rate normalized with pan evaporation (deWit, 1958). **(A)** Sorghum, **(B)** wheat, and **(C)** alfalfa.

likely be more advantageous, but for any crop species that has been subjected to breeding and selection for high yield, it seems likely that genotypes with low photosynthetic rates have already been discarded.

Direct measures of C_i/C_a tend to show values that are consistent with the maximum *c* values given above. Bunce (2005) measured in the field the C_i/C_a ratio of six C4 species and found the lowest ratio was in Japanese bristlegrass (*Seteria faberi*) with a ratio of 0.3 (maximum c = 0.7). In a comparison of a large number of sugarcane (*Saccharum* spp.) cultivars, Jackson et al. (2016) found the minimum C_i/C_a to be 0.34 (maximum c = 0.66). In C3 species, the value of C_i/C_a is much higher than in C4 species. In a field comparison of eight soybean [*Glycine max* (Merr.) culitvars, L.] at different stages of development, Tomeo and Rosenthal (2017) found the lowest value of C_i/C_a to be about 0.66 (maximum c = 0.34) with most observations in the range about 0.69 (maximum c = 0.31) to 0.79 (maximum c = 0.21). In a comparison of seven cotton (*Gossypium hirsutum* L.) cultivars, C_i/C_a ranged from 0.66 to 0.68 (maximum c = 0.34 to 0.32) (Stiller et al., 2005). Hence, the maximum experimental values of c in C4 and C3 are consistent with the stated values in the definition of k_d among species.

Given that both variables b and c are approximately stable with few practical options for major modification, it is concluded that the k_d term of TE does not appear to be a major priority target for increasing TE. The variable left for increasing TE is VPD. Unfortunately and importantly, VPD is often ignored in comparisons of TE even though it is clear that this variable can have a large impact on TE. Further, VPD is not simply defined by the changing ambient environmental conditions, but can be a physiological term resulting from plant adjustments in stomatal conductance over time and environmental conditions (Vadez et al., 2014).

Remembering that the VPD term in Eq. [2] represents daily VPD weighted for transpiration rate, the value of this term is decreased if the fraction of daily transpiration under high VPD conditions is decreased. There are two major approaches to result in decreased transpiration during the midday period of elevated VPD. One approach is the possibility of limited-transpiration rate due to the imposition of a maximum water transport to the guard cells due to plant hydraulic conductance limitations (Sinclair, 2017b). Under this condition, further increases in VPD result in partial stomatal closure so that the transpiration rate matches the water flow rate to the stomata. If there was not a limitation on transpiration rate due to partial stomatal closure, the leaf would rapidly desiccate due to limited water flow into the leaf. This stomatal response is sometimes observationally referred to as 'midday stomatal closure.' Sinclair et al. (2008) found that the limited-transpiration trait in soybean genotype PI 416937 was associated with low leaf hydraulic conductance, which was consistent with apparent aquaporin activity of this genotype (Sadok and Sinclair, 2010). Not surprising, in a study of peanut genotypes, Devi et al. (2009, 2010) found that those lines exhibiting

partial stomata closure at threshold VPDs also had significantly greater TE.

A second approach to decreasing daily VPD can result from a decrease partial stomatal closure as the soil dries. Decreasing soil hydraulic conductance with soil drying results in partial stomatal closure at midday when no more than one third or less of the transpirable soil water remains in the soil (Sinclair, 2005). If a genotype with a low plant hydraulic conductance is paired with low soil conductance resulting from soil drying, then the threshold of extractable soil water at which transpiration decrease is likely initiated is at a higher soil water content than the usual one third transpirable soil water (Sinclair, 2017a). Those genotypes that initiate stomatal closure at high transpirable soil water will have a lower weighted VPD, and consequently greater TE as the soil dries.

DECREASE IN WATER USE BY ENVIRONMENTALLY SENSITIVE STOMATAL REGULATION

Given that there appears to be limited possibilities for increasing k_d in crop species that have been subjected to breeding for yield increase, a more rewarding focus for increasing TE seems likely to be on plant traits associated with decreased effective VPD (Eq. [2]). An increase in TE as a result of decreased weighted VPD certainly indicates a major opportunity for yield increase as shown in the Eq. [1]. However, Eq. [1] represents a static view of crop yield and fails to account for the temporally dynamic processes of mass accumulation and water use through an entire growing season. Accounting for the dynamic changes in water use through the growing season is critical in resolving the impact of VPD. Not only does weather directly influence VPD, but fluctuating availability of soil water can have a major influence on weighted VPD. Further, variation through the season on possible crop transpiration rate can influence the determination of weighted VPD.

In terms of increasing crop yield, an important outcome of the two water-conservation traits discussed above is that they result in altered seasonal patterns of water use. Conservation of soil water, especially early in the growing season, can result in greater soil water availability later in the growing season so that the impact of late-season drought might be decreased as a result of sustained physiological activity, especially during seed fill. Richards and Passioura (1989) selected wheat genotypes with smaller diameter metaxylem vessels as an approach to achieve decreased plant hydraulic conductance and shift water use to later in the growing season. While they found yield increases of 3 – 11%, no commercial cultivars were released from their study

A concern for each of the two water-conservation traits discussed here is that partial stomatal closure to limit water loss also results in a restriction on current photosynthetic activity. A key question to be resolved is whether the gain in conservation of soil water (and increased TE) overcomes the early season loss in plant mass accumulation. This question cannot be resolved using a static equation such as Eq. [1] but requires a temporal analysis through the growing season requiring a dynamic, mechanistic crop model. The model needs to be applied over a number of seasons for each location to obtain enough simulation results to allow adequate information to generate average yields, and likely more importantly, probability estimates for yield change.

Simulations to assess the yield response by introducing the water-conservations traits into crop genotypes have been done using the Simple Simulation Model (SSM, Soltani and Sinclair, 2012). This model tracks soil water content on a daily basis by adding precipitation and irrigation to the soil and removing water as a result of soil evaporation and canopy transpiration. The daily amount of crop mass accumulation, transpiration, leaf area development, and nitrogen accumulation are all adjusted in SSM based on the fraction of transpiration soil water (FTSW) that exists in the soil on each day as the simulation progresses through the growing season. Hence, the simulations are temporally dynamic and directly account for plant responses to soil water status.

Assessment of Limited-Transpiration on Crop Yield

The impact of water conservation due to decreased transpiration rate under elevated VPD was first simulated for sorghum (*Sorghum bicolor* L.) in Australia (Sinclair et al., 2005). Weather data from four locations over more than 100 years was used to simulate sorghum plants with assumed, hourly limited-transpiration rates of 0.4 and 0.6 mm h^{-1}. Simulated yields were generally increased, or at least unchanged, at yield levels of about 4.5 t ha^{-1} and lower. Approximately 75 % of the growing seasons were in this lower-yield classification that would benefit from the limited-transpiration trait. Above 4.5 t ha^{-1}, yields were only slightly decreased due to the limited-transpiration trait. It was concluded that the limited-transpiration trait appeared advantageous for commercial production of sorghum in Australia.

Simulations were also done on the impact of the limited-transpiration trait on soybean in the United States (Sinclair et al., 2010). The limited-transpiration response was invoked whenever VPD during the daily cycle was greater than 2 kPa. Simulations were done at each grid location (30 km × 30 km) over the United States based on 50 years of weather data. Due to the sensitivity of N_2 fixation to soil drying, water conservation as a result of the limited-transpiration trait resulted in a high probability of yield increase of 85 % or greater for most locations (**Figure 2a**). Yields when ranked at each location showed yield increases at the 75 (wet), 50, and 25 (dry) percentile ranking in nearly all locations in the major areas of soybean production (**Figures 2b–d**). In the 25 percentile ranking, the yield increase ranged from 0.25 to 0.75 t ha^{-1}. Similar simulations for soybean in Africa were done with the threshold for limited-transpiration trait at 1.8 kPa (Sinclair et al., 2014). Roughly half of the area in both East and West Africa had an 85% or greater probability of yield increase. The probability of a 70% or greater yield increase included all but the wettest and driest locations in Africa.

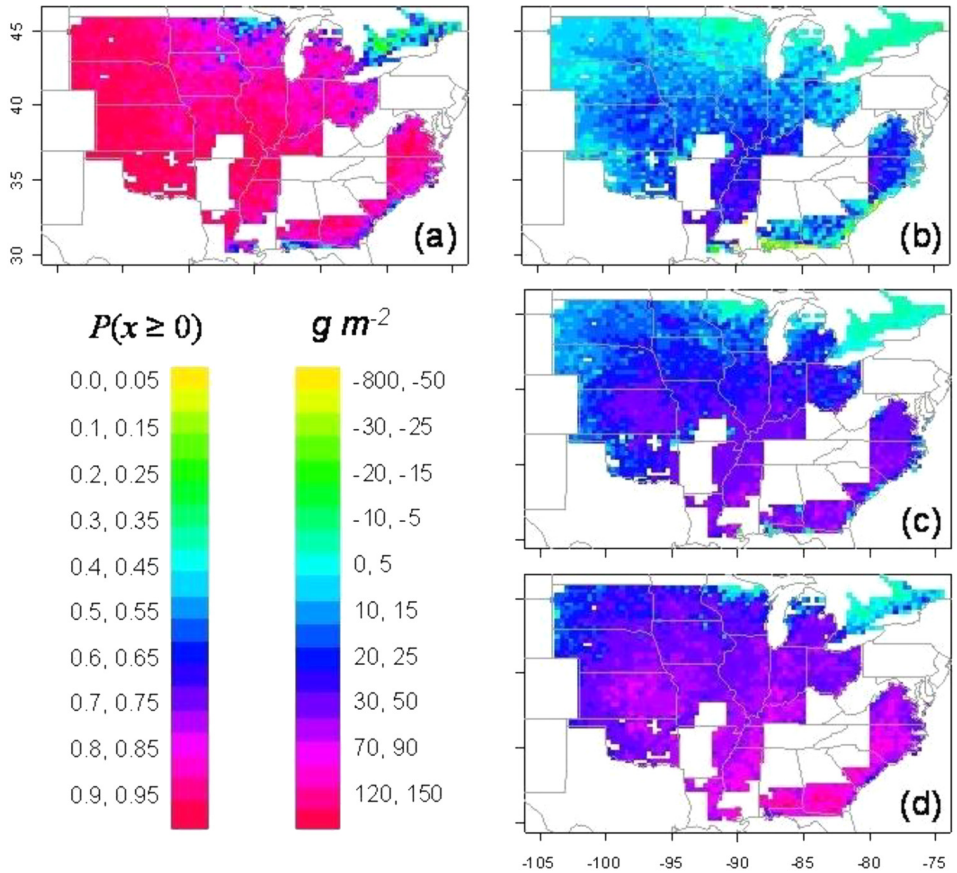

FIGURE 2 | Simulation of yield change for soybean in the United States as a result of the introduction of a limited-transpiration trait (threshold = 2 kPa). The probability of yield increase over the 50 simulated years is shown in panel **(a)**. The actual yield increase at each location for percentile rankings of **(b)** 75% (wet), **(c)** 50% (median), and **(d)** 25% (dry) (Sinclair et al., 2010).

Geospatial assessments have also been done for several other crop species and locations. In South Asia, lentil (*Lens culinaris* Medik) was simulated with limited-transpiration thresholds of 2.2 and 1.1 kPa (Guiguitant et al., 2017). Limited-transpiration with a 1.1 kPa threshold had yield increase probability greater than 55% for much of the central zone of the South Asia region. Outside the central region, however, the simulations indicated the trait would not give consistent yield increase. Also, in South Asia Kholova et al. (2014) simulated the yield response of sorghum to modification in several plant traits. The limited-transpiration trait was found to have highest positive effect on crop yield of the studied traits. Over a wide range of yield levels, yields were increased up to 0.2 t ha^{-1}.

The potential impact of the limited-transpiration trait on maize (*Zea mays* L.) yields in the United States was simulated by Messina et al. (2015). Using a 2.0 kPa limited-transpiration threshold, yield was generally increased in environments where yield without the trait was less than 10.5 t ha^{-1}, with the greatest yield increases occurring at yield levels less than 6.5 t ha^{-1}. Hence the greatest benefit in yield increase of the limited-transpiration trait was in the western regions of maize production in the United States, generally west of 95° west longitude. The results of these simulations are being used by Pioneer to guide the marketing of their AQUAmax hybrids, which have been shown to express the limited-transpiration trait.

Assessment of Soil-Drying Sensitivity on Crop Yield

Partial stomatal closure at a higher FTSW was simulated for maize grown at Columbia, MO. Yield in only 3 out of 20 simulated seasons was benefitted by initiating partial stomatal closure at higher soil water content than normally observed (Sinclair and Muchow, 2001). A much more extensive simulation of the response of soybean to higher FTSW for stomatal closure was included in the study for the United States described above by Sinclair et al. (2010). Due to the sensitivity to soil water deficit of symbiotic nitrogen fixation in soybean, the probability of yield increase was greater than 79% for three–fourths of the locations (**Figure 3a**). Yields when ranked at each location showed yield increases at the 75 (wet), 50, and 25 (dry) percentile rankings in nearly all locations in the major areas of soybean production (**Figures 3b–d**). Yields were increased especially in the drier growing seasons represented by the 25 percentile

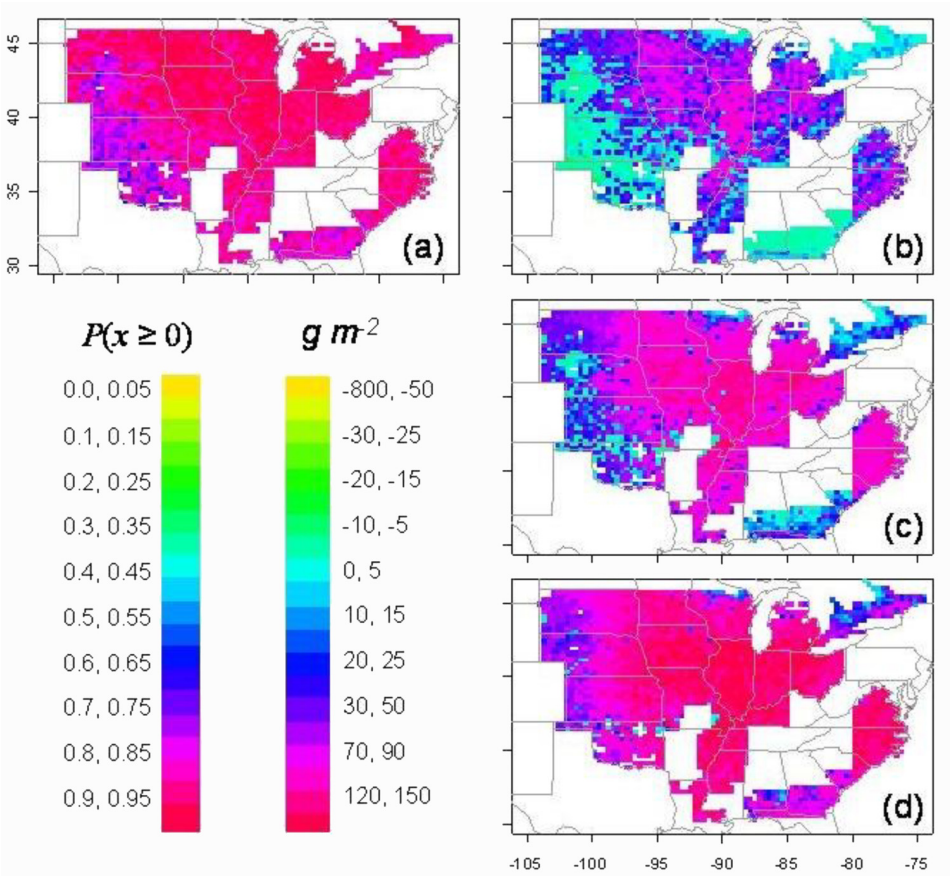

FIGURE 3 | Simulation of yield change for soybean in the United States as a result of the introduction of early partial stomatal closure with soil drying (breakpoint at FTSW = 0.33). The probability of yield increase over the 50 simulated years is shown in panel **(a)**. The actual yield increase at each location for percentile rankings of **(b)** 75% (wet), **(c)** 50% (median), and **(d)** 25% (dry) (Sinclair et al., 2010).

ranking. Therefore, available water was much more effectively used through the growing season as a result of the early initiation of stomatal closure at high FTSW.

EFFECTIVE WATER USE

The above discussion of water conservations traits either by limited-transpiration rate under elevated VPD or by early decline in transpiration rate with soil drying showed the importance of shifting water use from earlier in the cropping season to later in the season, especially to the seed-fill period. Increasing availability of water to the crop at the end of the season enhances the possibility of sustained crop physiological activity, and hence, decreasing the impact of water deficit on reproductive growth. That is, the key response variable to increase yield as expressed in the phenomenological perspective of Eq. [1] is an increased HI.

There are, of course, additional approaches to water-conservation by crops other than those discussed above to achieve effective water use through a cropping season. One simple management approach that was empirically developed from field trails is to shift the cropping season to cooler periods when the VPD is lower and the overall water requirement is less. Another management approach is to select shorter-season cultivars so the cropping season can be completed before water deficits develop. In the Midsouth of the United States, a major shift in soybean management to increase yields by avoiding drought, which commonly develops at the end of July (Purcell et al., 2003), was achieved by using a combination of early sowing and early-maturing cultivars (Bowers, 1995; Heatherly, 1999).

In contrast to the soybean experience, simulations of lentil production in east Africa indicated longer-season cultivars had a higher probability of yield increase (Ghanem et al., 2015). The longer-season cultivars were better suited to take full advantage of all rainfall to attain more effective water use. The optimum sowing date varied substantially across the region so that full consideration of the rainfall pattern is required to determine the appropriate crop sowing date for each location.

Other plant traits can potentially be altered to decrease plant water use in the early part of the cropping season. Lower leaf photosynthesis rates early in the growing season as a result of low leaf nitrogen content and low stomatal conductance, for example, will result in water conservation for late season water use. Slower leaf area development will also decrease the light intercepting

leaf area index so early-season transpiration rate is lessened. These traits are associated with the relative performance of maize, sorghum and millet with increasingly dry conditions favoring sorghum and then millet (Sinclair and Weiss, 2010). Slow root extension in the soil will also limit early season transpiration rate in favor of later season water use. The simulations of soybean production across the United States showed such traits would increase the probability of yield increase for much of the soybean production area (Sinclair et al., 2010). Of course, an important consideration in these early-season water conservation traits is minimization of water loss due to soil evaporation and competing weeds.

PERSPECTIVE

The phenomenological equation indicating the importance of TE turns out to be very complex at the mechanistic level. As found in the derivation of Tanner and Sinclair (1983), TE in the phenomenological equation is actually dependent on several physical and physiological variables as well as the environment. As a minimum, accounting for atmospheric humidity conditions is essential as was done in deWit's analysis 60 years ago. As shown in deWit's results, little variation within a crop species in TE normalized for VPD seemed to exist.

Even "intrinsic" TE may offer minimum insight. This term is usually assumed to be static, i.e., constant over a range a conditions. In fact, environmental variation over the growing season is likely to introduce instability that challenges the data requirements to fully establish intrinsic TE. Simply obtaining sufficient observations of intrinsic TE in a breeding population may be a major problem. The carbon isotope discrimination technique was developed in an effort to overcome this problem but the approach in practice is essentially empirical and is vulnerable to poor relationships with TE (Sinclair, 2012; Vadez et al., 2014).

For crop improvement, a major limitation in using "intrinsic" TE is that the potential improvement may be quite limited for crop species that already have been subjected to selection focused simply on improved yield in water-deficit environments. Intrinsic TE is limited by C_i, which appears to have well-defined limits with maximum values of C_i/C_a of approximately 0.3 and 0.7 for C4 and C3 species, respectively. Of course, if current cultivars deviate substantially above these limits, then potential for TE improvement clearly exist. Even in this case, the more direct breeding approach may be simply selection for superior yield under specified, water-limited conditions.

Rather than focus on TE, much greater return in yield improvement is expected from consideration of the temporal dynamics of water use through the growing season to improve the effective use of available water (Blum, 2009; Sinclair, 2012). This approach to a large extent likely focuses on decreasing water use early in the season or drying cycles to increase water availability to sustain physiological activity through seed fill. Drought during seed fill, especially those water deficits causing early termination of seed growth, can have large negative impacts on yield. As discussed above, simulation studies have shown under a range of conditions that improving plant water-conservation traits can results in high probabilities of yield increase, and absolute yield increases in drier environments can be substantial. Research to introduce these various options into commercial cultivars for increasing effective water use seems much more promising than the century-old, generally unfulfilled quest to improve static TE.

AUTHOR CONTRIBUTIONS

The author confirms being the sole contributor of this work and approved it for publication.

REFERENCES

Abbate, P. E., Dardanelli, J. L., Cantarero, M. G., Maturano, M., Melchiori, R. J. M., and Suero, E. E. (2004). Climate and water availability effects on water-use efficiency in wheat. *Crop Sci.* 44, 474–483. doi: 10.1111/plb.12883

Blum, A. (2009). Effective use of water (EUW) and not water-use efficiency (WUE) is the target of crop yield improvement under drought stress. *Field Crops Res.* 112, 119–123. doi: 10.1016/j.fcr.2009.03.009

Bowers, G. R. (1995). An early season production system for drought avoidance. *J. Prod. Agric.* 8, 112–119. doi: 10.2134/jpa1995.fpage

Bunce, J. A. (2005). What is the usual internal carbon dioxide concentration in C4 species under midday field conditions? *Photosynthetica* 43, 603–608. doi: 10.1007/s11099-005-0094-y

Devi, M. J., Sinclair, T. R., and Vadez, V. (2010). Genotypic variation in peanut for transpiration response to vapor pressure deficit. *Crop Sci.* 50, 191–196. doi: 10.2135/cropsci2009.04.0220

Devi, M. J., Sinclair, T. R., Vadez, V., and Krishnamurthy, L. (2009). Peanut genotypic variation in transpiration efficiency and decreased transpiration during progressive soil drying. *Field Crops Res.* 114, 280–285. doi: 10.1016/j.fcr.2009.08.012

deWit, C. T. (1958). *Transpiration and crop yield.* Verslag Landbouwk Onderz 64.6. Wageningen: Institute for Biological & Chemical Research.

Ghanem, M. E., Marrou, H., Birada, C., and Sinclair, T. R. (2015). Production potential of lentil (*Lens culinaris* Medik.) in East Africa. *Agric. Syst.* 137, 24–38. doi: 10.1016/j.agsy.2015.03.005

Guiguitant, J., Marrou, H., Vadez, V., Gupta, P., Kumar, S., Soltani, A., et al. (2017). Relevance of limited-transpiration trait for lentil (*Lens culinaris* Medik.) in South Asia. *Field Crops Res.* 209, 96–107. doi: 10.1016/j.fcr.2017.04.013

Heatherly, L. G. (1999). "Early soybean production system (ESPS)," in *Soybean Production in the Midsouth*, eds L. G. Heatherly and H. F. Hodges (Boca Raton, FL: CRS Press), 103–118.

Jackson, P., Basnayake, J., Inman-Bamber, G., Lakshamanan, P., Natarajan, S., and Stokes, C. (2016). Genetic variation in transpiration efficiency and relationships between whole plant and leaf gas exchange measurements in *Saccharum* spp. and related germplasm. *J. Exp. Bot.* 67, 861–871. doi: 10.1093/jxb/erv505

Kholova, J., Murugesan, T., Kaliamoorthy, S., Malayee, S., Baddam, R., Hammer, G. L., et al. (2014). Modeling the effect of plant water use traits on yield and stay-green expression in sorghum. *Funct. Plant Biol.* 41, 1019–1034. doi: 10.1071/FP13355

Messina, C. D., Sinclair, T. R., Hammer, G. L., Curan, D., Thompson, J., Oler, Z., et al. (2015). Limited-transpiration trait may increase maize drought tolerance in the US Corn Belt. *Agron. J.* 107, 1978–1986. doi: 10.2134/agronj15.0016

Passioura, J. B. (1977). Grain yield, harvest index and water use of wheat. *J. Aus. Inst. Agric. Sci.* 48, 117–121.

Purcell, L. C., Sinclair, T. R., and McNew, R. W. (2003). Drought avoidance assessment for summer annula crops using long-term weather data. *Agron. J.* 95, 1566–1576. doi: 10.2134/agronj2003.1566

Rebetzke, G. J., Condon, A. G., Richards, R. A., and Farquhar, G. D. (2002). Selection for reduced carbon isotope discrimination increases aerial biomass and grain yield of rainfed bread wheat. *Crop Sci.* 42, 739–745. doi: 10.2135/cropsci2002.7390

Richards, R. A., and Passioura, J. B. (1989). A breeding program to reduce the diameter of the major xylem vessel in the seminal roots of wheat and its effect on grain yield in rain-fed environments. *Aust. J. Agric. Res.* 40, 943–950. doi: 10.1071/AR9890943

Sadok, W., and Sinclair, T. R. (2010). Genetic variability of transpiration response of soybean (*Glycine max* (L.) Merr.) shoots to leaf hydraulic conductance inhibitor AgNO3. *Crop Sci.* 50, 1423–1430. doi: 10.2135/cropsci2009.10.0575

Sinclair, T. R. (2005). Theoretical analysis of soil and plant traits influencing daily plant water flux on drying soils. *Agron. J.* 97, 1148–1152. doi: 10.2134/agronj2004.0286

Sinclair, T. R. (2012). Is transpiration efficiency a viable plant trait in breeding for crop improvement? *Funct. Plant Biol.* 39, 359–365. doi: 10.1071/FP11198

Sinclair, T. R. (2017a). "Early partial stomata closure with soil drying," in *Water-Conservations Traits to Increase Crop Yields in Water-Deficit Environments: Case Studies*, ed. T. R. Sinclair (Switzerland: Springer). doi: 10.1007/978-3-319-56321-3

Sinclair, T. R. (2017b). "Limited transpiration rate under elevated atmospheric vapor pressure deficit," in *Water-Conservations Traits to Increase Crop Yields in Water-Deficit Environments: Case Studies*, ed. T. R. Sinclair (Switzerland: Springer). doi: 10.1007/978-3-319-56321-3

Sinclair, T. R., Hammer, G. L., and van Oosterom, E. J. (2005). Potential yield and water-use efficiency benefits in sorghum from limited maximum transpiration rate. *Funct. Plant Biol.* 32, 945–952. doi: 10.1071/FP05047

Sinclair, T. R., Marrou, H., Soltani, A., and Vadez, V. (2014). Soybean production potential in Africa. *Glob. Food Sec.* 3, 31–40. doi: 10.1016/j.gfs.2013.12.001

Sinclair, T. R., Messina, C. D., Beatty, A., and Samples, M. (2010). Assessment across the United States of the benefits of altered soybean drought traits. *Agron. J.* 102, 475–482. doi: 10.2134/agronj2009.0195

Sinclair, T. R., and Muchow, R. C. (2001). System analysis of plant traits to increase grain yield on limited water supplies. *Agron. J.* 93, 263–270. doi: 10.2134/agronj2001.932263x

Sinclair, T. R., and Weiss, A. (2010). *Principles of Ecology in Plant Production*, 2 Edn. Wallingford: CAB International. doi: 10.1079/9781845936549.0000

Sinclair, T. R., Zwieniecki, M. A., and Holbrook, N. M. (2008). Low leaf hydraulic conductance associated with drought tolerance in soybean. *Physiol. Plant.* 132, 446–451. doi: 10.1111/j.1399-3054.2007.01028.x

Soltani, A., and Sinclair, T. R. (2012). *Modeling Physiology of Crop Development, Growth and Yield*. Wallingford: CAB Intl. doi: 10.1079/9781845939700.0000

Stiller, W. N., Read, J. J., Constable, G. A., and Reid, P. E. (2005). Selection for water use efficiency traits in cotton breeding program: cultivar differences. *Crop Sci.* 45, 1107–1113. doi: 10.2135/cropsci2004.0545

Tanner, C. B., and Sinclair, T. R. (1983). "Efficient water use in crop production: research or re-search?," in *Limitation to Efficient Water Use in Crop Production*, eds H. M. Taylor, W. R. Jordan, and T. R. Sinclair (Madison, WI: American Society of Agronomy), 1–27.

Tomeo, N. J., and Rosenthal, D. M. (2017). Variable mesophyll conductance among soybean cultivars sets a tradeoff between photosynthesis and water-use efficiency. *Plant Phyiol.* 174, 241–252. doi: 10.1104/pp.16.01940

Vadez, V., Kholova, J., Medina, S., Kakkera, A., and Anderberg, H. (2014). Transpiration efficiency: new insights into an old story. *J. Exp. Bot.* 65, 6141–6153. doi: 10.1093/jxb/eru040

Conflict of Interest Statement: The author declares that the research was conducted in the absence of any commercial or financial relationships that could be construed as a potential conflict of interest.

frontiers in Plant Science

ORIGINAL RESEARCH
published: 11 September 2018
doi: 10.3389/fpls.2018.01290

Effects of 8-Year Nitrogen and Phosphorus Treatments on the Ecophysiological Traits of Two Key Species on Tibetan Plateau

Dan Wang[1], Tianqi Ling[1], Pengpeng Wang[1], Panpan Jing[1], Jiazhi Fan[1], Hao Wang[1] and Yaoqi Zhang[2]*

[1] International Center for Ecology, Meteorology and Environment, Jiangsu Key Laboratory of Agricultural Meteorology, Nanjing University of Information Science and Technology, Nanjing, China, [2] School of Forestry and Wildlife Sciences, Auburn University, Auburn, AL, United States

OPEN ACCESS

Edited by:
Jeffrey M. Warren, Oak Ridge National Laboratory (DOE), United States

Reviewed by:
Fernando José Cebola Lidon, Faculdade de Ciências e Tecnologia da Universidade Nova de Lisboa, Portugal
Anirban Guha, Oak Ridge National Laboratory (DOE), United States

***Correspondence:**
Dan Wang
wangdan@nuist.edu.cn;
wangdan.nuist@outlook.com

Specialty section:
This article was submitted to Plant Physiology, a section of the journal Frontiers in Plant Science

Received: *27 March 2018*
Accepted: *16 August 2018*
Published: *11 September 2018*

Citation:
Wang D, Ling T, Wang P, Jing P, Fan J, Wang H and Zhang Y (2018) Effects of 8-Year Nitrogen and Phosphorus Treatments on the Ecophysiological Traits of Two Key Species on Tibetan Plateau. Front. Plant Sci. 9:1290. doi: 10.3389/fpls.2018.01290

Understanding how nitrogen (N) and/or phosphorus (P) addition affects plants carbon- and water- related ecophysiological characteristics is essential for predicting the global change impact on the alpine meadow ecosystem structure and function in carbon and water cycling. The Qinghai-Tibetan Plateau (QTP) with the largest alpine meadow in the world is regarded as the third pole in the earth and has been experiencing increased atmospheric N deposition. In this project, we focused on two key species (*Elymus dahuricus* and *Gentiana straminea*) of the alpine meadow on the Tibetan Plateau and investigated the variability of photosynthetic and stomatal responses to 8-year N and/or P treatments through field measurements and modeling. We measured photosynthesis- and g_s-response curves to generate parameter estimates from individual leaves with two widely used stomatal models (the BWB model and MED model) for validation of growth and ecosystem models and to elucidate the physiological basis for observed differences in productivity and WUE. We assessed WUE by means of gas exchange measurements (WUE_i) and stable carbon isotope composition ($\Delta^{13}C$) to get the intrinsic and integrated estimates of WUE of the two species. P and N+P treatments, but not N, improved the photosynthetic capacity (A_{net} and V_{cmax}) for both species. Stomatal functions including instaneous measurements of stomatal conductance, intrinsic water-use efficiency and stomatal slope parameters of the two widely used stomatal models were altered by the addition of P or N+P treatment, but the impact varied across years and species. The inconsistent responses across species suggest that an understanding of photosynthetic, stomatal functions and water-use should be evaluated on species separately. WUE estimated by $\Delta^{13}C$ values had a positive relationship with A_{net} and g_s and a negative relationship with WUE_i. Our findings should be useful for understanding the underlying mechanisms of the response of alpine plants growth and alpine meadow ecosystem to global change.

Keywords: photosynthesis, stomatal conductance, intrinsic water-use efficiency, integrated water-use efficiency, stomatal slope parameter

INTRODUCTION

Terrestrial ecosystems worldwide are limited or co-limited by nutrients, especially by nitrogen (N) and phosphorus (P) (Elser et al., 2007; LeBauer and Treseder, 2008; Harpole et al., 2011). While it is well-known that N and P addition typically increases plant growth, less is known about how N and P addition affects plants ecophysiological characteristics related to carbon and water acquisition. The Qinghai-Tibetan Plateau (QTP) is regarded as the third pole and has one of the largest alpine grasslands in the world. The QTP has been experiencing much greater than average global changes, such as increased atmospheric N deposition and climate warming (IPCC, 2013). The wet nitrogen deposition was estimated 6.96–7.55 kg N hm^{-2} y^{-1} on the QTP (Lv and Tian, 2007). With the increase of global nitrogen deposition and the relative slow mineralization rate due to the low temperature at the high elevation, it is critical to investigate the ecophysiological responses of the alpine grasslands species to N and P addition. The information will be valuable in predicting the global change impact on the alpine meadow ecosystem structure and function in carbon and water cycling.

Alpine meadow system on the Tibetan Plateau is characterized as low N and P availability due to the slow mineralization processes at the low temperature. The addition of N and P is therefore anticipated to boost the growth of the alpine meadow species. Yang et al. (2014) reported that N and P additions both increased the aboveground biomass on QTP alpine meadow and the P effect was more evident than the N effect. Fu and Shen (2017) synthesized 51 studies on the QTP and confirmed that nitrogen addition significantly increased plant height and aboveground biomass. Photosynthetic carbon gain of leaves was mainly affected by N concentration and light availability (Field and Mooney, 1986). This observation is supported by the positive relationships between leaf N concentration and net photosynthesis observed in many different species (Turnbull et al., 2007; Wang et al., 2012). However, whether the alpine meadow species is photosynthetically N or P limited and whether different species respond to N/P addition differently remains unknown. Chlorophyll fluorescence parameters, stomatal conductance (g_s) and maximum rate of carboxylation (V_{cmax}) are important physiological parameters related to plant photosynthesis. All these physiological parameters are nutrient-dependent and probably affected under N and/or P addition conditions (Reich et al., 2009; Liu and Greaver, 2010). Measurements of photosynthetic and stomatal responses of the alpine meadow species to N and/or P addition are needed for validation of plant growth models and to elucidate the physiological basis for observed differences in plant growth responses to the addition of N and/or P.

Successfully simulating canopy and ecosystem photosynthesis and transpiration requires understanding the rate-impacting factors in leaf photosynthesis and stomatal activities (Laisk et al., 2005). Understanding and predicting larger scale carbon, water, and energy cycles also requires accurate estimates of the leaf diffusive (stomatal) conductance to water vapor using stomatal conductance models. The regulatory role of stomata in photosynthetic CO_2 assimilation and water vapor loss to the atmosphere is arguably the most fundamental constraint on plant function and most critical process in simulating and predicting larger scale carbon, water and energy fluxes. Empirical and mechanical models have been incorporated into land surface models to simulate stomatal conductance. The Ball, Woodrow & Berry (BWB model) and Medlyn model (MED model) are two widely used stomatal models to describe the complex behavior of stomata at the leaf level (Medlyn et al., 2001; Wolz et al., 2017). The parameters of these models (m and g_0 from BB model, g_1 and g_0 from MED model) are valuable for large-scale simulations and represent important physiological traits that determine plant water-use efficiency. Compared with instant measurements, the changes in stomatal slope parameters (m and g1) with plant's biophysical environment provide a simple but synthetic framework for studying climate-change related carbon and water cycling, because of its sensitivity to CO_2, vapor pressure deficient, and photosynthesis, as well as its crucial information about climate change impacts on photosynthesis and water-use efficiency (Oren et al., 1999). How stomatal slope parameters of alpine meadow species varies among different species and at different fertilization conditions requires further study and analysis.

Through gas exchange measurements, WUE can be expressed as intrinsic WUE (WUE_i, the ratio of net photosynthesis to stomatal conductance, A_{net}/g_s). Integrative WUE ($\Delta^{13}C$) can be assessed indirectly with measurements of the stable carbon isotope composition ($\delta^{13}C$) of leaves or other plant materials. This latter method is based on the linear relationship between $\delta^{13}C$ and the ratio of the concentration of CO_2 inside and outside of the leaf (Farquhar et al., 1982). Using gas exchange measurements (WUE_i) and carbon isotope composition would provide both instantaneous and integrated estimates of WUE (Seibt et al., 2008). Whether the integrated measurements matches with the instantaneous measurements of water-use efficiency, stomatal slope, and photosynthetic parameters for the alpine meadow species requires further investigation and analysis.

Previous studies indicated that N and P additions increased the aboveground biomass of grass but decreased forb biomass (Yang et al., 2014; Fu and Shen, 2017). To identify the ecophysiological responses of different PFTs to N/P addition, we will select two key species (*Elymus dahuricus*, a C_3 perennial grass and *Gentiana straminea*, a C_3 perennial forb) of the alpine meadow on the Tibetan Plateau and investigate the variability of photosynthetic and stomatal responses to N or P additions and associated leaf traits through field measurements and modeling. We measured photosynthesis- and g_s-response

Abbreviation: A_{net}, net CO_2 assimilation rate (umol m^{-2} s^{-1}); F_v'/F_m^i, the maximal photosystem II (PSII) efficiency in the light; g_s, stomatal conductance (mol m^{-2} s^{-1}); J_{max}, maximum electron transport rate (umol m^{-2} s^{-1}); N_{mass}, leaf mass-based nitrogen concentration (%); PFTs, plant functional types; Φ_{PSII}, the actual PSII efficiency; RuBP, ribulose-1,5-bisphosphate carboxylase; V_{cmax}, maximum carboxylation rate (umol m^{-2} s^{-1}); WUEi, intrinsic water-use efficiency (umol CO_2/mol H_2O); $\Delta^{13}C$, stable isotope ^{13}C discrimination values (‰).

curves to generate parameter estimates from individual leaves for two widely used stomatal models (the BWB model and MED model). We assessed WUE by means of gas exchange measurements (WUE_i) and stable carbon isotope composition ($\Delta^{13}C$) to get the intrinsic and integrated estimates of WUE of the two key alpine meadow species. The objectives of this study were (1) to determine whether P or N or both was the nutrient more limiting to the photosynthesis of two alpine meadow species growing in the field; (2) to investigate whether long-term fertilization treatments changes the stomatal slope parameters; (3) to identify the relationship of leaf traits to integrated water-use efficiency ($\Delta^{13}C$). We hypothesized that (1) as the effect on the aboveground biomass, both P and N addition will improve the photosynthetic capacity of the two species and the P effect will be more evident than the N effect; (2) the addition of N or P will not change the stomatal regulating properties; (3) the integrated water-use efficiency ($\Delta^{13}C$) will be correlated with the instantaneous measurements of water-use efficiency (WUE_i and stomatal slope parameters).

MATERIALS AND METHODS

Site Description

The study site was established in an alpine grassland at the Haibei Alpine Meadow Ecosystem Research Station (37°37′ N, 101°12′ E, 3240 m above the sea level), located on the northeastern Tibetan Plateau in Qinghai Province, China (Yang et al., 2014; Song and Yu, 2015). The historic mean annual temperature is −1.7°C and annual precipitation is 560 mm, 85% of which occurs in the growing season from May to September. The PAR (photosynthetically active radiation) reaches 370 W m^{-2} s^{-1} in the growing season, equivalent ot 10 MJ m^{-2} d^{-1}. The mean annual temperature was 2.89 and −0.02°C and the mean annual precipitation was 601 and 453 mm in 2015 and 2016, respectively. The mean daily day- and night-temperature and maximal temperature was 11.6, 4.6, and 28.4°C and 13.6, 5.2, and 28.9°C in the growing season in 2015 and 2016, respectively. The soil is classified as Mat Cry-gelic Cambisols (Chinese Soil Taxonomy Research Group, 1995), corresponding to Gelic Cambisol. Topsoil (0–10 cm) has a pH value of 7.5, and contains 71.4 g kg^{-1} organic C, 7.8 g kg^{-1} total N, and 0.77 g kg^{-1} total P before nutrient treatments were applied in 2009 (Huang et al., 2014). The experimental site was fenced before the experiment plot was established. The plant community at the experimental site is dominated by *Kobresia humilis*, *Stipa aliena*, *Elymus nutans*, *E. dahuricus*, *G. straminea*, and *Festuca ovina*.

Experimental Design and Sampling

The experimental design followed the standard protocols of Nutrient Network (NutNet[1]). In mid-May 2009, an experimental area of 1 ha was fenced to prevent grazing disturbance. Twenty-four plots of 6 m × 6 m were randomly assigned to four treatments with six replicates (blocks) in a complete randomized block design. The blocks were separated by a 2-m-wide buffer zone, and the plots within each block were separated by a 1-m-wide buffer zone to minimize disturbance from neighboring treatments. The four treatments consisted of the following: (1) Control (CK, no fertilizer was added); (2) N addition (in the form of urea, 100 kg N ha^{-1} $year^{-1}$); (3) P addition (in the form of triple superphosphate, 50 kg ha^{-1} $year^{-1}$); and (4) N+P addition (combined addition of N and P in the same amounts as the solo treatments). Pelletized fertilizer was evenly distributed by hand onto the plots after sunset in July from 2009 to 2016.

[1]http://nutnet.umn.edu

Photosynthetic Measurements

Gas exchange (including net photosynthetic rate and stomatal conductance) was measured with a portable infrared gas analyzer (LI-COR 6400LCF; LI-COR, Lincoln, NE, United States) on 1 randomly selected fully expanded healthy leaf from each plot of each treatment in August, 2015 and 2016. During measurements, leaves were exposed to a CO_2 concentration of 370 μmol mol^{-1}, leaf temperature of 25°C, and airflow through the chamber of 300 μmol s^{-1}. Leaves were acclimated to a photosynthetic photon flux (PPFD; 2000 μmol m^{-2} s^{-1}) until photosynthetic rates stabilized. The rate of photosynthesis at a PPFD of 2000 μmol m^{-2} s^{-1} was defined as the net photosynthetic rate (A_{net}). PSII efficiency in light-adapted leaves (F_v'/F_m') and PSII operating efficiency (Φ_{PSII}) were also measured using a Licor 6400-40 Leaf Chamber Fluorometer. The photosynthesis-CO_2 response (A–C_i) curves were measured each year in the middle of the growing season (August). During measurement, leaves were acclimated for 30–60 min before adjusting the CO_2 concentrations. Thereafter, CO_2 concentration was decreased in five steps (400, 300, 200, 100, and 50 ppm CO_2) and then increased in four steps (400, 600, 800, and 1000 μmol mol^{-1} CO_2). A–C_i curves were fit to the Farquhar-von Caemmerer-Berry model based on the methods developed by Miao et al. (2009). By using grid search and non-linear two-stage least square regression technique, the fitting model solves the A–C_i parameters including maximum ribulose 1·5-bisphosphate carboxylase/oxygenase (Rubisco) carboxylation rate (V_{cmax}, μmol m^{-2} s^{-1}) and potential light saturated electron transport rate (J_{max}, μmol m^{-2} s^{-1}), respectively.

Immediately following gas-exchange measurements, leaf samples were oven-dried till constant weight. Leaf samples were then ground and N concentration (N_{mass}, mass based nitrogen concentration) were measured with a Perkin Elmer CHN Analyzer (Model 2400).

Integrated Water-Use Efficiency ($\Delta^{13}C$)

Leaves were oven-dried at 65°C for 2 weeks, then ground to fine powder. Approximately, 2 mg of homogenized leaves were weighed into tin capsules and analyzed with an elemental analyzer coupled to an isotope ratio mass spectrometer (Elemental combustion system 4010, Costech instruments). Carbon isotope ratios were expressed in conventional δ notation and referenced to the Pee Dee Belemnite (PDB) standard for $\delta^{13}C$. Measurement error was less than 0.3‰ for $\delta^{13}C$.

The carbon isotope composition ($\delta^{13}C$) was calculated as the ratio (‰):

$$\delta^{13}C = \left[\left(\frac{R_{sample}}{R_{standard}}\right) - 1\right] \times 1000$$

Carbon isotope ratio values were converted to discrimination values (Δ, ‰) by the equation (Farquhar et al., 1989):

$$\Delta = (\delta a - \delta p)/\left(1 + \frac{\delta p}{1000}\right)$$

Where δa is the carbon isotope ratio of CO_2 in the atmosphere (assumed to be -8 pars per mil, Seibt et al., 2008) and δp is the measured carbon isotope ratio of the leaf tissue. Lower values of Δ indicate higher water-use efficiency values.

Stomatal Slope Parameter Calculations

The Ball et al. (1987) (Eq. 1) or Medlyn et al. (2001) (Eq. 2) models of g_s were used to calculate the stomatal slope parameters (m and g1).

$$Eq.\ 1 \quad g_s = g_0 + m\frac{Ah}{C_a}$$

where g_s is stomatal conductance (mol m^{-2} s^{-1}), A is the net rate of photosynthetic CO_2 uptake (μmol m^{-2} s^{-1}), h is atmospheric relative humidity (unitless), C_a is the atmospheric CO_2 concentration at the leaf surface (μmol mol^{-1}), g_0 is the y-axis intercept and m is the slope of the line.

$$Eq.\ 2 \quad g_s = g_0 + 1.6\left(1 + \frac{g_1}{\sqrt{D}}\right)\frac{A}{C_a}$$

where D is atmospheric vapor pressure deficit (kPa) and g_1 is the model parameter related to the slope of the line.

For each leaf, a linear least squares regression of Eq. 1 or Eq. 2 was used to estimate the intercept and slope parameters of the Ball et al. (1987) (*3*) model and Medlyn et al. (*5*) model, respectively. Biologically, the slope parameter of each model represents the sensitivity of g_s to changes in A_{net}, C_a and atmospheric water status and will be the focus of this analysis. A term for the y intercept of each model algorithm (g_0) can be used to describe variation in minimum g_s. Only leaves that provided a regression between modeled and observed stomatal conductance with an $R^2 > 0.8$ were included in further analyses (Wolz et al., 2017).

Statistical Analysis

Three-way analysis of variance (ANOVA) was used to test the fixed effects of year, species, fertilization treatment and their interaction on A_{net}, g_s, WUE_i, N_{mass}, F_v'/F_m', Φ_{PSII}, V_{cmax}, J_{max}, and $\Delta^{13}C$. *Post hoc* Tukey HSD tests were conducted on specific contrasts to examine significant treatment effects among groups. General linear models (GLMs) were used to assess the relationship between $\Delta^{13}C$, WUE_i and other physiological parameters. For all tests, the normality of the residuals was tested using the Shapiro–Wilk test. All statistical testes were considered significant at $p \leq 0.05$. Mean values of each variable were expressed with their standard error (SE). All analyses were conducted in R (R 2.14[2]).

RESULTS

The three-way ANOVA analysis revealed that effects of nutrient additions on photosynthetic traits varied among species, years, treatment and their interactions (**Figure 1** and **Table 1**). Photosynthetic and leaf traits varied between years and among species, with *G. straminea* possessing higher A_{net}, g_s, F_v'/F_m', Φ_{PSII}, V_{cmax}, J_{max}, N_{mass}, and $\Delta^{13}C$ and lower WUE_i and stomatal slope parameters compared with *E. dahuricus* (**Table 1**). A_{net} of plants with P and N+P treatments was significantly higher than those with N and CK treatments for *E. dahuricus* and *G. straminea* in 2015 and 2016 (**Figure 1**). Across species and years, the value of g_s of plants with P and N+P treatment was significantly higher than those with N and CK treatments. There were significant species, year and species * treatment effect on WUE_i. The value of WUE_i of *E. dahuricus* with N+P and P treatment was significantly higher than those with N and CK treatments.

Significant effects were detected among species, year, treatment and species × treatment for F_v'/F_m' and Φ_{PSII} (**Figure 2** and **Table 1**). For *E. dahuricus*, plants with P and N+P treatments had higher F_v'/F_m' and Φ_{PSII} than those with CK and N treatments. For *G. straminea*, P addition significantly increased F_v'/F_m' in 2016 and 2017 compared with CK treatments and Φ_{PSII} compared with CK, N and N+P treatments in 2017.

There were significant effects of species, year, treatment and their interactions for V_{cmax} and J_{max} (**Figure 3** and **Table 1**). Across *E. dahuricus* and *G. straminea* in 2 years, plants with P and N+P treatments had higher V_{cmax} and J_{max} than those with N and CK treatments.

There were no treatment, but species, year and treatment × year effects on stomatal slope parameters of m and g1 (**Figure 4** and **Table 1**). Variation in estimates of the g1 slope parameter from the Medlyn et al. model mirrored that of m, both in species rank and treatment effects. In 2015, plants with nutrient treatment had higher values of m and g1 than plants with CK treatments for both species. In 2016, plants with P and N+P treatments had lower values of m and g1 than plants with CK treatment for *E. dahuricus*. There were no significant treatment effects for *G. straminea* in 2016.

Significant effects were detected among species, years, treatment and their interactions for N_{mass} and $\Delta^{13}C$ (**Figure 5** and **Table 1**). Across the two species in the 2 years, plants with N and N+P treatment had higher N_{mass} than plants with P and CK treatments. The value of $\Delta^{13}C$ varied among species and treatments. Plants with N+P treatment had lower $\Delta^{13}C$ than plants with CK treatments across two species.

$\Delta^{13}C$ had a positive relationship with A_{net} and g_s, a negative relationship with WUE_i and no relationship with stomatal slope parameter of m or g1 (**Figure 6**).

[2]http://www.r-project.org/

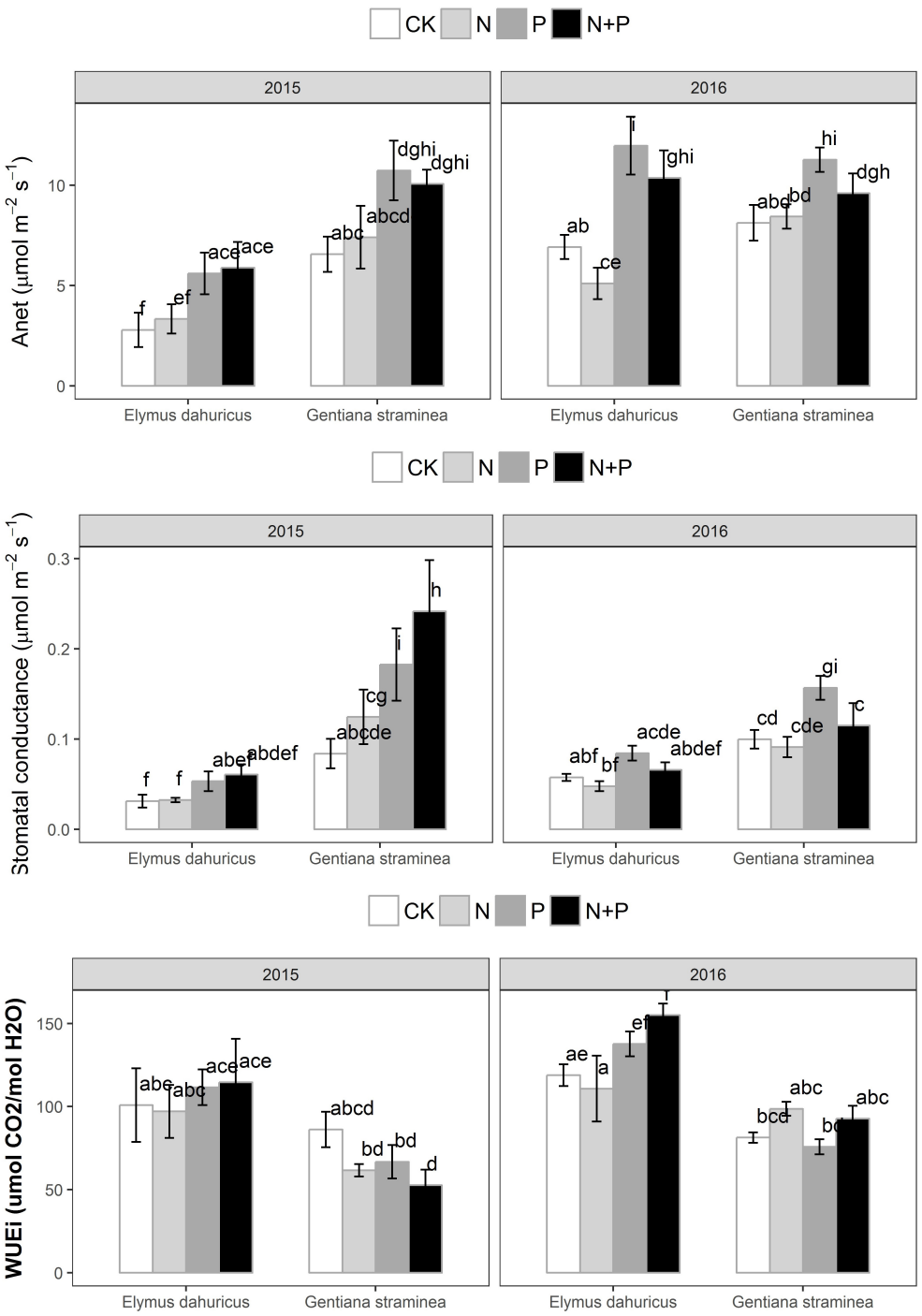

FIGURE 1 | The response of net photosynthetic CO_2 assimilation (A_{net}), stomatal conductance ($_{gs}$), and intrinsic water-use efficiency (WUE_i) to the nutrient addition for *Elymus dahuricus* and *Gentiana straminea*. Measurements were taken at CK (control), N (nitrogen), P (phosphorus), and N+P (nitrogen and phosphorus) treatments in the peak growing season in 2015 and 2016. Values are means ± 1 SE; $n = 5$. Bars sharing the same letters are not significantly different.

DISCUSSION

In order to investigate the variation in the ecophysiological responses to N and/or P treatment and detect whether there is stomatal acclimation with long-term fertilization treatment, we assessed leaf traits of two key species on Tibet alpine grassland across two growing seasons. The systematic measurements of gas exchange after long-term fertilization treatment are essential for validation of plant growth and ecosystem models and to elucidate the physiological basis for observed differences

TABLE 1 | Analysis of variance (*F*-value) of the effects of species, treatment, year and their interactions on net photosynthetic rate (A_{net}), stomatal conductance (g_s), intrinsic WUE (WUEi), leaf nitrogen concentration (N_{mass}), the maximal PSII efficiency in the light (F_v'/F_m'), the actual PSII efficiency (Φ_{PSII}), maximal carboxylation rate (V_{cmax}), potential light saturated electron transport rate (J_{max}), stomatal slope parameters m and g1, and $\Delta^{13}C$.

Variation	A_{net}	g_s	*iWUE*	F_v'/F_m'	Φ_{PSII}	V_{cmax}	J_{max}	g1	m	N_{mass}	$\Delta^{13}C$
Species	8.9**	96.9***	48.7***	110.4***	79.3***	4.9*	4.1*	9.9***	12.3***	565.6***	264.7***
Treatment	19.8***	11.5***	1.6	17.8***	11.6***	7.5***	8.2**	1.0	0.8	10.7***	2.9*
Year	19.9***	0.8	12.2***	48.9***	61.2***	21.9***	14.9***	15.4***	27.3***	15.8***	0.1
Species × treatment	1.1	3.3*	3.2*	4.6**	2.0	2.8*	0.7	0.8	0.3	0.4	0.3
Species × year	6.9**	15.1***	0.0	1.4	4.5*	5.2*	6.8**	2.7	0.7	8.0**	167.7***
Treatment × year	0.7	3.6*	0.9	1.7	1.0	1.8	2.6*	4.1**	4.1**	1.5	0.4

*** *Indicates significance level at 0.001, ** 0.01, * 0.05.*

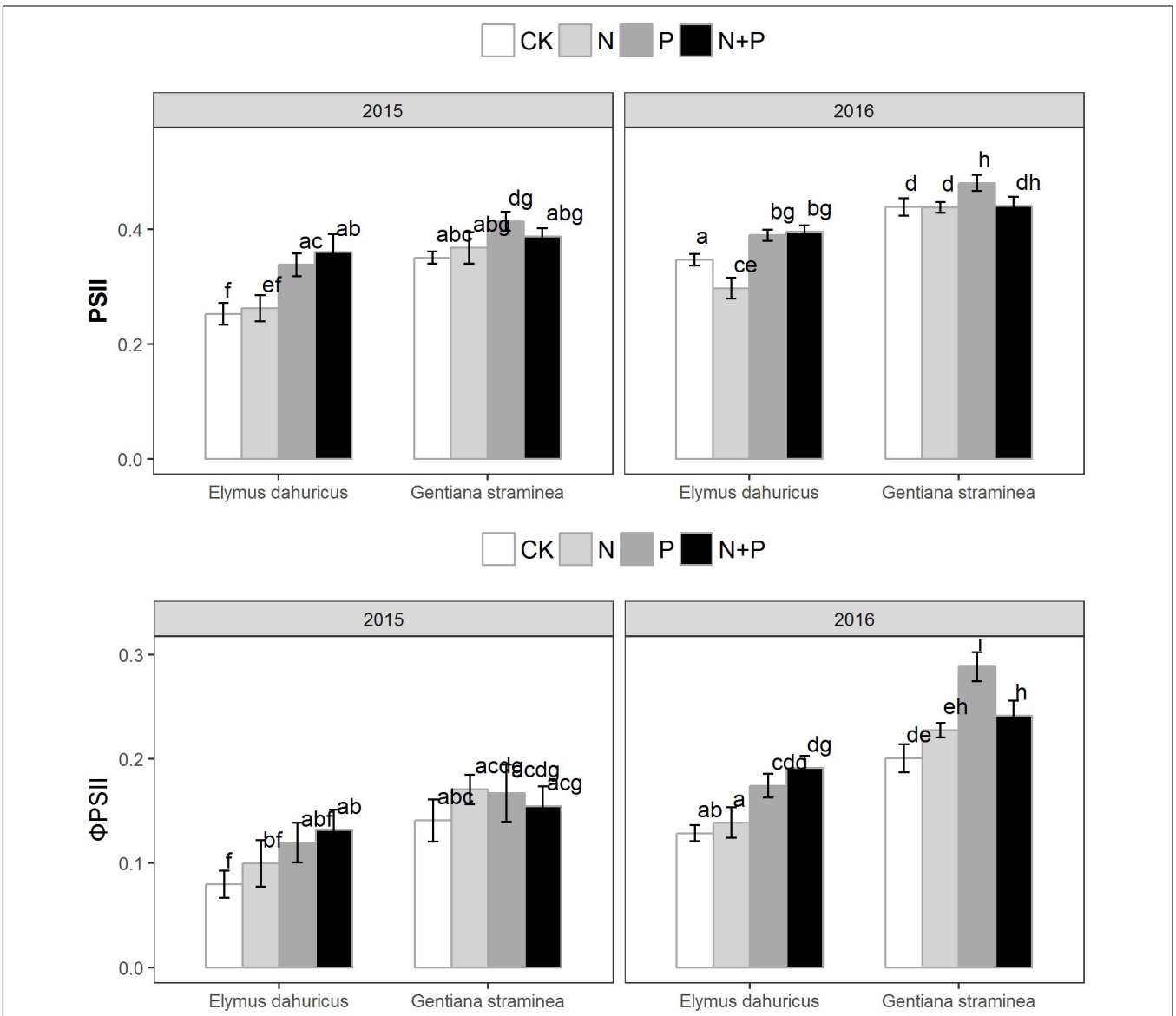

FIGURE 2 | The response of the maximal PSII efficiency in the light (F_v'/F_m') and the actual PSII efficiency (Φ_{PSII}) to the nutrient addition for *E. dahuricus* and *G. straminea*. Measurements were taken at CK (control), N (nitrogen), P (phosphorus), and N+P (nitrogen and phosphorus) treatments in the peak growing season in 2015 and 2016. Values are means ± 1 SE; $n = 5$. Bars sharing the same letters are not significantly different.

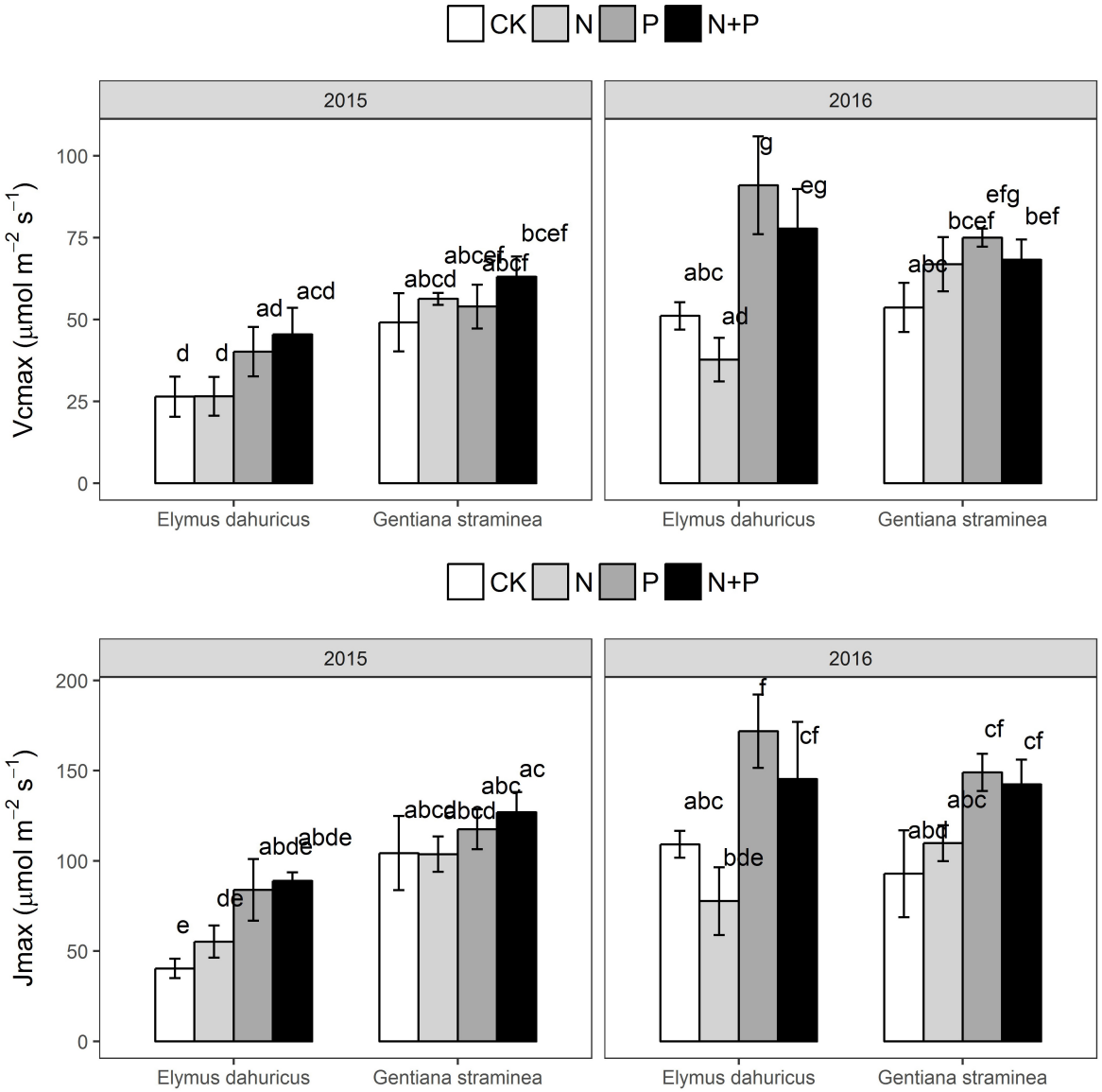

FIGURE 3 | The response of maximum rate of Rubisco activity (V_{cmax}) and potential light saturated electron transport rate (J_{max}) to the nutrient addition for *E. dahuricus* and *G. straminea*. Measurements were taken at CK (control), N (nitrogen), P (phosphorus), and N+P (nitrogen and phosphorus) treatments in the peak growing season in 2015 and 2016. Values are means ± 1 SE; n = 5. Bars sharing the same letters are not significantly different.

in the response of growth and water-use to N and/or P additions.

In our study, photosynthetic and leaf traits varied among species and treatment, with *G. straminea* possessing higher A_{net}, g_s, F_v'/F_m', Φ_{PSII}, V_{cmax}, J_{max}, N_{mass}, and $\Delta^{13}C$ and lower WUE_i and stomatal slope parameters compared with *E. dahuricus* (**Table 1**). Contrary to our first hypothesis, 8 years of N treatments had no effects on photosynthetic traits of either species, despite significant increases in foliar N for both species. No stimulation of photosynthetic traits by N treatment in the present study was not in line with other results from this experiment site demonstrating that N addition increased the aboveground biomass by 24% (Yang et al., 2014). Though nitrogen addition significantly increased plant productivity in the alpine meadow (Bassin et al., 2012; Fu and Shen, 2017) and other grasslands (LeBauer and Treseder, 2008; Lee et al., 2010), the effect of nitrogen addition on plants' photosynthetic performance on alpine meadow has not been investigated widely. The results implied that the elevated foliar N might not have been partitioned to photosynthetic components, i.e., RuBP carboxylase (Rubisco) or chlorophylls (Bauer et al., 2004), suggesting a decoupling of photosynthesis and elevated foliar N. The proportion of N allocation to Rubisco may not increase, as shown by the maximum Rubisco carboxylation efficiency, which was not altered by N fertilization. The effect of N on plant growth is generally due to both an effect on photosynthesis and leaf growth, which was mostly confirmed

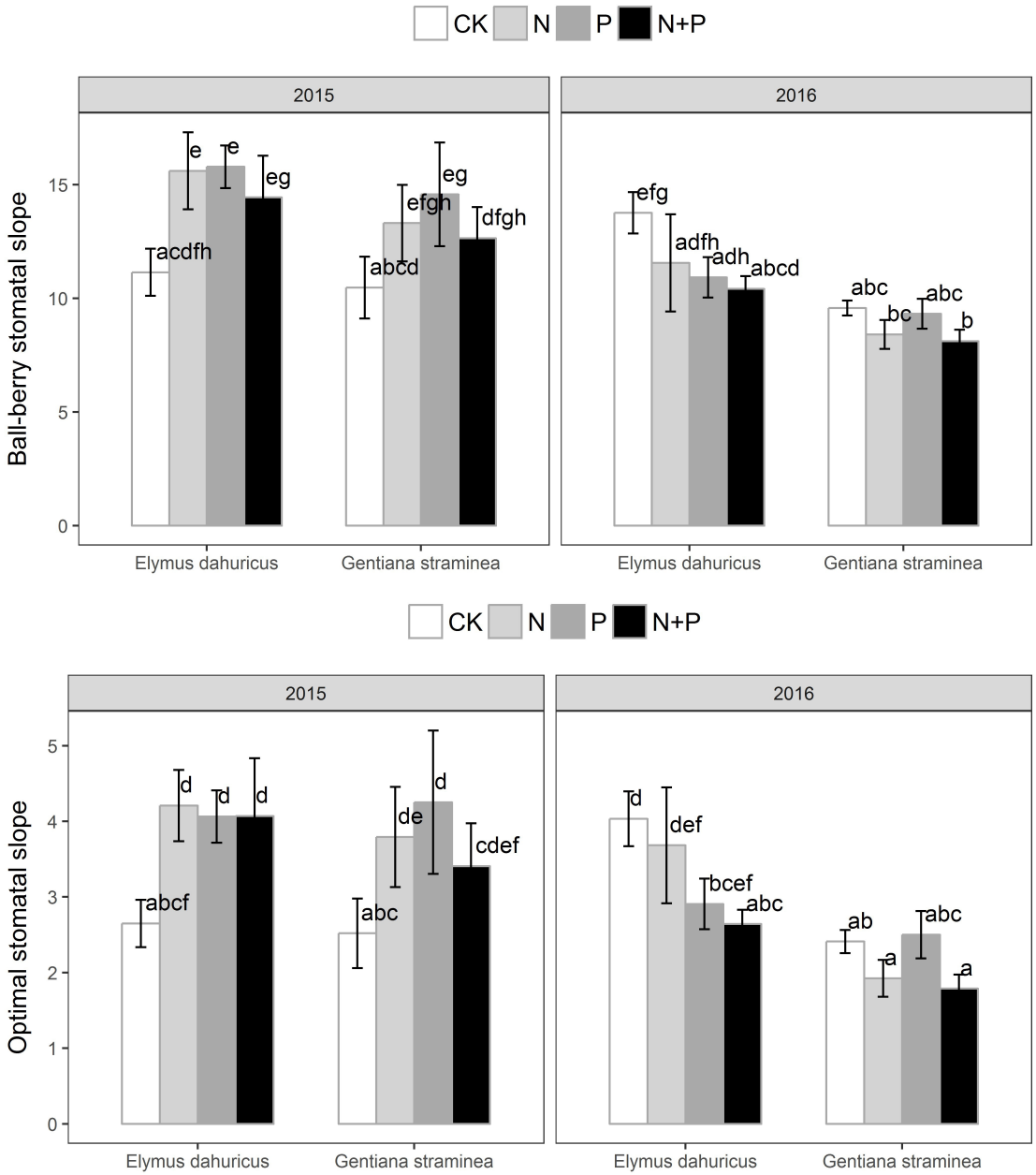

FIGURE 4 | The response of stomatal slope m from Ball-berry model and g1 from Medlyn model to the nutrient addition for *E. dahuricus* and *G. straminea*. Measurements were taken at CK (control), N (nitrogen), P (phosphorus), and N+P (nitrogen and phosphorus) treatments in the peak growing season in 2015 and 2016. Values are means ± 1 SE; $n = 5$. Bars sharing the same letters are not significantly different.

on C_3 species. Such long and high N treatments might have eliminated any N limitation to photosynthetic performances.

In consistent with earlier findings that P addition increased the aboveground biomass by 52% (Yang et al., 2014), P addition increased A_{net} for both species compared with CK treatment (**Figure 1**). The increase of A_{net} promoted by P addition may be attributed to increases in g_s, F_v'/F_m', Φ_{PSII} and Rubisco activity (V_{cmax} and J_{max}) for both species (**Figures 1**, **3**). Phosphorus (P) nutrient is essential to a variety of plant functions and a major component of nucleic acids, sugar phosphates, ATP, and phospholipids, all of which play important roles in photosynthesis. Low leaf P is thought to limit A_{net} through reductions in ribulose-1,5-bisphosphate (RuBP) regeneration, carboxylation activity, light use efficiency, and stomatal conductance (Campbell and Sage, 2006; Thomas et al., 2006). It had been shown that P supply influenced partitioning of

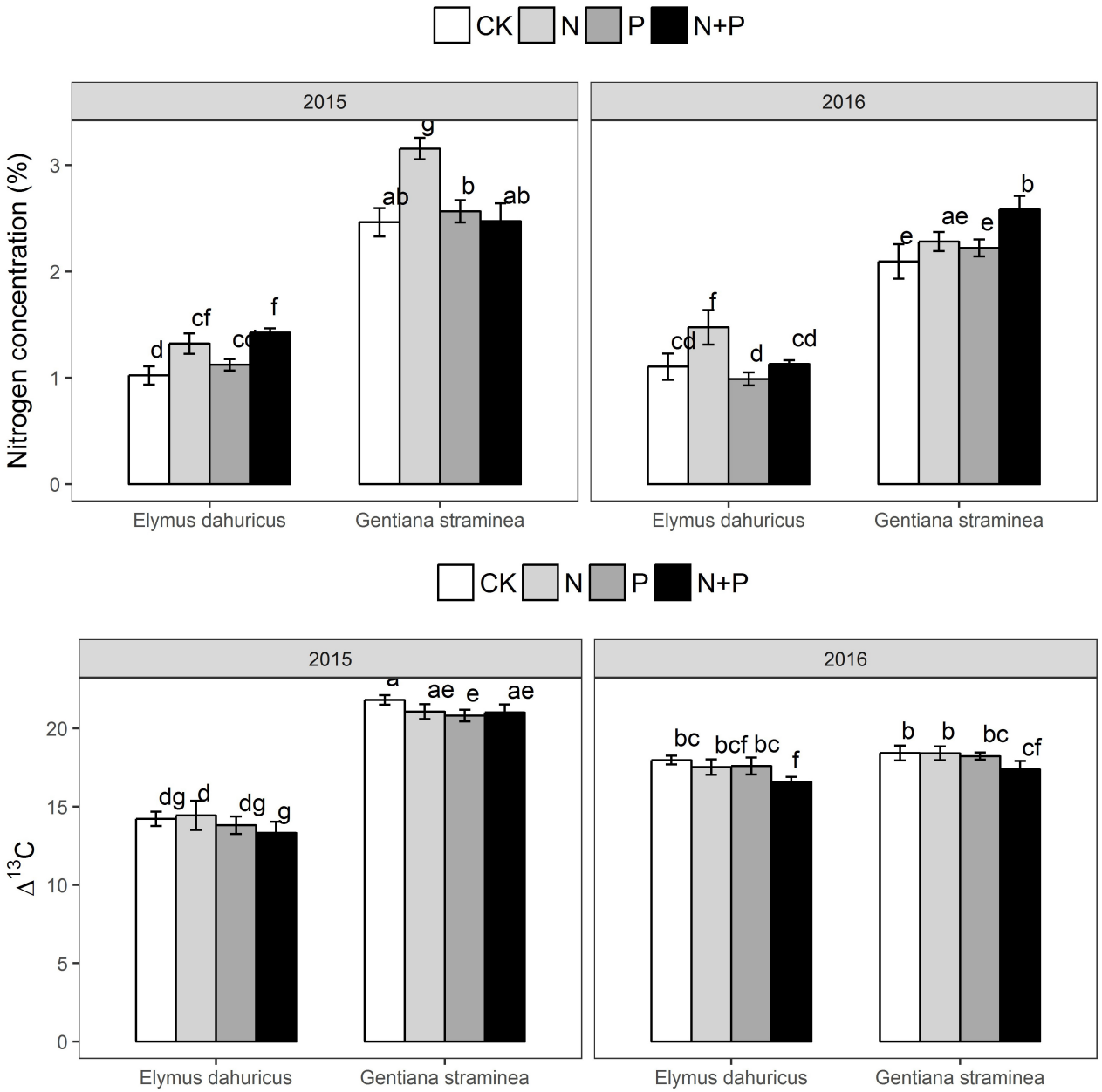

FIGURE 5 | The response of leaf N (N_{mass}) and integrated water-use efficiency ($\Delta^{13}C$) to the nutrient addition for *E. dahuricus* and *G. straminea*. Measurements were taken at CK (control), N (nitrogen), P (phosphorus), and N+P (nitrogen and phosphorus) treatments in the peak growing season in 2015 and 2016. Values are means ± 1 SE; $n = 5$. Bars sharing the same letters are not significantly different.

N to Rubisco and important for RuBP regeneration, suggesting there might be interactive effects of N and P availability on A_{net} (Warren et al., 2005). In a cross-biome analysis of the influence of P on the linear relationship between photosynthetic capacity (A_{max}) and foliar N, the slope of such linear relationship increased with leaf P (Reich et al., 2009). The results in this study indicated there was no additive effect of N+P treatment on the photosynthetic capacity of these two species. In alpine ecosystems on the Tibetan Plateau, these two species were limited by P rather than N availability photosynthetically and P addition will trigger a stronger positive response of plant photosynthesis than N addition. The findings here suggest that it is important to learn more about the physiology of P effects on A_{net} for modeling carbon and biogeochemical fluxes and vegetation–climate interactions, especially for regions where low P supply may play a role in limiting plant and ecosystem function. The significant year * species and year * treatment effects also suggested that the meteorological conditions might also play a significant effect on the ecophysiological responses of the two key species to the nutrient treatments.

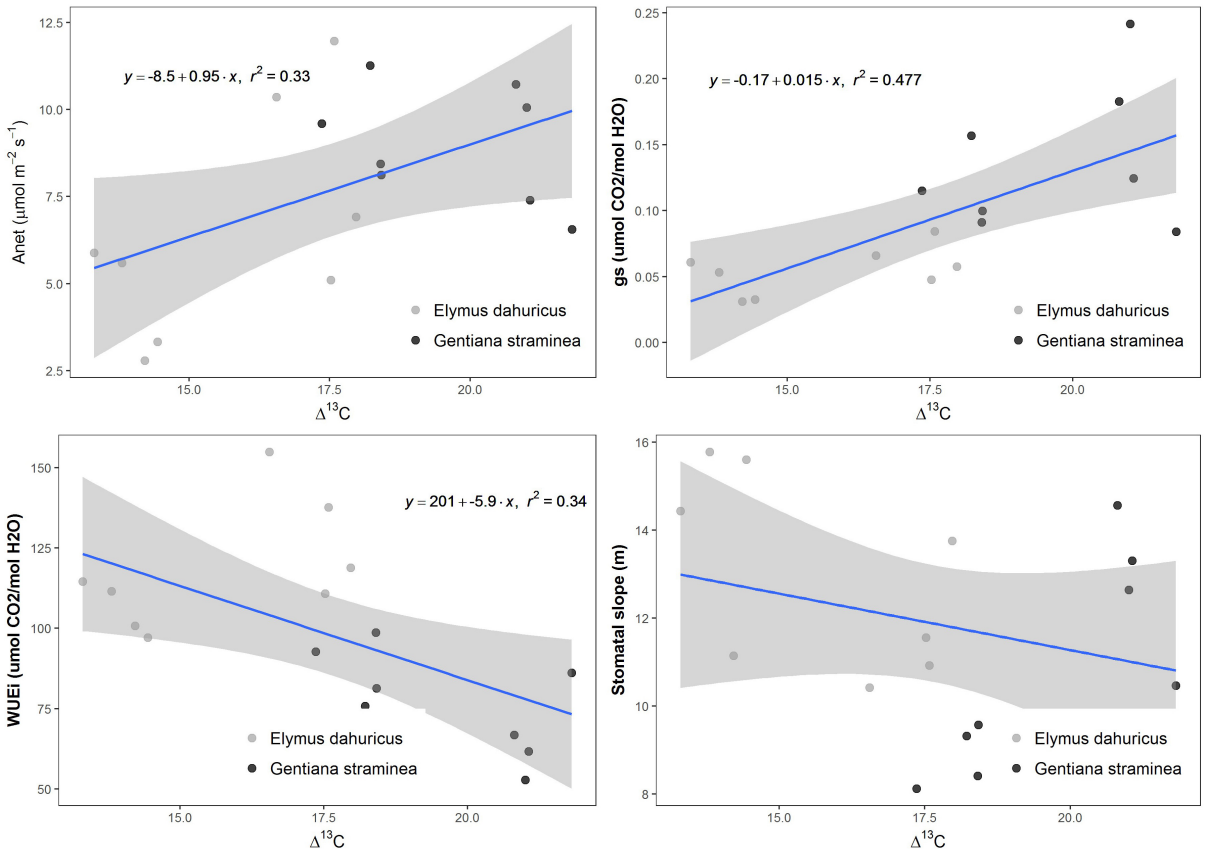

FIGURE 6 | The linear relationship between integrated water-use efficiency ($\Delta^{13}C$) and net photosynthetic CO_2 assimilation (A_{net}), stomatal conductance (g_s), intrinsic water-use efficiency (WUE_i), stomatal slope m from Ball-berry for *E. dahuricus* and *G. straminea*. Only significant relationships ($p < 0.05$) with equations were shown on the figures.

Nutrient addition not only affected plants carbon gain of these two species, but also their stomatal functions in water relations. P addition significantly increased g_s for *E. dahuricus* and *G. straminea*. P stimulation on stomatal conductance indicated that nutrient availability may limit stomatal function and thus was important for maximizing carbon gain. Higher stomatal conductance and thus higher transpiration can enhance nutrient uptake. Variation across PFTs and environmental gradients in the g_1 and m parameters had been reported widely (Medlyn et al., 2011; Lin et al., 2015; Wolz et al., 2017). Consistent with our prediction, there was no altered stomatal sensitivity under different nutrient addition treatments. N, P or N+P treatment increased m and g1 in 2015 ($p = 0.06$ for *E. dahuricus* and for *G. straminea*). The slope parameter g1 and m (dimensionless) relating g_s to AH/cs was obtained by fitting the equation to leaf gas-exchange data (Leakey et al., 2006). The values of g1 and m are largely representative of the ratio g_s/A, the reciprocal of intrinsic water-use efficiency (Franks et al., 2017). Therefore, it might be expected that plants with characteristically higher WUE_i will exhibit lower g1, which was the case for the stomatal slope parameter g1 and m in 2015 and 2016 for both species. The case study of 15 temperate C_3 tree species revealed that long-held assumptions about stomatal function were a substantial source of error in physiological models of carbon and water fluxes at the leaf scale (Wolz et al., 2017). Current modeling approaches assuming a universal stomatal slope parameter under different conditions could probably propagate the errors to simulations of crop performance, ecosystem function and global biogeochemical cycles.

The ratio C_i/C_a, measured under normal (light-saturated) conditions of leaf gas exchange or as a time-integrated value from carbon isotope discrimination ($\Delta^{13}C$) in plant material, has long been recognized as an index of plant water-use efficiency. A decline in C_i/C_a [and $\Delta^{13}C$] is equivalent to an increase in intrinsic water-use efficiency (Farquhar et al., 1989). This relationship can be difficult to resolve because the two variables integrate plant response over different time spans: WUE_i is an instantaneous measurement while $\Delta^{13}C$ is integrated over the growing season. There was evidence for a negative linear relationship between WUE_i and $\Delta^{13}C$ in different species and functional types (Roussel et al., 2009; Orchard et al., 2010; Wang et al., 2012). Recent analyses had suggested that using $\Delta^{13}C$ as an indicator of variation in WUE could be less effective when applied across species (Warren and Adams, 2006; Seibt et al., 2008; Wang et al., 2012; Cernusak et al., 2016). Our study showed that the diversity of $\Delta^{13}C$ had a negative relationship with WUE_i

of the two species, consistent with previous studies (**Figure 6**). Plants can increase WUE by increasing the efficiency of carbon fixation inside the leaf, either by increasing the efficiency of light harvesting or carboxylation processes. However, $\Delta^{13}C$ was positively correlated with A_{net}, implying that the decrease of WUE (increase of $\Delta^{13}C$) was more driven by the increase of g_s. The overall $\Delta^{13}C$ during carbon assimilation is dependent on the CO_2 concentration at the sites of carboxylation, which in turn is strongly dependent on mesophyll conductance (g_m). Many studies reported no significant relationship between $\Delta^{13}C$ and WUE_i (Seibt et al., 2008; McCarthy et al., 2011), claiming mesophyll conductance contributed to the observed variability of $\Delta^{13}C$.

CONCLUSION

This study provided an ecophysiological investigation of two alpine meadow species after 8-year N and/or P treatments with a systematic measurement of leaf traits across two growing seasons. P and N+P addition improved the photosynthetic capacity for both species. A_{net} of the two alpine species in this study responded similarly to N and/or P treatment and the P stimulation on the A_{net} was associated with increased g_s, F_v'/F_m' and V_{cmax} for *E. dahuricus* and *G. straminea*. The stomatal functions including instantaneous measurements of stomatal conductance, intrinsic water-use efficiency and the stomatal slope parameters of the two widely used stomatal models were altered by the addition of P or N+P treatment, but the impact varied across years or species. This suggests that an understanding of photosynthesis, stomatal functions, and water-use should be evaluated on species basis. The effectiveness of integrating $\Delta^{13}C$ and intrinsic water-use efficiency was confirmed. Our findings should be useful for understanding the underlying mechanisms of the response of alpine plants to global change.

AUTHOR CONTRIBUTIONS

DW came up with the idea and manage the experimental sites and wrote the paper. TL, PW, PJ, HW, and JF conducted the experiment and analyzed the data. YZ helped with the manuscript writing.

FUNDING

Funding for this research was provided by Nanjing University of Information Science and Technology (2013r115); Jiangsu Distinguished Professor Scholarship, Jiangsu six talent peaks (R2016L15); Jiangsu Natural Science Foundation (BK20150894); National Natural Science Foundation of China (31500503 and 31770485); Jiangsu Overseas Research & Training Program for University Prominent Young & Middle-aged Teachers and Presidents through DW; and International S&T Cooperation Program of China (2012DFA60830).

ACKNOWLEDGMENTS

We thank Dr. Jinsheng He, Dr. Zhenhua Zhang, and Zhiyuan Ma for their assistance with field sampling and measurements.

REFERENCES

Ball, J., Woodrow, I., and Berry, J. (1987). "A model predicting stomatal conductance," in *Progress in Photosynthesis Research*, ed. J. Biggens (Dordrecht: Martinus Nijhoff), 221–224.

Bassin, S., Schalajda, J., Vogel, A., and Suter, M. (2012). Different types of sub-alpine grassland respond similarly to elevated nitrogen deposition in terms of productivity and sedge abundance. *J. Veg. Sci.* 23, 1024–1034. doi: 10.1111/j.1654-1103.2012.01422.x

Bauer, G. A., Bazzaz, F. A., Minocha, R., Long, S., Magill, A., Aber, J., et al. (2004). Effects of chronic N additions on tissue chemistry, photosynthetic capacity, and carbon sequestration potential of a red pine (*Pinus resinosa* Ait.) stand in the NE United States. *For. Ecol. Manage.* 196, 173–186. doi: 10.1016/j.foreco.2004.03.032

Campbell, C. D., and Sage, R. F. (2006). Interactions between the effects of atmospheric CO2 content and P nutrition on photosynthesis in white lupin (*Lupinus albus* L.). *Plant Cell Environ.* 29, 844–853. doi: 10.1111/j.1365-3040.2005.01464.x

Cernusak, L. A., Barbour, M. M., Arndt, S. K., Cheesman, A. W., English, N. B., Feild, T. S., et al. (2016). Stable isotopes in leaf water of terrestrial plants. *Plant Cell Environ.* 39, 1087–1102. doi: 10.1111/pce.12703

Chinese Soil Taxonomy Research Group (1995). *Chinese Soil Taxonomy*. New York, NY: Science Press, 58–147.

Elser, J. J., Bracken, M. E., Cleland, E. E., Gruner, D. S., Harpole, W. S., Hillebrand, H., et al. (2007). Global analysis of nitrogen and phosphorus limitation of primary producers in freshwater, marine and terrestrial ecosystems. *Ecol. Lett.* 10, 1135–1142. doi: 10.1111/j.1461-0248.2007.01113.x

Farquhar, G. D., Ehleringer, J. R., and Hubick, K. T. (1989). Carbon isotope discrimination and photosynthesis. *Annu. Rev. Plant Physiol. Plant Mol. Biol.* 40, 503–537. doi: 10.1146/annurev.pp.40.060189.002443

Farquhar, G. D., O'Leary, M. H., and Berry, J. A. (1982). On the relationship between carbon isotope discrimination and the intercellular carbon dioxide concentration in leaves. *Funct. Plant Biol.* 9, 281–292.

Field, C. B., and Mooney, H. A. (1986). "The photosynthesis-nitrogen relationship in wild plants," in *On the Economy of Plant Form and Function*, ed. T. J. Givnish (Cambridge: Cambridge University Press), 35–55.

Franks, P. J., Berry, J. A., Lombardozzi, D. L., and Bonan, G. B. (2017). Stomatal function across temporal and spatial scales: deep-time trends, land-atmosphere coupling and global models. *Plant Physiol.* 174, 583–602. doi: 10.1104/pp.17.00287

Fu, G., and Shen, Z. (2017). Response of alpine soils to nitrogen addition on the Tibetan plateau: a meta-analysis. *Appl. Soil Ecol.* 114, 99–104. doi: 10.1016/j.apsoil.2017.03.008

Harpole, W. S., Ngai, J. T., Cleland, E. E., Seabloom, E. W., Borer, E. T., Bracken, M. E., et al. (2011). Nutrient co-limitation of primary producer communities. *Ecol. Lett.* 14, 852–862. doi: 10.1111/j.1461-0248.2011.01651.x

Huang, Y., Olbrecht, L., Yang, X., and He, J. (2014). Effects of nutrient additions on the arbuscular mycorrhizal fungal colonization in the alpine meadow on the Tibetan Plateau. *Beijing Daxue Xuebao (Ziran Kexue Ban). Acta Sci. Nat. Univ. Pekinensis* 50, 911–918.

IPCC (2013). *Climate Change 2013: The Physical Science Basis. Contribution of Working Group I to the Fifth Assessment Report of the Intergovernmental Panel on Climate Change*. Cambridge: Cambridge University Press.

Laisk, A., Eichelmann, H., Oja, V., Rasulov, B., Padu, E., Bichele, I., et al. (2005). Adjustment of leaf photosynthesis to shade in a natural canopy: rate parameters. *Plant Cell Environ.* 28, 375–388. doi: 10.1111/j.1365-3040.2004.01274.x

Leakey, A. D. B., Bernacchi, C. J., Ort, D. R., and Long, S. P. (2006). Long-term growth of soybean at elevated CO2 does not cause acclimation of stomatal conductance under fully open-air conditions. *Plant Cell Environ.* 29, 1794–1800. doi: 10.1111/j.1365-3040.2006.01556.x

LeBauer, D. S., and Treseder, K. K. (2008). Nitrogen limitation of net primary productivity in terrestrial ecosystems is globally distributed. *Ecology* 89, 371–379. doi: 10.1890/06-2057.1

Lee, M., Manning, P., Rist, J., Power, S. A., and Marsh, C. (2010). A global comparison of grassland biomass responses to CO2 and nitrogen enrichment. *Philos. Trans. R. Soc. B Biol. Sci.* 365, 2047–2056. doi: 10.1098/rstb.2010.0028

Lin, Y. S., Medlyn, B. E., Duursma, R. A., Prentice, I. C., Wang, H., Baig, S., et al. (2015). Optimal stomatal behaviour around the world. *Nat. Clim. Change* 5, 459–464. doi: 10.1038/nclimate2550

Liu, L., and Greaver, T. L. (2010). A global perspective on belowground carbon dynamics under nitrogen enrichment. *Ecol. Lett.* 13, 819–828. doi: 10.1111/j.1461-0248.2010.01482.x

Lv, C., and Tian, H. (2007). Spatial and temporal patterns of nitrogen deposition in China: synthesis of observational data. *J. Geophys. Res.* 112:D22S05.

McCarthy, H. R., Diane, P. E., and Jenerette, G. D. (2011). Plant water-use efficiency as a metric of urban ecosystem services. *Ecol. Appl.* 21, 3115–3127. doi: 10.1890/11-0048.1

Medlyn, B. E., Barton, C. V. M., Broadmeadow, M. S. J., Ceulemans, R., De Angelis, P., Forstreuter, M., et al. (2001). Stomatal conductance of forest species after long-term exposure to elevated CO_2 concentration: a synthesis. *New Phytol.* 149, 247–264. doi: 10.1046/j.1469-8137.2001.00028.x

Medlyn, B. E., Duursma, R. A., Eamus, D., Ellsworth, D. S., Prentice, I. C., Barton, C. V. M., et al. (2011). Reconciling the optimal and empirical approaches to modeling stomatal conductance. *Glob. Change Biol.* 17, 2134–2144. doi: 10.1111/j.1365-2486.2010.02375.x

Miao, Z., Xu, M., Richard, G., Lathrop, J. R., and Wang, Y. (2009). Comparison of the A–Cc curve fitting methods in determining maximum ribulose 1_5- bisphosphate carboxylase/oxygenase carboxylation rate, potential light saturated electron transport rate and leaf dark respiration. *Plant Cell Environ.* 32, 109–122. doi: 10.1111/j.1365-3040.2008.01900.x

Orchard, K. A., Cernusak, L. A., and Hutley, L. B. (2010). Photosynthesis and water-use efficiency of seedlings from northern Australian monsoon forest, savanna and swamp habitats grown in a common garden. *Funct. Plant Biol.* 37, 1050–1060. doi: 10.1071/FP09306

Oren, R., Sperry, J. S., Katul, G. G., Pataki, D. E., Ewers, B. E., Phillips, N., et al. (1999). Survey and synthesis of intra- and interspecific variation in stomatal sensitivity to vapour pressure deficit. *Plant Cell Environ.* 22, 1515–1526. doi: 10.1046/j.1365-3040.1999.00513.x

Reich, P. B., Oleksyn, J., and Wright, I. J. (2009). Leaf phosphorus influences the photosynthesis-nitrogen relation: a cross-biome analysis of 314 species. *Oecologia* 160, 207–212. doi: 10.1007/s00442-009-1291-3

Roussel, M., Dreyer, E., Montpied, P., Le-Provost, G., Guehl, J. M., and Brendel, O. (2009). The diversity of (13)C isotope discrimination in a *Quercus robur* fullsib family is associated with differences in intrinsic water use efficiency, transpiration efficiency, and stomatal conductance. *J. Exp. Bot.* 60, 2419–2431. doi: 10.1093/jxb/erp100

Seibt, U., Rajabi, A., Griffiths, H., and Berry, J. A. (2008). Carbon isotopes and water use efficiency: sense and sensitivity. *Oecologia* 155, 441–454. doi: 10.1007/s00442-007-0932-7

Song, M. H., and Yu, F. H. (2015). Reduced compensatory effects explain the nitrogen mediated reduction in stability of an alpine meadow on the Tibetan Plateau. *New Phytol.* 207, 70–77. doi: 10.1111/nph.13329

Thomas, D. S., Montagu, K. D., and Conroy, J. P. (2006). Leaf inorganic phosphorus as a potential indicator of phosphorus status, photosynthesis and growth of *Eucalyptus grandis* seedlings. *For. Ecol. Manage.* 223, 267–274. doi: 10.1016/j.foreco.2005.11.006

Turnbull, T. L., Kelly, N., Adams, M. A., and Warren, C. R. (2007). Within-canopy nitrogen and photosynthetic gradients are unaffected by soil fertility in field-grown *Eucalyptus globulus*. *Tree Physiol.* 27, 1607–1617. doi: 10.1093/treephys/27.11.1607

Wang, D., Maughan, M. W., Sun, J., Feng, X., Miguez, F., Lee, D., et al. (2012). Impact of nitrogen allocation on growth and photosynthesis of Miscanthus (*Miscanthus x giganteus*). *Glob. Change Biol. Bioenergy* 4, 688–697. doi: 10.1111/j.1757-1707.2012.01167.x

Warren, C. R., and Adams, M. A. (2006). Internal conductance does not scale with photosynthetic capacity: implications for carbon isotope discrimination and the economics of water and nitrogen use in photosynthesis. *Plant Cell Environ.* 29, 192–201. doi: 10.1111/j.1365-3040.2005.01412.x

Warren, C. R., McGrath, J. F., and Adams, M. A. (2005). Differential effe cts of N, P and K on photosynthesis and partitioning of N in *Pinus pinaster* needles. *Annu. For. Sci.* 62, 1–8. doi: 10.1051/forest:2004088

Wolz, K., Timothy, W., Mark, A., Wang, D., and Leakey, A. (2017). Diversity in stomatal function is integral to modelling plant carbon and water fluxes. *Nat. Ecol. Evol.* 1, 1292–1298. doi: 10.1038/s41559-017-0238-z

Yang, X. X., Ren, F., Zhou, H. K., and He, J. S. (2014). Responses of plant community biomass to nitrogen and phosphorus additions in an alpine meadow on the Qinghai-Xizang Plateau. *Chin. J. Plant Ecol.* 38, 159–166. doi: 10.3724/SP.J.1258.2014.00014

Conflict of Interest Statement: The authors declare that the research was conducted in the absence of any commercial or financial relationships that could be construed as a potential conflict of interest.

The reviewer AG and handling Editor declared their shared affiliation.

Advantages of publishing in Frontiers

OPEN ACCESS
Articles are free to read for greatest visibility and readership

FAST PUBLICATION
Around 90 days from submission to decision

HIGH QUALITY PEER-REVIEW
Rigorous, collaborative, and constructive peer-review

TRANSPARENT PEER-REVIEW
Editors and reviewers acknowledged by name on published articles

Frontiers
Avenue du Tribunal-Fédéral 34
1005 Lausanne | Switzerland

Visit us: www.frontiersin.org
Contact us: info@frontiersin.org | +41 21 510 17 00

REPRODUCIBILITY OF RESEARCH
Support open data and methods to enhance research reproducibility

DIGITAL PUBLISHING
Articles designed for optimal readership across devices

FOLLOW US
@frontiersin

IMPACT METRICS
Advanced article metrics track visibility across digital media

EXTENSIVE PROMOTION
Marketing and promotion of impactful research

LOOP RESEARCH NETWORK
Our network increases your article's readership